

Ecohydrology of a Mixed Savanna-Agricultural Catchment in South-East Burkina Faso, West Africa

THÈSE N° 6040 (2014)

PRÉSENTÉE LE 17 JANVIER 2014

À LA FACULTÉ DE L'ENVIRONNEMENT NATUREL, ARCHITECTURAL ET CONSTRUIT
LABORATOIRE DE MÉCANIQUE DES FLUIDES DE L'ENVIRONNEMENT
PROGRAMME DOCTORAL EN ENVIRONNEMENT

ÉCOLE POLYTECHNIQUE FÉDÉRALE DE LAUSANNE

POUR L'OBTENTION DU GRADE DE DOCTEUR ÈS SCIENCES

PAR

Natalie Claire CEPERLEY

acceptée sur proposition du jury:

Prof. F. Golay, président du jury
Prof. M. Parlange, Prof. J.-C. Bolay, directeurs de thèse
Prof. A. Buttler, rapporteur
Prof. S. Gaskin, rapporteur
Prof. N. C. van de Giesen, rapporteur



ÉCOLE POLYTECHNIQUE
FÉDÉRALE DE LAUSANNE

Suisse
2014

I later learned that there was a connection between the fig tree's root system and the underground water reservoirs. The roots burrowed deep into the ground, breaking through the rocks beneath the surface soil and diving into the underground water table. The water travelled up along the roots until it hit a depression or weak place in the ground and gushed out as a spring. Indeed, wherever these trees stood, there were likely to be streams. The reverence the community had for the fig tree helped preserve the stream and the tadpoles that so captivated me. The trees also held the soil together, reducing erosion and landslides. In such ways, without conscious or deliberate effort, these cultural and spiritual practices contributed to the conservation of biodiversity.

- Wangari Maathai, *Unbowed*, 2006.

To my grandparents, *James McCoy Davis*, *Phyllis Ruth Rowe Davis*, *Ellen Axson Rodes Ceperley*, and *Florian Fairchild Ceperley*, from whom I inherited my passion for the pursuit of education, the discovery of global cultures, and the marvel of the natural world.



Acknowledgements

A huge thank you to the entire village of Tambarga and the Commune of Madjoari. You so enthusiastically tolerated us through all our trials, participatory meetings, and installations of instruments that looked like they came from another planet. I owe a special *ndjanda* to Dramane Yonli, who maintained our equipment and samples even when we could not be there, to Sabordja Koare who helped me immensely with so many tasks, and to Aisha Kouadima who taught me my few words of Gourmançema. The mayor, Mamoudou Ouoba, made sure that we were always respected and taken care of in the village and our work would have been impossible without so many others including Issa Koadima, Boundia Kouare, Brigitte Amoussou, Amadou Lankoande, Assou Bande, all of their children and families, the teachers in the two schools, the farmers who owned the fields, and all of the workers who helped dig holes, carry equipment, translate and install instruments. I am forever grateful to all the children and unnamed who made my time in Tambarga meaningful and I hope you learned even a fraction from me of what I learned from you. The most individually significant sacrifice to this work was perhaps made by the man who lost his life near the village of Nagré, when we first transported equipment to the village in 2009. May we always remember that tragedy that taints our presence and may his sacrifice not have been in vain.

Second, I would like to thank everyone at ZiE for the support I received. Desire Koakou, in particular, maintained our stations and worked hard while we were focusing on scientific analysis. Each of the drivers at ZiE performed a thankless task, that I hope hasn't totally turned them off to Tambarga. The professors and researchers, in particular Hamma Yacouba and Dial Niang, were always generous with their time. Also, I am grateful to the students at ZiE who came to stay with us in the field. In Ouagadougou, above all, thank you to Seydou Kabore, for all his support, both logistic and personal, as well as that of his staff at the PRCUU. This project would not be possible without them. More personally, Chantal Kolongo gave personality to my time in Ouagadougou. Finally, I would like to thank the various officials who afforded us their time, especially at the beginning of the project.

In Switzerland, my co-advisor, Jean-Claude Bolay, and the entire CoDev team provided a much-appreciated second academic home as I attempted to do socially relevant science on two continents. In particular, I owe a huge thank you to Alexandre Repetti who initiated the project. In this light, I would like to acknowledge the Velux and 3rd Millennium foundations that funded the first years. In addition, the KFPE – jeunes chercheurs grant supported a large part of my fieldwork.

I would like to thank the members of Rolf Siegwolf's group at PSI in Villigen for their help with the extraction of water from soil and xylem. At EPFL, Michael Bensimmon's as well as Elena and Karine, and Felipe's team's help in their respective labs was indispensable. The Sensorscope team, especially Guillermo and Davis, perhaps got more than they bargained for when they jumped on board and I am grateful they stuck with us. Closer to home, I would first like to thank all of those who came with us to the field, Thierry, Olivier, and Francesca, as well as Nick Van de Geisen and Scott Tyler who were particularly supportive in the field at the start and remotely later on. And of course, the entire EFLUM lab who accompany us technically and personally – Vincent, Chad, Holly, Hendrick, Nikki, Megan, Jacques, Valentin, Marie-Jo and the rest of the team, current and past. I am grateful for my exchanges with each of the visitors who we hosted – Wilfred Brutsaert, Amilcare Porporato, Ron Calhoun, Paolo D'Odorico, Eric Pardyjak, Greg Characklis, Chris Williams, Andreas Christen, Gaby Katul, Jan Hopmans, and others – and I only wish I had been able to benefit more from each of our exchanges. The students and interns who worked with me each helped and taught me in many ways – Maoya, Camille, Christine, Pierre-Adil, Malik, Ariane, Lucile, Matthieu, Brendan, Guillaume, Georges, Antonia and others.

Above all, I would like to thank Theophile Mande for being my partner on this project. We were really a team in so many senses of the word, and I hope we continue to take measurements in the remote corners of the earth together. And last, but far from least, I owe so much to Marc Parlange. He believed in this project and convinced me to be an "expert" who took EFLUM to Africa. Although, I must admit, sometimes I questioned the "cowboy" style; ultimately I have come to appreciate the foresight and genius it disguises. I learned so much from these years and hope they continue to shape both of our research trajectories. Finally, though they deserve far more than this last line, I would like to thank my family and friends near and far who accompanied me in this journey, in particular my mother, who even helped with fieldwork, and my father who is my first academic role model.

Natalie Ceperley
Lausanne, 14 October 2013



Abstract

Understanding water use by agroforestry trees and diverse land uses in dry-land ecosystems is essential for improving water management in some of the most precarious parts of the world. Agroforestry trees, as well as other land covers whose use is secondary to agriculture, are valued and promoted for many of their ecologic and economic benefits, but are often criticized as competing for valuable water resources. In addition, increasing knowledge about the hydrologic roles of vegetation and land cover will allow us to better predict and anticipate consequences of changing settlements and climate. This is especially important as rural economies are becoming less able to provide for the costs of modern life and there is stronger impetus for rural exodus. It is imperative for the quality of rural life that the environmental resources necessary for the long-term viability of farming be secure.

My thesis brings together five interrelated analyses that each further understanding of hydrologic function of vegetation at different scales, in particular *Sclerocarya birrea* agroforestry trees, in the catchment surrounding the ephemeral stream near Tambarga, Burkina Faso, in the context of improving agro-systems. First, I examine the fluxes of sensible and latent heat to understand how the seasonal variations in land cover and topography affect the transfer of energy and water vapor in the catchment. Second, I use eddy covariance measurements of latent heat flux together with an energy balance – similarity theory formulation to obtain evaporation at each of the sixteen wireless meteorological stations. In this case, I calculate ground heat flux as a fraction of net radiation that I apply over the catchment in terms of land-cover. From this spatial analysis, I refine my understanding of the land cover controls on the catchment scale hydrologic exchanges with the soil moisture and atmosphere. Third, I use my observations of sensible and latent heat flux to improve my interpretation of the land surface controls on the evaporative fraction. This step is an important foundation for eventual upscaling using. Fourth, this informed a simple model of soil moisture surrounding the tree, using an innovative arrangement of a wireless sensor network to partition precipitation into interception, infiltration, evapotranspiration, and runoff under the canopy and in the open. And fifth, I use an analysis of the stable isotopes of soil and xylem water extracted from branches and soil underneath a *Sclerocarya birrea* as well as that from surface and ground water in the catchment to understand what water sources the tree is using when. This analysis has huge potential for local livelihood improvement, as these steps can be built upon to provide environmental information services for small-scale farmers as well as recommendation regarding agroforestry improvement.

My examination of the energy fluxes over the seasons demonstrates the strong controls on evaporative fraction by vegetation through modification of the surface roughness, albedo, and available moisture. Despite these variations, I demonstrate that energy balance together similarity theory applied to distributed weather stations can give reasonable estimates of the evaporation over the catchment and thus provides a very practical and applicable tool for evaporation estimates to be made in a lower-cost more distributed manner than is currently possible. I also demonstrated the evaporative fraction's response to the land surface controls, which is another useful tool for eventual upscaling. This is especially important in this part of the world where meteorological data are scarce. My balance of tree water partitioning showed that soil moisture under agroforestry trees did remain humid further into the dry season than that in the open, suggesting that the trees can be beneficial to neighboring crops. From this, I propose concrete incentives for local farmers to maintain and increase current woody vegetation cover in the form of agroforestry interventions in their cropland. Later, examination of the time series of enriched stable isotope concentrations in water confirm that values in soil and xylem are coupled, both becoming enriched during the dry season and depleted during the rainy season. Xylem water δO_{18} levels drop in early March when trees access groundwater for leafing out, however soil water does not reach this level until soil moisture increases in mid-June. This suggests that *Sclerocarya birrea* performs hydraulic redistribution, or lifting of deep ground water, during dry season to allow for this initial leaf-out. These conclusions have implications not only for local farmers, but also for the scientific community and the global environment.

Keywords: Agroforestry, Burkina Faso, *Sclerocarya birrea*, Stable Isotopes, Surface Energy Balance, Evaporative Fraction

Résumé

Comprendre l'utilisation de l'eau par les arbres agroforestiers dans les écosystèmes des terres arides est essentiel pour améliorer la gestion de l'eau. Par rapport à leurs avantages écologiques et économiques, les arbres agroforestiers ont des grandes qualités cependant on leur reproche souvent de trop monopoliser les ressources en eau si précieuses. De plus, améliorer notre compréhension de l'impact hydrologique de la végétation et du couvert végétal nous permettra de mieux prédire et de se préparer aux conséquences des changements d'occupation de sol et de climat. Ceci se révèle particulièrement important dans la mesure où, dans un contexte d'exode rural toujours plus grand, la difficulté pour les populations rurales de supporter les coûts de la vie moderne se fait de plus en plus grande. Il est impératif pour que la qualité de vie en milieu rural soit augmentée que ressources environnementales nécessaires pour une agriculture durable soit sécurisée.

Ma thèse rassemble cinq analyses interdépendantes qui avancent notre compréhension du fonctionnement hydrologique de la végétation, en particulier les arbres agroforestiers *Sclerocarya birrea*, dans le bassin entourant le ruisseau éphémère près de Tambarga, Burkina Faso. Tout d'abord, j'examine les flux de chaleur sensible et latente afin de comprendre comment les variations saisonnières de la couverture du sol et de la topographie influencent le transfert d'énergie et de vapeur d'eau dans le bassin versant. Deuxièmement, je me sers de mes mesures de flux de chaleur latente avec un bilan énergétique – selon la théorie de similarité pour obtenir l'évaporation à chacune des dix-sept stations météorologiques. Dans ce cas, je calcule le flux de chaleur du sol comme une fraction du rayonnement net. De cette analyse spatiale, j'affine ma compréhension des contrôles d'occupation des sols sur les bassins hydrologiques échelle échanges avec l'humidité et l'atmosphère du sol. Troisièmement, j'utilise mes observations des flux de chaleur sensible et latent pour améliorer ma compréhension des contrôles exigés par la surface terroir sur la fraction évaporé. Cette étape ouvre les portes vers la possibilité de monter en échelle. Quatrièmement, mes mesures décrivent un modèle simple de l'humidité du sol autour de l'arbre, en utilisant un dispositif novateur réseau de capteurs sans fil. Ce réseau de capteurs permet alors de connaître la répartition entre les précipitations, l'infiltration, l'évapotranspiration ainsi que le ruissellement sous le couvert et le ruissellement en plein air. Cinquième, j'utilise l'analyse des isotopes du xylème extraits des branches du *Sclerocarya birrea* et du sol sous l'arbre sol sous un *Sclerocarya birrea* ainsi que celle de la surface et des eaux souterraines dans le bassin versant de comprendre quelles sont les sources d'eau de l'arbre utilise. Cette analyse a un énorme potentiel terme d'amélioration de la subsistance locale dans la mesure où les données de ce réseau de capteurs sans fil peuvent être transmises en temps réel via une connexion GSM partout dans le monde et par conséquent être disponibles pour les utilisateurs locaux. Dans mon analyse, je propose un modèle de paiement pour des services écologiques fait sur la base de mes résultats au niveau de l'arbre ainsi qu'à l'échelle du bassin. Cela permettrait de motiver financièrement les agriculteurs à entretenir des arbres agroforestiers sur leurs terres afin que l'intégrité hydrologique du paysage puisse être maintenue.

Mon examen des flux d'énergie au cours des saisons démontre les contrôles rigoureux sur la fraction évaporatoire par la végétation grâce à la modification de la rugosité de surface, l'albédo et l'humidité disponible. Malgré ces variations, j'ai démontré qu'un modèle basé sur la théorie de similarité appliqué aux stations météorologiques réparties peut donner des estimations raisonnables de l'évaporation sur le bassin versant et ainsi fournir un outil très pratique et applicable pour estimer l'évaporation. J'ai aussi démontré la réponse de la fraction évaporée aux contrôles de la surface terroir, qui est aussi un utile pratique pour monter l'échelle. Ceci est particulièrement important dans cette partie du monde où les données météorologiques sont rares. Mon équilibre de l'arbre de partitionnement de l'eau a montré que le sol sous les arbres agroforestiers reste humide plus longtemps durant la saison sèche que le sol exposé à l'air libre. Cela suggère que les arbres peuvent être bénéfiques pour les cultures voisines. Enfin, je propose des solutions concrètes pour inciter les agriculteurs locaux à maintenir et accroître la couverture de la végétation ligneuse sous la forme d'agroforesterie qui interviendrait dans leurs terres arables. La série temporelle des concentrations $\delta O18$ confirme qu'il existe une corrélation entre les valeurs dans le sol et l'eau du xylème, les deux devenant enrichis pendant la saison sèche et appauvris pendant la saison des pluies. Xylème $\delta O18$ baisse de niveaux au début de Mars, lorsque les arbres accèdent à l'eau souterraine pour la feuillaison, cependant l'eau du sol n'atteint ce niveau que lorsque l'humidité augmente à la mi-Juin. Cela suggère que *Sclerocarya birrea* fait la redistribution hydraulique, ou la remonter de l'eau sous terrain profond pendant la saison sèche pour permettre cette première feuille de départ. Ces conclusions ont d'énormes implications non seulement pour les agriculteurs locaux, mais aussi pour la communauté scientifique et l'environnement mondial.

Mots-clés: agroforesterie, Burkina Faso, *Sclerocarya birrea*, isotopes stables, bilan énergétique de surface, fraction évaporé

Mi mayutaanma

Ki bandi mi ñima n todi ti tiidi bi findima po maama ki tinkuonga nni pia mayuli boncianla ki baa fidi ki todi mi ñima kubima yeni n suagi liiga. Tin kuo yaa tiidi pia mayuli kelima bi pia ku tingbangu po todima ki go findi ti loagu, ama laa tiidi mo tagili tie ke bi bua mi ñima boncianla bi findima po ke nan sua ke ban kpedi yaa tinga nni yeni ñima waa. Li pia mayuli boncianla kelima naani mi yema n lebidi maama ke a dociamama (galo) tuada kua mi dobimu yeni, li teni ke yaa niba n fuo a dobila nni yema paagidi. Naani mi yema n paagidi maama teni ke bi tianba yen fii ki ñaa bi dogu ki gedi potogu.

Li pia mayuli ki dagidi ke yaa niba n fuo mu dobimu nni yeni miali yema n fidi ki ñanbi ki pugini. Laa lebidima sanu tie ki ñanbi ki kubi i loagi leni bu kpaabu n kpendinni yaa loagu kuli. N tuonli tie ki taani mayuciamama muu ke bi kuli pia tuginyema ki baa fidi ki todi ti tin pia yaa banma ke li tuugi leni tin kuo yaa tiidi yeni n suagi liiga. Laa tiidi yeni yii *Bunamarigbu*, bi fini lindi yaa baagu n kuu leni Tangbaaga dogu Bulicina Faso nni. N baa kpa cili ki diidi mi fawatonma n cuoni maama ki fidi ki bandi ku tingbangu n tie maama leni ku lebidima ku siagu leni ku tontongu yogunu n pia yaa fuoma yaa fawatonma (yaa manma) n ñaa ku baagu nni.

N baa suagi ki taa min pia yaa bonbiigikaala ke li baa fidi ki todinni min biigi mi fawatonma n cuoni maama ke li tuugi leni yaa banma buolu ke mi yii. Laa biigima baa tieni piiga n tuonsoanjaana lele nni; yaa tuonsoanjaana ke bi yii meteyo yeni. Lan kani n baa fidi ki tieni li kanli yaali n tuugi leni ki tinga tonu. N baa yaa tiendi laa kanli dana lele kuli ki taa laa cuada ki tugini leni ku baagu yeni tingbangu ki go biigi. Laa biigima baa todinni mi bandi cain yaali n tuugi leni mi fawatonma n cuoni maama yaa tinmu n kuu ku baagu yeni. N baa suagi ki taa mi tama leni bu tibu beni ñima leni ki tinga ñima. Laa tibu leni ki tinga ñima kuli baa yaa tie yaa tibu n yii *Bunamarigbu* yeni tiipo yaale. N go baa ñani ku baagu yeni ñima leni ku tiipo ñima ki biigi likuli lan todinni min fidi ki bandi bu tibu n ñuu yaa ñima bu findima po. Laa puoli pendima n baa taa yaa tuonsoantiagu n baa todinni mi bandi bu tibu lindima n kuugi maama. Laa tuonsoantiagu baa fidi ki teni min bandi ki taaga n mini ke li daa maama, mi ñima n lundi ki kua ki tinga nni maama, man tiini maama ki kua ku baagu nni, man cuoni maama ki tinga tiipo leni ki tapoli.

Laa biigima pia u fidu ke li yabi a dobila niba yema findima po. Laa biigima n mali yaala tie yaala ke bi baa fidi ki diidi kaanu kuli dunia nni mi biigima yeni yogunu kelima li tuugi leni yaa banma n yii interineti yeni. N tuonli nni n bua ki taa nannanli ki waani i pani yaala n tuugi leni ti tiidi yeni kpaabu lan fidi ki paagi a kpakpaala pala ban fidi ki kubi ñama ban kuo yaa tiidi yeni bi tinmu nni ki daa biidi ku tingbangu n pia yaa ñima. Mi biigima doagidi ki waani ke ti tiidi beni ñima leni ku tingbangu ñima yen pugini ku tontongu yogunu ama ki nan yen wadi ku siagu yaa yogu. Ti tiidi beni ñima yen wadi citaa ñmaalo yaa yogunu ke ti tiidi jiini yen moandi ki bua ki pundi ku tingbangu tiipo ñima ti faadi findima po yeni. Ama laa yogunu tiipo ñima yeni kaanu foagi kelima mi wadi. Ki tinga kugima yen pugidi ciluoba ñmaalo boagima yogunu.

Laa bonla kuli taanma todinni ke n baa fidi ki yedi ke yaa tibu n yii *Bunamarigbu* yeni yen kubi mi ñima o gbanu nni ku tontongu yogunu lani n todi o cicili faadi findima. Laa bonbiigikaala wani cain ke tin kuo yaa tiidi yeni tiipo kugima ki cie yaa tinga n kaa pia tibu ku tontongu yogunu. Li doagidi ti po ke tin kuo yaa tiidi kpaabu pia mi todima tin baa fidi ki kuo yaala u kuanu nni kuli po. Min cogi yaa cogu ke li tuugi leni ki tinga leni mi ñima n lebidi maama li binli tugu nni doagidi ti po ke baa ke ki tingbangu ñima gbeni, ti tiidi pia ban tagi yaa sanbila ki fidi ki yaa fuo. Li tie moamoani ke mi lebidima tiendi, ama baa lankuli, n fidi ki taa yaa bangima ke li tuugi leni ti tiidi n bua yaa bontodikaala bi findima po yeni ki doagidi ke laa banma yaa tugini leni meteyo tuonsontiadi baa todi tin bandi ku baagu ñima gbenma n tiendi maama. Laa banma baa fidi moko ki tua ti po u cogu buolu yaala n baa todi ti tin fidi ki biigidi ku baagu ñima gbenma tontoni ki nan kan biidi i ligi. Laa banma pia mayuli boncianla yaa dogi n kaa pia meteyo banma ke mi yabi.

Mi juodima, n go waani a sanbila ke li baa todi a kpakpaala ki go paagi bi pala ban fidi ki kuo bi tinmu nni ti tiidi ki baa ti ñuadi laa yabi. Line cogu kuli taanma pia li mayuli mu dobimu kpakpaala po leni mi bancianma danba mo po leni li ñandunli kuli tingbangu bonpiakaala kuli po.



Contents

Acknowledgements	vi
Abstract	viii
Résumé	ix
Mi mayutaanma	x
Chapter 1 Introduction	5
1.1 Ecohydrology for Agriculture.....	5
1.2 Chosen Approach	6
1.3 Community Participation.....	7
1.4 Interview Methods	7
1.5 Introduction to <i>Sclerocarya birrea</i>	9
1.6 Results from Interviews.....	10
1.7 Study Site.....	11
1.8 Overview	14
1.9 References.....	15
Chapter 2 Observation of Sensible and Latent Heat Fluxes Over a Mixed Savanna-Agricultural Catchment	18
2.1 Introduction.....	18
2.2 Methods	20
2.2.1 Geographical Context	20
2.2.2 Equipment set-up	21
2.2.3 Eddy - Covariance.....	22
2.2.4 Data Preparation and Correction.....	22
2.2.5 Ground Heat Flux	23
2.2.6 Additional Data	23
2.3 Results	23
2.3.1 Seasonal Changes in Coupled Hydrologic and Energy Balances	23
2.3.2 Energy Balance Comparison	26

2.3.3	Ground Heat Flux	27
2.3.4	Fluxes by wind sector	30
2.4	Discussion	31
2.4.1	Summary of our data	31
2.4.2	Comparison with regional data	32
2.4.3	Relation to plant growth	33
2.4.4	Timing of Peaks	33
2.4.5	State of Flux Measurement Regionally	33
2.5	Conclusion	34
2.6	References	34
Chapter 3	Calculation of The Energy Balance Using a Distributed Network of Sensors	38
3.1	Introduction	38
3.2	Methods	40
3.2.1	Study Site	40
3.2.2	Measurement of Evaporation	42
3.2.3	Ground Heat Flux and Albedo	42
3.2.4	Radiation	43
3.2.5	Roughness length	44
3.2.6	Monin-Obukhov Theory	46
3.2.7	Analysis of variance	48
3.3	Results	48
3.3.1	Energy budget	48
3.3.2	Roughness length	51
3.3.3	Albedo	52
3.3.4	Conversion to Ground Heat Flux	53
3.3.5	Net Radiation	55
3.3.6	Latent Heat Flux	56
3.4	Discussions & Conclusions	57
3.4.1	References	58
Chapter 4	Evaporative Fraction Influenced By Land Surface Controls	59
4.1	Introduction	59
4.2	Methods	61
4.2.1	Evaporative Fraction	61
4.2.2	Cloud Cover Calculation	62
4.2.3	Soil Moisture	63
4.2.4	Vegetation Index	63
4.3	Results	64

4.4	Discussion and Conclusions	68
4.5	References	69
Chapter 5	Soil Water Balance Under agroforestry trees indicate spatial heterogeneity	70
5.1	Introduction.....	70
5.1.1	Problem.....	70
5.1.2	Agroforestry.....	71
5.1.3	Objectives	72
5.2	Methods	73
5.2.1	Site Description.....	73
5.2.2	Species Choice.....	74
5.2.3	Measurements	76
5.3	Results	77
5.4	Discussion.....	81
5.5	Social Perspective.....	83
5.6	Conclusions.....	84
5.7	References.....	85
Chapter 6	Detection of seasonal leaf out and groundwater recharge with stable isotopes of water	89
6.1	Introduction.....	89
6.1.1	Open question of agroforestry's benefit	89
6.1.2	Review of Stable Isotopes in Water	89
6.1.3	Monitoring of Stable Isotopes in West Africa	90
6.1.4	Stable Isotopes are useful tracers to understand plant water use	90
6.1.5	Research goals	91
6.1.6	Sampling and Measurement.....	91
6.1.7	Sampling, Extraction	92
6.1.8	Cavity Ring Down Spectroscopy.....	92
6.1.9	Sap flow	93
6.1.10	Additional Measurements	93
6.1.11	Canopy Shading.....	93
6.2	Results	94
6.3	Discussion.....	108
6.3.1	Enrichment.....	108
6.3.2	Water Storage.....	109
6.3.3	Root groundwater access	109
6.3.4	Monsoon Effect.....	110
6.3.5	Innovative tool.....	110
6.3.6	Indicators	110

6.4	Conclusions.....	111
6.5	References.....	111
Chapter 7	Conclusion	113
7.1	Current Research.....	113
7.2	Future Research	114
7.2.1	Improved Technologies and Use of Equipment	114
Postface: Lessons Learned		116
	Looking forward.....	116
	Personal Story.....	118
Appendices.....		120
Appendix I.	Species Inventory.....	120
Appendix II.	Sensorscope Station Inventory.....	121
Appendix III.	Calculation of the Hydraulic Properties of Soils	125
	Reference	127
Appendix IV.	Wireless Sensor Networks.....	127
	References.....	128

Chapter 1 Introduction

When Wangari Maathai accepted the Nobel Peace Prize in 2004 for her work with the Green Belt Movement, she described how women in villages in Kenya are no longer able to meet their basic needs because of the degradation of their immediate environment and the expansion of commercial agriculture. She planted trees to not only restore degraded farms but also to educate and empower the women and communities surrounding them. An effort to guarantee the food and water for future generations through more careful resource management and restoration emerged from her efforts and, less expectedly, previously excluded women demanded democracy from their governments. She concluded her Nobel acceptance speech by evoking an image of a stream next to her childhood home that no longer flows but once flowed generously and sheltered entire ecosystems. In her biography, she attributes this stream's clarity and continuity to a fig tree that cultural practices forbade cutting (Maathai, 2006). However, as times changed, the cultural practices were disrespected and the natural environment correspondingly degraded.

The image of Wangari Maathai's idyllic childhood village is powerful because it evokes an ancient concept of interdependence between components of the environment and cultural practices. This image makes it clear that though environmental degradation may have initially targeted vegetation, for example the cutting of a tree, or the conversion of small farms for industrial agriculture, it eventually impacts many other ecosystem services, such as the provision of water, and eventually the quality of life of the villagers. This concept of the interrelationships between vegetation and hydrologic processes is by no means a new one, however it has only recently been articulated as such by science.

1.1 Ecohydrology for Agriculture

Ingram (1987) was perhaps one of the first scientists to use the term *ecohydrology* prominently to explain the methods by which acrotelm in a Scottish peat land regulates the water flow between the soil and atmosphere. The term was then adopted by the integrated water resources management community to refer to management of freshwater ecosystems coupled with the management of the water resources, emphasizing the application of coupling hydraulic and biological resource management (Zalewski et al., 1997). And when Malin Falkenmark and Johan Rockström titled their book *Balancing Water for Humans and Nature: The New Approach in Ecohydrology* (2004), they emphasized the use of this holistic approach for managing terrestrial and aquatic resources together, but this time with an articulated value for the sustainability of human use.

However, when Rodriguez-Iturbe (2000) brought the term into the environmental engineering community in his "vision for the future", he focused on the study of the hydrologic mechanisms that underlie the ecologic patterns and processes, specifically the climate-soil-vegetation dynamics. He discussed the need to use a quantitative scientific basis to understand the dynamics of biomes. He emphasized soil moisture as the intermediary between hydrologic and biologic processes, both above and below ground as well as their stochastic and fluctuating patterns. Thus he opened a theoretical line of inquiry that focused mainly on natural systems, fairly distinct from the evolving applied field. Subsequently, much of this line of research has focused on the ecohydrology of dryland and semi-arid systems because in these ecosystems, water is so essential and drives the system (D'Odorico and Porporato, 2006). As Parlange and Rinaldo (2012) explained, ecohydrology is a field on the move, transcending boundaries of

any single discipline. It focuses on the feedbacks that emerge from the interactions between hydrologic processes and ecosystems, and is not isolated from anthropogenic influence.

Ecohydrology is a particularly timely tool for West Africa. It offers a theoretical framework, in a sense, a disciplinary framework, permitting us to move beyond any single discipline, and any single scale or approach, and to find solutions to urgent environmental problems by thinking about interrelationships between elements of our environment. In the past rainy season, over 6712 people in Burkina Faso alone have been affected by flooding, and that number is much higher in the neighboring countries of Niger, Nigeria, Benin, and Senegal (Reliefweb, 2013a). Simultaneously, there is a “Sahel Crises” caused by the converging consequences of a food shortage, erosion of food security, and ramifications of political instability only some of which are directly environmentally related (Reliefweb, 2013b). Although an indicator like child mortality does not respond directly to climatic indicators, like precipitation variation, there are many interrelated factors that link human life security with climate including type of farming and vegetation cover in the immediate environment (Henry and Dos Santos, 2013). Thus, ecohydrology is well suited to both address the complicated relationships between land cover and hydrology in this dry-land ecosystem given the human dependence on those relationships and the need to find applied solutions to natural resource management challenges.

Due to anthropogenic changes to the global environment, the global climate is undergoing significant changes. Although few of the original causes are in West Africa, the region is predicted to experience the consequences, and with a population mainly dependent on rainfed agriculture, more than elsewhere. Rainfall in West Africa is predicted to become much more variable (Nicholson, 1993, 2013). Simultaneously, human populations are growing and migrating, and industrial agriculture is becoming more widespread. Flooding is an extreme response to a rainfall – runoff process that is also mediated by the vegetative cover (Séguis et al., 2011). Changing precipitation patterns will result in more extremes in flooding and in less adaptive agriculture (Zorom et al., 2013; Cooper et al., 2008).

Local populations are extremely aware of these challenges and these changes, but often are unaware of appropriate adaptations that would increase their resilience. As William G. Moseley said, in the *Good Governance of Africa* (2012), food insecurity is not going to be solved by increasing production or expanding large agribusinesses, but rather must introduce low-cost, sustainable enhancement to farming including agroforestry and mixed cropping that the poorest can access. Additionally, mitigating the hydrologic consequences of changing land cover and climate will most effectively be addressed at a scale that incorporates consequences for different parts of a water basin and global economy, based on who has the largest impact and ability to adapt (Falkenmark, 2013). Science has an important role to play, first to document and understand the processes, and second to predict and support the political processes. In addition, new technologies can provide direct access to information, for example cell phones connected by wireless to a database communicating with soil moisture sensors can give real time alerts to farmers when urgent irrigation is needed (Knoche et al., 2010).

1.2 Chosen Approach

To address these problems, we take an ecohydrologic approach to examine the exchanges between vegetation and hydrology in a quantitatively rigorous way but one that still leaves room for the human context and applied solutions for the bottom of the pyramid farmers. We examine two general aspects of farming practices in the village of Tambarga (Commune de Madjoari, Burkina Faso) – varying adjacent land uses and agroforestry.

First, the farms where we are focused are situated around a small ephemeral stream surrounded by a rocky escarpment with a natural Sudanian savanna growing on it and a forested corridor at the stream’s origin. This represents a practice of mixing farmland, fallow land, savanna, and gallery forests in an immediate vicinity that maintains the local landscape diversity and

presents an interesting opportunity to study the variations and interrelationships between different-land cover types. The first three chapters (2 to 4) of this thesis focus on the variations in hydrologic exchanges over different land-covers.

Second, agroforestry is widely practiced in this village. Understanding water use by agroforestry trees in dry-land ecosystems is essential for improving water management. Agroforestry trees are valued and promoted for many of their ecologic and economic benefits but are often criticized as competing for valuable water resources. The next two chapters (5 and 6) use different tools to examine *Sclerocarya birrea* agroforestry. The postface focuses on human dimensions to these questions. Throughout all five chapters, we ask what is the role of the vegetation in the water-soil-atmosphere transfer. We do this using several scales and tools, and eventually make observations that are more directly useful to local farmers.

1.3 Community Participation

This project began with an interdisciplinary team that brought together cutting edge information technology (wireless sensor networks) with environmental scientists and engineers from hydrology, social sciences, and micrometeorology. The overarching hope of this project is that the new technologies can empower rural landholders to have direct contact with the data and make autonomous decisions regarding farming, land, and water management. In addition this project began not only with an academic agenda and academic players, but was initially launched with a participatory mapping workshop where stakeholders from the entire catchment discussed and diagrammed various environmental challenges, opportunities, and conflicts on top of aerial satellite images of the river basin shown in Figure 1-1. Focus groups at the workshop used satellite images printed at a large scale as a tool to discuss natural resource management conflicts and knowledge that could guide the research directions. Of particular interest to this specific research was the knowledge supplied by a few of the elders present in regards to variation between species of agroforestry trees in terms of soil moisture conservation. Additionally, they provided a certain historical context for how vegetation patterns have changed over time. These discussions guided both the placement of the instrumentation for intensive study and the choice of species of *Sclerocarya birrea*. The location was chosen both because of the input of the participants present and the topography which could be used to define a catchment, and the species was chosen because of both its local abundance in the focus watershed and the mention of it as a species valued for its soil moisture retention beyond the rainy season. Upon completion, results and implications will be presented to the community and have the opportunity to improve use of agroforestry for water and land management.

In addition, the scientific study was bracketed by a set of interviews that assessed the importance of *Sclerocarya birrea* to the local community, the local perception of climate change, the local history and development of land use, the traditional knowledge of farming and rain prediction and influencing practices, the local technological needs, and local perception of current development, specifically over the time period of the project. The goal of these interviews was to understand the local community's perspective on the scientific questions, basis, and propositions of our research project. By framing the project within two different organized dialogues with the village, we are able to make conclusions of the social importance and potential impact of this research.

1.4 Interview Methods

In 2009, 100 people were interviewed in two cycles of interviews, a first round in the fields and the second in homes, in the three villages of Madjoari, Matambima, and Tambarga. In 2010 21 people were interviewed in their homes, mostly older than 50 years old, including only 5 women, and 3 Peulhs – or members of the greater Fulani ethnic group who are responsible for cow-herding (Bordes, 2010). Interviews were conducted one on one with the help of a translator and covered 6 subjects: Importance of *Sclerocarya birrea*, climate change, land use history, data and technology needs and information, development of the village, and traditional knowledge of farming and rain prediction and bringing systems. All interviews took place in the village of Tambarga

Results of Participatory Mapping Workshop of Singou River Basin Burkina Faso, August 2008

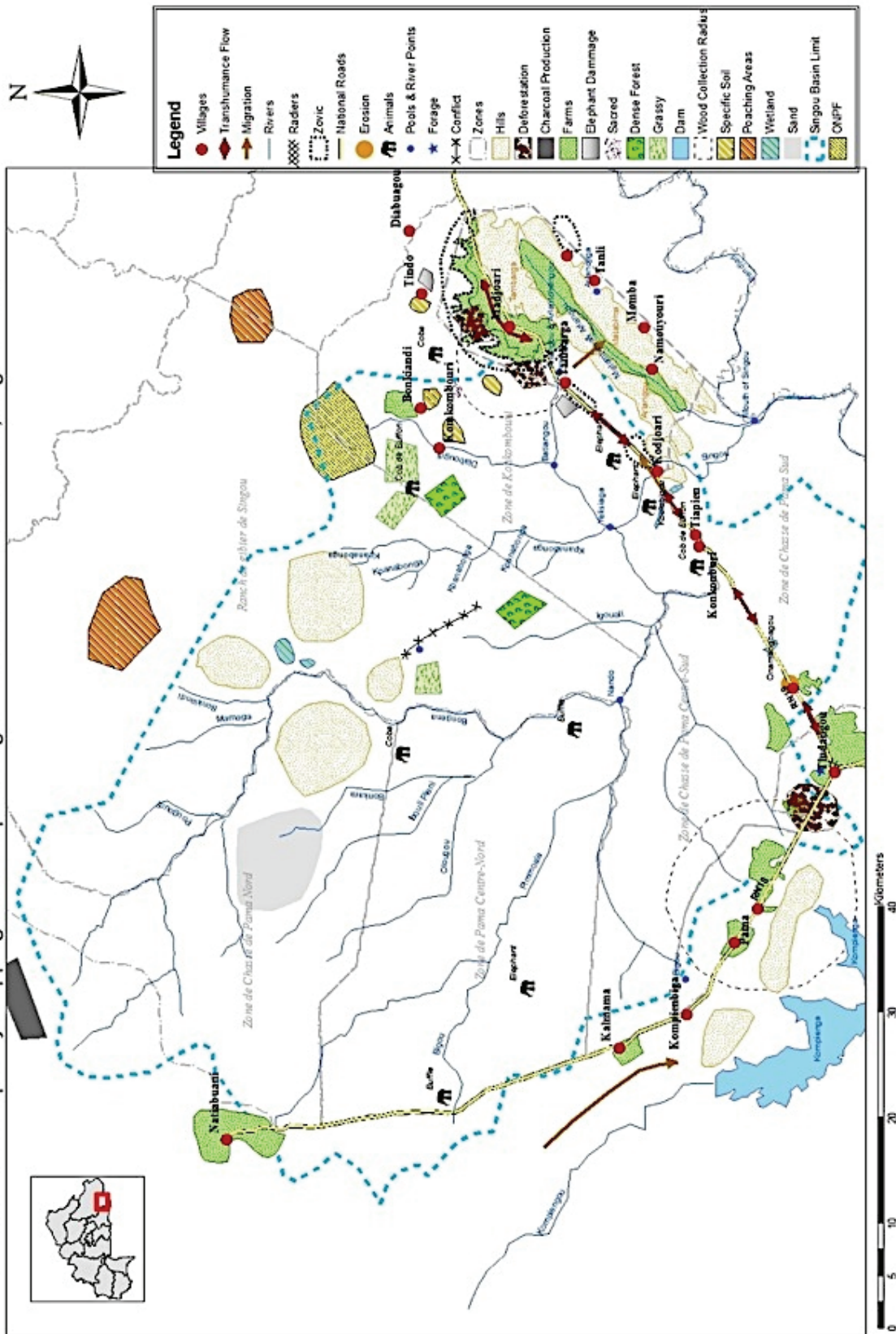


Figure 1-1 Map of Singou River Basin showing the results of the initial participatory mapping workshop. In the original workshop, participants were split into four small groups: Forest, Water, Urban, and Land Use; and asked to draw on Landsat satellite images according to the theme. The drawings from these issues were compiled in this map. Notes the local names for waterways, the different land use categories, places of animal observations, and the sites of high activity. This mapping activity provided an opportunity for learning by both the researchers and the participants. These discussions guided our site choice and research direction.

or the neighboring Peuhl camps. In addition, a baseline vegetation inventory was completed by identifying all species in plots of 50 square meters in the upper and lower parts of the catchment.

1.5 Introduction to *Sclerocarya birrea*

Namagili Namagili // The seeds of Marula, The seeds of Marula
Em pani ni ba mi ño // Give me your milk so I can nurse
Sa buenleni kankanli // When I get a new baby
Yin pu ni mi bima mi ñew // I will give you some milk and you will drink
Namagili namagili pani mi biima min no // The seeds of Marula give your milk to me
 [Song sung in Tambarga, Burkina Faso in the old times – *Bwaba Tchombiano*]

Sclerocarya birrea is wide spread throughout the semi-arid savannas of West, East, and Southern Africa. It is well established which services the *Sclerocarya birrea* tree provides. Throughout its range, it is considered valuable for food, medicine, and occasionally for its contribution to agroforestry. It is known by many names: *Prunier* (French); *Marula* (English); *Gna, kuna, kunan, n'guna* (Bambara); *Dania* (Hausa); *Bunamagabu, noabega, noabegha, nobega* (Moore); *Beri, edi, eri, hedehi, hedi, kede, eedy, dri, kede, ddeh* (Peulh/Fulani); *Ari(k)* (Serer); *Tauila'h, touhila* (Tamachek); *Ber, birr* (Wolof); *Unle* (Bomo); *Bin* (Dogon); *Luley, diney, moru-moru* (Dendi); *Bunamagbu, bunamashiabu* (female), *bunamangjabu* (male), *bu namagbu, namabu* (Gourmantche); *Ubamingbu* (M'berme); *Dambahabu, damakharu, damarkarbu* (Warma); *Namuak* (Berba); *Kutan dao* (Soce); And *manyi* (Bariba) (DeSouzo, 2008; Maydel, 1986; Smith, 2010; Gouwakinnou, 2011a; Gonzalez, 2001; Lykke, 2000; Glew, 2004)

The *Sclerocarya birrea* fruit is nutritious, in particular the nut offers a high level of rare fatty acids (Ogbobe, 1992; Glew, 2004); it has commercial value as a non-timber forest product in southern Africa (Wynberg et al., 2002); It has also demonstrated medicinal value such as antibacterial properties (Eloff, 2001; Moyo et al., 2010) and a hypoglycemic effect (Ojewole 2003). There is some evidence to show that it can increase the arbuscular mycorrhizal fungi presence when intercropped with millet or corn (Muok et al., 2009), which is useful for the mobilization of nutrients. Attempts to domesticate the tree have begun in Southern Africa (Leakey et al., 2005, Leakey, 2005). However, it currently remains under used in West Africa (Gouwakinnou, 2011a), compared to Southern Africa where the sale of beer brewed from its fruit has now become common (Shackleton, 2004; Verlinden and Dayot, 2005; Plessis et al., 2002) and valued at 0.03 to 1.40 USD per kg of fruit (Shackleton, 1996). As far north as the Ferlo of Northern Senegal it is valued for the contribution to the diet of its nuts and is encouraged in the fields (Becker, 1983). In Mali, the frequency of the tree has been observed to have significantly decreased, although it is valued for its wood, fruits, nuts, and alcohol production in Bwa and Dogon communities (Smith, 2010). *Sclerocarya birrea* was preferred as fodder by goats in particular but also by sheep and cattle in the Sahelian zone of Burkina Faso (Sanon et al., 2007). In Niger, it is valued for its nutrition, shade, wind buffering, and fertilization (Wezel and Haigis, 1999). In Benin, it is valued for both food and medicine (Assogbadjo et al., 2011). Similarly, in Zambia and Cameroon, it is particularly valued for its fruit (Sileshi et al., 2007; Wassouni 2006).

It is usually present in open farmlands or natural savanna, but can be used as live fences and thus be present near residences. Saplings emerge in fallow fields but it is rare in flooded areas. It has a higher presence in agricultural parklands (74 %) than in the natural Sudanian vegetation (30 %) in Northern Benin. People agree that its presence has declined in recent times (98% in Northern Benin) due to agricultural, human use, grazing, decreasing soil fertility, natural death, and drought (Gouwakinnou et al., 2011b). It is considered a multi-use tree with the bark used as medicine to treat bacterial infections (stomach ache, diarrhea, wounds, and coughs). The nuts were consistently used as a food. The use of the wood for carving and the juice of the fruit for alcohol production are rarely practiced presently but were in the past. Leaves and fruit can also be eaten directly or in cooking. *Sclerocarya birrea* is a sexual dimorphic species, which is recognized by over half of local people, but this does not affect its spatial distribution in northern Benin (Gouwakinnou, 2011b), but is a determinant for selection near human settlements in northern Namibia (Nghitoolwa, 2003).

In Northern Burkina Faso, it is the 5th most common woody species present in the fields of farmers in Dangadé and Katchari and tied for 5th in Sambona (Leenders et al., 2005). It is considered to decrease the amount of sand deposited in fields and does not have a significant effect on erosion, however it is valued for its fodder and food provision primarily, and secondarily for its medicinal and domestic uses (Leenders et al., 2005). *Sclerocarya birrea* has been shown to store water for the entire dry season in order to produce early leaves when rainy season onset is delayed (Kulmatiski et al., 2010).

However, in the site of Tambarga, Burkina Faso there exists some ambivalence or contradiction in its perceived importance as determined by three rounds of interviews; a participatory workshop at the start, intensive interviewing about agroforestry practices in June - August 2009, and rapid one-on-one interviews focused on *Sclerocarya birrea* in September and October 2010. In addition, throughout the duration, observations continued as researchers were continually present in the site or in contact with community members. Parallel to the research project, out-reach activities, specifically a youth center and botanical garden, involved the residents of Tambarga.

1.6 Results from Interviews

In 2009 people reported that the fruit of *Sclerocarya birrea* is edible, especially liked by children and animals, who eat the leaves, and the bark and leaves are important for medicine. Children like the fruits more than adults, and even the inner nut is edible. Farming under the tree's canopy will not be productive, it does not maintain the humidity, the roots are on the surface, the branches break easily, the bark is not fire resistant, it keeps its leaves into the dry season, and the seeds germinate easily. Some say wind and fire have caused a decline in the population (55%), others say that it has increased (36%), and a single respondent said that the population has not changed.

Interviews that focused on *Sclerocarya birrea* in 2010 found that above all it is valued for its fruit, which children and animals eat (cited by 76%). The nut inside can be extracted and eaten (as reported by 38% of people) particularly by elders (10%) and young children (10%) who used to sell it in small cans for 25 cents but no longer do because of school. The nut also contains oil that can be extracted. Since it is most frequently eaten by domestic animals, it is defecated near villages by domestic animals, which leads to the tree seeming to "follow" human settlements - growing at former village sites (14%). The fruit can also be turned into a juice called *anamargha*, which once was used by young girls to make a pretend "dolo" or local beer that they would offer to young men that they are interested in (24%). The bark and root can heal children (33%), particularly red eye, diseases of the anus, diarrhea including dysentery (24%), and the leaves can be used to wash children (14%). The tree can also be used to make a medicine to treat fainting, dizziness, and fever (19%), a hurt leg, broken bone, jaundice, a stomach ache (24%), cough (25%), yellow fever, toothache, hemorrhoids (14%), itching, wounds (29%), and similar ailments in animals. The tree should be left growing in fields for use as medicine (10%). Its wood is good for cooking (29%), especially for preparing *dolo* because of its large flame.

Some say that it is not good for building, but others use it to build hangers to sit under (10%), and say that the wood can be sold (10%). Branches are also good to make whips for discipline. *Sclerocarya birrea* often grows next to fields, though some people say it gives too much shade (5%). However a majority of people (76%) believe that this species indicates a nearby water source and that the roots actively maintain and attract moisture, particularly where there are young plants. Elders recommend digging wells close to this tree since it grows where it does because of water (10%). One person pointed out that *Lannea sp.* and *Vitellaria sp.* bring more humidity. The leaves can increase soil nutrients by decomposing (71%), it is sensitive to fire, only grows near the hills (10%), pretty, and monkeys and birds like it. More people agreed that it provides valuable shade for animals and people to rest under (48%), especially during funerals, it breaks the wind (14%), provides fodder for animals (52%), and some people pointed out that since the leaves last for a long time without decomposing, the nutrients are minimal (19%). The leaves are produced early in the season, which is good for forage for animals, and the fruit appears when the guinea fowl should lay eggs, so some bring home fruits

to give to the poultry to motivate them to lay eggs. The leaves mixed with salt, makes an animal feed that is good for increasing milk production in livestock. It cannot grow high on the hill since it can only grows close to where there is water (14%), and more people think that it will lessen erosion by slowing the water and increasing infiltration (33%). Soy, pepper, and tomatoes can be grown under its canopy.

It can grow anywhere, does not have special needs, some claim that it does not keep the humidity or lessen erosion because of the small leaves and has to be cleared for new fields. There are lots in the wild lands, but many people say that it is not a true “*brousse*” if you find *Sclerocarya birrea*, but rather the site of a former village (62%). It is deciduous, and according to some, this helps maintain the humidity, and thus stays cool and moist in the hot season (29%). It traps rain, particularly if there are lots of trees, they will be able to break up the clouds and bring rain (29%). These trees are disappearing because people cut them from fields (19%), and have gotten old and died (48%), but once there were more in the village (10%). In the bush, elephants have destroyed many trees (10%). Some think that the name means that it will heal, other thinks it means “nuts of the cow” since the cows eat the fruit (10%). Some claim a genie lives in the tree, which is why it makes so much noise (14%), it is also used for the circumcision ritual, and others say there is bad luck when you walk across the roots, but other say there is no magic and no story associated (19%). Some people say that this tree comes on its own and does not need to be planted, but others advocate planting and caring for them since people are cutting and burning more now. The tree may have come from Niger, and it may have no commercial value (19%), or only is worthwhile if you heal someone with its products (19%).



Figure 1-2. From left to right: *Sclerocarya birrea* in an agroforestry context. Experimental garden for knowledge transfer. Sensorscope wireless sensor network meteorological station. Use of *Sclerocarya birrea* agroforestry system by livestock for fodder.

1.7 Study Site

The study site is located in a catchment defined by an ephemeral stream (figure 1-3) and framed by a rocky catchment. It is located near the village of Tambarga, in the Commune of Madjoari, in South Eastern Burkina Faso in West Africa. The stream flows into the Volta Water Basin that occupies much of the countries of Burkina Faso and Ghana. The study catchment is a small part of the Singou basin that is about 50 km². It is in the Sudanian vegetation type characterized by an open savanna. The study site is surrounded by hunting concessions and national parks, so it often seems to be an inhabited island inside of an area with relatively dense vegetation and abundant animals. The village of Tambarga neighbors our catchment. It homes between 2500-5000 people depending on the season. It is accessible by dirt road for part of the year.

The study catchment spans a number of different land uses in its 3.5 km². The open savanna on top of the rocky escarpment and the rain fed millet or cornfields are the dominant land cover. There is also a denser, gallery forest in the valley formed by the escarpment where there are perennial springs. Near the measured outlet of the stream, there is an ephemeral wetland that is used for rice cultivation. The escarpment is about 100 meters higher than the fields, but there are also rocky points that reach higher than this to 550 meters. In each chapter, I will present the relevant aspects of the study site. All chapters take place in the same site, however the map that follows is meant to guide you through the entire document. More detail regarding various aspects of the study site will be in each chapter. Appendices I-III contain species list, soil types, and photographs.

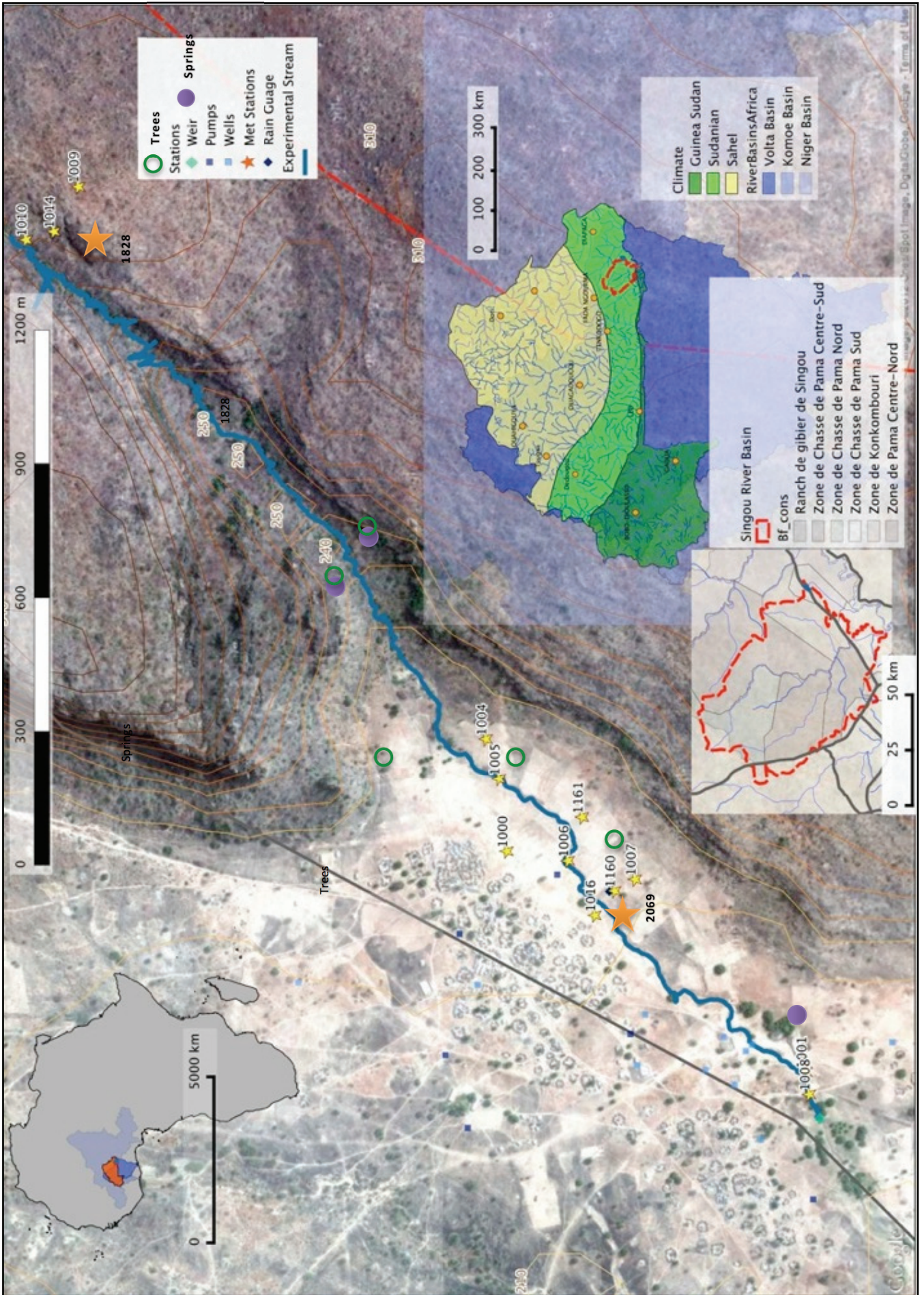


Figure 1-3 shows the position of the experimental catchment over a geoeye image from January 2010. The ephemeral stream is the blue line and the research equipment is indicated by the symbols corresponding to the legend. In the upper left, is a positioning of Burkina Faso (red) in the African continent (grey) laid over the three water basins in Burkina Faso: Niger, Volta, and Komoe. Our site is located in Burkina Faso (red) and the Volta catchment (darkest blue). In the lower right is a positioning of the greater Singou basin (dotted red) in the country of Burkina Faso (outline), all the river ways in Burkina Faso (blue lines), and the 3 major vegetation types: Sahel (yellow), Sudanian (bright green), and Guinean Sudanian (dark green). Also visible in the background are the blue outlines of the water basins. Our site is in the Sudanian (bright green zone) characterized by open savanna and is a subcatchment in the greater Singou Catchment. In the lower center map is a sketch of the hunting concessions and natural parks surrounding the Singou Basin. Our subcatchment is a tiny blue streak and is essentially an island in a sea of hunting concessions. Finally our experimental catchment is the major frame. Individual houses of the village of Tambarga are visible in this image as is the general land cover type. Agricultural areas appear mostly white in this image, although if they were recently burned, they are black. Some trees are still green but most open savanna is reddish. The ephemeral stream is in blue. Sensorscope stations (Appendix Iv) are marked with a yellow star and their initial number and isotope sampling sites are labeled as well with various symbols. Met stations are orange stars and springs are purple circles. Stream outlet is shown with a green diamond labeled weir. Topographic lines show the elevation change (210 to 310 m). Also visible are the national roads and the river. Below are some photographs of and from the hill that gave the village its name.



1.8 Overview

This thesis includes five chapters in addition to a more personal postface. All research took place in a single village, Tambarga, in the community of Madjoari in the Gourma Region of South West Burkina Faso. Most research took place in the “experimental catchment” defined by a small ephemeral stream. This stream flows into the Singou River, which flows into the Pendjari River, which flows into the White Volta that eventually joins the main Volta which discharges into the Atlantic Ocean in Ghana. The natural vegetation is in White’s category of Sudanian (1986). However, this is a bit misleading, because Sudanian areas can include vegetation that is usually considered Guinean in the humid pockets as well as areas that could nearly be Sahelian where there is less access to moisture. Our site is primarily Sudanian open wooded savanna, however there is a gallery forest with characteristic Guinean vegetation and there is a small patch that has trees usually only found in Sahelian climates. A species list of the majority of woody vegetation is in the Appendix I. In addition, vegetation varies according to use. A large part of the catchment is farmed and another part is grazed. Only a small area is relatively undisturbed. In addition, the site is located in an area primarily occupied by hunting concessions and national parks. It is one of the few areas open to human use and consequently, in addition to the farming communities, is home to herds of cattle and their nomadic drivers twice a year when they move from their dry season pastures to their rainy season homes and vice versa. The location also reveals some of the local livelihood history. People originally inhabited this area for the game resources but since hunting has become regulated, they rely predominately on rain fed agriculture.

Each chapter addresses the question of seasonal variations in the soil – vegetation – atmosphere hydrologic transfer process and how we study and apply understanding of it at a different scale and using a new technology or system. In most cases, an aspect of the technology is new for this part of the world and for this application.

Chapter	Spatial Scale	Technology / Innovation	Soil – Vegetation - Atmosphere
2	2 patches	Eddy correlation	(s-v) – <u>Atmosphere</u>
3	Distributed network of 12 points	Wireless sensor network of meteorological stations	(v) - <u>Atmosphere</u>
4	3.5 km ² catchment	Evaporative Fraction - Satellite	(s-v) – <u>Atmosphere</u>
5	Tree – crop comparison	Simple soil moisture model	(h) -> <u>Soil Moisture</u> – (v – a)
6	1-5 agroforestry trees	Stable isotopes – sap flow – canopy shading	(s) – <u>Vegetation</u> – (a)
Postface	Global research-development	Cooperation for science	<u>Human</u> -> (s-v-a)

Table 1-1. This thesis presents analyses at different spatial scales, using different technologies, and different components of the soil-vegetation-atmosphere transfer of humidity and interaction with humanity.

In Table 1-1, I present the 5 chapters in terms of the variations in scale, technology, and interest on the soil vegetation atmosphere transfer and related to humanity. The postface examines our project in the context of the research development discourse that motivated it, instead of just the results from inside. Clearly, a holistic approach to this research was essential and it was dependent on interdisciplinary collaborations and exchanges. Figure 1-3 demonstrates the multiplicity of interrelationships between the chapters and between the different flow pathways. We cannot consider one without the whole.

In general, we use a distributed sensor network of sixteen wireless meteorological stations including soil moisture sensors in addition to two eddy covariance stations and sap flow probes to understand land cover controls on variations in evapotranspiration and infiltration over a semi-arid watershed in Southeastern Burkina Faso. Our equipment was dispersed across cultivated rice and millet fields, natural savanna, fallow fields, and around agroforestry trees, specifically *Sclerocarya birrea*. Normalized difference vegetation indexes taken from weekly MODIS images as well as personal field observations and photographs were used to inform seasonal and spatial variations in albedo, ground heat flux, and roughness length. Samples from rain, ground, surface, soil, and xylem water were collected for analysis of isotopic δO_{18} and $\delta D H$ fractions, and ground water, stream temperature, and discharge

were monitored. Finally, interviews with the local community were conducted towards the beginning, middle, and end of the intensive research. In each chapter, I will address the methods in more detail.

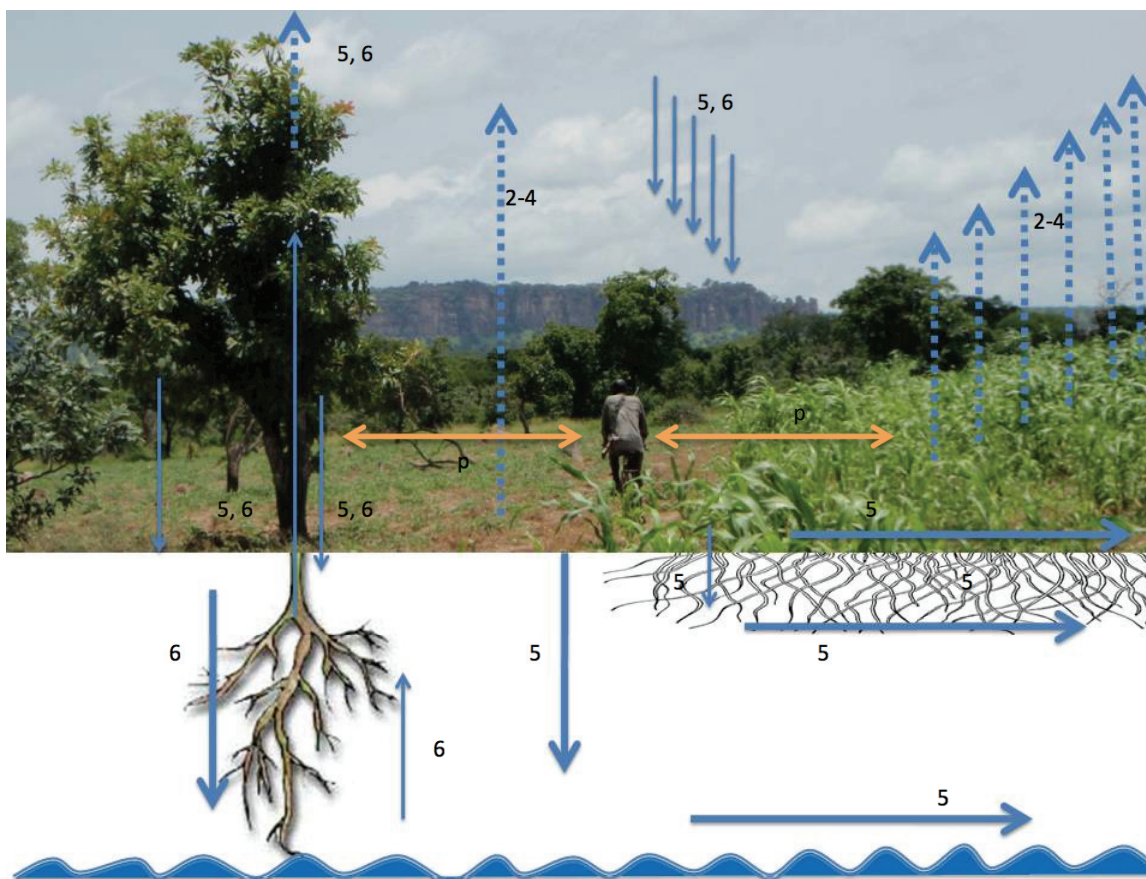


Figure 1-3. This is an overview illustration of the different processes of interest to me. Numbers correspond to the relevant chapter. Blue arrows represent flows of water and orange arrows represent flows of tangible and non-tangible benefit in terms of livelihood.

In this thesis I will identify basin level exchanges of energy and moisture, their spatial variability, and test simple models to predict them. I will improve understanding of the role of a single tree in storing and retrieving soil moisture and the pattern of “wet up” and “dry down”. I will conceptualize the energetic and hydrologic consequences of local conversion to agriculture. And finally, I will contribute to improved environmental and agricultural management.

Wangari Maathai said in 2004 when she accepted her Nobel prize, that “we are faced with a challenge that calls for a shift in our thinking so that humanity stops threatening its life support system. We are called to assist the earth to heal her wounds. And in the process, heal our own...In the course of history there comes a time when humanity is called to shift to a new level of consciousness”. I hope that the results from this work will contribute to our understanding of how to make farms in some of the most precarious ecosystems in this planet while minimizing the irreversible, long-term consequences. This is a first step to improving understanding of the vegetative controls on the hydrologic exchanges with the soil and the atmosphere.

1.9 References

Assogbadjo, A. E., Glèlè Kakaï, R., Vodouhê, F. G., Djagoun, C. A. M. S., Codjia, J. T. C., & Sinsin, B. (2011). Biodiversity and socioeconomic factors supporting farmers' choice of wild edible trees in the agroforestry systems of Benin (West Africa). *Forest Policy and Economics*. Elsevier B.V.

- Becker, B. (1983). The contribution of wild plants to human nutrition in the Ferlo (Northern Senegal) Members of four ethnic groups live in the Ferlo : Peulhs , Wolofs , Moors and. *Agroforestry Systems*, 257-267.
- Bordes, C. (2010). La Gestion Des Arbres Par Les Paysans: Etude d'une enclave au milieu de reserves forestieres au sud-est du Burkina Faso. ISTOM. ISTOM.
- DeSouzo, S. (2008). La flore du Benin: 3rd Edition. Paris, France.
- Eloff, J. N. (2001). Antibacterial activity of Marula (*Sclerocarya birrea* (Anacardiaceae) bark and leaves. *Journal of Ethnopharmacology*, 76, 305- 308.
- Glew, R. S., Vanderjagt, D. J., Huang, Y., Chuang, L., Bosse, R., & Glew, R. H. (2004). Nutritional analysis of the edible pit of *Sclerocarya birrea* in the Republic of Niger (daniya, Hausa). *Journal of Food Composition and Analysis*, 17, 99-111.
- Gonzalez, P. (2001). Desertification and a shift of forest species in the West African Sahel. *Climate Research*, 17, 217-228.
- Gouwakinnou, Gerard N, Lykke, A. M., Assogbadjo, A. E., & Sinsin, B. (2011a). Local knowledge, pattern and diversity of use of *Sclerocarya birrea*. *Journal of ethnobiology and ethnomedicine*, 7(1), 8. BioMed Central Ltd.
- Gouwakinnou, Gerard Nounagnon, Lykke, A. M., Djossa, B. A., & Sinsin, B. (2011b). Folk perception of sexual dimorphism, sex ratio, and spatial repartition: implications for population dynamics of *Sclerocarya birrea* [(A. Rich) Hochst] populations in Benin, West Africa. *Agroforestry Systems*, 82(1), 25-35.
- Knoche, H., Rao, P.R.S., Huang, J., (2010). Voices in the field: A mobile phone based application to improve marginal farmers livelihoods. *MobileHCI*, September 7-10, Lisboa, Portugal.
- Kulmatiski, A., Beard, K. H., Verweij, R. J. T., & February, E. C. (2010). A depth-controlled tracer technique measures vertical, horizontal and temporal patterns of water use by trees and grasses in a subtropical savanna. *The New phytologist*, 188(1), 199-209.
- Leakey, R. (2005). Domestication potential of Marula (*Sclerocarya birrea* subsp . *caffra*) in South Africa and Namibia : 3 . Multiple trait selection. *Agroforestry Systems*, 51-59.
- Leakey, R., Pate, K., & Lombard, C. (2005). Domestication potential of Marula (*Sclerocarya birrea* subsp *caffra*) in South Africa and Namibia : 2 . Phenotypic variation in nut and kernel traits. *Agroforestry Systems*, 37-49.
- Leenders, J. K., Visser, S. M., & Stroosnijder, L. (2005). Farmers Perceptions of the Role of Scattered Vegetation in Wind Erosion Control on Arable Land in Burkina Faso. *Soil and Water*, 16, 327-337.
- Lykke, A. (2000). Local perceptions of vegetation change and priorities for conservation of woody-savanna vegetation in Senegal. *Journal of Environmental Management*, 59(2), 107-120.
- Maydell, H.-J. von. (1986). *Trees and Shrubs of the Sahel* (p. 525). Eschborn: GTZ.
- Moyo, M., Finnie, J. F., & Van Staden, J. (2011). Antimicrobial and cyclooxygenase enzyme inhibitory activities of *Sclerocarya birrea* and *Harpephyllum caffrum* (Anacardiaceae) plant extracts. *South African Journal of Botany*, 77(3), 592-597. Elsevier B.V.
- Muok, B. O., Matsumura, A., Ishii, T., & Odee, D. W. (2009). The effect of intercropping *Sclerocarya birrea* (A . Rich .) Hochst ., millet and corn in the presence of arbuscular mycorrhizal fungi. *Journal of Biotechnology*, 8(5), 807-812.
- Nghitoolwa, E., Hall, J. B., & Sinclair, F. L. (2003). Population status and gender imbalance of the marula tree , *Sclerocarya birrea* subsp . *caffra* in northern Namibia. *Agroforestry Systems*, (Goosen 1985), 289-294.
- Ogbobe, O. (1992). *Sclerocarya birrea*. *Plant Foods for Human Nutrition*, 201-206.
- Ojewole, J. A O. (2003). Hypoglycemic effect of *Sclerocarya birrea* [(A. Rich.) Hochst.] [Anacardiaceae] stem-bark aqueous extract in rats. *Phytomedicine : international journal of phytotherapy and phytopharmacology*, 10(8), 675-81. Retrieved from <http://www.ncbi.nlm.nih.gov/pubmed/14692729>
- Plessis, P., Lombard, C., & Adel, S. D. (2002). Marula In Namibia: Commercial Chain Analysis. *Forestry* (pp. 1-28).
- Sanon, H., Kaborezoungrana, C., & Ledin, I. (2007). Behaviour of goats, sheep and cattle and their selection of browse species on natural pasture in a Sahelian area. *Small Ruminant Research*, 67(1), 64-74.
- Shackleton, C. M. (1996). Potential Stimulation of Local Rural Economies by Harvesting Secondary Products: A Case Study of the Central Transvaal Lowveld, South Africa. *Ambio*, 25(1), 33-38.
- Shackleton, S. (2004). Livelihood benefits from the local level commercial- ization of savanna resources : a case study of the new and expanding trade in marula (*Sclerocarya birrea*) beer in Bushbuckridge , South Africa. *South African Journal Of Science*, (December), 651-657.
- Sileshi, G. W., Kuntashula, E., Matakala, P., & Nkunika, P. O. (2007). Farmers perceptions of tree mortality, pests and pest management practices in agroforestry in Malawi, Mozambique and Zambia. *Agroforestry Systems*, 72(2), 87-101.

- Smith, E. F. C. (2010). Local Knowledge of Natural Regeneration and Tree Management in Sahelian Parklands North of Tominian, Mali. North. University of London, Wye College.
- Verlinden, A., & Dayot, B. (2005). A comparison between indigenous environmental knowledge and a conventional vegetation analysis in north central Namibia. *Journal of Arid Environments*, 62(1), 143-175.
- Wassouni. (2006). Bushland in Mindif Region, Cameroon: Functions, Decline, Context and Prospects. Prospects. Leiden University.
- Wezel, A., & Haigis, J. (2000). Farmers Perception of Vegetation Changes in Semi-Arid Niger. *Land Degradation & Development*, 11, 523-534.
- Wynberg, R., Cribbins, J., Lombard, C., & Mander, M. (2002). Knowledge on *Sclerocarya birrea* subsp. *caffra* with emphasis on its importance as a non-timber forest product in South and southern Africa : A Summary. *Southern African Forestry Journal*, (196), 67-79.

Chapter 2 Observation of Sensible and Latent Heat Fluxes Over a Mixed Savanna-Agricultural Catchment

Evaporation and the surface energy balance over two land-cover types in Sudanian savanna were investigated in terms of seasonal and interannual variability using four years of eddy covariance measurements (2009-2013). The observations demonstrate the strong controls on evaporation by vegetation through modification of the surface roughness, albedo, and available moisture related to seasonal variations in land cover and topography. Two characteristic land uses of semi-arid West Africa (Burkina Faso) were monitored: agricultural fields and gallery forest. The sites receive around 800 mm of rain most years, typically between the months of May and October, with up to approximately 20% being transferred to runoff. Seasonal variation in all components of the energy balance was found to be greater over the agricultural landscape; the total latent energy flux over the gallery forest was higher by approximately 30%. Improved understanding of the variability of fluxes over diverse land cover will allow us to improve the estimation of evaporation to the atmosphere over the entire watershed.

2.1 Introduction

Quantification of the global hydrological cycle is dependent on balancing the energy budget around the world (Brutsaert, 1982; Parlange, 1995; Szilagyi and Parlange, 1999; Guyot et al., 2009). The latent heat is the energy that is transferred from the ground to the atmosphere when evaporation takes place and can be directly converted to the quantity of water evaporated. It is the shared term in the hydrologic and energetic cycles and is also the hardest to measure.

Monitoring, understanding, and predicting the interchanging global energy and water budgets have huge implications for our ability to model meteorological processes, make agricultural recommendations, predict droughts, ensure food security, manage freshwater resources, calculate appropriate withdrawals, and many other applications. It is no secret that as global climate change becomes more and more widespread each one of these applications will become even more crucial for humanity and biodiversity alike. Furthermore, understanding the variability in the hydrologic cycle and predicting how it will be affected by changes in the global atmosphere and land surface depend on comprehension of the relationship between land surfaces and atmospheric processes (Timouk et al., 2009; Siqueira et al., 2009). Specifically, each land cover type in each climate present on our planet needs be systematically studied. Currently, certain regions of the world are under represented among measurements, and consequently, less well understood. Africa, as whole, homes significantly fewer long-term meteorological stations than any other continent; and in particular, only a fraction of those are situated in West Africa (Timouk et al., 2009).

Despite the lack of monitoring, one could argue that West Africa is among the most important places to monitor fluxes (Bagayoko et al., 2007; Gourtorbe et al., 1994). Land surface in this region may amplify the West African Monsoon's inter-annual variability, which is controlled by changes in Atlantic Sea Surface Temperature (Timouk et al., 2009). The rainfall pattern of the region, governed by the monsoon's movement, and the corresponding surface hydrology are both defined by their extreme variations between years and seasons. This unpredictability influences all land surface processes that, in turn, determine small-scale, rain-fed agriculture, the cornerstone of most local livelihoods. Since entire communities depend on such a variable water source and years

of abundance and scarcity are frequent, famine is regular. Local production and viability would be improved by better understanding and thus prediction of rainfall timing and quantity, as determined by land surface – atmosphere exchanges.

The surface energy balance is based on the principle that energy must be conserved at the earth's surface, and is the essence of the surface atmosphere exchange. Each component of the energy balance can be measured and observed independently. It is diurnally forced, as the sun is the primary energy source. Surface vegetation and substrate will affect components independently. The energy budget can be written in a general way as (Brutsaert, 1982:128):

$$\frac{\partial W}{\partial t} = R_n - L_e E - H + L_p F_p - G + A_h \quad (2-1)$$

Where R_n is the net radiated flux, L_e , the latent heat of vaporization, E , the evaporative flux, H , the sensible heat flux, L_p , the thermal conversion factor for fixation of carbon dioxide, F_p , the specific flux of CO_2 , G the specific energy flux leaving the layer at the lower boundary, A_h the energy advection into the layer expressed as a specific flux, and dW/dt , the rate of energy storage per unit area in the layer. In the case of a simple lumped system, that neglects unsteadiness, ice melt, photosynthesis and lateral advection, the energy balance can be written as (Brutsaert, 1982:2):

$$R_n = L_e E + H + G \quad (2-2)$$

Successful closure of the energy budget, above, is dependent on each component being measured over identical control spaces (Foken, 2008). The energy balance is hard to close in areas and regions with extensive data sets and accessibility (Burba et al., 2005; Foken et al., 2010; Farhadi, 2012; Krishnan et al., 2012; Guo, 2006; Williams, 2012). This partition of energy into sensible heat, evaporation, and downward conduction heat according to the above energy balance drives global atmospheric processes and is controlled by interacting surface and atmospheric conditions (Szilagyi and Parlange, 1999; Foken, 2008). Therefore, it is essential that we account for as many potential controls on the energy budget as possible and explore its response to changing land cover in order to improve modeling and eventually predictions of both meteorological and hydrologic processes.

Current measurement equipment does not allow these fluxes to be measured at comparable scales (Beyrich et al., 2006; Albertson and Parlange, 1999; Brutsaert, 1998; Parlange et al., 1995; Eichinger et al., 1996; Bou-zeid et al., 2004). The area of measurement for net radiation can be fairly well controlled, although, in the case of vegetation, it maybe hard to maintain consistent separation between the radiation that is reflected from the ground and that from canopy surface. Eddy flux equipment, that measures the latent and sensible heat fluxes, does not take into account all scales of eddies and the source area fluctuates depending on the wind speed and direction (Baldocchi and Rao, 1995; Burba et al., 2005; Hsieh et al., 2000; Horst, 1999). And ground heat flux plates are installed a few centimeters below the surface and thus do not take into account what happens at the soil surface or in a vegetation layer (Liebethal et al., 2005; Verhoef et al., 2012). Tools exist to correct the heat fluxes and net radiation, but correctly measuring the ground heat flux and storage (excluded from equation above) are reoccurring problems for closure and may create up to 50% error each (Foken, 2008). To avoid this particular debate, for the purposes of our work, we are not including measurements of ground heat flux. Rather, we are calculating ground heat flux (including any storage) as the residual after subtracting the latent and sensible heat fluxes from net radiation (below). Our future studies will undoubtedly examine this particular assumption for our site and for the various vegetation covers. A short comparison of ground heat flux measured with the residual is presented.

$$G = R_n - L_e E - H \quad (2-3)$$

In West Africa various large, long-term campaigns including AMMA/Catch, SEBEX, HAPEX-Sahel, and GLOWA-Volta have each set up similar instrumentations. However, for the most part, they focused on the “dry-down” phase, or were less well equipped to capture the latent energy flux (Verhoef, 1999; Gash, 1998; Ramier, 2009; Bagayoko, 2007).

This measurement and analysis of fluxes is a significant contribution to global flux monitoring because it took place in a very the Sudanian Savanna, which has hardly been studied in this way either as vegetation type or climate zone. The site itself was difficult to access – only in the rainy season by car and in the wet season by motorcycle and car. This area is undergoing rapid transformation both due to local human activity and global climate change (Ezzahar et al., 2009). The transformations in land cover could result in dramatic changes in the soil moisture, precipitation, and groundwater regimes that may be irreversible (Rigby, 2009; Clark, 2004, 2001; Goodrich et al., 2000). The neighboring Sahel underwent a similar dramatic land cover change that was triggered both by droughts and land use change, the exact cause is debated, but the results were drastic for local livelihoods and farming who both witnessed a loss of productivity (Gash et al., 1997; Schuttemeyer et al., 2006; Verhoef et al., 2012; Kabat et al., 1997; Le Barbé, 2002). In fact, some authors claim that this destabilization went far beyond environmental consequences of degradation, drying of water resources, and loss of vegetation and many social conflicts have their origins in the original land degradation (Taylor et al., 2008; Goutourbe et al., 1994; Boulain, 2009; Cappelaere et al., 2009). Finally, human livelihoods are intimately connected to agricultural production in West Africa, so small changes in agricultural productivity can have enormous consequences in livelihoods, quality of life, and human mortality. For example, each drought year has direct consequences in terms of mortality. Thus the impact of improving understanding of they hydrologic flows surrounding agriculture and the consequences of changes to any of the many parts of that system go far beyond the natural resources or agriculture themselves and affect human health, survival, and society.

Additionally, this study is unique from the few there are, because it compares gallery forests with neighboring agricultural fields, which otherwise has not been accomplished (Bagayoko et al., 2007; Guyot et al., 2009; Ezzahar et al., 2009, Mauder, 2007). Gallery forests occur in areas of extremely irregular topography and thus measurement was challenging. In total, we include 18 months of gallery forest measurements and 37 months over the agricultural field. Challenges in measurement and data collection were, at times, significant, so our 37 months are not continuous (Table 2-2). This chapter concludes by describing these challenges and recommendations for future eddy covariance measurements at similar sites.

Our primary goal in this paper is to examine the partition of fluxes over a mixed savanna agricultural catchment in West Africa over multiple seasons. The extreme seasonality of the environment and corresponding changing land cover allows us to look at the relationships between vegetative surface, moisture availability, and energy balance partition. We will begin by examining the most significant components, R_n , LeE , H , and G in more detail.

2.2 Methods

2.2.1 Geographical Context

The general site of the community Madjoari was initially selected based on a participatory process, incorporating the voices of villagers from communities surrounding the Singou River Basin, scientific researchers from Burkina Faso and abroad, and political official from various levels of government, focused on the Southeastern region surrounding the Singou River Basin of Burkina, that is less studied and visited despite its high level of vegetation cover and thus corresponding complex human – environment interactions. The participatory dialogue led us to Tambarga, one of the 8 villages of commune of Madjoari, because there was a catchment that was topographically defined and the village residents were ready to engage in the research. There were no

previous ongoing measurements and thus a need existed for monitoring of hydro-meteorological variables that was validated by a personal invitation from the local community. The region represents an interesting human – environment conflict or juxtaposition. The community of Madjoari is the main human settlement inside a region that is composed of a patchwork of hunting reserves and national parks. The reserves and parks have various owners and regulations controlling use and access, but in all cases forbid farming on their lands. The enforcement of these regulations has varied, but currently, residents may only farm in land designated for farming by the community of Madjoari. This means that there are essentially farmed islands surrounded by land protected from farming and managed for wild animals consisting of open forest and savanna. People suffer from two problems that are related to the community’s “island” position: crop damage by elephants, and a lack of road development that makes the village relatively inaccessible during the rainy season. This geographic situation also makes the village a prime location to study the consequences of land use change from Sudanian savanna to agricultural fields, as the savannas are less impacted and the fields are exploited to the maximum. In addition the Sudanian savanna, which is characterized by fire-selected grasses ranging from 20 centimeters to 1.5 meters also includes patches of woody scrubland, open forests, gallery forests, and riparian stands (Arbonnier, 2004). Agroforestry parks, fallow fields and active farming of millet, corn, cotton, rice, sunflowers and sorghum make up farmlands. In addition, there are a small number of vegetable and tobacco gardens. Soil is predominantly sandy-loam at the site (Appendix III).

The community of Madjori is made up of eight villages that were involved in a participatory mapping project that helped guide where and what micrometeorological and hydrologic variables were collected. It was decided that understanding the flows components of the interrelated energy and water balances surrounding the village was importance for future natural resource management as well as adaptations to changes in the regional precipitation and climate. Specifically, there was an interest in understanding the difference between natural and anthropomorphic land uses. Evaporation is the main term that pairs the two balances, and for this chapter we will focus on the energy balance and in particular evaporation. Eddy covariance is the optimal method for measurement of evaporation, and could be placed in sites both more and less impacted by human land use. Eddy covariance stations were placed in 2 locations in a small catchment (~4 square kilometers), defined by a rocky escarpment of about 100 m elevation and an ephemeral stream near the village of Tambarga.

2.2.2 Equipment set-up

Instrument	Measurement	Height/ Depth	Number	Interval
CSAT-3 Sonic Anemometer (Campbell Scientific)	3D Wind speed and Direction, Air Temperature	2.2 m	3	20 Hz, proc. 30 min.
LI-7500 Infrared Gas Analyzer (LICOR)	CO ₂ H ₂ O Concentration	2.2 m	3	20 Hz, proc. 30 min.
CNR2 Radiometer (Kipp & Zonen)	SW-net, LW-net Radiation	2.1 m	2	1 min.
HMP450/Campbell Scientific with Radiation Shield	Air Temperature, Air Humidity	2.25 m	2	1 min.
Apogee/ Campbell Scientific	Surface Temperature	2 m	2	1 min.
Hukseflux Heat Flux Plates	Ground Heat Flux	< 5 cm	2	1 min.
(Campbell Scientific)	Wind Speed	2.25 m	2	1 min.
Precis Instruments (3029)	Precipitation	1 m	1	0.1 mm

Table 2-1. Inventory of Instruments used for Energy Balance Analysis: The name of the sensor or instrument is followed by the measurement it performs, the height and depth of each sensor, the number present, and the interval of measurement.

One station was placed in a millet field and the other on the edge of the rocky escarpment overlooking the gallery forest (Figure 1-3; 0). Each station was equipped with a CS Sonic Anemometer, LICOR gas analyzer, surface temperature sensor, rototronic temperature and relative humidity sensor, fine wire thermocouple, wind vein, ground heat flux plates, and rain gauge (Table 2-1). In addition the lower station had a second sonic anemometer and Licor gas analyzer installed in the opposite direction. Placement of the eddy-correlation in opposite directions allows us to measure fluxes when the wind is blowing from all 360°. Map

showing position in climatic zones, neighboring watersheds larger watersheds, hunting concessions, and position of equipment in relation to the village and local topography and land cover is in the introduction (Figure 1-1).

Instruments were installed from May 2009 to October 2010, however continual measurements were not always possible (Table 2-2). A smaller equipment set up was installed in July 2011 and made the observations used in this paper until May 2013. Eddy correlation data was only used from the sonic Licor in the direction of incoming wind, when possible. The dominant wind direction was 240° or South West. The eddy-correlation equipment obstructs the path of the wind when it comes from behind, and thus that data is unreliable. Further in the analysis, we examined the fluxes by 60° sector and compared the quantity of transport as well as the frequency in each sector.

	Jan	Feb	Mar	Apr	May	Jun	Jul	Aug	Sept	Oct	Nov	Dec	
2009	-	-	-	16	15	11	17	4	15	18	-	-	field
	-	-	-	21	15	25	29	13	15	9	24	31	hill
2010	-	11	2	21	3	23	2	3	2	-	-	-	field
	26	29	26	31	3	31	31	3	26	-	-	-	hill
2011	-	-	-	-	-	-	29	3	3	3	29	29	field
	-	-	-	-	-	-	-	-	-	-	-	-	hill
2012	29	31	3	2	1	31	31	3	25	3	25	16	field
	-	-	-	-	-	-	-	-	-	-	-	-	hill
2013	21	24	9	17	-	-	-	-	-	-	-	-	field
	-	-	-	-	-	-	-	-	-	-	-	-	hill

Table 2-2. Calendar of successful Eddy Correlation Data (days per month at respective stations). The field is shown above the hill station. The years are shown in larger rows. The dashes mean that no data was present. For all comparisons in the chapter, however, we only use years 2009-2010 because both stations were taking measurements. And for direct comparisons, we only used times when both were present, which is highlighted.

2.2.3 Eddy - Covariance

$$\text{Sensible heat flux} \quad H = \rho c_p \overline{w'T'} \quad [W/m^2] \quad (2-4)$$

$$\text{Latent energy flux:} \quad LE = L_e \rho \overline{w'q'} \quad [W/m^2] \quad (2-5)$$

We calculate the covariances in equations 2-4 to 2-5 using measurements at a frequency of 20 Hertz and over an averaging window 30 minutes. The sensible heat flux (H) is the product of the air density (ρ), the specific heat of air (c_p), and the covariance of vertical wind speed (w) and air temperature (T). The latent energy flux is a product of the latent heat of vaporization (L_e), air density (ρ), and the covariances of wind speed (w) and humidity (q). Thirty minutes is a large enough frame to see eddies that catch a range of transport processes and eddies of different sizes (Foken, 2008). Constants used for this and following equations are presented in the following chapter (Table 3-3).

2.2.4 Data Preparation and Correction

However, before we were able to analyze and compare the fluxes, we had to process and prepare the data. Data was first extracted in the field using LoggerPro software. It was compiled and parsed into approximately monthly segments. As described by Rebman et al. mean vertical velocity was non-zero over an approximate month (2012). Since, we trust and therefore are most interested in the fluxes perpendicular to the main flow direction, there was significant lift in the case of the hill station that biased the results (Burba et al., 2005). In order to prepare the data for flux calculation, we used the planar-fit method proposed by Wilczak, Oncley, & Stage (2001) to adjust the flow to correct for this lift before analysis of the covariances. This was particularly important because our hill station was located at the top of a canyon, so updraft was significant. Corrections also

changed values for the lower station as well, demonstrating the significance of even apparent nuances in topography. We effectively tilted measurements of the three components of the wind field perpendicular to the direction of flow so that the vertical wind component equaled zero over 1 month averaging periods and the mean wind direction was in the x direction. We then performed a linear regression using the mean wind vectors to obtain a matrix that we used to obtain the mean wind vectors and stress tensors in a new coordinate system with a z-axis perpendicular to the mean streamline. Then, we rotated the intermediate winds and stress tensors.

After the planar fit (Burba et al.; 2005; Aubinet, 2012; Wilczak, Oncley, & Stage, 2001), we proceeded with flux calculations. The eddy correlation method relies on direct measurements of vertical velocity (w) and scalar concentrations (c). At a moment in time, eddies will move air parcels up and down with a certain speed. Each parcel will have certain characteristics. If we measure those characteristics such as gas concentrations, temperature, humidity, we can calculate the flux by calculating the covariance of the vertical velocity and the concentration. The temperature and humidity fluctuates over the course of measurements, causing fluctuations in trace gas concentrations that we do not want to measure. These fluctuations can occur differently in upward and downward eddies, creating an illusion of flux. We correct this illusion using the Webb-Pearman-Leuning (WPL) equations (2-6; Webb et al., 1980; Leuning, 2007; Foken et al., 2012).

$$\mathbf{WPL}_{\text{corr}} \quad E = (1 + \mu\sigma) \overline{(w'\rho'_v + \frac{\bar{T}}{\rho_v} w'T')} \quad (2-6)$$

2.2.5 Ground Heat Flux

Ground heat flux and other terms of the energy budget were lumped together for the purposes of this analysis. This is a simplification that allows for closure. However it is important to note that, by doing this, we are grouping together error and storage in the term names "ground heat flux". For reference, we additionally measured the ground heat flux at each site with 2 ground heat flux plates (Table 2-1). However, for energy closure, we used the residual (2-7).

$$G + \varepsilon = R_n - L_e E - H; \quad \varepsilon = \frac{\partial W}{\partial t} - L_p F_p - A_h \quad (2-7)$$

2.2.6 Additional Data

Hydrologic data included rainfall, runoff, and soil moisture that were collected simultaneously as the micrometeorology data. They are treated more in detail in other chapters, but rainfall is presented in this chapter for seasonal context, as available moisture is the main determinant of hydrological and corresponding energetic processes in this semi-arid system. It was measured by a *précis* rain gauge with a resolution of 0.1 mm, and gaps were filled with a nearby Davis rain gauge.

2.3 Results

2.3.1 Seasonal Changes in Coupled Hydrologic and Energy Balances

Rain begins in April or May and falls mainly June through August and a little in September (Table 2-3). By October, it has already declined. The annual rainfall was relatively consistent in 2009, 2010, and 2012, but 2011 was a drought year with less than half the rainfall as the other years. The river flowed from May to December most years, but only had significant rates of discharge in September and October each year. The ground water indicated by the depth of the water table decreases to its annual minimum in April most years before rising to its peak in September or October. Soil moisture followed a similar cycle to that of groundwater in the field. On the hill, it had a similar pattern, though seems to have both a later moistening and drying, which occurs more in November than October.

	Hydrology		Soil						Average Daily Heat Flux						Maximum Daily Heat Flux													
	Rain mm	Ground water m below surface	WVC 15cm	WVC 30cm	WVC 15cm	WVC 30cm	WVC 5cm	WVC 10cm	WVC 20cm	WVC 40cm	H Field Avg Daily	H Hill Avg Daily	LeE Field Avg Daily	LeE Hill Avg Daily	Rn Field Avg Daily	Rn Hill Avg Daily	G Field Avg Daily	G Hill Avg Daily	H Field Max Daily	H Hill Max Daily	LeE Field Max Daily	LeE Hill Max Daily	Rn Field Max Daily	Rn Hill Max Daily	G Field Max Daily	G Hill Max Daily		
5	May-09	64.1	-5.3702								39.7052	52.4851	76.2871	103.0519					268.5	268.5	1493	1184.2						
6	Jun-09	177.1	-4.869								43.9905	50.8312	71.3707	103.836					308.1	308.1	1094.1	1137.7						
7	Jul-09	176.2	-2.4193								29.8186	41.9872	70.5755	104.4568					203.6	203.6	711	1286.1						
8	Aug-09	186									31.092	39.6847	101.007	112.6148					229	229	894.2	786.4						
9	Sep-09	118.7	-0.5779								28.1141	35.9473	57.738	131.9481					553.5	553.5	524.2	1013.6						
10	Oct-09	66.8									31.6982	63.5799	81.8668	123.6481	142.7478	120.0226	29.6574	67.2054	225	225	502.4	673.9	774.2	460.7	774.2	460.7	354	
11	Nov-09	0	-2.2								33.6395	54.8774	56.2839	71.133	119.8006	98.9375	29.8773	-27.073	221.7	221.7	452.7	568.4	685.8	693.4	437.4	389.4		
12	Dec-09	0	-2.9406								31.6706		59.6449	63.9709				27.3447				341.5					406.5	
1	Jan-10	0	-3.2568								37.4193		64.7904	62.791				40.8518				347.5					611.6	
2	Feb-10	0	-3.9775								47.5418		67.8246	85.7088				29.368				364.5					652.5	
3	Mar-10	0	-4.749								39.7797	57.8825	30.2273	63.0066	109.8815	96.4081	46.4388	-24.4809	220.3	220.3	116.5	498.5	1193	659.1	1045.7	1045.7	872.9	
4	Apr-10	0	-5.1605								64.3663	75.6004	37.2277	63.8718	107.7105	120.6203	107.949	-18.4321	363.5	363.5	726	918.1	599.1	720.2	438.2	438.2	726.8	
5	May-10	41.8	-5.7714	0.2242	0.0376	0.1017	0.091				60.4762	76.088	44.4001	88.6838	123.9903	136.4556	28.6813	-30.1281	434.4	434.4	434.4	981.6	975.2	681.7	826.8	625.6	999.7	
6	Jun-10	137.1	-5.235	0.2419	0.0702	0.1611	0.1748				42.0801	63.3744	52.8788	109.413	141.2154	132.2873	51.8519	-40.4372	443.8	443.8	1087.6	1067.7	778.3	767.2	899.9	817.2		
7	Jul-10	130	-4.5128	0.0969	0.1764	0.1876					23.8	38.8948	51.0017	82.825	122.5663	112.9462	50.2368	-8.8404	762.4	762.4	943.8	662.9	800.1	771.1	807	807	515.6	
8	Aug-10	224.2	-4.05	0.1349	0.1767	0.1948					24.5667	36.4081	59.5197	103.0042	139.5947	117.7738	58.0493	-21.5158	268.7	268.7	1021.8	1159.5	751.6	802.4	799.9	966.4		
9	Sep-10	188.7	-0.9617	0.1775	0.1815	0.2051					27.7364	39.1284	96.7404	123.6406	141.7331	130.7746	21.3507	-31.7255	803.9	803.9	981.1	830.2	857.5	1159	909.1	776.5		
10	Oct-10	57.1	-	0.1616	0.1816	0.1942					30.8901	62.2251	101.0701	140.0761	158.0867	128.0409	29.0724	74.2603	244.1	244.1	627.9	1013	846.3	807.4	680.9	993.9		
8	Aug-11	124.9	-4.8779								16.2854		23.3801	133.34				92.5152	154.2	154.2	545.9					955.6	673	
9	Sep-11	134.2	-4.3179								21.7035		38.2973	150.583				90.9579	161.9	161.9	472.6					884.5	624.7	
10	Oct-11	35.7	-3.9769								30.2913		48.685	160.3944				85.1581	242	242	393					785.6	484.5	
11	Nov-11	0.5	-4.8439								45.8991		38.5241	103.6983				19.21	308.6	308.6	358.9					654.4	432.8	
12	Dec-11	0	-								34.1377		42.5538	80.0133				3.3218	328.1	328.1	251.4					523	412.9	
1	Jan-12	0	-5.7184								35.125		51.5335	88.6062				19.0003	374.7	374.7	322					555.7	385	
2	Feb-12	4.2	-6.656								39.1338		53.2903	91.0001				-1.4241	302.2	302.2	395.4					689.4	406.4	
3	Mar-12	0.1	-6.9525								51.0817		54.0943	100.8768				-4.4755	297.8	297.8	326.2					653.2	362.9	
4	Apr-12	42.4	-7.1591								56.2302		34.8555	126.0377				35.097	377.2	377.2	327.2	638.9				684	492.2	
5	May-12	60.7	-7.2251								46.3406		39.4729	128.6163				42.8028	347.9	347.9	347.9	1235.4				700.6	489.5	
6	Jun-12	53.5	-7.2966								17.8827		67.9488	131.6878				50.6615	216.4	216.4	1479.5					833.4	606.9	
7	Jul-12	181.3	-6.552								14.2148		44.9624	130.0594				71.1954	177	177	1281.2					926.6	664	
8	Aug-12	95.1	-5.5118								21.3766		51.2948	151.2901				79.7756	471.9	471.9	705.5					859.7	661	
9	Sep-12	212.7	-2.7931								25.8691		66.856	155.4345				65.3272	211.9	211.9	756.1					832.7	585.8	
10	Oct-12	83.2	-1.9544								43.7458		58.494	121.4481				19.2082	278.4	278.4	518					720.6	341.4	
11	Nov-12	1.5	-3.1446								33.437		45.5717	91.3307				12.322	265.6	265.6	283.2					644.5	312	
12	Dec-12	0	-4.3828								27.3874		50.7747					18.8521	182.1	182.1	197.7					612.8	385.4	
1	Jan-13	0	-4.7653								42.9052		43.3031	99.8698				13.8524	352.4	352.4	302					612.8	385.4	
2	Feb-13	0	-5.5356								63.6695		30.168	113.5324				21.9067	335.4	335.4	397.6					622.7	474.4	
3	Mar-13	0	-6.3978								51.6284		83.9943						315.9	315.9	552.8					622.7	474.4	
4	Apr-13	0	-6.6738								51.7786		83.9943						585.8	585.8	585.8					622.7	474.4	
5	May-13	0	-6.608																585.8	585.8	585.8					622.7	474.4	

Table 2-3. Table shows the monthly summary data of the energy budget components and hydrologic parameters. From left to right (bottom to top): Rain, groundwater depth, discharge of stream, soil moisture at multiple depths, average daily heat flux (sensible, latent, net radiation, and ground), and daily maximum heat fluxes (sensible, latent, net radiation, and ground). Alternating field and hill for all appropriate variables.



Table 2-4 Shows the two eddy-covariance stations through a single year (2010) by month. Land-cover behaved very similarly other years for both stations. Land cover surrounding two stations in characteristic of the different covers present in the basin. Field station shows a typical semi-fallow farmland and hill station shows what is happening over the hill on the cliff.

The energy balance has a corresponding annual cycle to the hydrological cycle and vegetation change. Figure 2-1 shows the daily monthly behavior of the energy balance at each of the two cycles. Average daily net radiation is bimodal with a peak in May and another in September on the hill, and in June and October in the field. It seems to be slightly higher in field. Latent energy flux, however, is considerably higher on the hill, with the highest average daily sensible heat flux occurring in October. The latent heat flux in the field shows more variation between years and is less high in August to October in particular. Sensible heat flux is similar over the two land covers, though a bit higher in the hill. It has a slight increase from January and peaking in April, then decreases and is lowest in August before increasing again in October, on the hill, and November, in the field. Average values of

ground heat flux show the most discrepancy between sites. On the hill, they are consistently below zero, indicating a flux into the soil of up to 75 W/m^2 , whereas they range between -5 and 100 W/m^2 in the field (Figure 2-1; Table 2-3).

2.3.2 Energy Balance Comparison

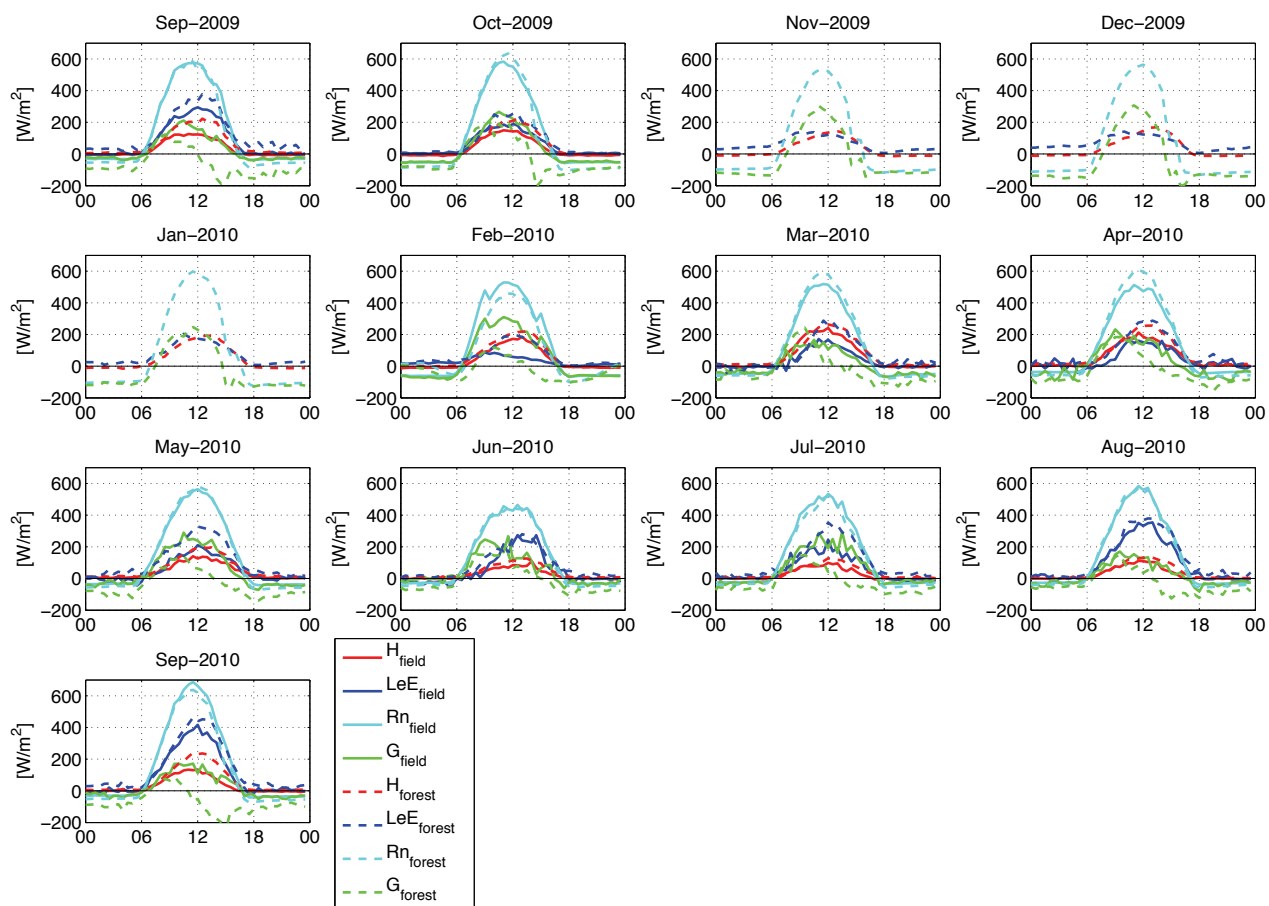


Figure 2-1. Energy balance by month, showing each station independently. Each month from September 2009 to September 2010 is shown separately. Graphs show the average fluxes over the day in Watts per square meter, labeled with hours. Red indicates sensible heat flux, blue latent, cyan net radiation, and green ground over the field, solid, and hill/forest, dashed.

Daily maximum values of the components of the energy balance show similar trends to their averages, but most remarkable is the variation in peak of latent heat flux. Although the average values did not vary so much over the course of the year, the maximum daily values increased dramatically in May, June, July, and August, up to 1500 W/m^2 in the field, and 1200 W/m^2 over the hill as opposed to a dry season daily peaks of 120 W/m^2 and 340 W/m^2 (Table 2-4 and Figure 2-1).

The ground heat flux is at its maximum in June in the field, whereas over the hill it is in April and September. The difference is related to the surface substrate in the two fields. In June, the field has just become wet but has not started growing dramatically yet. Whereas in the field, the substrate under the station is rock, so the behavior of ground heat flux is dramatically different. April and September peaks could be associated with the high radiation during those months of equinox relative to the atmospheric humidity. Finally, time of daily maximum is fairly consistent for all fluxes except for latent energy flux. In particular, over the field it happens much later in the day (after noon) during the growing season, (June - September) and very early during the dry season (December to March). This is also true for the hill.

Examination of the average diurnal fluxes by month (Figure 2-1) reveals more detail of how the fluxes vary between the two land covers. The net radiation is very similar for the months that have data from both sites, in October 2009, March 2010, and April 2010, the hill seems to have a higher peak, but in February 2010, the peak in the field is higher. Latent heat flux is significantly higher on the hill in all months. In particular, it is clear that the field's latent heat flux peaks early in dry months, like February 2010. The sensible heat looks similar in all months, although it is slightly higher in many months, September 2009, October 2009, March 2010, and April 2010. The most consistent difference between the two sites is the afternoon drop in ground heat flux on the hill site. In September, both 2009 and 2010, it is the most pronounced, sometimes dropping to as low as -200 W/m^2 .

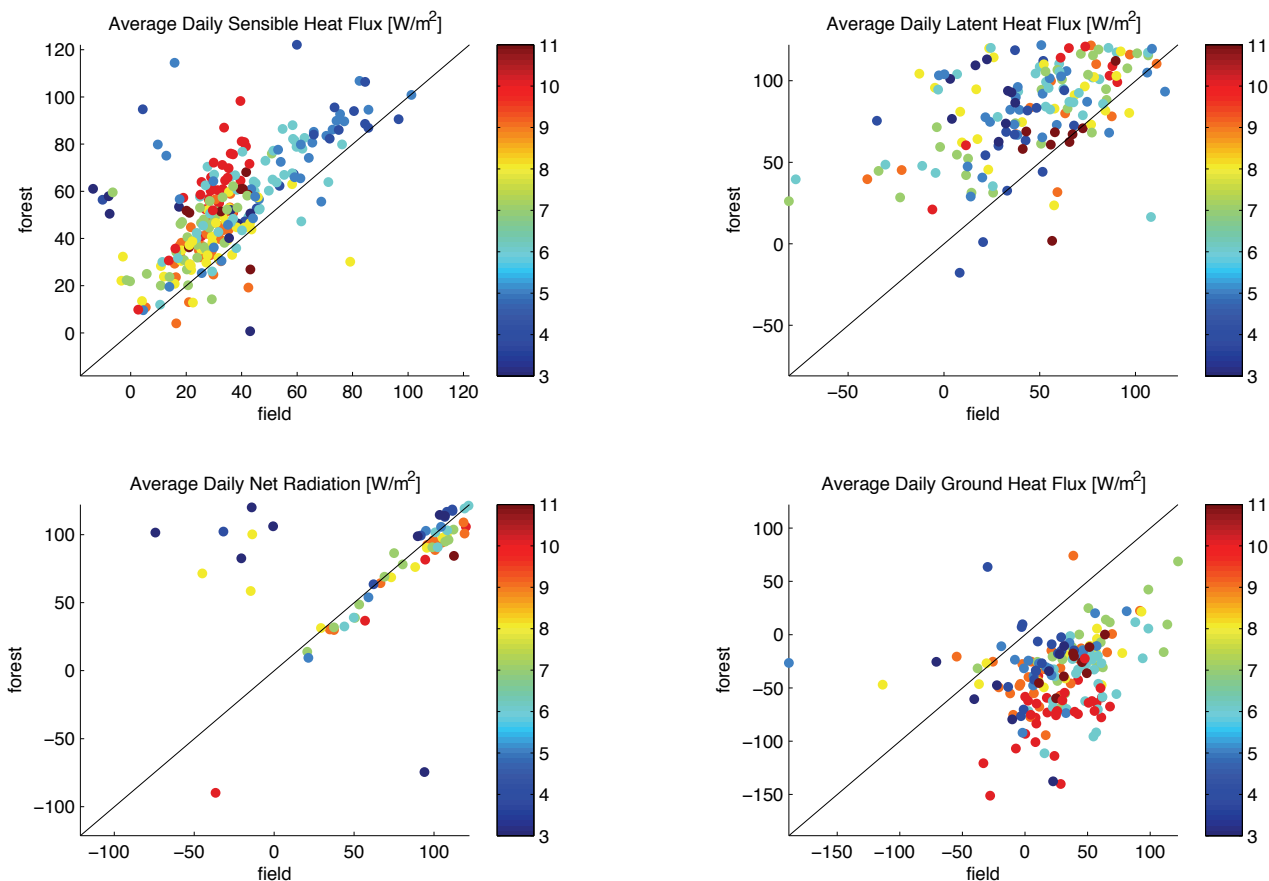


Figure 2-2. Comparison of the Average Daily Fluxes over the Field and over the Forest or Hill. This figure compares each of the components of the energy balance by daily average between the two sites. Color scale shows the month, in this case we are pooling data from the 13-month span that begins in September 2009 and ends in September 2010. Since during the months of December, January, and February, the stations did not share any valid data, they are excluded from this comparison. Black line shows the 1:1 line.

Both sensible and latent heat fluxes were greater on the hill or forest than in the field (Figure 2-2). Average daily ground heat flux was, as already observed negative on the hill and positive over the forest. The daily net radiation has the closest correspondence between sites.

2.3.3 Ground Heat Flux

Figure 2-3 compares the residual that is used for the energy budget above with that which was measured at a varying depth with heat flux plates. Data from heat flux plates were not used in the previous display of the energy budget because they are considered to drastically underestimate the ground heat flux. As the figure shows, the residual is about four times the size of the measured value. Heat flux plates were not located at the exact surface of the soil. Initially they were installed close to the surface,

however they experienced a downward migration to do litter accumulation and at other times were moved upward. In addition ground heat flux plates have been known to alter moisture and thus energy transfer in their immediate vicinity and thus cannot be considered to be an exact measurement of the ground heat flux. However what is clear from this figure, is the similarity in the tendencies. The diurnal cycle is visible, with negative nighttime values and higher daytime values peaking in green (near noon). There is more scatter on the hill, and a higher magnitude of negative values on the hill. The residual is more likely to be negative in the afternoon, whereas the measured heat flux plate only becomes negative after sunset. The positioning of the heat flux plate under the soil surface results it not including any flux that takes place above it (in the top 5 cm of soil and at the surface) and neglecting any storage between the soil surface and the 2m high flux measurements, which is included in the ground heat flux as a residual.

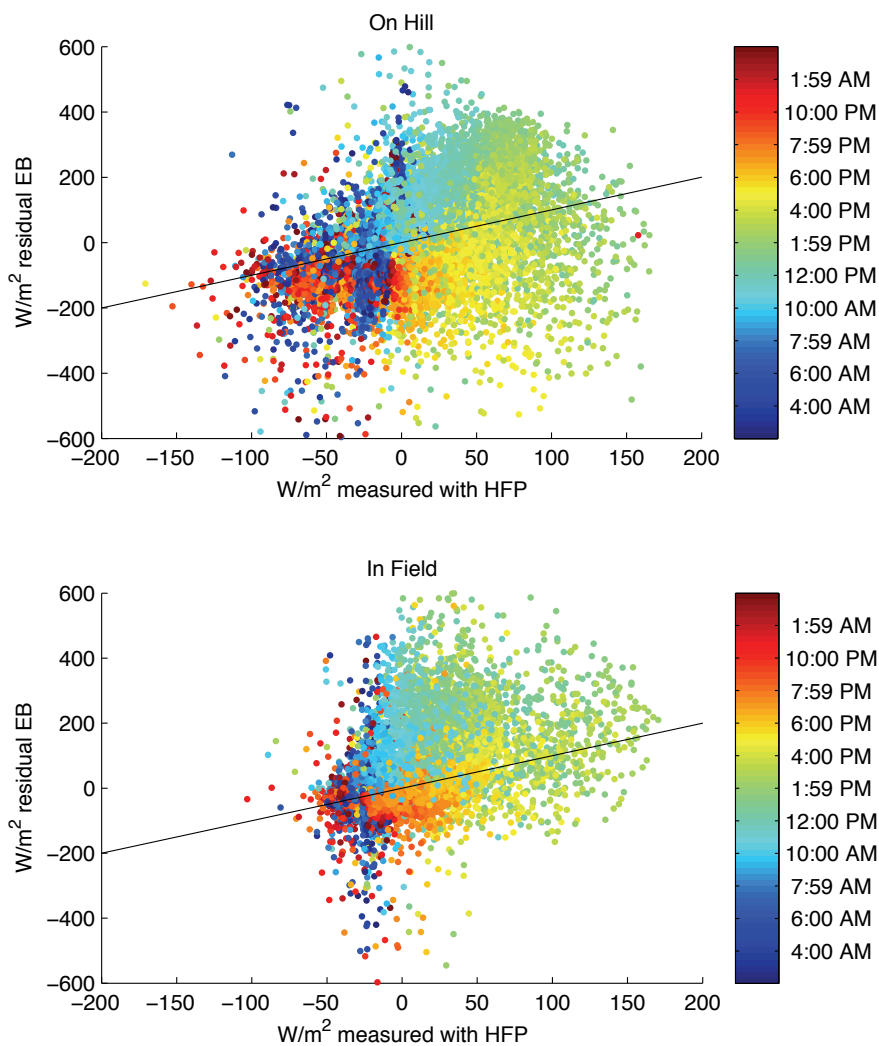


Figure 2-3 Comparison of G determined with residual of energy balance with the G measured with Heat Flux Plates (HFP) for hill and for field. The one to one line is shown in black. The time of day is shown with color. One day point is shown for every half hour of data collected from September 2009 – September 2010. No trends were found according to season (not shown). HFP were located close to, but not at, the soil surface. Depth varied between 0 – 5 cm, as soil was added and removed by wind and erosion throughout the period.

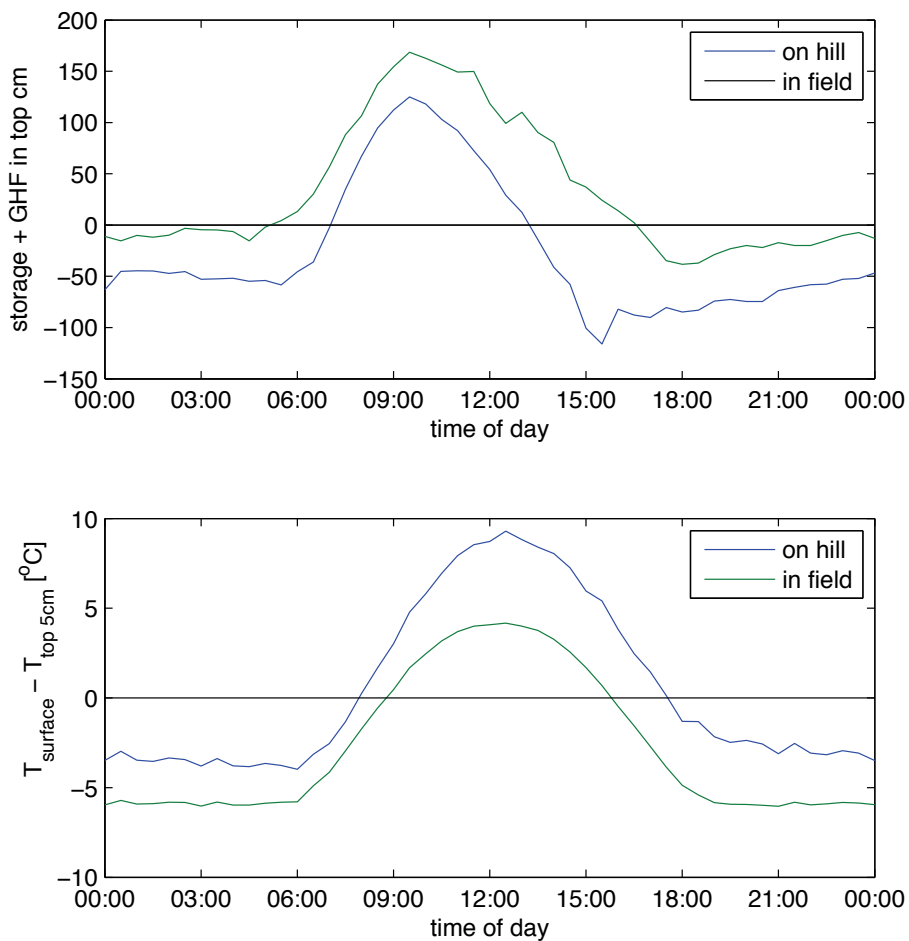


Figure 2-4 Shows the remainder when the ground heat flux plate measurements are subtracted from the residual from the energy balance in the upper plot. And the temperature difference between the surface and the 5-cm below ground in the lower plot. The hill or forest is shown in blue and the field is shown in green. The time of day is on the x-axis. This plot is the average between all 2009 and 2010 data. The seasonal changes were not significant (not shown). In the field, the temperature measurements are taken right at the station, but for the hill, they are from the nearest possible station with soil (for the subsurface temperature).

In figure 2-4, we examine that residual. In the top subplot, we see the difference between diurnal cycle of the residual G from the energy budget and the ground heat flux measured. We see that comparatively, in the field it is net positive. This suggests that there is a storage term in the field between 5 cm below the surface and 2 m above the surface, where the eddy-covariance measurements are taking place. In contrast, the hill does not seem to be accumulating heat over time. Its daily cycle is more or less zero, creating a stable energy balance. The main difference between these two sites, in terms of ground surface, is that the hill station is situated on top of a rocky escarpment, whereas the field station is over a sandy-loam soil. The dense rock is much denser than the porous soil. We expect the rock to have a higher thermal storage capacity as well as a higher thermal diffusivity. This means that it will gain more energy during the day, but also lose it more at night. This is confirmed by the steady state diurnal cycle. In the lower subplot, we see the difference in temperature between the ground surface and the soil surface. However in the lower plot, because the subsurface measurements, both ground heat flux and subsurface temperature, are not taken right at the station (due to the rock presence), it is not confirmed. The heat flux plates are in a crevice in the rock, whereas the temperature measurements are at the nearby sandy soil site. However we do see that there is an extremely high temperature difference in the hill compared to the field at noon, but a narrower temperature difference at night. This suggests that our above hypothesis is true, and we would expect to have even lower hill nighttime temperature difference measurements at night, when the rock surface would be losing all of its heat.

2.3.4 Fluxes by wind sector

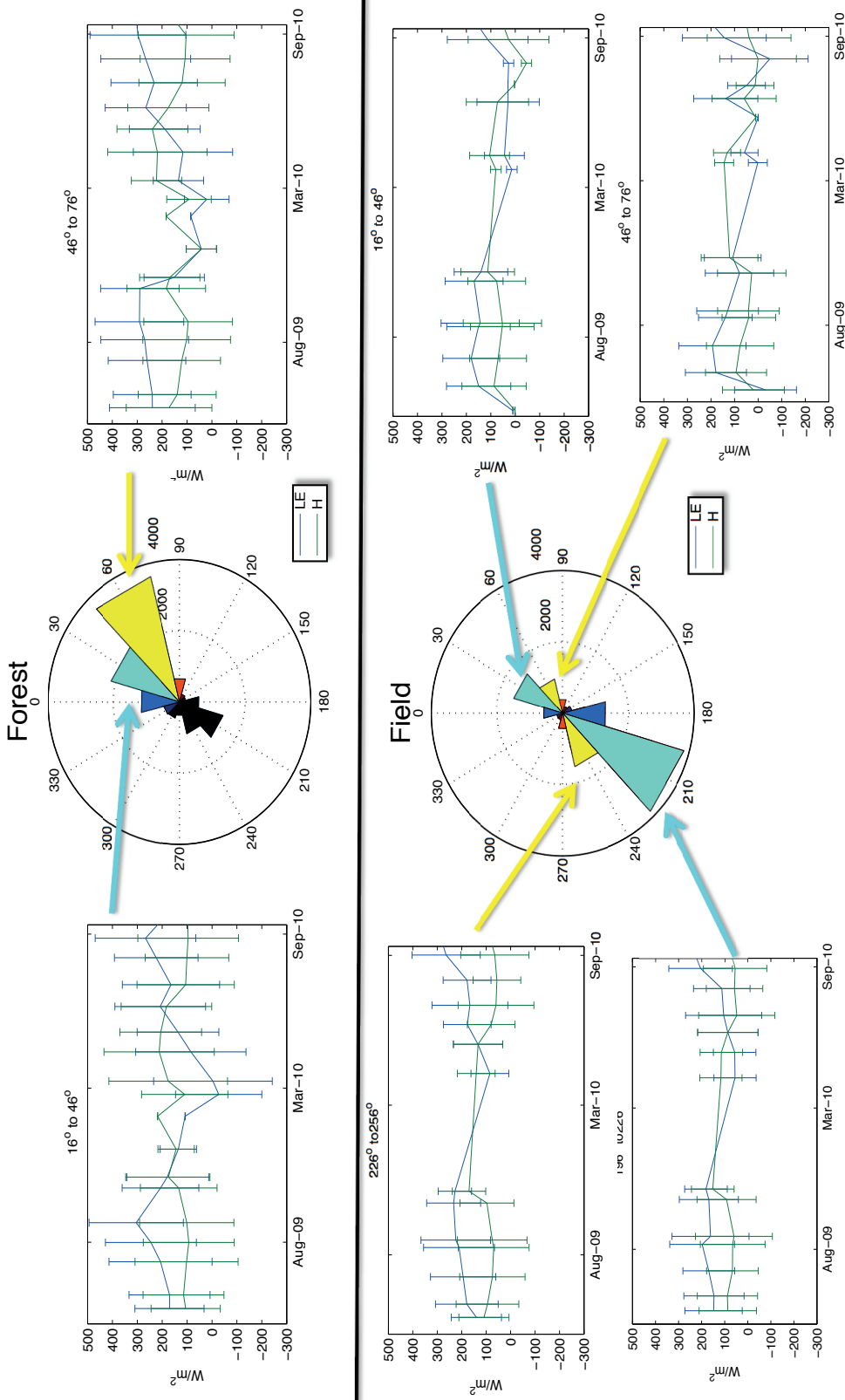


Figure 2-5 Comparison of fluxes by wind sector. We separated the fluxes measured in each 30o sector. In this figure we compare the latent (LE - blue) and sensible (H - green) heat fluxes in the wind sectors to the immediate left and right of each set of eddy covariance equipment. The wind rose in the center shows the frequency (number of half hour points) that the wind flew

in these points over 2009 and 2010. The seasonal bar graphs show the mean and standard deviation of the 24-hour flux in each direction.

Figure 2-5 shows the sensible and latent heat flux in each of the 30-degree wind sectors to the immediate left and right of each set of eddy covariance equipment as well as the frequency that the wind blew in each direction. Our stations are oriented in the predominant wind directions, which improves the overall reliability of our measurements, since measurements are most accurate when the wind is blowing directly into the eddy-covariance instruments. In the field plots, the four wind sectors look very similar. The main difference is in the final months, July – September 2010, the wind coming from 226 to 256° shows the highest level of latent energy flux. This would be the direction from the ephemeral wetlands near the outlet of the stream that would still be inundated at this point. This is from where we would expect the highest level of latent energy flux because it maintains a certain level of humidity and even standing water even when the surrounding vegetation and landscape begins to dry out. In addition, when we compare the two directions shown on the hill, we see that « drying » from October to December 2009 is much more abrupt in the sector from 46 to 76° compared to that from 16 to 46° which is more gradual. This is what we would expect because 46-76° spans the upland savanna whereas 16-46° spans the gallery forest. The gallery forest can only exist where moisture is available for longer and more continuously than in the surrounding Sudanian forest. It is located in the steep valley where springs flow year round from the rocky escarpment. Many of these trees are not deciduous and keep their leaves year round. Whereas the Sudanian forests visibly turns yellow (grass) and is deciduous (trees) as soon as water is less available in October.

2.4 Discussion

2.4.1 Summary of our data

The most striking observation is that across all months, the forest had higher levels of both sensible and latent heat flux. Sensible heat flux showed the highest difference in November and March (unfortunately we cannot compare December through February). Latent heat flux is for the most part most significantly different between the two land uses in August and May, times when the access to water in the catchment is not uniform. At its highest levels, there is the most similarity between the two land covers, in May through September. Net radiation is similar between the two sites.

The ground heat flux, as calculated as a residual, is much lower over the forest compared to the field. In fact, it is often negative. This could be a result of the fact that the net radiometer is situated over a rocky ledge as opposed to the eddy-flux instruments that capture the fluxes from the canopy, and thus is an error due to a variation in scale (Foken, 2008). But, in addition, these differences in ground heat flux are likely due to the high level of thermal conductivity and heat storage capacity in the dense rocky escarpment compared to the sandy loam. Larmuth (1978) and Childs and Flint (1990) explored the role of rocky substrates for thermal diffusivity and corresponding energy budgets. They were looking at the presence of rocks in the soil layer, instead of solid rock ground covers, but they also found there to be differences in the thermal diffusivity according to rock presence that resulted from the difference in conductivity and storage capacity of the different substrates due to their differing porosities and densities.

Finally, partitioning the heat fluxes by wind sector further supported our understanding of the availability of moisture in the basin. The wind coming from both the gallery forest and the ephemeral wetlands contained moisture farther into the dry season than that coming off of the fallow cropland or the Sudanian savanna. This supports the idea that small differences in topography and in moisture availability can have large differences in the seasonal changes in moisture availability. This supports the idea that maintaining many land-uses with correspondingly different moisture cycles will affect the overall moisture availability in the catchment due to atmospheric transport.

2.4.2 Comparison with regional data

Our fluxes of latent and sensible are, across the board, much higher than any mentioned in the literature. Our absolute highest flux of latent heat flux was 1493 W/m² but this could have been a spike during that single half hour period. The highest average daily flux of latent energy was over 400 W/m² in September 2010, and higher over the forest than in the fields by about 50 W/m². The highest sensible heat flux was in April and March 2010 when both the field and the forest were over 200 W/m² (Table 2-3; Figure 2-1).

Table 2-5 presents a summary of sensible and latent heat flux measurements elsewhere in the region of West Africa. Our values of sensible and latent heat flux are most similar to those measured by Schuttemeyer et al. (2006) in Ejura, Ghana in 2002. Ejura is about 500 km from our site, and though quite far and typically placed in a different category of climate and vegetation, so it is quite unexpected that we measure similar values. However, Schuttemeyer measured during the month of November, when the vegetation would be most similar to that at our site. Bagayoko's site is by far the most similar and closest to ours (less than 100 km). Though overlapping in terms of seasons, his measurements are still lower than ours. This might be explained by Tambarga-Madjoari's location in the midst of a natural park and hunting concession as well as our measurement of a the gallery forest, which would demonstrate the importance of neighboring vegetation cover. On the whole our measurements are comparable to those elsewhere in West Africa, given that most of these sites (Mali, Niger) are more sahelian, and thus have less moisture availability, and others (Nigeria, Benin, Ghana) are considerably south and thus have denser vegetation (White, 1986).

Who	Location	Years	max daily H (W/m ²)	max daily LE (W/m ²)	Reference
GLOWA	Ejura, Ghana (7°20'N; 1°16'W)	2002 (doy 307-349) Nov	100-200	150-400	Schuttemeyer et al., 2006
GLOWA	Tamale, Ghana (9°29'N, 0°55'W)	2002-03 (doy 313-28) Jan	150-300	150	
GLOWA	Kompienga, Burkina Faso (11°07'N; 0°31'E).	May 2003- Nov. 2004	50-250	25-350	Bagayoko et al., 2007
NIMEX-1	Ile-Ife, Nigeria (7°33'N, 4°33'E)	Feb. - Mar. 2004	102-320	50-320	Mauder et al., 2006
AMMA	Agoufou, Mali (15° 20'40"N and 1°28'45"W)	2002-2007	only Rn		Guichard et al., 2009
AMMA	Hombori, Mali (15.3°N)	0-120 (avg) 200		0-50 (avg)	Timouk et al., 2009
	Bamba, Mali (17.1°N)	40-70 (avg) 400		0-200	
HAPEX-Sahel	Niamey, Niger (13°32.60' N, 2°30.68' E)	Sept-Oct 1992		25-35 mmol/m ² /d	Goutorbe et al., 1994
HAPEX-Sahel	Niamey, Niger	237-285 doy	160-220 – LE /45 days	160 mm/45 days	Gash et al., 1997
AMMA	Ara, Benin (9.74°N, 1.60°E)				Guyot et al., 2009

Table 2-5 Comparison of regional measurements of sensible and latent heat flux. Measurements of sensible heat flux range from 50 to 320 W/m² and latent heat flux from 25 to 400 W/m².

Contrary to Guyot (2009), who attributed their lack of closure to surface water heat storage during floods, our failure to close is more likely due error because of the scale incongruity between the turbulent flux (sensible and latent) flux measurements and the net radiation. This could be perceived as question of advection as the fluxes are measuring the heat and moisture transported over the forest canopy, whereas the net radiometer is measuring the reflection from the land surface directly under the station. However, it is more likely related to the difference in the heat transport by the rock surface on the hill and the sandy loam substrate in the field. Thus the ground heat flux term is not including the errors associated with, in particular, storage in addition to the flux that we are measuring.

2.4.3 Relation to plant growth

The Amma team found that during the rainy season, the growth of plants plus the available soil moisture resulted in a higher surface net radiation, perhaps because of the changing albedo (Guichard et al., 2009). They also observed that their Agoufou site, which is more forested similar to our site and that of Bagayoko (2007), received more net radiation and less sensible heat during the dry season. We found net radiation to be fairly similar between the two sites when the whole day was taken into account, but the field was more often higher in when vegetation was present (June to December) and the hill was higher during April and May. Note that the upper net radiometer was placed over a rocky outcrop, and so this does not reflect any phenology of the forest canopy. The daily maximums of net radiation between the two stations are fairly equal. The change in albedo due to plants will be strongest when the plants are absorbing the radiation and assimilating carbon. For most plants, this occurs in the morning and not at midday, since opening of stomata in midday often leads to the loss of more moisture than desired or manageable. Our observation of differing net radiation during periods of plant assimilation is logical in this physiological light.

2.4.4 Timing of Peaks

The timing of the peaks of latent energy serves as a flag signaling when the system is moisture limited. We would expect latent energy flux to come short of its potential when the system is moisture limited, and in contrary decline due to declining incoming radiation when the system is saturated. Since this is a semi-arid savanna, we expect these changes to correspond to the wet and dry seasons. If there is a little bit of moisture available, we will see a small peak in latent energy in the early part of the day. In fact, during the early part of the year, the dry season through May 2009, the latent energy peaks over both the forest and the field during the mid morning, from 9 to 10 am, whereas over the forest, the peak is already after noon in April 2009. In 2012, when there is also enough data for this assessment, but just in the field, we see that the peak is earlier, but there was also more rain earlier in 2012.

This limitation of moisture is again visible in our observation of the contribution of the six sectors of wind direction to latent energy flux. We observed that the wind coming off of the ephemeral wetland was much longer lasting into the dry land than that from dried or burned crops and fallow fields. Similarly, we saw that the wind coming from over the gallery forest transported moisture into the dry season, corresponding to the year long moisture availability to in the valley and accessed by the gallery forest, compared to the upland savanna vegetation which quickly dried as the dry season began.

2.4.5 State of Flux Measurement Regionally

Accurate measurements of sensible and latent heat fluxes from the diverse and varied vegetation types in West Africa are essential for understanding the nuances of the extreme seasonality over different land covers. Especially in light of changing land-use and climatic patterns, long term management of the land-atmosphere hydrologic exchanges have a crucial role to play in observing and predicting consequences of the changes to the hydrologic cycle. With data such as ours, we begin to understand the controls on these exchanges.

Fafre Bagayoko, (2007) studied a site very similar to ours and not far (~70 km) from 2003 to 2004, which he claimed were the longest reported measurements (18 months). We measured 40 months all together, but 22 months was our longest continuous streak, and we only had 15 months with both towers. Although this is a long time span, there were many human and technical errors that resulted in holes during many of those months. In the mean time, many of the other long-term eddy flux sites in West Africa have been retired due to regional conflict. How can we ensure that micrometeorology measurements continue to be taken in West Africa? Fluxnet has established elsewhere in the world and provides years of continuous data at over 150 sites

(Williams et al., 2012). But because of the high costs of these stations and the high level of maintenance and quality control required, many of them are also being abandoned.

In addition to installing additional and more permanent eddy-flux stations that benefit from past experiences, we could turn to calculations from less-expensive meteorological data and satellite data. The next two chapters will explore these possibilities. Our measurements are significant because they could allow calibration and comparison for calculations from lower cost and more easily maintained and obtained stations and corresponding data (chapter 3) or calculations from satellite imagery (chapter 4).

2.5 Conclusion

This study presents a significant observation of the energy balance over the many land covers, both natural and anthropogenic, in the Sudanian savanna. We found that both sensible and latent heat fluxes were higher over the gallery forest than the semi-cultivated fields. We observed the seasonality of the system expressed itself independently in each component of the energy budget's diurnal cycle in terms of average values, peaks, and timing of those peaks. Net radiation differed the most between the two sites, vegetated and non-vegetated, when the plants were growing. Furthermore, our observations suggest that the plants alter the albedo according to time of day. Latent energy was found to become peak earlier in the dry season, suggesting depletion of all available moisture. In contrast, during the rainy season, it declined followed the cycle of available radiation. Ground heat flux was taken as a residual of the energy balance, to allow for closure, but which resulting in this terms also including any error and storage. Storage of heat was found to respond to the thermal diffusivity of the substrate. The density of the rock surface that under laid the hill or forest site meant that it had significantly different thermal conductivity and storage potential than the sandy loam over which the field station was placed. The albedo of the station was taken to be that over the rock surface and not over the entire forest canopy. This resulted in scale discrepancies between the measurements of net radiation and the turbulent fluxes meant that the former did not receive advected moisture from the gallery forests in the same way.

Our measurements were also higher than those previously measured in the region, suggesting the significance of this site's location inside a semi-protected area. However when fluxes were separated by 60° wind sector, we saw that particular sectors, corresponding to the location of particular features led to the increased fluxes, for example the ephemeral wetland and the gallery forest. Our site may also have a higher level of topography than regional sites, creating these anomalies. The significance of these irregularities for surface-atmosphere interactions, suggested that their contribution is more important than their area alone. Conservation efforts focused on preserving the hydrologic services of a region need to take these anomalies into particular account and cultural institutions that protect, for example, wetlands and gallery forests need to be reinforced. In addition to fully comprehend their contribution to regional surface-atmosphere exchange, more thorough measurements and estimations need to be developed. These anomalies in the exchanges mean that scarce observations could have enormous consequences for regional calculations. Monitoring needs to occur at a high resolution in order to observe these important anomalies. We recommend developing of techniques to use eddy-covariance measurement to improve estimates with more easily maintained and obtained meteorological data and stations and satellite data and explore these possibilities in subsequent chapters.

2.6 References

- Albertson, J.D., Parlange, M.B. (1999). Surface length scales and shear stress: Implications for land-atmosphere interaction over complex terrain. *Water Resources Research*, 35(7), 2121-2132.
- Arbonnier, M. (2004). *Trees, Shrubs and lianas of West African dry Zones*. MNHN: CIRAD.

- Aubinet, M., Feigenwinter, C., Heinesch, B., Laffineur, Q., Papale, D., Reichstein, M., Rinne, J., Van Gorsel, E. (2012). Nighttime Flux Correction. In: Aubinet, M. et al. (eds.), *Eddy Covariance: A Practical Guide to Measurement and Data Analysis*, Springer Atmospheric Sciences.
- Bagayoko, F., Yonkeu, S., Elbers, J., & van de Giesen, N. (2007). Energy partitioning over the West African savanna: Multi-year evaporation and surface conductance measurements in Eastern Burkina Faso. *Journal of Hydrology*, 334(3-4), 545–559.
- Baldocchi, D. D., & Rao, K. S. (1995). Intra-field variability of scalar flux densities across a transition between a desert and an irrigated potato field. *Boundary-Layer Meteorology*, 76, 109–136.
- Beyrich, F., & Mengelkamp, H.-T. (2006). Evaporation over a Heterogeneous Land Surface: EVA_GRIPS and the LITFASS-2003 Experiment—An Overview. *Boundary-Layer Meteorology*, 121(1), 5–32.
- Bou-Zeid, E., Meneveau, C., & Parlange, M. B. (2004). Large-eddy simulation of neutral atmospheric boundary layer flow over heterogeneous surfaces: Blending height and effective surface roughness. *Water Resources Research*, 40(2).
- Boulain, N., Cappelaere, B., Ramier, D., Issoufou, H. B. A., Halilou, O., Seghier, J., & Timouk, F. (2009). Towards an understanding of coupled physical and biological processes in the cultivated Sahel—2. Vegetation and carbon dynamics. *Journal of Hydrology*, 375(1), 190-203.
- Brutsaert, W. (1982). *Evaporation into the Atmosphere: Theory, History, and Applications*. Dordrecht, The Netherlands: Kluwer Academic Publishers.
- Brutsaert, W., & Parlange, M. B. (1998). Hydrologic cycle explains the evaporation paradox. *Nature*, 396(6706), 30-30.
- Burba, G. (2005). *Eddy Covariance Method for Scientific, Industrial, Agricultural and Regulatory Applications*. Licor Biosciences.
- Cappelaere, B., Descroix, L., Lebel, T., Boulain, N., Ramier, D., Laurent, J. P., & Quantin, G. (2009). The AMMA-CATCH experiment in the cultivated Sahelian area of south-west Niger—Investigating water cycle response to a fluctuating climate and changing environment. *Journal of Hydrology*, 375(1), 34-51.
- Childs, S.W. and Flint, A.L. (1990). Physical properties of forest soils containing rock fragments. In: Gessel, S.P., Lacate, D.S., Weetman, G.F., Powers, R.F. (Eds.), *Sustained Productivity of Forest Soils*, University of British Columbia, Faculty of Forestry Publications, Vancouver, B.C. 95–121
- Clark, A. (2001). Modeling the Impact of Land Surface Degradation on the Climate of Tropical North Africa, (1995), 1809–1822.
- Clark, A. (2004). Feedback between the Land Surface and Rainfall at Convective Length Scales, 625–639.
- Compaore, H., Hendrickx, J. M., Hong, S. H., Friesen, J., van de Giesen, N. C., Rodgers, C., & Vlek, P. L. (2008). Evaporation mapping at two scales using optical imagery in the White Volta Basin, Upper East Ghana. *Physics and Chemistry of the Earth, Parts A/B/C*, 33(1), 127-140.
- Eichinger, W. E., Parlange, M. B., & Stricker, H. (1996). On the Concept of Equilibrium Evaporation and the Value of the Priestley-Taylor Coefficient. *Water Resources Research*, 32(1), 161–164.
- Ezzahar, J., Chehbouni, A., Hoedjes, J., Ramier, D., Boulain, N., Boubkraoui, S., & Timouk, F. (2009). Combining scintillometer measurements and an aggregation scheme to estimate area-averaged latent heat flux during the AMMA experiment. *Journal of Hydrology*, 375(1), 217-226.
- Farhadi, L. (2012). *Estimation of Land Surface Water and Energy Balance Flux Components and Closure Relation Using Conditional Sampling*. PhD Dissertation. Department of Civil and Environmental Engineering, Massachusetts Institute of Technology.
- Foken, T. (2008). The energy balance closure problem: An overview. *Ecological Applications*, 18(6), 1351-1367.
- Foken, T., Leuning, R., Oncley, S.R., Mauder, M., Aubinet, M. (2012). Corrections and Data Quality Control. In: Aubinet, M. et al. (eds.), *Eddy Covariance: A Practical Guide to Measurement and Data Analysis*, Springer Atmospheric Sciences.
- Foken, T., Mauder, M., Liebethal, C., Wimmer, F., Beyrich, F., Leps, J.-P., Raasch, S., DeBruin, H.A.R., Meijninger, W.M.L., Bange, J. (2010). Energy balance closure for the LITFASS-2003 experiment. *Theoretical and Applied Climatology*, 101(1-2), 149–160.
- Gash, J. H. C., Shuttleworth, W. J., Lloyd, C. R., André, J.-C., Goutorbe, J.-P., & Gelpe, J. (1989). Micrometeorological measurements in Les Landes Forest during HAPEX-MOBILHY. *Agricultural and Forest Meteorology*, 46(1), 131–147.
- Goodrich, D. C., Chehbouni, A., Goff, B., Macnish, B., Maddock, T., Moran, S., Shuttleworth, W.J., Williams, D.G., Watts, C., Hipps, L.H., Cooper, D.I., Schieldge, J., Kerr, Y.H., Arias, H., Kirkland, M., Carlose, R., Cayrol, P., Kepner, W., Jones, B., Avissar, R., Begue, A., Nonnefond, J.-M., Boulet, G., Branan, B., Brunel, J.P., Chen, L.C., Clarke, T., Davis, M.R., DeBruin, H., Dedieu, G., Eguero, E., Eichinger, W.E., Everitt, J., Garatuza-Payan, J., Gempko, V.L., Gupta, H., Harlow, C., Hartogensis, O., Helfert, M., Holifield, C., Hymer, D., Kahle, A., Keefer, T., Krishnamoorthy, S., Lhomme, J.-P., Lagouarde, J.-P., Lo Seen, D., Luquet, D., Marsett, R., Monteny, B., Ni, W., Nouvellon, Y., Pinker, R., Peters, C., Pool, D., Qi, J., Rambal, S., Rodriguez, J., Santiago, F., Sano, E., Schaeffer, S.M., Schulte, M., Scott, R., Shao, X., Snyder, K.A., Sorooshian, S., Unkrich, C.L., Whitaker, M., Yucel, I., (2000). Preface paper to the Semi-Arid Land-Surface-Atmosphere (SALSA) Program special issue, 105(D), 3–20.

- Goutorbe, J.-P., Lebel, T., Tinga, A., Bessemoulin, P., Brouwer, J., Dolman, A. J., Engman, E.T., Gash, J.H.C., Hoepffner, M., Kabat, P., Kerr, Y.H., Monteny, B., Prince, S., Said, F., Sellers, P., Wallace, J. S. (1994). HAPEX-Sahel: a large-scale study of land-atmosphere interactions in the semi-arid tropics. *Annales Geophysicae*, 12(1), 53–64.
- Guichard, F., Lergoat, L., Mougin, E., Timouk, F., Baup, F., Hiernaux, P., & Lavenu, F. (2009) Surface thermodynamics and radiative budget in the Sahelian Gourma: Seasonal and diurnal cycles. *Journal of Hydrology*. 375: 161-177.
- Guo, Z., Dirmeyer, P. A., Koster, R. D., Bonan, G., Chan, E., Cox, P., Gordon, C.T., Kanae, S., Kowalczyk, E., Lawrence, D., Liu, P., Mocko, D., Oki, T., Oleson, K.W., Pitman, A., Sud, Y.C., Taylor, C.M., Verseghy, D., Vasic, R., Youngkang, X., Yamada, T. (2006). GLACE : The Global Land – Atmosphere Coupling Experiment . Part II : Analysis. *American Meteorological Society*, 7, 611–625.
- Guyot, A., Cohard, J. M., Anquetin, S., Galle, S., & Lloyd, C. R. (2009). Combined analysis of energy and water balances to estimate latent heat flux of a sudanian small catchment. *Journal of Hydrology*, 375(1), 227-240.
- Horst, T. W. (1999). The footprint for estimation of atmosphere-surface exchange fluxes by profile techniques, (July 1998), 171–188.
- Hsieh, C. I., Katul, G., & Chi, T. W. (2000). An approximate analytical model for footprint estimation of scalar fluxes in thermally stratified atmospheric flows. *Advances in Water Resources*, 23(7), 765-772.
- Kabat, P., Dolman, A.J., Elbers, J.A. (1997). Evaporation sensible heat and canopy conductance of fallow savanna and patterned woodland in the Sahel. *Journal of Hydrology*, 188-189, 494-515.
- Krishnan, P., Meyers, T. P., Scott, R. L., Kennedy, L., & Heuer, M. (2012). Energy exchange and evapotranspiration over two temperate semi-arid grasslands in North America. *Agricultural and Forest Meteorology*, 153, 31–44.
- Larmuth, L. (1978). Temperatures beneath stones used as daytime retreats by desert animals. *Journal of Arid Environments*, 1, 34–40.
- Le Barbé, L., Lebel, T., & Tapsoba, D. (2002). Rainfall variability in West Africa during the years 1950-90. *Journal of Climate*, 15(2), 187-202.
- Leuning, R. (2007). The correct form of the Webb, Pearman and Leuning equation for eddy fluxes of trace gases in steady and non-steady state, horizontally homogeneous flows. *Boundary-Layer Meteorology*, 123, 263-267.
- Liebethal, C., Huwe, B., & Foken, T. (2005). Sensitivity analysis for two ground heat flux calculation approaches. *Agricultural and Forest Meteorology*, 132(3), 253-262.
- Mauder, M., Jegede, O. O., Okogbue, E. C., Wimmer, F., & Foken, T. (2006). Surface energy balance measurements at a tropical site in West Africa during the transition from dry to wet season. *Theoretical and Applied Climatology*, 89(3-4), 171–183.
- Parlange, M. B., Eichinger, W. E., & Albertson, J. D. (1995). Regional scale evaporation and the atmospheric boundary layer. *Reviews of Geophysics*, 33(1), 99-124.
- Ramier, D., Boulain, N., Cappelaere, B., Timouk, F., Rabanit, M., Lloyd, C. R., & Wawrzyniak, V. (2009). Towards an understanding of coupled physical and biological processes in the cultivated Sahel–1. Energy and water. *Journal of Hydrology*, 375(1), 204–216.
- Rebmann, C., Kolle, O., Heinesch, B., Queck, R., Ibrom, A., & Aubinet, M. (2012). Data acquisition and flux calculations. In *Eddy Covariance* (pp. 59-83). Springer Netherlands.
- Rigby, J.R. (2009). Intermittency and Irreversibility in the Soil-Plant-Atmosphere System Intermittency and Irreversibility in the Soil-Plant-Atmosphere System. Duke University.
- Schüttemeyer, D., Moene, A. F., Holtslag, A. A. M., De Bruin, H. A. R., & Van De Giesen, N. (2006). Surface fluxes and characteristics of drying semi-arid terrain in West Africa. *Boundary-layer meteorology*, 118(3), 583-612.
- Siqueira, M., Katul, G., & Porporato, A. (2009). Soil Moisture Feedbacks on Convection Triggers: The Role of Soil–Plant Hydrodynamics. *Journal of Hydrometeorology*, 10(1), 96–112.
- Szilagy, J., & Parlange, M. B. (1999). Defining Watershed-Scale Evaporation Using a Normalized Difference Vegetation Index. *Journal Of The American Water Resources Association*, 35(5), 1245–1255.
- Taylor, C. M. (2008). Intraseasonal Land–Atmosphere Coupling in the West African Monsoon. *Journal of Climate*, 21(24), 6636–6648.
- Timouk, F., Kergoat, L., Mougin, E., Lloyd, C. R., Ceshia, E., Cohard, J.-M., de Rosnay, P., Hiernaux, P., Demarez, V., Taylor, C. M. (2009). Response of surface energy balance to water regime and vegetation development in a Sahelian landscape. *Journal of Hydrology*, 1–43.

- Verhoef, A., Ottlé, C., Cappelaere, B., Murray, T., Saux-Picart, S., Zribi, M., Maignan, F., Boulain, N., Demarty, J., Ramier, D. (2012). Spatio-temporal surface soil heat flux estimates from satellite data; results for the AMMA experiment at the Fakara (Niger) supersite. *Agricultural and Forest Meteorology*, 154-155, 55–66.
- Webb, E.K., Pearman, G.I., Leuning, R. (1980). Correction of flux measurements for density effects due to heat and water vapour transfer. *Quarterly Journal Royal Meteorology Society*, 106, 85–100.
- White, F. (1986). *La végétation de l'Afrique: Memoire accompagnant la carte de vegetation de l'Afrique* (p. 389).
- Wilczak, J. M., Oncley, S. P., & Stage, S. A. (2001). Sonic anemometer tilt correction algorithms, 127–150.
- Williams, C. A., Reichstein, M., Buchmann, N., Baldocchi, D., Beer, C., Schwalm, C., Schaefer, K. (2012). Climate and vegetation controls on the surface water balance: Synthesis of evapotranspiration measured across a global network of flux towers. *Water Resources Research*, 48(6), W06523.

Fascination with evaporation is not a new phenomenon, for example, Leonardo Da Vinci described the “humidity excess that is in the air” falling and rising sustained by heat over 500 years ago (Pfister, 2009). Hesiod in the 8th century B.C. observed that mist is drawn from rivers, travels by wind, and returns by storm and rain (Brutsaert, 1982). However quantifying evaporation presents a complex challenge that is not just a sampling or measurement technique problem, but also a scale problem. When we measure evaporation, it is not over a point, but rather a changing area (Brutsaert, 1982). Overcoming these challenges has been attempted by direct measurements, such as pans and lysimeters, formulae using knowledge of the atmospheric processes, and budget methods that close coupled or separate energy and water budgets in a given area (Jackson, 1999).

More precisely, because water vapor, momentum, and sensible heat are all transported by turbulent fluxes, they can be calculated using direct measurements of vertical velocity fluctuations and scalar concentration fluctuations (Brutsaert, 1982). The latent energy flux is the product of the vertical velocity fluctuations and those of water vapor concentration. Sensible heat flux is similarly calculated as the product of the vertical velocity fluctuations and the temperature fluctuations. Although simple theoretically, it requires that measurements take place at least at 5 Hz and preferably at 20 Hz, thus instrumentation is quite expensive and requires considerable expertise to maintain. The eddy-covariance method has only been used a limited number of times in West Africa, as discussed in the previous chapter (Schuttemeyer et al., 2006; Bagayoko et al., 2007; Mauder et al., 2006; Guichard et al., 2009; Timouk et al., 2009; Goutorbe et al., 1994; Gash et al., 1997; Guyot et al., 2009).

A number of theoretical methods have been proposed in order to estimate evaporation with less expensive equipment, but each also has its own challenges of measurement, scale, and precision. In 1956, Monin-Obukov proposed the use of a similarity theory that only requires simple measurements at multiple heights. Monin Obukov similarity theory allows estimation of the vertical profiles of wind speed, momentum, heat and water vapor fluxes. The theory is based on the assumption that the turbulent transport of one quantity is proportional to the turbulent diffusivity and the vertical gradient in mean concentration (Hippis & Kustas, 2000).

Monin-Obukhov hypothesized that atmospheric properties, normalized by the friction velocity, u^* , and Monin-Obukhov length, L , are universal functions of the non-dimensional number, reference height over Monin-Obukhov length, z/L . This method has proved essential for many surface boundary studies, however its universality and the methods used to determine unknown coefficients iteratively or empirically have been questioned by Farhadi (2012). Moreover, the application of Monin-Obukhov similarity theory is specific for the surface layer, which is the part of the boundary layer at the surface whose depth will vary less 10% in 1000 km (Stull, 1988). Note that Monin-Obukhov similarity works only when there is wind and u^* , the friction and shear velocity, is not zero. Homogeneity is such an important aspect that deviation from Monin-Obukhov similarity theory predictions has been used as an indicator of heterogeneity (Hippis & Kustas, 2000). On strongly convective days when L is much greater than the roughness length, there is a layer that both MOST and a mixed-layer theory can apply. Deardorf (1970) suggested that as soon as convection develops, the eddy size is proportional to the mixing depth and turbulence occupies the whole space.

In the previous chapter, we successfully compared evaporation from a catchment in South Eastern Burkina Faso over an agricultural-fallow area and a natural wooded savanna- forest using established eddy-covariance methods. Here, we use similarity theory to demonstrate the use of small, less expensive, and easily deployable meteorological stations to calculate evaporation.

The calculation of evaporation using data from these stations allows us to observe the variation in evaporation according to land cover. This calculation allows for improved scientific understanding of evaporation from West African vegetation and land surfaces and has the potential to inform local reforestation and agricultural management. In addition, results from this work could be incorporated into an agricultural extension project, so that farmers can make more informed decisions regarding their land-use. For example, Knoche et al. (2010) discuss their efforts to bring similar information and communication technologies to rural farmers in

India who share many characteristics in terms of education, farming strategy, and climatic constraints with our farmers. In their case, they focus on soil moisture, but they found that information about basic hydrological processes governing crop prediction is extremely interesting to local farmers and that similar technology had a place overcoming challenges of farming in extremes of climate/weather.

In this chapter, we present our calculation of evaporation from the low-cost meteorological stations using similarity theory. We discuss the advantages and shortcomings of this method in the context of a remote site where information could make a difference to both immediate, local livelihoods and in global predictions.

3.2 Methods

In general, we determined the evaporation across the catchment by first deterring several specific constant ratios and a reference energy balance at points of high precision and then computing each component consecutively through an iterative cycle of the energy budget using these constant ratios across the catchment. The points of high precision were situated over different land covers from each other in order to begin to capture the variation of the catchment. These were the 2 eddy-covariance stations described in the last chapter. The constant ratios were albedo (α), conversion rate (cr) from ground heat flux to net radiation, and roughness length (z_0). These constant ratios were needed for all steps of the calculation of evaporation at the stations. To capture the variability of the watershed, our distributed sensors was composed of relatively less expensive metrological equipment situated on as many different land covers as possible. We began the calculation at each of these stations by first calculating net radiation based on measurements of incoming shortwave radiation and temperature and the corresponding estimate of ground heat flux. We then solved the similarity equations for sensible heat flux and monin-obukov length using wind speed and temperature data from each station. We then solved for evaporation by assuming closure of the energy budget, since we knew the three other components. We then iterated by using this estimate of evaporation to improve our calculation of Monin-Obukov length. I will now go into more detail regarding each of those steps and the data collection locations and processes.

3.2.1 Study Site

This study took place in a catchment near the village of Tambarga in the commune of Madjoari in the Kompienga region of Burkina Faso defined by the discharge point at 11.44176°N and 1.215841°E (Figure 1-1). The study site is located in the Sudanian woodland vegetation zone. As White (1986) describes, most trees in this endemic group are spread out over a large area, along both east west and north south transects, are very adaptive phenotypically and in terms of ecologic communities. This vegetation type has also witnessed some of the largest impact from human agricultural use, and thus is perhaps one of the most anthropogenic driven assemblages on the continent, meaning the evolution of both the species and the communities as been heavily influence by human behavior (White, 1986). Topographical relief is minimal in this area - and variations between vegetation types are gradual. The experimental watershed was chosen in the community of Tambarga based on regional land cover transects and a participatory mapping workshop which helped to align local needs with scientific questions surrounding links between vegetation and hydrology. The watershed covers 4 km² and includes agricultural parkland (rice, millet, and corn fields interspersed with mango, marula, and fig trees), Sudanian savanna used for grazing of cattle, and a dense gallery forest in the valley surrounding persistent springs emerging from the escarpment. The catchment is defined by a small ephemeral stream with an average discharge of 0.03 m³/s and a maximum discharge of 0.52 m³/s during the rainy season. Vegetation varies seasonally with the rainy season that begins in May and lasts through October, and by December most vegetation has been burned.

Two large meteorological stations equipped to calculate and measure three components of the energy budget from measurements of sensible and latent heat fluxes and net radiation and 11 small meteorological stations which could measurement air

temperature, humidity, surface temperature, wind speed, wind direction, rainfall, solar radiation and soil moisture and temperature, were installed at points representative of the topographic and land cover variation and extremes in the catchment, specifically representing heterogeneous land cover: rocky escarpment, seasonal tall grass savanna, wooded savanna, bare ground, fallow fields, millet, corn, and rice cultivated fields, river bank, and ephemeral wetlands. Equipment was installed in May 2009, maintained through October 2010, reinstalled in May 2011 to a lesser extent and is still being maintained (October 2013). These continuous meteorological measurements were complimented by field observation, hand measurements, and additional hydrological and botanical observation.

Small meteorological stations (Sensorscope) made up a network of wireless sensors (Appendix IV) that upload data directly through a GSM connection in a local base station. Sensorscope stations route data through the network of stations to be delivered by a GPRS connection to a main server. Sensorscope meteorological stations rely on a multi-hop network of wireless sensors that are energetically autonomous with their own solar panel and allow for an easy, quick deployment, adapted to this environment, and uniquely configured (Inglrest, 2010). This network allows data to be gathered over a large area and quickly adapts to changes in station performance, for example if donkeys took down one station. Data are available in real time via a website that can be accessed by a mobile phone. Small photovoltaic panels power the stations autonomously. This deployment is the first time that these meteorological stations have been used on the African continent. Details of all stations and sensors in the catchment that are used in this analysis are presented in Table 3-1; 0 & IV.



Figure 3-1S. Sensorscope station in the savanna (May 28, 2009). Anemometer, temperature and humidity sensor, surface temperature, radiometer, wires leading to soil moisture sensors, and rain gauge are visible.

Instrument	Measurement	Height/ Depth	Number Present	Interval
Large Meteorological Station				
CSAT-3 Sonic Anemometer (Campbell Scientific)	3D Wind speed and Direction, Air Temperature	2.2 m	3	20 Hz, proc. 30 min.
LI-7500 Infrared Gas Analyzer (LICOR)	CO ₂ H ₂ O Concentration	2.2 m	3	20 Hz, proc. 30 min.
CNR2 Radiometer (Kipp & Zonen)	SW-net, LW-net Radiation	2.1 m	2	1 min.
HMP450/Campbell Scientific with Radiation Shield	Air Temperature, Air Humidity	2.25 m	2	1 min.
Apogee/ Campbell Scientific	Surface Temperature	2 m	2	1 min.
Hukseflux Heat Flux Plates (Campbell Scientific)	Ground Heat Flux	< 5 cm	2	1 min.
Precis Instruments (3029)	Precipitation	1 m	1	0.1 mm
Sensorscope Stations				
Davis Anemometer	Wind Speed, Direction	1.9 m	12	1 min.
Sesirion SHT7	Air Temperature, Air Humidity	1.7 m	12	1 min.
TNX Near Infra Red Sensor	Surface Temperature	1.1 m	12	1 min.
Davis Radiometer	Incoming Short Wave Radiation	1.8 m	12	1 min.
Decagon 5TM, ECTM, MPS1	Soil Moisture, Soil Temperature, Water Pressure	5-30 cm	24*	1 min.
Rain Gauge (Davis)	Precipitation	52 cm	12	1 min.

Table 3-1. Sensors present at the Eddy – Correlation and Sensorscope stations with the name of each instrument, the measurement taken, the height or depth, the number present and the interval for each.

3.2.2 Measurement of Evaporation

Evaporation was first determined by calculating the eddy covariance from the energy balance station. Evaporation is determined by computing the cross correlation of the measured fluctuations of vertical wind speed and humidity (chapter 2). Energy fluxes were monitored simultaneously at two points, in the field and on top of the rocky escarpment, as described in more detail in the previous chapter, but following the general equations repeated below and using the equipment listed in Table 3-1. Of particular interest in our calculation is that ground heat flux was calculated as a remainder of the sensible heat flux (H) and latent heat flux (LE) subtracted from the net radiation (R_n). We then can calculate a conversion ratio, Cr, which is the fraction of net radiation that is converted to ground heat flux.

$$\text{Sensible heat flux:} \quad H = \rho c_p \overline{w'T'} \quad [W/m^2] \quad (3-1)$$

$$\text{Latent energy flux:} \quad LeE = L_e \rho \overline{w'q'} \quad [W/m^2] \quad (3-2)$$

$$\text{Conversion Ratio:} \quad Cr = \frac{R_n - LE - H}{R_n} \quad [\%] \quad (3-3)$$

$$\text{Ground heat flux:} \quad G = Cr * R_n = R_n - LeE - H \quad [W/m^2] \quad (3-4)$$

The measurement of evaporation was determined by eddy covariance at two points, up on the hill, and down in the field, which are the two most distinct land covers in this basin. These points were used as references to compare with the nearest low-cost meteorological stations.

3.2.3 Ground Heat Flux and Albedo

Values of albedo, α , and ground heat flux as a percent of total net radiation, Cr, are calculated at each flux tower by day with a 3-day window, which is thought to be a sufficiently long period to overlook fluctuations due to the diurnal cycle or irregularities within the day, but short enough to observe changes to due vegetation growth. Energy flux measurements calculated at the flux tower are used as a comparison with those calculated at the closest point in the distributed sensor network. Initial calibration with

measures from 2 eddy covariance stations (EC) allows us to calculate the energy balance at each of the Sensorscope stations (SS). Albedo is the ratio of the reflected radiation (R_{su}) to the incoming radiation (R_{sd}). Darker surfaces will absorb more light whereas lighter surfaces will reflected it all.

Albedo:
$$\alpha = \frac{R_{su}}{R_{sd}} = 1 - \frac{R_{sn}}{R_{sd}} = 1 - \frac{R_{sd} - R_{su}}{R_{sd}} \quad (3-5)$$

In order to obtain a daily value, I performed a robust multilinear regression of, for albedo, the net shortwave measured (R_{sn}) at the eddy-covariance station against the incoming short wave at each SS station. Albedo is then equal to one minus the slope of this line (3-5). To determine, C_r , the same method is used but the fit is between the net radiation and the remainder after the sensible and latent heat fluxes was subtracted from the net radiation. This robust fit uses iteratively reweighted least squares and bisquare weighting (Huber, 1981).

In addition, a sunny day was defined as having more than 70% of the theoretical incoming radiation according to Whiteman & Alline (1996). The other days were excluded for this calculation. Also, values of albedo greater than 0.4, the highest non-snow value, were eliminated because they are not realistic for our study site (Brutsaert 1982). Missing values for days were interpolated linear using those calculated.

Radiative shields surrounding air temperature sensors created sensor heating, leading to a bias in measurement. These errors can be corrected for with equation 3-7 (Huwald et. al 2009). This correction takes into account radiative errors caused by the surface-reflected short wave error. Temperature error was found to fall along the curve as expected by Huwald et al. (2009) for both stations. This correction was used for all temperature measurements in standard solar radiation shields.

Air Temperature Correction
$$\Delta T = 3.1 \left(\frac{SW_u 10^3}{\rho c_p u T} \right)^{0.5} \quad (3-6)$$

3.2.4 Radiation

Net radiation is the sum of net long- and short - wave radiation. Where shortwave radiation in the albedo subtracted from one multiplied by the incoming shortwave radiation, and net long wave radiation is the sum of incoming long wave radiation and reflected long wave radiation (equation 3-8). The long wave upward radiation was calculated as the product of the surface emissivity, the Stefan-Boltzmann constant, and the fourth power of the surface temperature (3-9). And the incoming long wave radiation was calculated using the saturation vapor pressure, the Stefan-Boltzmann constant, and the air temperature (3-10 and 3-11). These were determined according to Brutsaert (1982) for each Sensorscope station and compared with the closest net radiometer. Emissivity, $\epsilon_s = 0.97$ for grass; ϵ_{ac} is a constant dependent on the saturation vapor pressure; Stefan-Boltzmann Constant, $\sigma = 0.97$ Radiation was calculated at each small station separately for short and long wave components. Constants and variables are explained in more detail in the following tables (Table 3-2; Table 3-3).

Net Radiation :
$$R_n = R_s(1 - \alpha) + \epsilon_s R_{lu} - R_{ld} \quad (3-7)$$

Long wave upward radiation :
$$R_{lu} = \epsilon_s \sigma T_s^4 \quad (3-8)$$

Long wave down radiation :
$$R_{ld} = \epsilon_{ac} \sigma T_a^4 \quad \text{where} \quad \epsilon_{ac} = a \left(\frac{e_a}{T_a} \right)^m \quad (3-9)$$

Vapor Pressure near surface :
$$e_a = \frac{RH * e_{sat}}{100} \quad [\text{mb}] \quad (3-10)$$

Where e_{sat} is a function of the temperature ratio between the steam point temperature (373.16°K) and the air temperature and the saturation vapor pressure at steam point (1013.25 hPa). We let m equal 1/7 and calculated as a function of, ultimately, T_a (Brutsaert 2005, 1982).

3.2.5 Roughness length

Roughness length (z_0) at the surface is a measure in length of how smooth or rough the surface is. It is a central variable in the similarity equations (3-12). We calculated it by solving the similarity equations at the EC station where we had measures of sensible heat (H), humidity (θ), and Monin-Obukov length (L) for z_0 independently for the two directions with 10 iterations each and then averaging by month (3-11). Since eddy covariance equipment were sonics and Licors pointing in both directions, we could make the calculation independently for each set, and thus obtaining an idea of the roughness in the two opposite cardinal directions. We began the iterative calculation with the initial monthly values for the region from Bagayoko (2007). Brutsaert (1982) would expect that for short average crops, $z_0=0.25$ m. We set the displacement height (d_0) equal to zero.

$$\ln\left(\frac{z-d_0}{z_0}\right) = \frac{\bar{u}k}{u_*} + \Psi_m\left(\frac{z-d_0}{L}\right) - \Psi_m\left(\frac{z_0}{L}\right)$$

$$\ln\left(\frac{z-d_0}{z_{0h}}\right) = \frac{(\theta_s - \bar{\theta})(ku_*\rho c_p)}{H} + \Psi_h\left(\frac{z-d_0}{L}\right) - \Psi_h\left(\frac{z_{0h}}{L}\right) \quad (3-11)$$

We calculated vapor pressure and specific humidity according to Brutsaert (2005).

We used the Monin-Obukov length (L) calculated at the EC station to initiate, but once we had latent heat flux estimates for each station, we used a value specific to each station. We only used daytime values and the friction velocity is greater than 0.25. We solved the similarity equations below for roughness length by iterating ten times and using the average of all ten outputs. Notice there are two roughness lengths – z_0 and z_{0h} , one is for momentum and the other for heat.

Roughness Reynolds number $z_0^+ = u^*/k_{vi}$ **(3-12)**

The roughness Reynolds number is less than 0.13 when a surface is hydronamically smooth and greater than 2 when hydronamically rough (Brutsaert, 1982). For smooth surfaces, the roughness length of heat can be calculated as

Smooth z_{0h} $z_{0h} = 0.395 v/u^*$ **(Brutsaert, 1982, pp123) (3-13)**

Bluff z_{0h} $z_{0h} = z_0 * 7.4 * e^{-2.46 * z_0^+.25}$ **(Brutsaert, 1982, pp123) (3-14)**

The Schmidt number $Sc = \nu/k_v$ **Brutsaert, 1982 (3-15)**

The Schmidt number is a non-dimensional number, and we need to calculate to calculate the Dalton number, another non-dimensional number. .

The Dalton number $Da_0 = C_R z_0^{+1/4} Sc^{-1/2}$ **Brutsaert, 1982 p94 (3-16)**

Permeable Bluff $z_{0h} = z_0 / e^{k(a_{vh} St_0^{-1} - Cd_0^{-1/2})}$ **Brutsaert, 1982 p105 (3-17)**

With the canopy layer drag coefficient, $Cd_0^{-1/2}$, ranging from 2.5 to 15 depending on the upper boundary of the interfacial sublayer (Brutsaert, 1982: 93-105). With $av_h=1.35$ and $k=0.35$ (Brutsaert, 1982: 68). We found a drag coefficient of 15 by comparing the

roughness length for sensible heat with that calculated (Figure 3-4). The permeable bluff surface requires the Stanton number, another non-dimensional number.

The Stanton number is given as

$$\frac{H}{\rho u^* c_p (\theta_s - \theta_a)}$$

Brutsaert 1982 p88 (3-18)

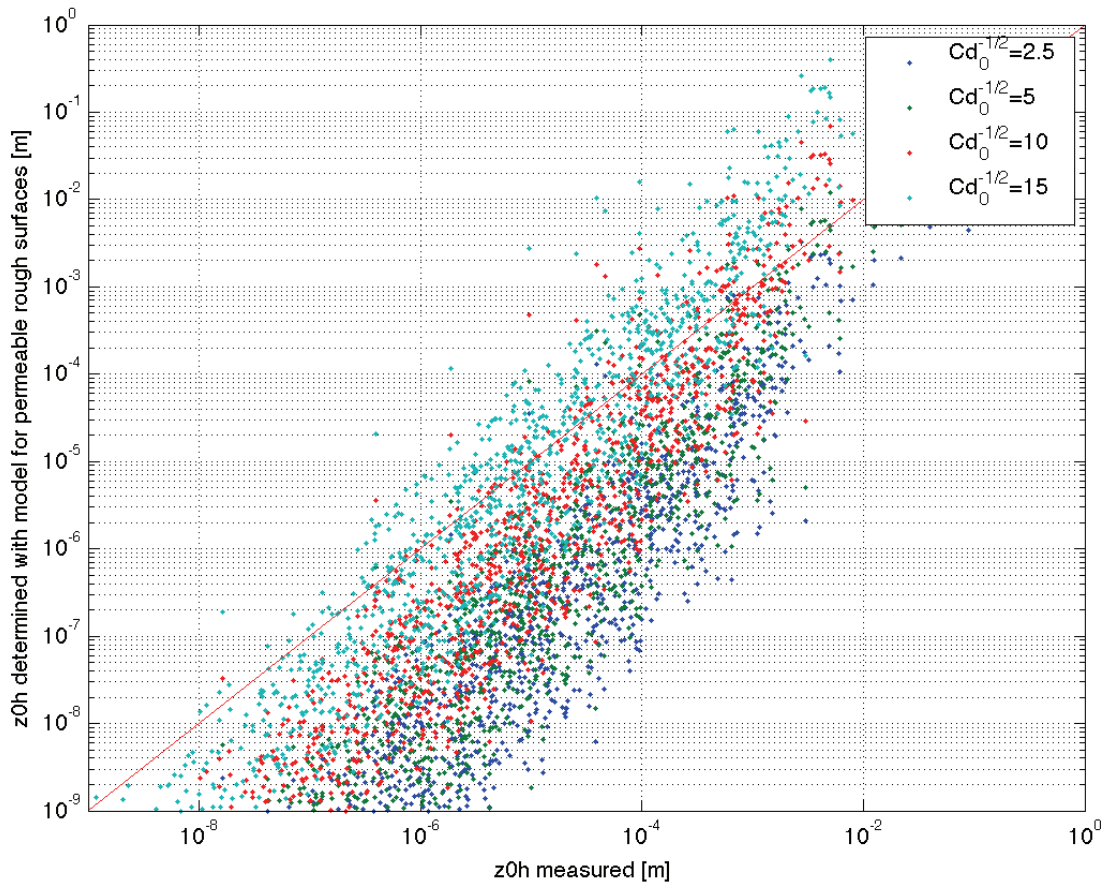


Figure 3-2 Comparison of Z_{0h} determined 2 ways. On the x – axis is Z_{0h} that was determined at the eddy-covariance equipment from the measurements of wind speed and on the y-axis is Z_{0h} determined with equation (3-17) for permeable bluff surfaces based on the Dalton number and drag coefficient. We solved for the best drag coefficient shown with the color. The correct drag coefficient to the order of 15, in turquoise, gave the best fit between modeled and measured roughness lengths.

By comparing our calculations with the modeled values (Figure 3-5), we observe that our surface conforms best to the permeable rough calculation of z_{0h} . The rule of thumb of 10%, that the roughness length for heat, z_{0h} , is ten percent of the general roughness length, z_0 , applies for April through June but by July, there is considerable scatter in the data. By late October, the bluff rough surface is the only one that our data conforms to. Brutsaert's points correspond to short grass (1), medium grass (2), bean crop (3), savanna scrub (4), and 5 and 6 are pine forest (1982). Our measurements over the agricultural field conform to points 1-3 for part of the season (Figure 3-5).

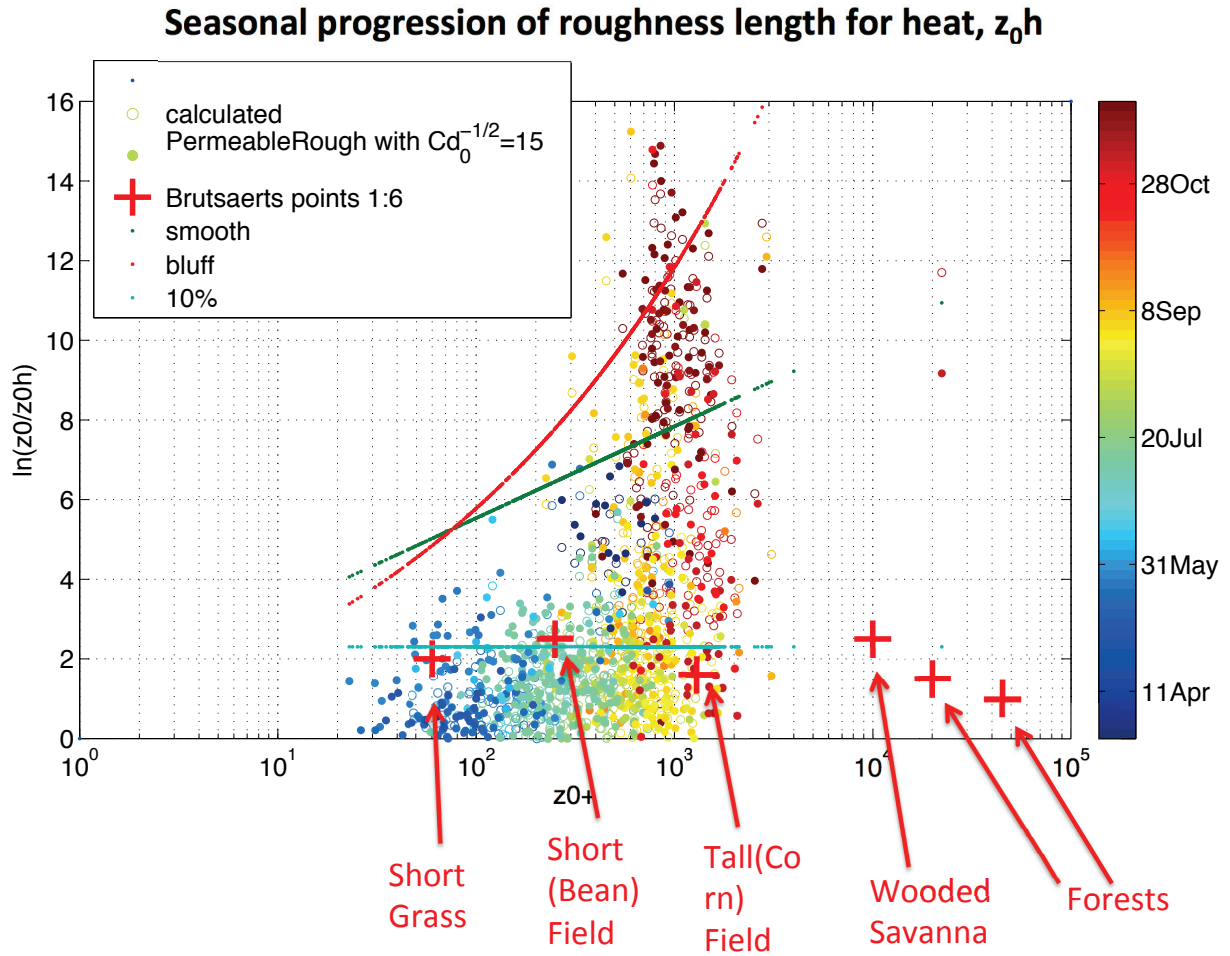


Figure 3-3 Seasonal Progression of Roughness Length For Heat : compares the calculation of the roughness length for heat, z_0h (displayed as $\ln(z_0/z_0h)$) through a number of different means and the season. The season is shown with the colorbar – April in blue to November in Red, corresponding with the growth of vegetation. The points calculated with the measured high resolution wind speeds are open circles whereas those that follow the equations for permeable bluff (3-17) are closed circles, those that follow a « smooth » surface are green (equation 3-13), those that follow a « bluff » surface are red (equation 3-14), and finally the rule of thumb that the roughness length for heat is a tenth of the general roughness length are in turquoise. Additionally, six points are shown that were calculated from different land surfaces ranging in vegetation height from short grass to forests. Our data, taken from the field, clearly falls in the range expected for short grass, short fields, and tall fields during all but the final months – October and November when the vegetation is very dry and rough. Similarly, the ten percent rule seems to be a reasonable estimate for all but the final months as well. During the the final months, it varies quite a bit with an upper limit defined by the red, bluff surface, a reasonable average by the smooth surface, but by far the best prediction estimated by the permeable rough.

3.2.6 Monin-Obukhov Theory

Thirty minute averaged data are used to estimate components of the energy budget based on the Monin-Obukov similarity theory (Monin, 1959). Tables 3-2 and 3-3 show the overview of the variables and constants used in the following equations. Initially, friction velocity is calculated just as a function of wind speed, and roughness lengths; Sensible heat flux as a function of temperature, friction velocity, and roughness lengths; And latent heat flux as a remainder subtracted from the net radiation.

Friction velocity
$$u^* = \frac{uk}{\ln\left(\frac{z}{z_0}\right)} \quad [\text{m/s}] \quad (3-19)$$

$$\text{Sensible Heat Flux} \quad H = \frac{(T_s - T_a)k\rho C_p u^*}{\ln\left(\frac{z_h}{z_{0h}}\right)} \quad [\text{W/m}^2] \quad (3-20)$$

$$\text{Latent Energy Flux} \quad LeE = Rn - G - H = Rn(1 - Cr) - H \quad [\text{W/m}^2] \quad (3-19)$$

But in order to calculate the evaporative flux using Monin-Obukov theory, ten iterations, recalculating each of friction velocity, H, and LE followed by a recalculation of Monin-Obukov Length, L, are performed. Latent heat flux is then recalculated with the new value of H. Note that in our calculation, we left d₀ equal to 0. Ψ_m and Ψ_h are similarity equations (3-25 and 3-26).

$$\text{Monin- Obukhov Length} \quad L = \frac{-u^{*3}}{\frac{kg}{T_a\rho}\left(\frac{H}{C_p} + 0.61T_a\left(\frac{LE}{Lvap}\right)\right)} \quad [\text{m}] \quad (3-20)$$

$$\text{Friction velocity} \quad u^* = \frac{uk}{\ln\left(\frac{z}{z_0}\right)} - \Psi_m\left(\frac{z}{L}\right) + \Psi_m\left(\frac{z_0}{L}\right) \quad [\text{m/s}] \quad (3-21)$$

$$\text{Sensible Heat Flux} \quad H = \frac{(T_s - T_a)k\rho C_p u^*}{\ln\left(\frac{z_h}{z_{0h}}\right)} - \Psi_h\left(\frac{z_h}{L}\right) + \Psi_h\left(\frac{z_{0h}}{L}\right) \quad [\text{W/m}^2] \quad (3-22)$$

$$\text{Similarity equation for momentum} \quad \ln\left(\frac{z-d_0}{z_0}\right) = \frac{\bar{u}k}{u^*} + \Psi_m\left(\frac{z-d_0}{L}\right) - \Psi_m\left(\frac{z_0}{L}\right) \quad (3-23)$$

$$\text{Similarity equation for heat flux} \quad \ln\left(\frac{z-d_0}{z_{0h}}\right) = \frac{(\theta_s - \bar{\theta})(ku^* \rho c_p)}{u^*} + \Psi_h\left(\frac{z-d_0}{L}\right) - \Psi_h\left(\frac{z_{0h}}{L}\right) \quad (3-24)$$

Measured Variable	Station where measured (or directly calculated)	Used for the Calculation of :	Calculated at SS Using :	
			Measured & Calculated Variables :	Constants :
Wind speed, <i>u</i>	SS, EC	<i>u</i> [*] , <i>z</i> ₀ , <i>z</i> _{0h}	-	-
Incoming Short-wave Solar Radiation, <i>Rsd</i>	SS	α	α , <i>Rsn</i> , <i>Rln</i> (at EC)	-
Air Temperature, <i>Ta</i>	SS, EC	<i>H</i> , <i>Rln</i> , <i>z</i> ₀ , <i>z</i> _{0h} , <i>ε</i> _{ac}	-	-
Surface Temperature, <i>Ts</i>	SS, EC	<i>H</i> , <i>Rln</i> , <i>z</i> ₀ , <i>z</i> _{0h}	-	-
Relative Humidity, <i>RH</i>	SS, EC	<i>z</i> ₀ , <i>z</i> _{0h} , <i>ε</i> _{ac}	-	-
Net Long Wave Radiation, <i>Rln</i>	EC	<i>Ref</i> , <i>Cr</i> , α	<i>Ts</i> , <i>Ta</i> , <i>ε</i> _{ac}	<i>ε</i> _s , <i>σ</i> , <i>a</i> , <i>m</i>
Net Short Wave Radiation, <i>Rsn</i>	EC	<i>Ref</i> , <i>Cr</i> , α	<i>Rsd</i> , α	-
Sensible Heat, <i>H</i>	EC (calc)	<i>Ref</i> , <i>Cr</i> , <i>z</i> ₀ , <i>z</i> _{0h}	<i>Ts</i> , <i>Ta</i> , <i>u</i> [*] , <i>z</i> _{0h} , <i>L</i>	<i>k</i> , <i>ρ</i> , <i>Cp</i> , <i>z</i> _h
Latent Heat, <i>LE</i>	EC (calc)	<i>Ref</i> , <i>Cr</i> , <i>z</i> ₀ , <i>z</i> _{0h}	<i>Cr</i> , <i>Rln</i> , <i>Rsn</i> , <i>H</i>	<i>Lvap</i>
Scalar Roughness, <i>u</i> [*]	EC (calc)	<i>z</i> ₀ , <i>z</i> _{0h}	<i>u</i> , <i>z</i> ₀ , <i>L</i>	<i>k</i> , <i>z</i>
Monin-Obukhov Length (<i>L</i>)	EC (calc)	<i>H</i>	<i>H</i> , <i>E</i> , <i>u</i> [*] , <i>Ta</i> ,	<i>Cp</i> , <i>ρ</i> , <i>k</i> , <i>g</i>
Atmospheric Pressure, <i>P</i>	EC	<i>z</i> ₀ , <i>z</i> _{0h}	-	-

Table 3-2 Interrelationships between variables measured and calculated. This table is meant to help keep the various interdependences between the variables separate. Note that in make cases, a variable is initial measured at the eddy covariance station but is then recalculated at each of the distributed points using a set of parameters determined at the eddy-covariance station as well but adapted to the land cover at the distributed points. The constants are explained in table 3-3.

Constants
Specific Heat (<i>Cp</i>) = 1012 J/kgK
Gravity (<i>g</i>) = 9.8 m/s ²
Von Karmen constant (<i>k</i>) = 0.41
Latent Heat of Vaporization (<i>Le</i>) = 2.430*10 ⁶ J/kg at 30°C

<p>Height of Wind Measurement (z) = 2 m</p> <p>Height of Temperature Measurement (z_h) = 1.7 m for SS and 2 m for EC</p> <p>Atmospheric emissivity for clear skies (ϵ_{ac}) = $(ea/Ta)^m$; $m = 1/7$</p> <p>Emissivity for grass (ϵ_s) = 0.97</p> <p>Density of dry Air (ρ) = 1.2923 kg/m³</p> <p>Stefan Boltzmann Constant (σ) = 5.8897×10^{-8} W/m²/K⁴</p> <p>Saturation Vapor Pressure (e_{sat}) = $10^{-7.90298 \cdot (TR-1) + 5.02808 \cdot \log_{10}(TR) - 1.3816e-7 \cdot (10^{(11.344 \cdot (1-TR)) - 1}) + 8.1328e-3 \cdot (10^{(-3.19149 \cdot (TR-1)) - 1}) + \log_{10}(esst)}$ [hPA]</p> <p>Coefficients : $a = m \cdot A \cdot \beta(k_1/k_2, m) \cdot (0.622 / ((k_2 \cdot R_d) \cdot 10e-5))^m$ [(mass/length²)^{1/7}]</p> <p>Intermediary Calculations $k_1 = k_2 + 4 \cdot y/T_a$; $y = atnp \cdot 288$; $atnp = 2.26e-2$ [km⁻¹]; $k_2 = k_w + k_p/2$; $k_w = 0.44$ km⁻¹; $k_p = 0.13$ km⁻¹; $m = 1/7$; $A = 0.75$</p> <p>$R_d = 287.04$ [J/kg/K]</p> <p>Vapor Pressure $ea = humidity_{air} \cdot e^{*3}$ [kpa]</p> <p>$e^{*3} = a_0 + T \cdot (a_1 + T \cdot (a_2 + T \cdot (a_3 + T \cdot (a_4 + T \cdot (a_5 + T \cdot a_6))))$); $a_0 = 6984.505294$; $a_1 = -188.9039310$; $a_2 = 2.133357675$; $a_3 = -1.288580973 \cdot 10^{-2}$; $a_4 = 4.393587233 \cdot 10^{-5}$; $a_5 = -8.023923082 \cdot 10^{-8}$; $a_6 = 6.136820929 \cdot 10^{-11}$</p>

Table 3-3 Constants Used for calculations in table 3-2 and previous equations (Brutsaert, 1982, 2005).

Once again, to summarize, I calculated evaporation using the data from a distributed sensor network of small meteorological stations. I performed this calculation using Monin-Obukov similarity theory (Monin, 1959). First, I determined the sensible heat flux from the wind speed, roughness length, and temperature of the air and surface. The total net radiation was then calculated using the measured shortwave radiation, the albedo, and the air and surface temperatures. The ground heat flux was estimated as a constant fraction of net radiation ($\frac{G}{R_n}$), and then the latent energy flux, which can be converted to mm of evaporation, was found by balancing the incoming and outgoing radiation. The necessary constants – albedo (α), $\frac{G}{R_n}$, and roughness length (z_0) – were determined at the reference eddy – covariance stations and found to be strongly controlled by vegetation and thus seasonally dependent.

3.2.7 Analysis of variance

Independence validates the importance of these measurements and calculations. Lack of dependence would negate the need for us to perform this calculation in these distributed locations. We use the Kruskal-Wallis one-way analysis of variance to examine, first if our micrometeorological input data from the different stations are independent from each other. This is the preferred statistical test to determine if these samples are in fact independent, because it does not assume a normal distribution of the residuals, can be used when the groups are of unequal size, although it does assume a common distribution (Kruskal Wallis, 1952).

3.3 Results

3.3.1 Energy budget

I first compare average energy balance per month compared between that calculated at a small station (station number 1007) and that measured at the field eddy correlation station (figure 3-4). The energy balance is composed of net radiation (R_n), latent energy flux (Le), sensible heat flux (H), and ground heat flux (G). This is an overview plot of the average flux at each half hour point as calculated through the described formulation of similarity theory at the station closest to the flux station, 1007, dotted, and that measured by the eddy-covariance station. There are months, when the measurements at one of the two stations is incomplete, hence the missing lines in some months. Net radiation (red) aligns very well in some months – March, May, June, July, August, September, November – but is extremely under estimated by the similarity calculation in others – April and December – and even overestimated in October. This may actually be explained by the small differences in land surface related to the fact that the reference station was protected from animals, farming, and burning and the other stations were not initially. Sensible heat flux (black) is similarly well estimated for some months – March, April, and August – and under estimated for others- September and November – and over estimated in May, June, and July. Latent heat flux (blue) is mostly lower with the similarity theory calculation – March through September – but higher in November. This also could be attributed to the difference in land use (Figure 2-4 Appendix II). Finally, ground heat flux (green) is often lower with the similarity theory calculation.

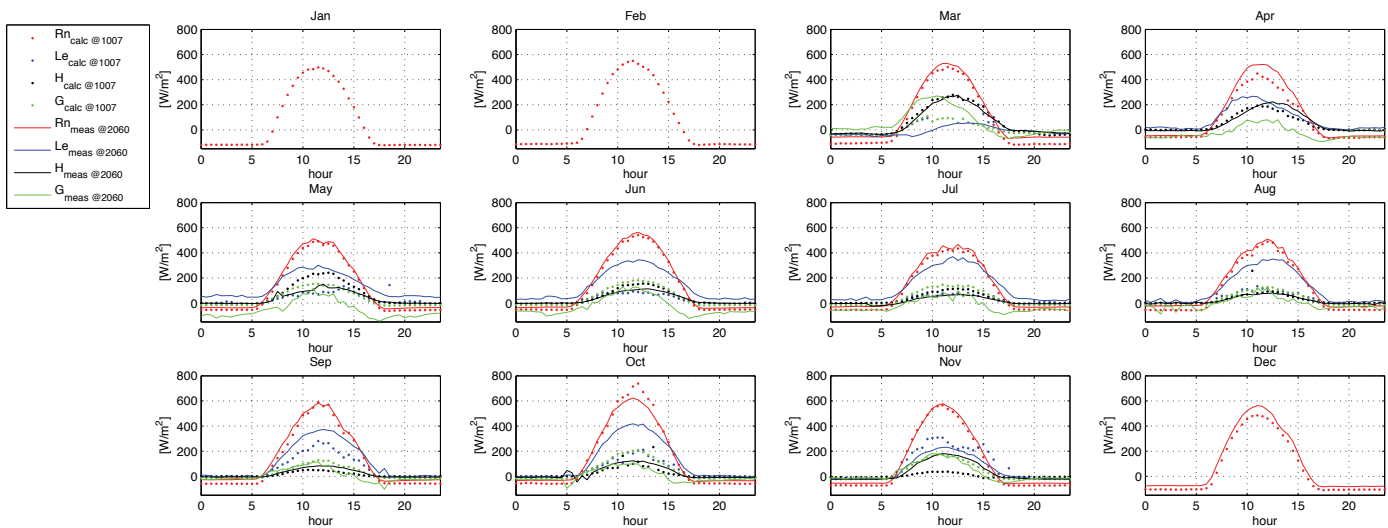


Figure 3-4. Diurnal Energy Budget. This figure shows the average diurnal cycle of the energy budget in each of twelve months. The dots show what was calculated at a Sensorscope station, 1007, which is the closed to the field eddy covariance station. The solid lines show the measurements at the eddy covariance station in the field. All four components of the energy balance are shown: net radiation (red), latent energy flux (blue), sensible heat flux (black), and ground heat flux (green). All fluxes are shown in W/m^2 on a 24-hour period. Data is missing when technical problems resulted in data gaps.

In Figure 3-5, we see that air humidity is quite dependent on season and, for example in November, we see that stations 1006 and 1008, near the river, stay humid while others dry out (Map – figure 1-3). The Kruskal-Wallis test was used to prove this quantitatively, with all months for all input variables as significant ($\chi^2 >> 1$, $p < 0.05$, Kruskal & Wallis, 1952). Of particular interest is the difference visible in the stations, 1000, located closer to the village, which is often lower than all the others, and the river, 1006, 1008, and 1001 which are higher in many months.

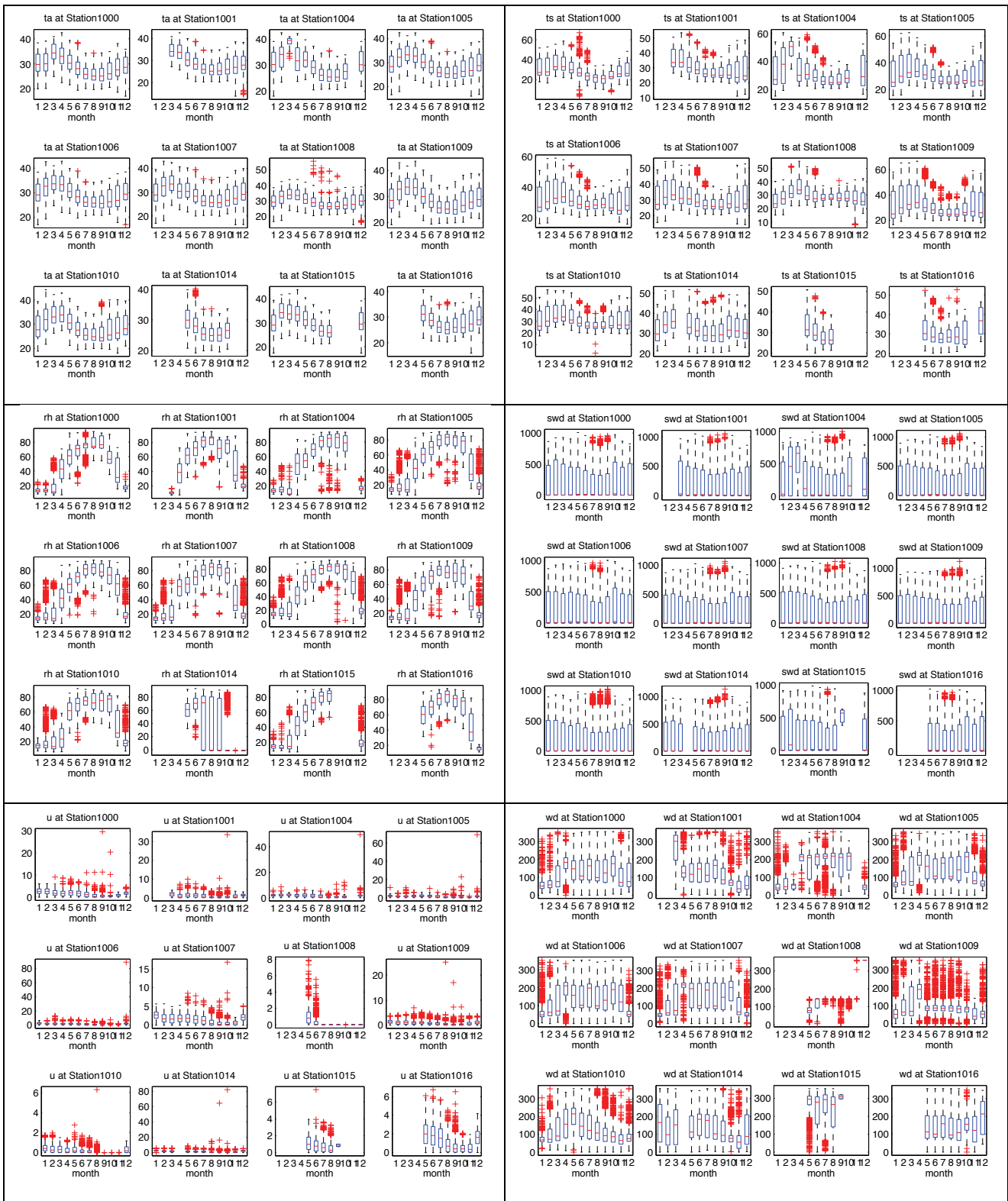


Figure 3-5. Seasonal Change of Variables. Bar graphs show the median (red), 25-75 quartiles (box), 5-95 (whiskers), and outliers (red crosses) for 12 months for the 12 Sensorscope stations where calculations took place. In upper left, the air temperature (ta) in °C is shown. In the upper right, the surface temperature (ts) is shown in °C. In the middle left the relative humidity (rh) in % is shown and in the middle right, the incoming short wave radiation (swd) is in W/m². The lower left shows the wind speed (u) in m/s and in the lower right is the wind direction (wd), in degrees. Months are organized from January to December, left to right, as indicated by the numbers on the x-axis. This is a pooling of all 2009 and 2010 data used in the distributed calculation of evaporation. Stations are from top to bottom, left to right: 1000, 1001, 1004, 1005, 1006, 1007, 1008, 1009, 1010, 1014, 1015, and 1016. Numbers are consistent with the map (figure 1-3) and the appendix (II). All samples were tested for independence and were found to be independent from each other ($\chi^2 \gg 1$; $p \ll 0.05$).

3.3.2 Roughness length

The seasonal progression of roughness length (figure 3-6) in the field demonstrates the seasonal progression. Roughness length is highest in the late part of the rainy season when the grasses are higher. This is more apparent at the field station than at the forest station. At the forest station, we see quite a bit a variability in the early part of the year, which corresponds to when the vegetation is partially deciduous and developing, by the end of the growing season, the roughness length is much more consistent. Our measurements are often ten-fold lower than those of Bagayoko (2007), which can be understood by the more variable vegetation in his site that had more trees scattered in the fields, even though it is physically close. The seasonal cycles are similar between our two sites.

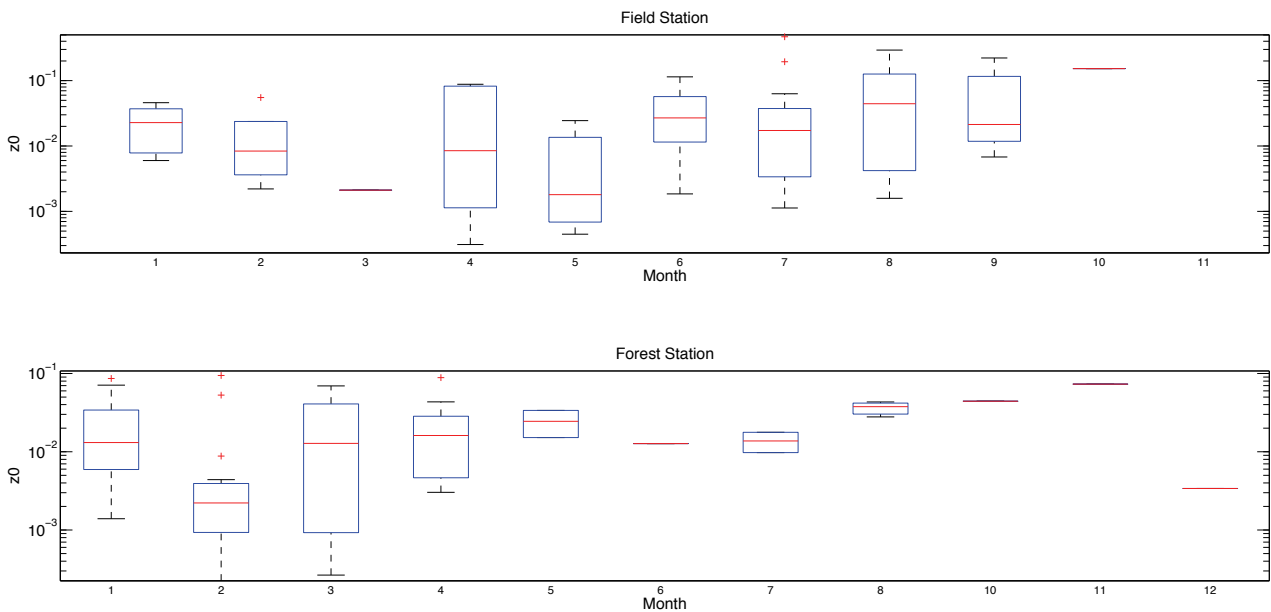


Figure 3-6. Roughness length (z_0 in meters) determined at the field station (above) and forest/hill station (below) determined independently for each day on a log plot. Plots show the median value (red line), and 25% and 75% quartiles (blue box), the 5 and 95 % distribution (whiskers) and outliers (ret crosses).

Roughness length was found to be strongly seasonal at both of the eddy correlation stations. The effect of the growth of vegetation was more apparent in the field station, as expected. In the first part of the year, a decline is visible as the grasses dry and the soil becomes barer. Once June began, there is an increase in roughness length that corresponds to the growth of vegetation. On the hill roughness length is more consistent, with a gentle increase into November as the vegetation becomes longer that only declines in December as drying, leaf loss, and burning takes place.

The roughness length for sensible heat (z_{0h}) in particular showed interesting results (figure 3-7) – followed the usual 10% of the roughness length described above until the late rainy season. Roughness length for heat (z_{0h}) also followed a seasonal cycle that is related to that of roughness length. We see that the roughness lengths for heat determined in the opposite direction, over a more irregular topography are much less than 10% of z_0 all lengths. This suggests that direction of wind, in addition to seasonality plays an important role in the roughness length calculation. We can also conclude that the 10% rule only applies for parts of the year.

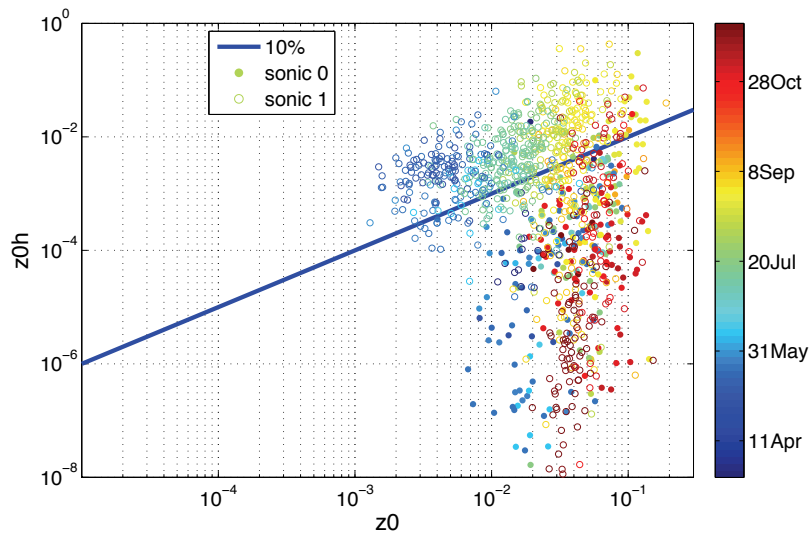


Figure 3-7. Seasonal Progression of the heat roughness length, z_0h , in meters on y-axis, as a compared the roughness length of z_0 , in meters on the x-axis. Here we see a comparison between the roughness lengths determined at the two sonics, pointing in opposite directions in the field. Sonic anemometer “0”, solid circles, points upstream towards the rocky escarpment, whereas sonic anemometer “1”, open circles, points downstream towards the outlet of the village. The seasonal cycle is shown in colors ranging from April 2010, in blue, to November 2010, in red.

3.3.3 Albedo

Albedo changes throughout the year and is different at the two sites. It is clear that albedo increases in the dry season, as the ground becomes barer (maximum in April) and decreases into the rainy season as the vegetation grows (minimum in September). The albedo varies by both month and station. The overall average is 0.1279, which is, according to Brutsaert (1982), in the appropriate range for moist dark soils, plowed fields and coniferous forest. The albedo rarely goes above 0.2, so it falls into the range of gray soils, bare fields, green grass and other short vegetation, dry prairie and savanna, dry soils, and desert. It never reaches the levels for snow or white sand, and rarely for water, as we would expect since these covers are never present at the site. Dry vegetation seems to similarly low to bare ground as demonstrated by values in October and November.

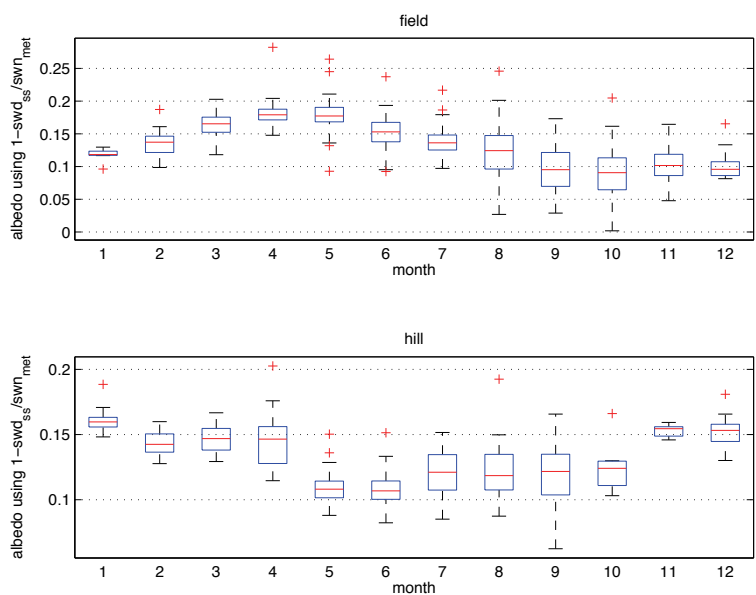


Figure 3-8. Comparison of Albedo by Station and by Month (x-axis). Field is show in the upper plot. It varies between 0.05 and 0.25 whereas the hill-forest (below) only varies between 0.1 and 0.2. Red lines indicate the median, blue box, the 25 and 75 % quartiles, whiskers, the 5 and 95 % quartiles, and outliers are the red crosses.

3.3.4 Conversion to Ground Heat Flux

As vegetation starts to have more a presence, in July in the field and August on the hill, the ground heat flux is then converted more likely to latent heat flux. Variations in the conversion rate from net radiation to ground heat flux also show variation at the two stations. Although, the two sites surprisingly follow similar patterns. In both cases, there seems to be a bimodal effect with lows in April and September and highs in January or December and July or June. In the dry but hazy months, when there is a low level of vegetation and humidity but more dust in the atmosphere, more net radiation is converted to ground heat flux. Similarly, near the summer solstice, before the humidity of the growing season begins, there is also a high level of transfer net radiation to ground heat flux. The decrease of the conversion rate in April could be attributed to thermal transfer and less into the ground.

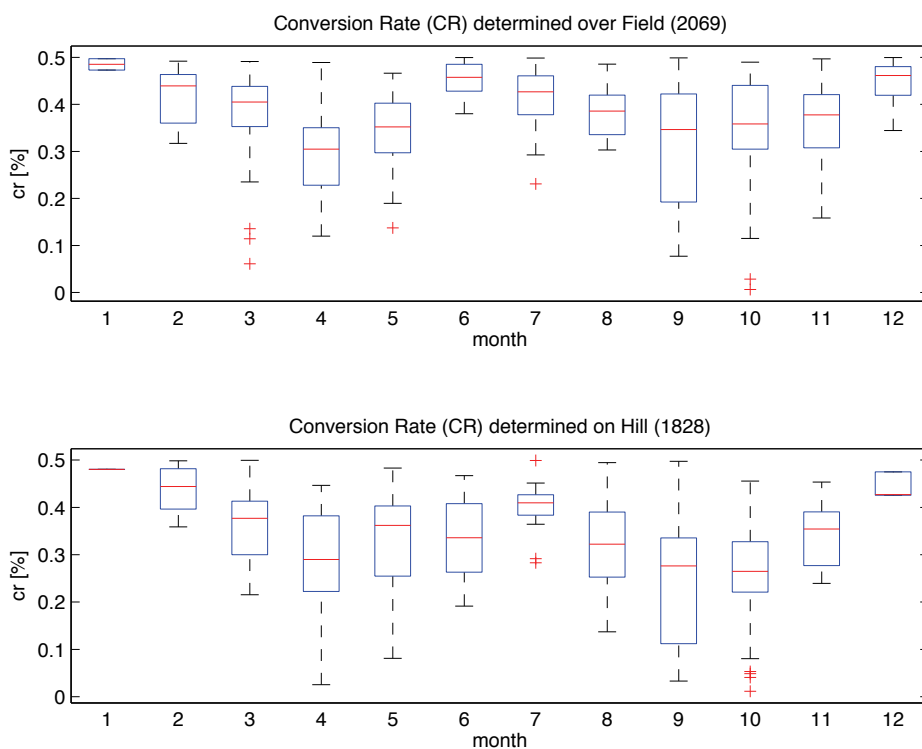


Figure 3-9. Comparison of conversion rate from net radiation to ground heat flux for two Eddy Covariance Stations by Month. The field is shown above and the hill-forest site below. The medians are shown in red lines, the 25 and 75 quartiles by the blue box, the 5 and 95 by the whiskers and the outliers by crosses. Months are sequentially on the x-axis from 1 to 12.

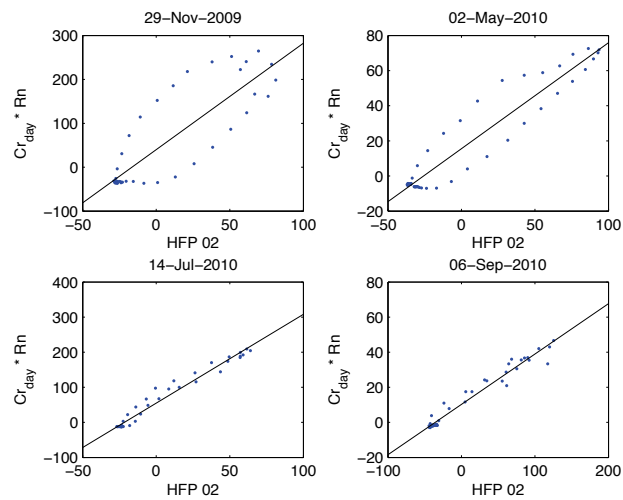


Figure 3-10. Comparison of the ground heat flux obtained from conversion rate ($Cr * Rn$) with that measured with the heat flux plates (HFP 02) in the field on 4 days (24 November 2009, 2 May 2010, 14 July 2010, and 06 September 2010). This heat flux plate was close to the surface (<5 cm). One dot per half hour calculation. The black line shows the best fit.

Figure 3-10 compares the estimation of ground heat flux (G) using the conversion rate (cr). We see that in the four days shown, the days with less vegetation and more bare ground (November and May) have less agreement on the half hour scale, but that over all they have a consistent relationship. On the other hand, when vegetation is present, in July and September, there is a much more linear fit and less evidence of hysteresis. However, in all cases there is a mismatch of scale between the two variables. The calculated G is about 4 times greater than that measured by the heat flux plates, with the exception of September when the heat flux plates seems to measure twice the calculated rates.

3.3.5 Net Radiation

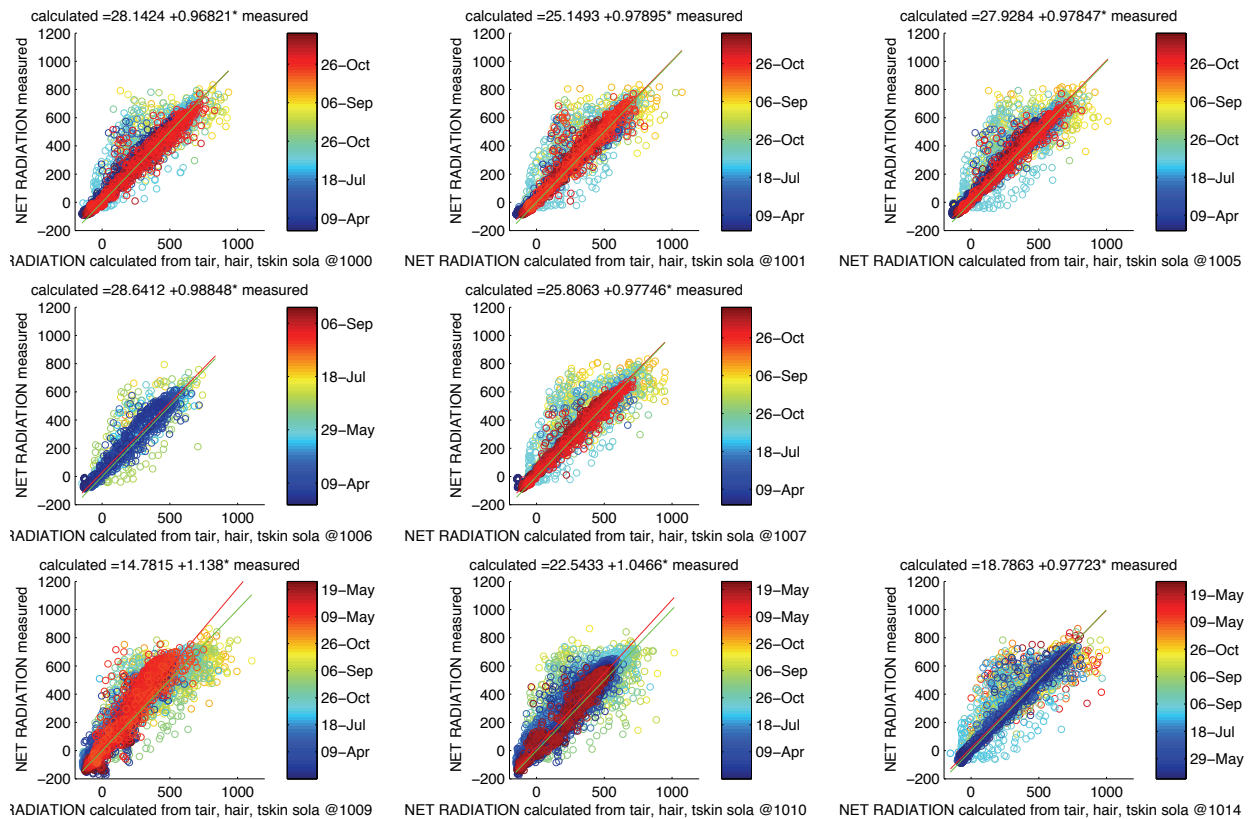


Figure 3-11. Comparison of net radiation calculated (x-axis) at each of the sensorcopes stations (left to right, top to bottom: 1000, 1001, 1005, 1006, 1007, 1009, 1010, 1014) compared with that measured (y-axis). Numbers correspond to those shown on map figure 1-3 and in appendix II Best fit is shown by a red line and 1:1: line is shown in green. All units are in W/m^2 . Color in scatter plot shows the day of year. Because data was not consistently available for each station, color bar shifts according to site, but in most ranges from April 2009 (blue) to May 2010 (red). Best-fit equations are written above the plot for each subplot.

Fits of the calculated net radiation to the measured were between 0.91 and 1.093. Color shows day of year. For most stations and most time of the year, there was a high level of correlation. Most of the scatter occurred in August or September, when the grasses reach their tallest heights and the sensors are no longer a reasonable distance above the land surface to satisfy the assumptions of the similarity theory formulation.

3.3.6 Latent Heat Flux

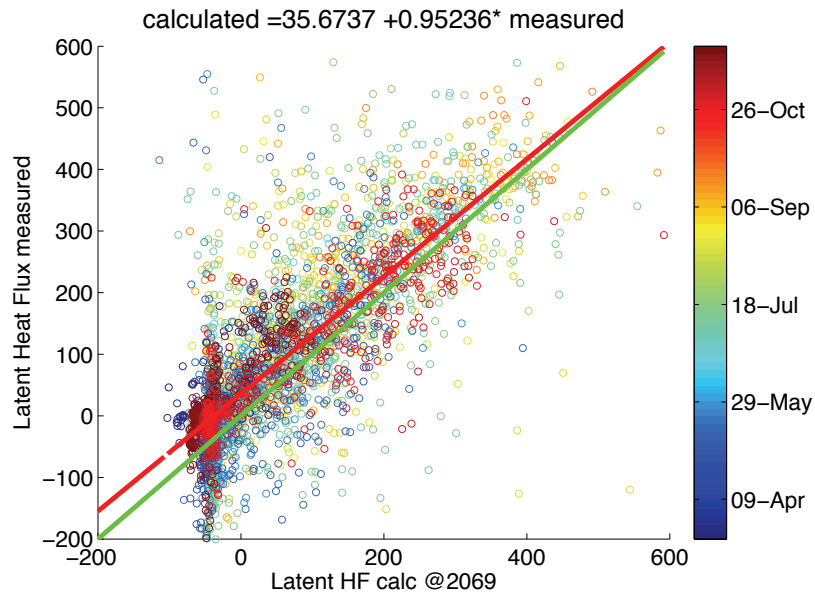


Figure 3-12. Comparison of latent energy flux (W/m^2) calculated with slow sensors at field eddy-correlation station (x-axis) and measured at same station (y-axis). Best-fit line is red, and 1:1 line is green. Color bar shows seasonal progression from April 2010 (blue) to November 2010 (red), although there is some scatter; there is a reasonable fit between the two variables. Best-fit equation is written above the plot.

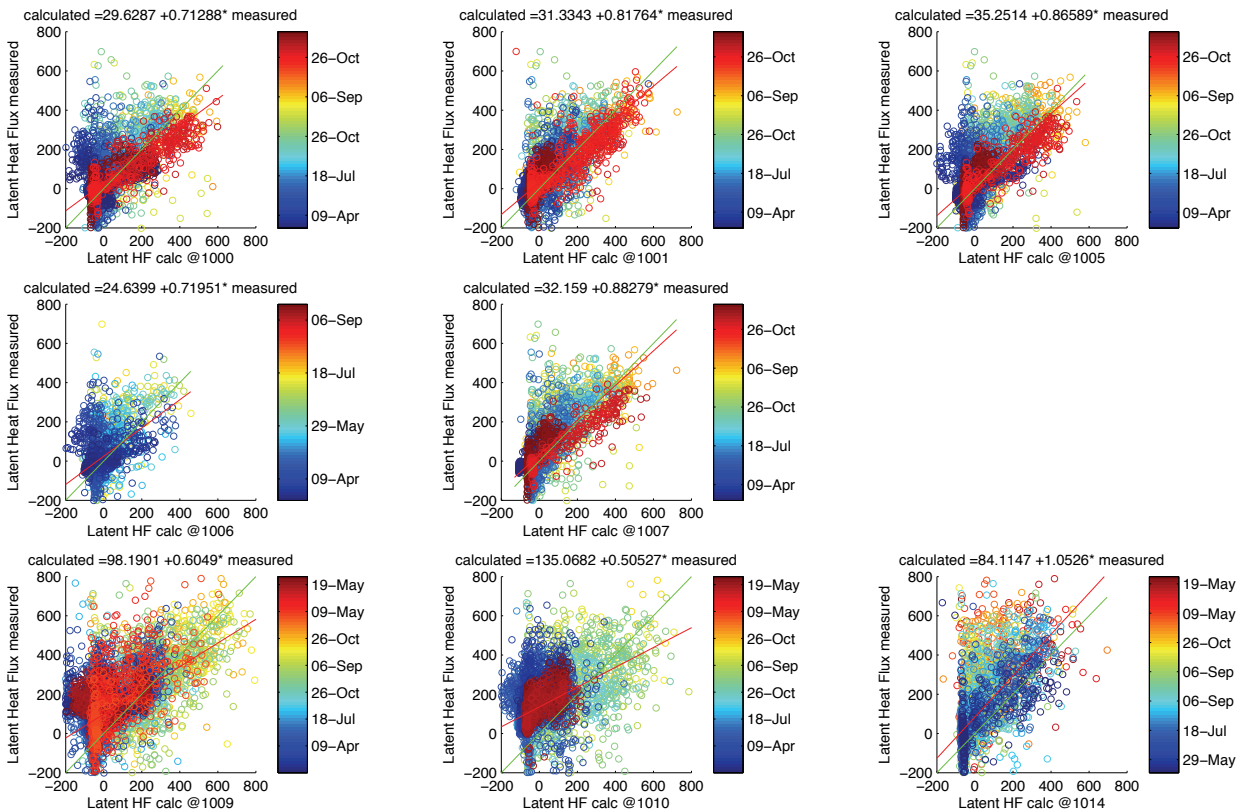


Figure 3-13. Comparison of Latent Heat flux calculated at each of the stations (x-axis), and measured at the nearest eddy covariance station (y-axis). Station numbers correspond to those in map and appendix (Figure 1-3, A-II). Color bar shows yearly time scale. One to one line in green. Best fit line in red. Equation of red line above each graph. All units in are W/m^2 . Color bars indicate the date.

There was a high level of correlation between the latent heat flux measured and calculated at the main eddy-flux station (Figure 3-12). Scattering occurred at low values, which makes sense because these values are often erroneous when energy exchange is lowest. When latent heat flux was calculated (figure 3-13) at the other stations, there was much more variation and scattering. These variations are likely due to changes in the roughness length or conversion rate to ground heat flux that vary over the catchment. Our assumption that each station would resemble the station closest to it was not always correct. The annual cycle was similar, but not uniform over the area of the watershed. As expected, stations closer to the reference stations were more similar due to their similar land cover. Agreement between measurements is highly variable, and can be associated with differences in vegetative cover. Stations with high agreement (1007, 1014) have similar vegetation whereas those with low agreement (1009, 1010, 1008) have different land cover. Seasonal variations in level of agreement are also visible as shown by the color of the scatter. Again, August and September seem to have the most variation.

3.4 Discussions & Conclusions

In this chapter, we observed variations in the energy balance across a small watershed and throughout a yearly cycle. This would not have been feasible with a standard eddy-covariance set up. In the process, we demonstrated the use of a simple model based on Monin-Obukhov similarity theory to estimate evaporation over a remote, rural watershed in Burkina Faso. The model did perform reasonably well when calculated at a single point. However, it requires the calculation of roughness length (z_0), albedo (α), and conversion rate (Cr) to ground heat flux. We were able to model albedo at each simple meteorological station using incoming solar radiation and air and surface temperatures, however Cr and z_0 require closing the energy balance at each station. Calculation of the four components of the energy budget (net radiation, latent heat flux, sensible heat flux, and ground heat flux) required inputs for α , Cr , and z_0 in addition to measures of air temperature, surface temperature, relative humidity, wind speed, and incoming solar radiation that are measured at each station. Thus in order to fully resolve the model at each station, we need to obtain spatially resolved estimations for Cr and z_0 . Seasonal cycles of the coefficients, conversion rate, roughness length, and albedo, were apparent. Variation in the roughness length over the seasonal cycle is currently unaccounted for in most West African meteorological models (Budyoko, 2007).

Spatially, there was significant variation in the input variables of temperature, wind, solar radiation and humidity over the watershed according to the Kruskal - Wallis test. The annual cycle was similar, but not uniform over the area of the watershed. As expected, stations closer to the reference stations were more similar. Agreement between measurements is highly variable, and can be associated with differences in vegetative cover. Stations with high agreement (1007, 1014) have similar vegetation whereas those with low agreement (1009, 1010, 1008) have different land cover. This suggests that vegetation plays a major role in determining the components of the energy budget. Similarly, Cr , or the percent of net radiation converted to ground heat flux, lowers in the wet season over the rocky escarpment, but not for the vegetated field. Albedo varies seasonally, and lowers over course of growing season over agricultural land but more constant over forested valley – savanna.

It is possible to successfully model the energy balance from data available from low-cost, portable Sensorscope stations in semi-arid West Africa. Preliminary results show the importance of vegetation heterogeneity as an evaporative control. Future work will focus on predicting roughness length and ground heat flux conversion rate based on seasonal and spatial changes in vegetation. Improved understanding of vegetative controls on evaporation will be used to inform farming practices by coupling the energy balance calculated here with a water balance. Eventually, after much social work, outreach, and collaboration, local farmers will be more able to adapt to changing weather patterns and land cover with increased access to information of these coupled energy and water budgets. Data such as this will improve global understanding of the variations in soil moisture, crop water use, runoff and other hydrological calculations as well as our ability to predict future changes.

3.4.1 References

- Bagayoko, F., Yonkeu, S., Elbers, J., & van de Giesen, N. (2007). Energy partitioning over the West African savanna: Multi-year evaporation and surface conductance measurements in Eastern Burkina Faso. *Journal of Hydrology*, 334(3-4), 545–559.
- Brutsaert, W. (1982). *Evaporation into the Atmosphere: Theory, History, and Applications*. Dordrecht, The Netherlands: Kluwer Academic Publishers.
- Deardorff, J. W. (1970). A numerical study of three-dimensional turbulent channel flow at large Reynolds numbers. *J. Fluid Mech*, 41(2), 453-480.
- Farhadi, L. (2012). *Estimation of Land Surface Water and Energy Balance Flux Components and Closure Relation Using Conditional Sampling*. PhD Dissertation. Environmental and Civil Engineering, Massachusetts Institute of Technology.
- Gash, J. H. C., Shuttleworth, W. J., Lloyd, C. R., André, J.-C., Goutorbe, J.-P., & Gelpe, J. (1989). Micrometeorological measurements in Les Landes Forest during HAPEX-MOBILHY. *Agricultural and Forest Meteorology*, 46(1), 131–147.
- Gleick, P. H., Cooley, H., Famiglietti, J. S., Lettenmaier, D. P., Oki, T., Vörösmarty, C. J., & Wood, E. F. (2013). Improving Understanding of the Global Hydrologic Cycle. In *Climate Science for Serving Society* (pp. 151-184). Springer Netherlands.
- Goutorbe, J.-P., Lebel, T., Tinga, A., Bessemoulin, P., Brouwer, J., Dolman, A. J., Engman, E.T., Gash, J.H.C., Hoepffner, M., Kabat, P., Kerr, Y.H., Monteny, B., Prince, S., Said, F., Sellers, P., Wallace, J. S. (1994). HAPEX-Sahel: a large-scale study of land-atmosphere interactions in the semi-arid tropics. *Annales Geophysicae*, 12(1), 53–64.
- Guichard, F., Lergoat, L., Mougou, E., Timouk, F., Baup, F., Hiernaux, P., & Lavenu, F. (2009) Surface thermodynamics and radiative budget in the Sahelian Gourma: Seasonal and diurnal cycles. *Journal of Hydrology*. 375: 161-177.
- Guyot, A., Cohard, J. M., Anquetin, S., Galle, S., & Lloyd, C. R. (2009). Combined analysis of energy and water balances to estimate latent heat flux of a sudanian small catchment. *Journal of Hydrology*, 375(1), 227-240.
- Hipps, L. E., & Kustas, W. P. (2000). Surface evaporation and its spatial variations. In R. B. Grayson & G. Blöschl (Eds.), *Spatial patterns in catchment hydrology*. Cambridge, UK: Cambridge University Press.
- Huber, P. J. (1981). *Robust statistics* (pp. 1248-1251). Springer Berlin Heidelberg.
- Huwald, H., Higgins, C. W., Boldi, M. O., Bou-Zeid, E., Lehning, M., & Parlange, M. B. (2009). Albedo effect on radiative errors in air temperature measurements. *Water Resources Research*, 45(8).
- Ingelrest, F., Barrenetxea, G., Schaefer, G., Vetterli, M., Couach, O., & Parlange, M. (2010). Sensorscope: Application-specific sensor network for environmental monitoring. *ACM Transactions on Sensor Networks (TOSN)*, 6(2), 17.
- Jackson, P. C., Meinzer, F. C., Bustamante, M., Goldstein, G., Franco, A., Rundel, P. W., Caldas, L., Iglar, E., Causin, F. (1999). Partitioning of soil water among tree species in a Brazilian Cerrado ecosystem. *Tree physiology*, 19(11), 717–724.
- Knoche, H., Rao, P.R.S., Huang, J., (2010). Voices in the field: A mobile phone based application to improve marginal farmers livelihoods. *MobileHCI*, September 7-10, Lisboa, Portugal.
- Kruskal, W. H., & Wallis, W. A. (1952). Use of ranks in one-criterion variance analysis. *Journal of the American statistical Association*, 47(260), 583-621.
- Mauder, M., Jegede, O. O., Okogbue, E. C., Wimmer, F., & Foken, T. (2006). Surface energy balance measurements at a tropical site in West Africa during the transition from dry to wet season. *Theoretical and Applied Climatology*, 89(3-4), 171–183.
- Monin, A. S. (1959). On the similarity of turbulence in the presence of a mean vertical temperature gradient. *Journal of Geophysical Research*, 64(12), 2196–2197.
- Pfister L., H.H. G. Savenije, F. Fenicia. 2009. Leonardo Da Vinci's Water Theory: On the origin and fate of water. IAHS Special Publication 9. Unesco.
- Schüttemeyer, D., Moene, A. F., Holtslag, A. A. M., De Bruin, H. A. R., & Van De Giesen, N. (2006). Surface fluxes and characteristics of drying semi-arid terrain in West Africa. *Boundary-layer meteorology*, 118(3), 583-612.
- Stull, R. B. (1998). *An Introduction to Boundary Layer Meteorology* (p. 666). Kluwer Academic Publishers.
- Timouk, F., Kergoat, L., Mougou, E., Lloyd, C. R., Ceschia, E., Cohard, J. M., Rosnay, P., Hiernaux, P., Demarez, V., Taylor, C. M. (2009). Response of surface energy balance to water regime and vegetation development in a Sahelian landscape. *Journal of hydrology*, 375(1), 178-189.
- White, F. (1986). *la vegetation de l'Afrique: Memoire accompagnant la carte de vegetation de l'Afrique* (p. 389).
- Whiteman, C. D., Allwine, K. J., Fritzchen, L. J., Orgill, M. M., & Simpson, J. R. (1989). Deep valley radiation and surface energy budget microclimates. Part I Radiation. *Journal of Applied Meteorology*, 28, 414.

Chapter 4 Evaporative Fraction Influenced By Land Surface Controls

4.1 Introduction

The exchange of energy and water between the land surfaces and atmosphere over the West African region is central to the coupling of the energy and water budgets, as we have discussed in previous chapters. This exchange is a driving force for many of the hydrologic and meteorological processes. In fact, actual evaporation from vegetated surfaces remains the component of the global distribution of water that is the least frequently measured and thus the least well understood (Brutsaert, 1982). As we have seen, anomalies in vegetation and topography as well seasonal cycles of vegetation and moisture presence are a driving force behind this exchange. In addition, populations in this region have a high dependence on rainfed agricultural and thus false estimations; predictions, recommendations or incomplete understanding or information can have dire consequences for human livelihood. Unfortunately, as previously discussed, many parts of West Africa and other semi-arid systems coincide with areas of scarce and incomplete information. This is in part due to the presence of meteorological research equipment that can document evaporative fluxes into the atmosphere.

In the previous chapter, we examined one method to use small and low-cost stations to calculate evaporation. This has an enormous potential to increase the regional understanding of evaporation if these stations can be distributed over a large area. However, obtaining such stations is still a hurdle to cross, and the data from them is not immediately present. Satellite data presents another opportunity for filling this need. Satellites have been circulating and collecting images of our planet for the last decades. Although African satellite data is still not preserved to the degree as it is on other continents, it is continually collected and often captured. In this chapter, I will explore one concept that could help transform satellite data into relevant evaporation estimates. I will not go into great detail regarding satellite information but instead examine out one ratio, the evaporative fraction, varies in our site and over our study period.

The evaporative fraction (EF, equation 4-1), or the ratio of latent energy flux, (LeE) to total available energy, the sum of sensible (H) and latent energy fluxes, is a useful concept to estimate total daily evaporation with measurements of a single component of the energy balance and to up-scale surface measurements using remote sensing products (Szilagyi and Parlange, 1999; Szilagyi et al., 1998; Compaore et al., 2008).

Evaporative Fraction
$$Ef = \frac{LeE}{H+LeE} \quad (4-1)$$

It is based on the concept of self-preservation in diurnal evolution of surface energy budget (Brutsaert & Sugita, 1992). The self-preservation concept is based on the idea that the diurnal cycle each of the energetic fluxes, will resemble that of available energy, or net radiation. Clearly, there are many variations in the quantity of available energy, but self-preservation predicts that the diurnal pattern will be similar. Thus from this assumption, we can deduce that by resolving the budget of energy at one point in the

day, we will be able to estimate its behavior for the entire day. This is particularly useful for remote sensing because satellites may only pass once a day. This means that if we obtain adequate data at that one point, we can estimate the entire day's budget.

Compaore et al. (2008) demonstrated that in West Africa, the self-preservation concept applied to the evaporative fraction could be used together with variables such as albedo, temperature at the surface, and a vegetation index to obtain a reasonable estimate of evaporation. Farah et al. (2004) found there to be a high correlation in mid-day evaporation and the evaporative fraction for Kenyan grasslands. Brutsaert and Sugita (1992) warned that evaporation fraction might be altered by variations in incoming radiation by cloud cover. But Dos Santos et al. (2010) concluded that cloudiness is not related to the stability of evaporative fraction in his studies in the 2005-2006 in Brazil.

Evaporative fraction may also be related to other environmental variables that are becoming more and more reliable from satellites. For example, Hall et al. (1992) found that above 20% soil moisture, there is not a relation between evaporative fraction and soil moisture but there is a rapid decrease below 20% in the Konza prairie, Kansas. Similarity Crago (1996) found that evaporative fraction responded to soil moisture and was able to calibrate curved fits.

The state of the global monitoring of fluxes makes the implications of this work even more significant – we need more precise and diurnally resolved methods to measure fluxes at higher spatial scales, in hard to access areas. We need evaporation estimates that are possible with minimal investments in meteorological stations in maintenance. However, we need to use the flux measurements, such as those described in chapter 2, to improve our interpretation of satellite data for this purpose. More flux measurements in combination with new analytical techniques that can transform satellite data into real evaporation estimates are extremely valuable.

This is particularly valuable in sites such as ours, when the data set is often discontinuous. EF is equal to the flux of latent heat divided by the total available energy (4-1). The Bowen ratio (Br, 4-2) is related linearly to the evaporative fraction as $\beta = \frac{1}{EF} - 1$, and thus has a similar utility (Cho, et al., 2011; Crago, 2013). We will focus our work on the EF, but we introduce the Br, because important analytical work has been applied to it that could be transferred to understanding of the EF.

Bowen Ratio

$$Br = \frac{H}{L_e E} \quad (4-2)$$

Porporato (2009) showed analytically that the relatively constant Bowen ratio during midday hours is due to its insensitivity to atmospheric conditions for large values of net available energy. However, this daily approximation is dependent on a well-mixed layer. When the boundary layer is not well mixed, the influence from dry air entrainment from above will interact with the influence of the surface. In the absence of large-scale advection, the moisture content in the convective boundary layer is determined by both evaporation at the land surface and entrainment of dry air at the top of the convective boundary layer (Van Heerwaarden, 2009).

In this chapter, I calculate the evaporative fraction for our site, building on the work of the last two chapters. I explore how cloud cover influences the quality of the EF calculation. I examine the role of filtering for improving the evaporative fractions relationship to the land surface controls. Specifically I examine satellite derived vegetation index and soil moisture. This work lays the basis for a future upscaling by validating the concepts of self-preservation. Upscaling using remotely sensed data would not be possible without this level of ground trothing.

4.2 Methods

4.2.1 Evaporative Fraction

Evaporative fraction was calculated according to equation 4-1 for each half hour of data, separately for upper and lower station, over the forest/hill and the field respectively. Sensible and latent heat fluxes were calculated for the two sites as described in chapter 2. The eddy-covariance stations and data were the same. This is the same site. Daily values of evaporative fraction were obtained by averaging all values between 10 and 14 hours. Tests were done to determine what hours were the best for this average, and this was found to be the most consistent. In order to separate the evaporative fraction due to evaporation from the surface and that due to dry air entrainment, we filter low covariances, when $\overline{q'T'} < 0$, and then recalculate the evaporative fraction. This filtering will allow us to focus our observations on the land surface controls of variation in the partition of fluxes.

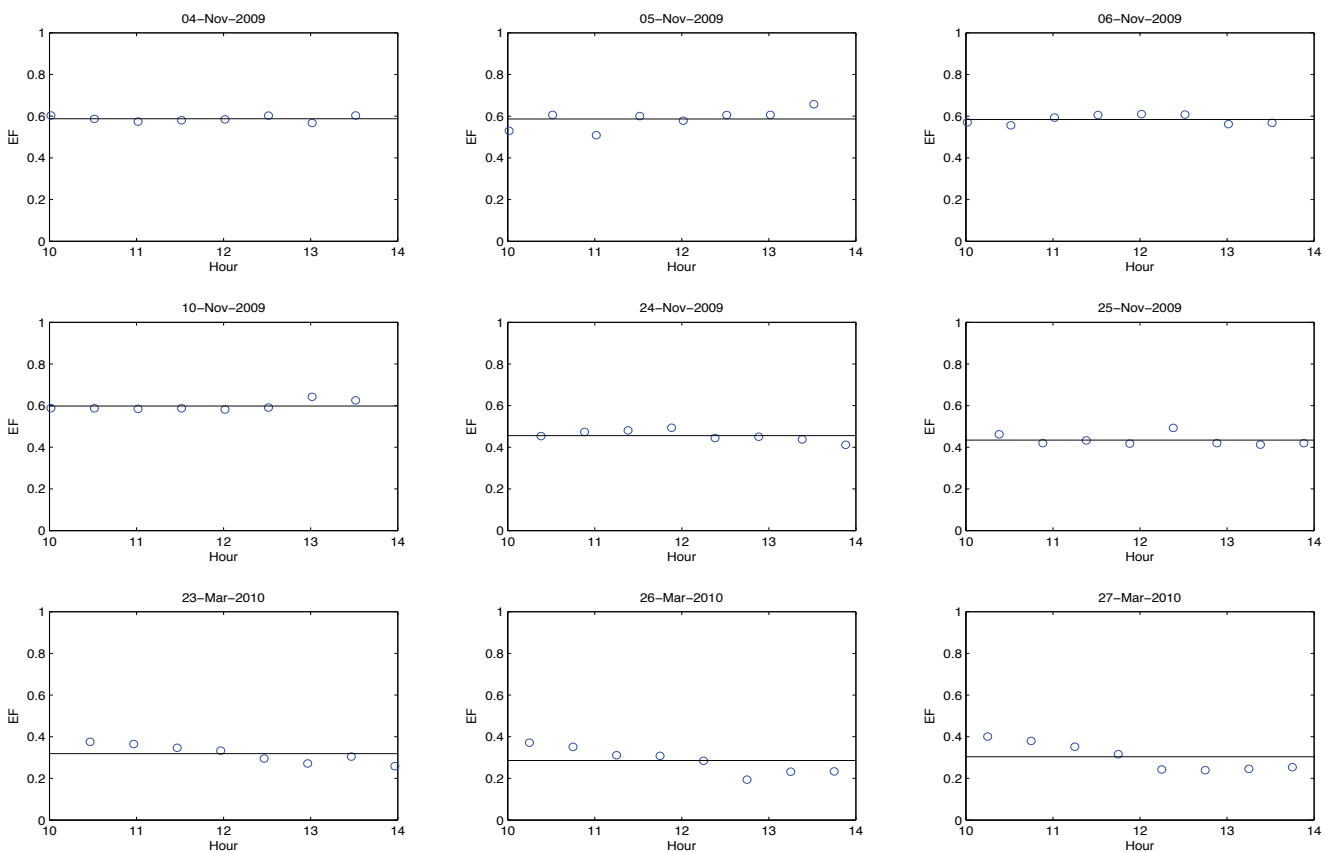


Figure 4-1. . Evaporative Fraction calculated by half hour shown here for nine example days for station on the hill. Values between 10 and 14 o'clock were averaged (black line).

4.2.2 Cloud Cover Calculation

Cloud cover was calculated by dividing the incoming shortwave infrared radiation measured with a Davis Radiometer by the theoretical incoming radiation calculated with a simple model by Whiteman and Allwine (1986) for all Sensorscope stations operating on any given day (equation 4-3). It was calculated per day independently for all stations and then averaged to give a single value per day.

$$CC = \frac{SW_m}{SW_{Th}} \tag{4-3}$$

Cloud Cover Fraction

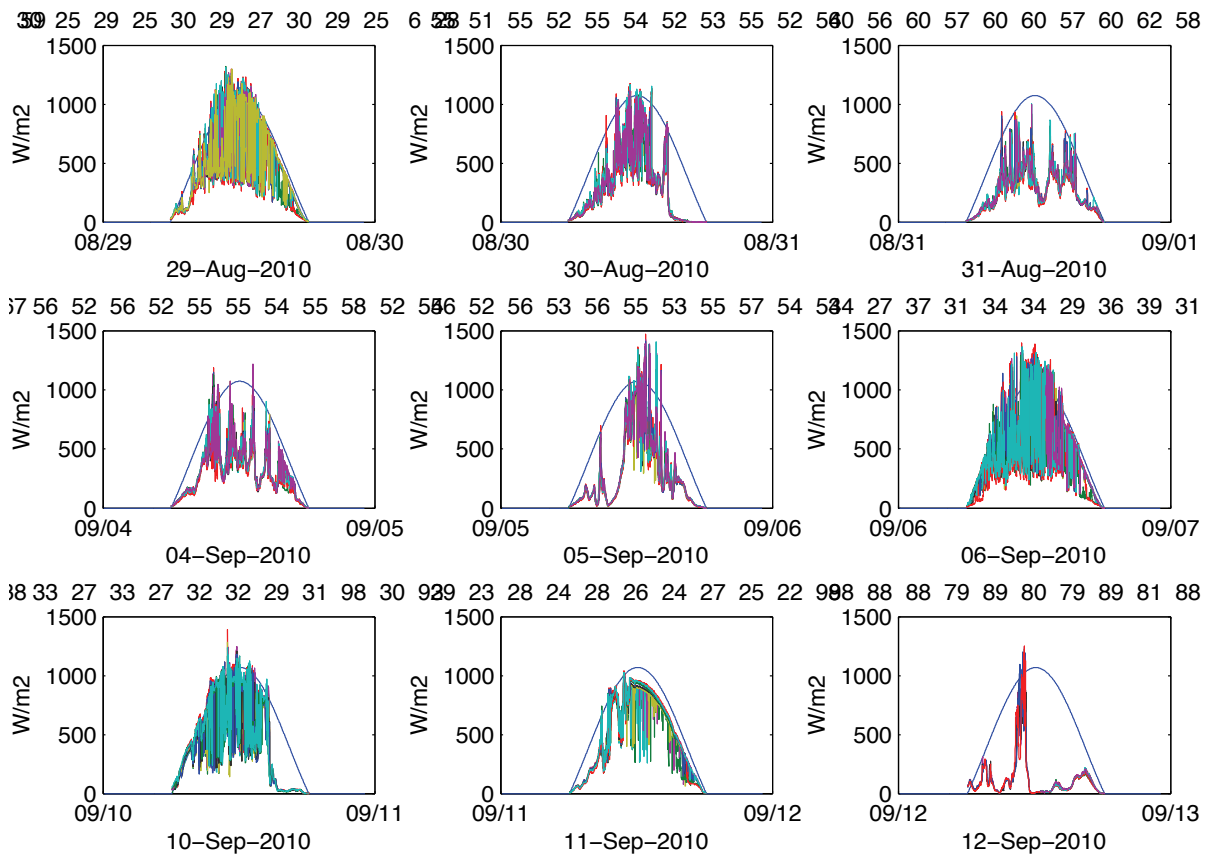


Figure 4-2. An example of nine days determination of cloud cover fraction. The theoretical solar radiation is in blue and the measured solar radiation at each of the stations is in different colors. The total sum under the curve for each station was divided by the total sum under the curve for the theoretical solar radiation.

4.2.3 Soil Moisture

In general, volumetric soil moisture (VWC) is the volume of water divided by the total volume of water, soil, and air in the soil space (4-4). However it is possible to calculate soil moisture from dielectric potential using Topp equation as described in more detail Appendix III. Soil moisture was monitored over the entire catchment at many of the Sensorscope stations (Figure 1-2, Appendix II) For this analysis, soil moisture was monitored using Decagon ECTM, 5TM, and 5TE dielectric sensors at locations less than 5 meters from each micrometeorology station at depths of 15 and 30 cm or 5 and 20 cm, respectively.

$$VWC = \frac{V_w}{V_w + V_s + V_a} \quad (4-4)$$

Volumetric Soil Moisture

4.2.4 Vegetation Index

Normalized difference vegetation index (NDVI) is an index based on the amount of infrared radiation absorbed, which is related to the amount of photosynthesis taking place. NDVI is a ratio of the near infra-red (NIR) to red wavelengths (equation 4-5).

$$NDVI = \frac{NIR - RED}{NIR + RED} \quad (4-5)$$

Volumetric Soil Moisture

It is considered a measure of the density of chlorophyll. It has been corrected for molecular scattering, ozone absorption, and aerosols and then smoothed using a least square linear regression (Swets et al., 1999). Seasonal change in normalized difference vegetation index observed by extraction of the area of interest from the 250 meter resolution West Africa eMODIS satellite data (U.S. Geological Survey). It was temporally smoothed NDVI over 10 days for 2010. The NDVI values are validated with photographic monitoring of the site (Appendix II). The pixels that contained our stations were extracted to give a basin – wide seasonal impression of the vegetation change.

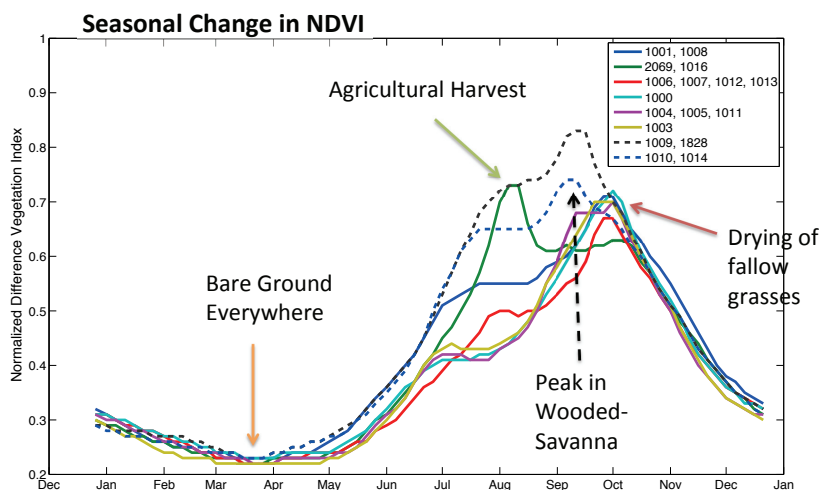


Figure 4-3 Normalized Difference Vegetation Index for 2010 extracted from 10-day composite product of Modis images (USGS-FEWS, 2010). Each line is a single pixel. The station numbers in the legend correspond to the map (figure 1-3) and to the appendix II. Notes on the plot indicate the interpreted processes from presence in the field and photographs.

Comparison of satellite NDVI over the course of the year illustrates many of the trends that we have encountered in the energy balance and in variations in roughness length, conversion coefficient, and albedo (chapter 3). Even at the coarse pixel resolution, the behavior of different parts of the watershed is visible. The vegetation is at a minimum in April and March, increases uniformly

in May and June. However in July there is a divergence. Over the hill it is much higher, which is probably due to the presence of woody vegetation and tall savanna grasses. In the field, at the site occupied by 2069, the energy balance station, and 1016, the NDVI continued to increase, and dropped suddenly in September. The site of the main station, 2069, was planted with a short season millet crop. In contrast, stations 1000, 1004, and 1003 all flattened out at this point. These areas were plowed and farmed. The red line was likely plowed later, but still had a late peak. The mixed signature could show a « mixed » pixel that was partly farmed with early and late crops. A mixed pixel would average the processes contained within its area.

4.3 Results

Examination of the monthly time series of evaporative fraction, volumetric water content, NDVI, and cloud cover shows pronounced seasonal cycles for all variables (figure 4-4). Separation between the field (blue) and the hill (red) is most apparent in the NDVI time series, where the field consistently stays more green from May to September, although the magnitude of that difference varies by year, and is most apparent in 2009 and 2010. In 2011, the drought year, the hill stayed slightly greener during the dry down. The few months that there was a significant discrepancy in cloud cover, the agricultural field had more and it was in the dry season, with the exception of 2009, when, for 3 months out of 4, the hill had more cloud cover. Although the catchment is very small and there is only 100 meters of elevation change, it is possible that humidity was higher at the lower elevations and the wind displaced any clouds forming higher. Volumetric water content in the field increases steadily starting in April and peaking in September and falling quickly in October. These time series become more interesting when we look at their interrelationships.

Evaporative fraction to changes in volumetric water content, NDVI, and cloud cover (figure 4-5). There is the greatest dependence of evaporative fraction on the soil moisture over the forest and on the NDVI over the forest. The other relationships are weak. All relationships seem to be more dependent on higher levels of moisture – when NDVI is greater than 0.1, when NDVI is greater than 0.6, and when cloud cover is greater than 0.6. This corresponds to months 8 – August and 9 – September (orange and dark yellow) in most cases.

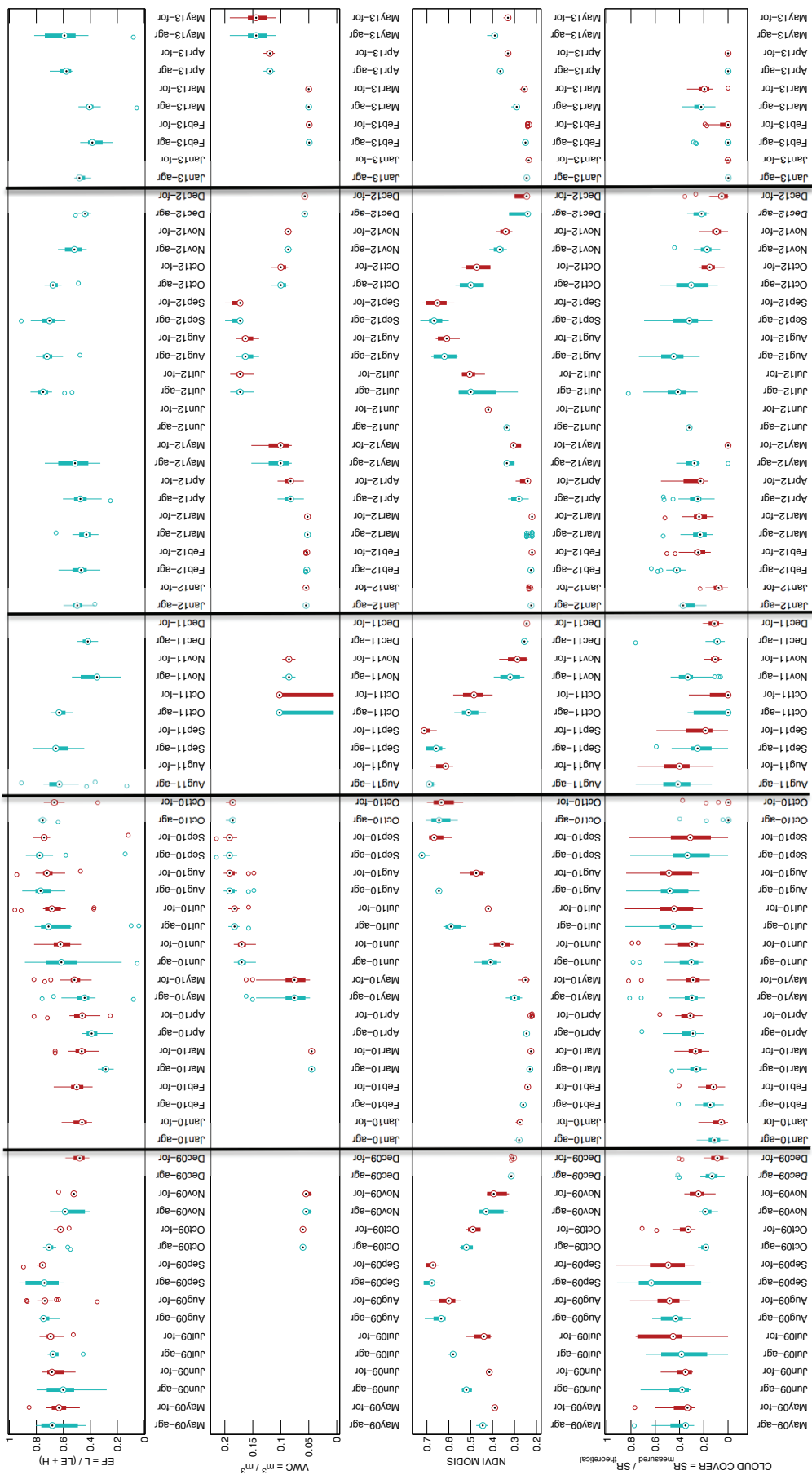


Figure 4-4. Bar graph comparing the evaporative fraction, the volumetric water content, and cloud cover over 4 years. Evaporative fraction is at the top followed by soil moisture (VWC), vegetation index (NDVI), and cloud cover. Separation between the field (blue) and the hill (red). Months of data along x-axis. Not all data present for all months.

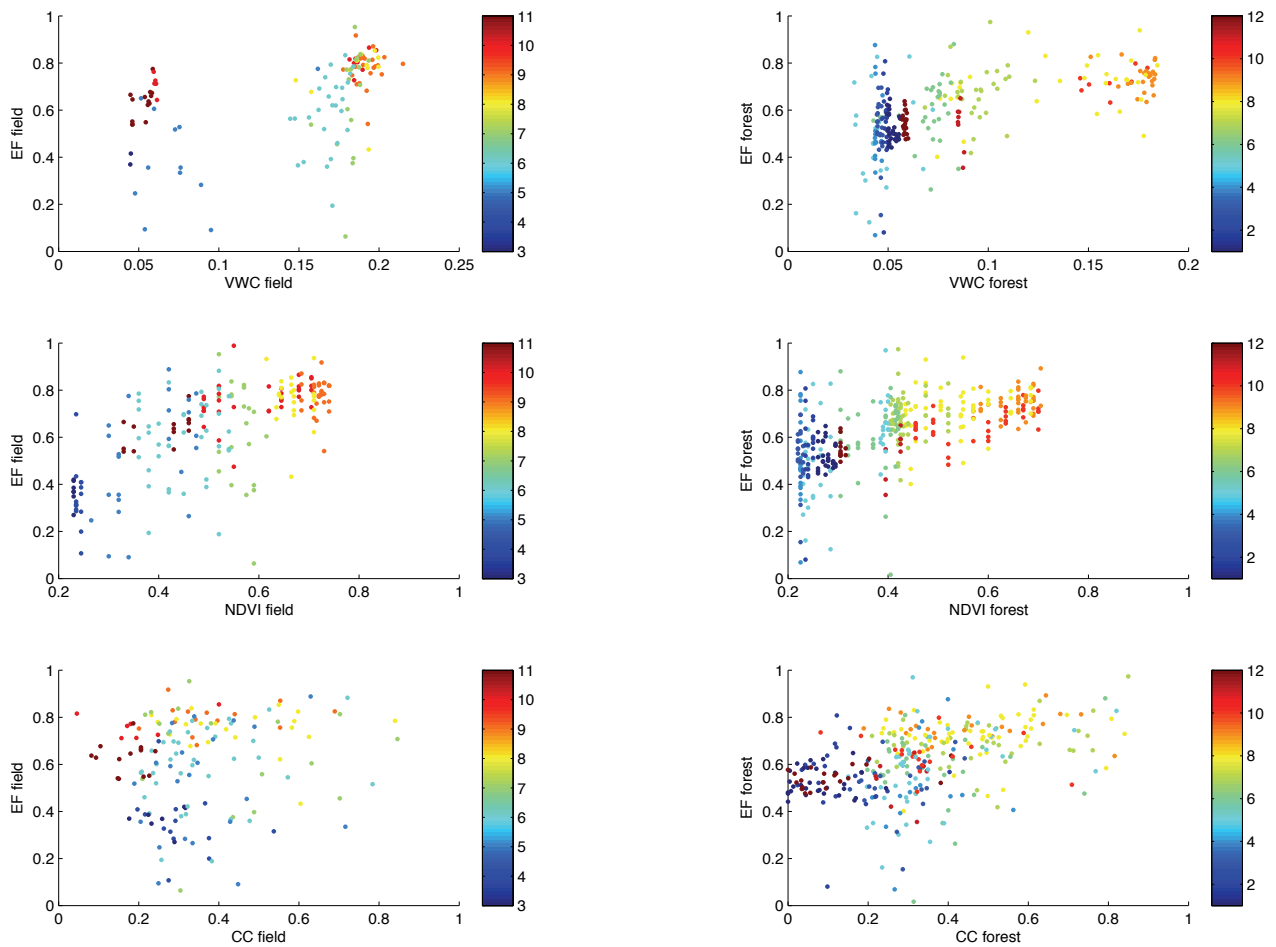


Figure 4-5. Response of Evaporative Fraction to changes in volumetric water content (VWC – upper row), vegetation index (NDVI – middle row), and cloud cover (CC – lowest row). Field station is on left, Forest station is on right. Color bar indicates month. All data from 2009 and 2010 are pooled and months include all available data.

Filtering of low frequency covariance between temperature and humidity affects each component of the energy balance differently (figure 4-6). In the calculated sensible heat flux, negative values appear. Similarly, high values become higher. Latent heat flux also becomes more variable. The evaporative fraction however does not show a significant shift, although there is a fair amount of scatter. The comparison of daily averages between those calculated with a filter and without a filter results in a strange set of negative values for H in the dry season that translates into the EF - again more in the forest than in the field (Figure 4-6). To some extent as well in the forest, we see that the filtering increases both the H and the LeE , thus has a neutral effect on the EF. The filtering removes the covariances that are not well mixed – when the dry air entrainment from the top of the boundary layers is interacting with surface influences. Thus, we should see that the land surface effects on the evaporative fraction are more pronounced when the filtering has been performed.

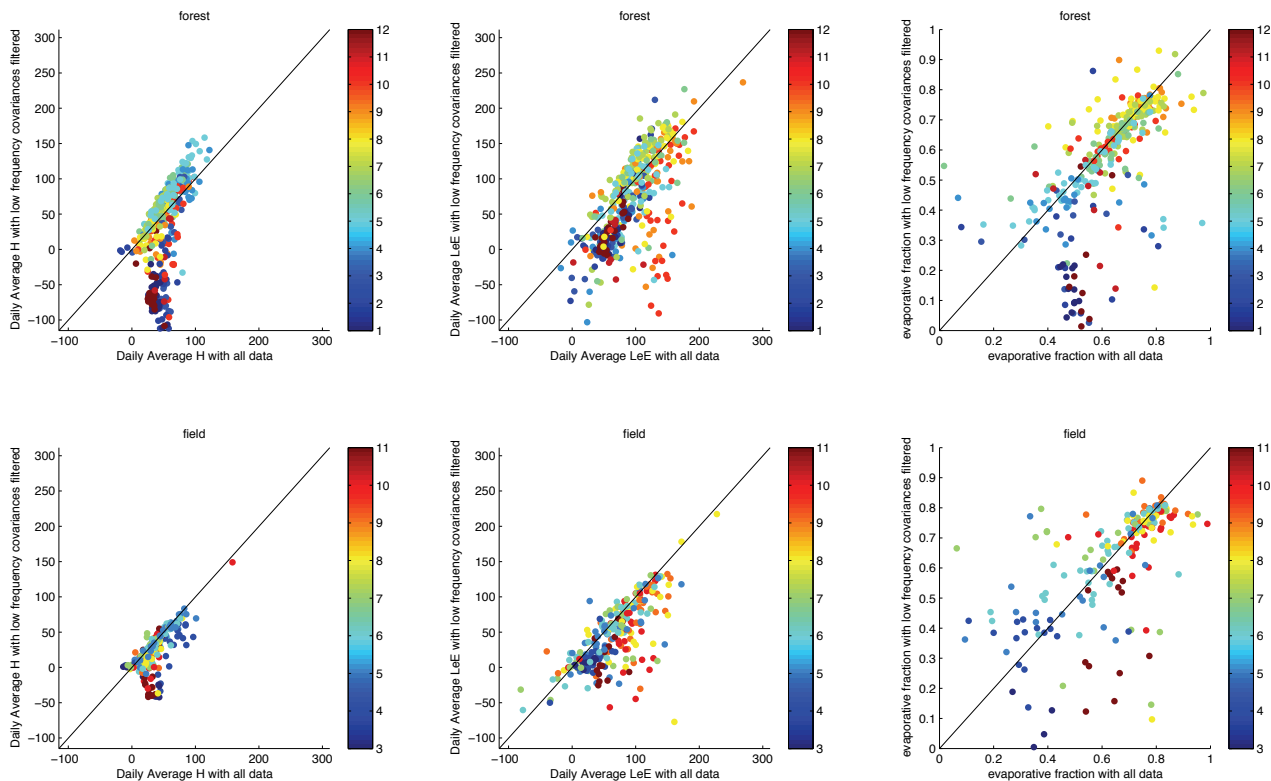


Figure 4-6. Comparison of Daily Averages of Each Flux Component between those with all low spectrum filtered, and those with nothing filtered.

When low frequency covariances are filtered, evaporative fraction shows a much higher dependence on all considered variables, volumetric water content, NDVI, and even cloud cover. EF over the field shows a somewhat linear dependence on NDVI for periods of low greenness that becomes less pronounced at levels of high greenness. Evaporative fraction shows a linear dependence on cloud cover at times of low cloud cover over the forest. Once cloud cover reaches a level of about 0.4, the evaporative fraction remains equally high (figure 4-6).

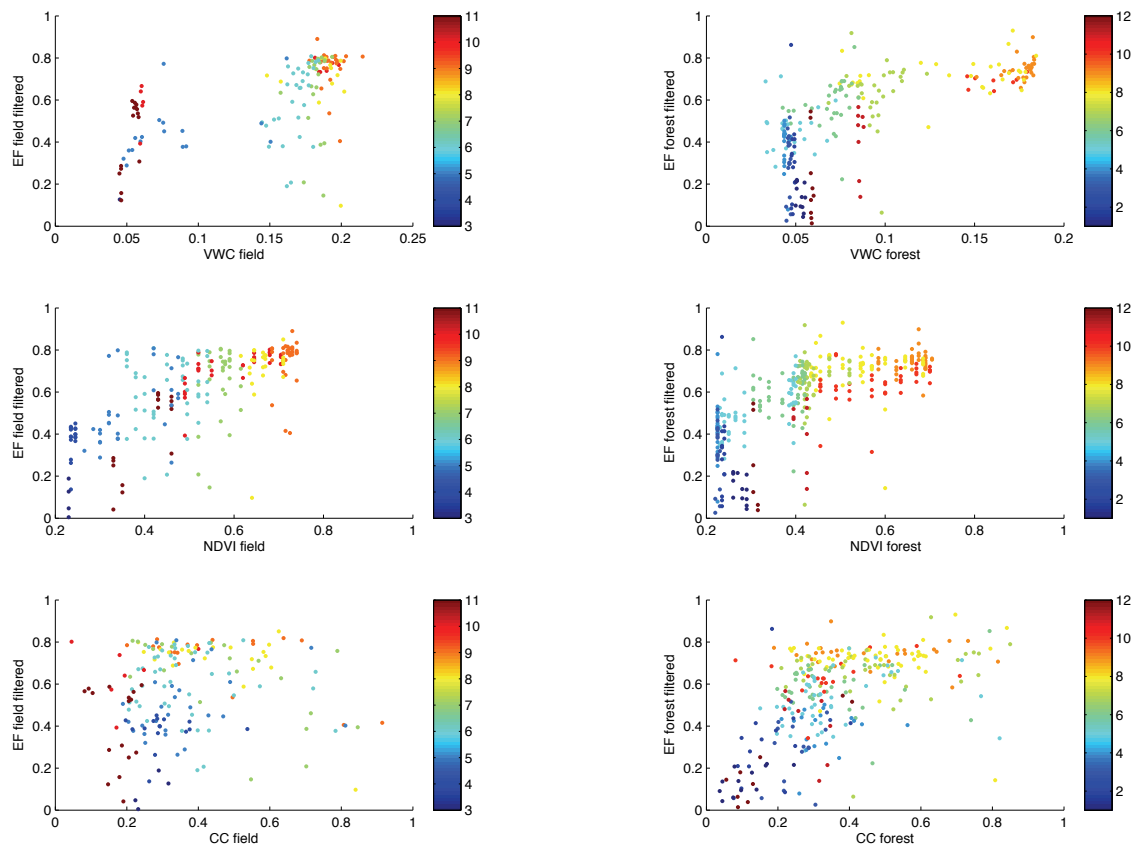


Figure 4-7. Response of Evaporative Fraction computed with low frequency covariances filtered to changes in volumetric water content (VWC – upper row), vegetation index (NDVI – middle row), and cloud cover (CC – lowest row). Field station is on left, Forest station is on right. Color bar indicates month. All data from 2009 and 2010 are pooled and months include all available data.

In the land surface conditions plot (figure 4-7), we see that in particular, over the forest, there is more dependence on cloud cover, vegetation index, and soil moisture with the filter. And all 3 follow a general rule that there is higher dependence at lower levels. In the field there is much less of an effect, in particular with cloud and soil moistures. Vegetation index shows a small dependence. It is important to distinguish the effect of available moisture either from soil moisture or transpiring (green) vegetation and available energy that may be limited by the cloud cover.

Because the filtering had a greater effect over the forest, and the filtered data showed a greater dependence on the land surface properties, we can deduce that there is more influence of dry air entrainment over the forest, and at both sites we can see a dependence of evaporative fraction on vegetation index, and at the forest site on the soil moisture and cloud cover as well.

4.4 Discussion and Conclusions

We see that soil moisture has a more pronounced effect on the evaporative fraction when the dry air entrainment is filtered, however we would suppose that vapor pressure deficit (VPD) would exert a stronger control on entrainment of dry air. The filtering of the flux measurements affected by the entrainment of dry air makes it clear that there are stronger hydrologic controls

on evaporative fraction than originally visible. Although in this example, only NDVI is determined from satellites, all three, cloud cover, NDVI, and soil moisture, have the potential to be determined from satellites.

Higher levels of soil moisture provide higher levels of moisture to the system, so it is logical that a positive correlation is found. Vegetation also provides moisture through transpiration. In these two examples, we see that landscape controls exert a strong influence on the evaporative processes. Cloud cover, on the other hand, exerts its control by limiting radiation into the system.

Removal of the influence of dry air entrainment revealed the hydrologic and vegetation controls on evaporative fraction. This study demonstrates that with better measures of soil moisture, vegetation index, and cloud cover from satellites; it would be possible to make estimations of evaporative fraction only from satellite data. However, in the mean time ground truthing with real time flux measurements is essential.

4.5 References

- Brutsaert, W. (1982). *Evaporation into the Atmosphere: Theory, History, and Applications*. Dordrecht, The Netherlands: Kluwer Academic Publishers.
- Brutsaert, W., & Sugita, M. (1992). Application of Self-Preservation in the Diurnal Evolution of the Surface Energy Budget to Determine Daily Evaporation. *Journal of Geophysical Research*, 97(D17), 18377–18382.
- Cho, J., Oki, T., Yeh, P. J. F., Kim, W., Kanae, S., & Otsuki, K. (2012). On the relationship between the Bowen ratio and the near-surface air temperature. *Theoretical and Applied Climatology*, 108(1-2), 135-145.
- Compaoré, H. (2006). The impact of savannah vegetation on the spatial and temporal variation of the actual evapotranspiration in the Volta Basin, Navrongo, Upper East Ghana. *Ecology and Development Series*, (36).
- Compaoré, H., Hendrickx, J. M. H. H., Hong, S., Friesen, J., Van de Giesen, N. C., Rodgers, C., Szarzynski, J., Vlek, P. L. G. (2008). Evaporation mapping at two scales using optical imagery in the White Volta Basin, Upper East Ghana. *Physics and Chemistry of the Earth, Parts A/B/C*, 33(1-2), 127–140.
- Crago, R. D. (1996). Conservation and variability of the evaporative fraction during the daytime. *Journal of Hydrology*, 180(1-4), 173–194
- Crago, R. D., & Qualls, R. (2013). The value of intuitive concepts in evaporation research. *Water Resources Researches*, 49(1-5).
- Dos Santos, C. A. C., Silva, B. B. Da, & Rao, T. V. R. (2010). Analysis of the Evaporative Fraction Using Eddy Covariance and Remote Sensing Techniques. *Revista Brasileira de Meteorologia*, 25(4), 427–436.
- Farah, H. O., Bastiaanssen, W. G. M., & Feddes, R. A. (2004). Evaluation of the temporal variability of the evaporative fraction in a tropical watershed. *International Journal of Applied Earth Observation and Geoinformation*, 5(2), 129–140.
- Hall, F. G., Huemmrich, K. F., Goetz, S. J., Sellers, P. J., & Nickeson, J. E. (1992). Satellite Remote Sensing of Surface Energy Balance: Success, Failures, and Unresolved Issues in FIFE. *Journal of Geophysical Research*, 97(D17), 19061–19089.
- Knoche, H., Rao, P.R.S., Huang, J., (2010). Voices in the field: A mobile phone based application to improve marginal farmers livelihoods. *MobileHCI*, September 7-10, Lisboa, Portugal.
- Porporato, A. (2009). Atmospheric Boundary-Layer Dynamics with Constant Bowen Ratio. *Boundary-Layer Meteorology*, 132(2), 227–240.
- Swets, D.L., Reed, B.C., Rowland, J.D. & Marko, S.E. (1999). A weighted least-squares approach to temporal NDVI smoothing. In: 1999 ASPRS Annual Conference: From Image to Information, Portland, Oregon, May 17-21. Proceedings: Bethesda, Maryland, American Society for Photogrammetry and Remote Sensing.
- Szilagyi, J., & Parlange, M. B. (1999). Defining Watershed-Scale Evaporation Using a Normalized Difference Vegetation Index. *Journal Of The American Water Resources Association*, 35(5), 1245–1255.
- Szilagyi, J., Rundquist, D. C., Gosselin, D. C., & Parlange, M. B. (1998). NDVI relationship to monthly evaporation. *Geophysical Research Letters*, 25(10), 1753–1756.
- Van Heerwaarden, C. C., Vil, J., Arellano, D., Moene, A. F., & Holtslag, A. A. M. (2009). Interactions between dry-air entrainment , surface evaporation and convective boundary-layer development. *Quarterly Journal of the Royal Meteorological Society*, 135, 1277–1291.

Chapter 5 Soil Water Balance Under agroforestry trees indicate spatial heterogeneity¹

5.1 Introduction

5.1.1 Problem

Seasonally dry forests and savannas consisting of sparse tree canopies and dominated by open grassland make up about 16 million square kilometers of tropical land of which only 1 million km² worldwide remains as natural vegetation (Miles et al., 2006). Natural vegetation is adapted to the extreme seasonality, characterized by deep tap root systems and seasonal deciduousness, whereas human propagated vegetation is not (Griffith, 1961). The remaining seasonally dry regions are cultivated (Williams 2008).

Watercourses and water bodies in these areas are ephemeral because of the extreme seasonality of the hydro-climatic regime, which is further exacerbated by the presence of unusually high inter-annual rainfall variability (Murphy and Lugo, 1986; Furley 2004). For example, the average total annual rainfall is 900 mm in Burkina Faso, but it is not unusual to have years with as little as 300 mm or as much as 1500 mm of rain.

These regions are predicted to be sites of strong climate changes (Donner and Large 2008). In Burkina Faso, precipitation isohyets have shifted to the South, reducing the average rainfall overall in the last four decades, although some recovery has been seen in the most recent decade (Wittig et al., 2007). Up to 20% rainfall reduction and 60% runoff reduction in Burkina Faso has been documented in the middle to end of the last century (Mahe et al., 2005; Kallis 2008). Climate change is expected to further alter the precipitation patterns in terms of timing, even if original quantities are maintained (Hulme et al., 2000). These changes can be attributed both to regional land use, specifically vegetation change, and to global weather response to increased green house gases. As a result, especially towards the middle and end of the dry season, lakes and streams become dry while groundwater levels drop.

¹ A previous version of this document was published as : Ceperley, N., Repetti, A., & Parlange, M. (2012). Chapter 15: Application of Soil Moisture Model to Marula (*Sclerocarya birrea*): Millet (*Pennisetum Glaucum*) Agroforestry System in Burkina Faso. In J.-C. Bolay, M. Schmid, G. Tejada, & E. Hazboun (Eds.), *Technologies and Innovations for Development* (pp. 211-229). Paris: Springer Paris.

In the Sudanian savanna landscape, which occupies much of the country, these shifts in precipitation can be accompanied by a dramatic shift in species composition or a *sahelisation* that is irreversible due to the corresponding changes in soil physics and albedo. Zheng and Eltahir (1998) found that at a regional scale, deforestation along the coast in addition to the desert border of West Africa might be responsible for the decrease in precipitation in especially the Sahelian zone.

Resource poor farmers are among the most vulnerable groups to climate change in West Africa. Although in the Sudanian zone, less than 10% of water resources are currently exploited, these farmers have little access to the technology needed to increase access to water. Their livelihoods are almost entirely dependent on rain fed agricultural which is highly sensitive to even small fluctuations in the variability and quantity of rain. Since they are both the consumers and producers of their agricultural products, there is little external impetus for investment in climate change adaptation; however, failure to adapt may result in large scale poverty, famine, migration, and possible conversion to livelihood strategies which further threaten global biodiversity and ecosystem services (Downing et al., 1997). Important adaptations include technological support to rural farmers that will allow them to predict, prepare for, and buffer the damages of climate hazards on their livelihoods.

Seasonality is the core principle of farming systems in these areas, as opposed to the temperature-driven agriculture present in temperate zones. Soils are generally fertile and the rain is sufficient for rainfed cotton, maize, millet, and sorghum production, although the farmer must be especially attentive to anticipate and predict the rain. For example, the Yoruba know that the rain will arrive by observing changes in the leaves, the sky, and bird songs (Richards, 1985). Late rainfall and poor timing of planting in relation to the rain can cause fatal problems. Although the most prosperous farmers can produce competitive crops in seasonally dry ecosystems, most farmers and their communities live in poor conditions, with food shortages, water stress, and related symptoms of poverty. Farming in valleys, floodplains, and wetlands is a frequently used tool in West Africa that is used to cope with the challenge of droughts in place of irrigation, although it can increase diversification of the generally limited crops. Paul Richards argued in 1985 that most rural farmers in West Africa (Nigeria and Sierra Leone) knew most of what agricultural science has to offer, however they still had problems, and those were for the most part unsolved by scientific inquiry.

Two reasons explain the lack of exploitation of the water resources. The first is the difficulty for the local population to manage a water resource defined by very intense rainfalls followed by long dry seasons. During the wet season, runoff and erosion are intense, but the recharge is limited due to superficial soils that reduce deep infiltration. This suggests that lack of water is not necessarily the primary constraint and that even a doubling of crop yields would be hydrologically possible with relatively small manipulations of rainwater partitioning in the water balance. The second reason is the poor management of agricultural lands, which includes grazing practices (Rockstrom and Falkenmark 2000), fires induced by humans (Delmas et al., 1991), and forest clearing (Fries and Heermans, 1992; Savadogo et al., 2007). These activities have increased erosion, soil loss, loss of nutrients and organic matter, and altered natural stream ecology and regime. An overall poor management may be due to the low understanding of natural phenomena, lack of management tools, and a low level of environmental education of the communities and the authorities but the consequences are further exasperated by the population density reaching the limit of the potential productivity of the land (Wallace and Gregory 2002; Schuol et al., 2008).

5.1.2 Agroforestry

Seasonally dry ecosystems offer great possibilities for sustainable and profitable management of cultivated and natural areas (Fries and Heermans, 1992). Improving rainfed agriculture could take place by increasing the use of the portion of rainfall that infiltrates the soil and is subsequently accessible by plants for biomass growth (Falkenmark and Rockstrom 2006) is a commonly suggested solution.

Agroforestry, or the mixed planting of trees with crops, has long been practiced in West Africa (Neumann et al., 1998). Cannell proposed the central biophysical hypothesis of agroforestry to be that “*the benefits of trees and crops only exist when trees can acquire resources of water, light, and nutrients that crops would otherwise not acquire*” (1996). When they are water limiting, they increase the yield when they increase the fraction of rainfall in plant growth. Improving water use efficiency by crops is an important tool to promote resilience in the face of occurring and predicted climate change (Thomas 2008). Optimizing the water use by trees benefitting from the unused crop water is an opportunity for adaptation. The livelihood benefits are even more significant when one considers the added value that trees offer to agricultural land in terms of non timber products, particularly in years of crop failure due to irregular weather patterns which are expected to become common in West Africa. Non timber forest products includes, edible fruits and leaves, medicines, fodder, wood, and services such as shade, soil and moisture retention.

Reductions in soil moisture are one of the main reasons why farmers are resistant to adopting intensive agroforestry practices (Ong and Leaky, 1999). Agroforestry solutions that emphasize the spatial arrangement of trees and crops in terms of differences in topography and soil variation may be the most beneficial to minimize root competition between crops and trees (Ong et al., 2002). Pruning or separating roots is shown to be effective to separate the root space of the crops and trees. Some argue that agriculture must mimic a natural savanna ecosystem, where there is evidence of clear niche partitioning between the shallow water used by grasses and the deep water drawn by trees.

Shade offered by tree canopies may alter the sub-canopy microclimate and thus the optimal species in adjacent areas. Jonsson et al. (1999) found significant competition for light resources demonstrated by reduction in yields between millet crops and parkland Shea-nut (*Vitellaria paradoxa*) and African mustard trees (*Parkia biglobosa*). Optimizing agroforestry potential may be a matter of matching possible shade preferring crops with appropriate radiation shields offered by specific canopies rather than incorporating the dominant crop into canopy space (Jonsson et al., 1999). Cotton yield, in contrast to that of millet and sorghum, is not reduced by shading by sheanut and African mustard trees, perhaps because water capture is improved with by the shading with little effect on assimilation rates in species that rely on C₃ carbon fixation (Ong and Leaky, 1999). However, Payne (2000) found that reduction of vapor pressure deficit over stands of Pearl Millet, through shading, in combination with soil nutrient supplements could help improve Pearl Millet yields.

Regardless, it is clear that benefits from tree products must outweigh losses in productivity due to shading and water competition for them to be preferred. Matching species that can occupy the same small space or have different requirements in terms of sun, water, and timing can compensate the total yields (Kessler, 1992). *Sclerocarya birrea* was found to be one of the 4 most preferred vegetation species in 60 farmers’ fields in Northern Burkina Faso and was most often valued for food (49%), fodder (21.4%), erosion control (3.9%), domestic use (7.8%), and shade in agricultural area (2%) (Leenders et al., 2005).

A diversification of rural economic activities and a social reorganization must accompany agricultural advances to provide the resilience to changing social and climate pressures (Turner and Robbins, 2008). Improvements should be based on furthered understanding of the water and energy fluxes in natural savannas from observations and modeling (Brümmer et al., 2008a; Brümmer et al., 2008b; Brümmer et al., 2009; Grote et al., 2009). In addition, these improvements to the exchanges between natural and cultivated land, should be compatible with local cultural and economic tendencies (DeFries, 2008; Hobbs and Cramer, 2008).

5.1.3 Objectives

Soil moisture emerges as the crucial variable necessary to understand in order to optimize the resource partitioning between agroforestry trees and surrounding crops, knowledge and interpretation of soil moisture offers scientific support to rural farmers in

countries such as Burkina Faso. Rodriguez-Iturbe et al. (1999) proposed an equation for calculating daily soil moisture as a balance between the stochastic arrival of rainfall events and the deterministic rate of soil moisture losses at a point. They average over the rooting space or the product of soil porosity and the depth of the active rooting level. Although a stochastic model of plant water interactions has been demonstrated, the challenge of upscaling to account for competition between crops and trees is significant (Katul et al., 2007). This chapter takes the first step in exploring the applicability of such a model to a mixed *Pennisetum glaucum* and *Sclerocarya birrea* agroforestry parkland.

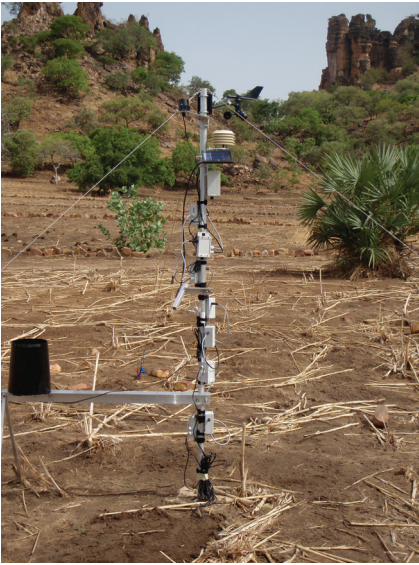


Figure 5-1. Wireless sensing device, Sensorscope used for observation in agricultural field.

Data for this research was collected using wireless sensing devices (Appendix II), making it the first experiment of this type using the Sensorscope Network of wireless sensing devices both in an African rural development context and to study the environmental heterogeneity attributed to trees in an agricultural savanna landscape. Solar panels provided all the energy for this project. Valuable lessons were learned regarding the feasibility of using this technology in this context and the potential of transferring this technology to rural farmers to improve agroforestry practices in the face of climate change.

In this chapter we will run a simple model of soil moisture using the actual measured rainfall from the beginning to the end of the rainy season (May to October) as the sole input for both an herbaceous, millet dominated vegetation cover and directly under a *Sclerocarya birrea* agro-forestry tree. We will then compare the predicted soil moisture with measured values distributed over the rooting depth, through the end of July. Finally, we will identify discrepancies between the modeled and the measured system to guide further study. This is a preliminary analysis of data that will guide subsequent research and indicate the direction for agricultural outreach inquiries specifically regarding the arrangement of agroforestry trees. In addition, we will explore hydrologic flows measured around the agroforestry tree.

5.2 Methods

5.2.1 Site Description

The Singou River Basin is located in South East Burkina Faso in the province of Kompienga (Figure 1-3). It is home to a rare diversity and abundance of wildlife as well as particularly dense vegetation cover, which is in part due to its protection by hunting concessions and national parks and in part due to its relative inaccessibility. However, residents of areas surrounding the protected

areas have been forced to intensify agriculture that has resulted in soil degradation as well as increases in the frequency and severity of flooding and droughts. Local communities are heavily dependent on rain fed agriculture, cultivating a mix of millet, corn, rice, sorghum, tubers in a parkland cropping system interspersed with Karite or Shea butter (*Vitellaria paradoxa*), Niere or African mustard (*Parkia biglobosa*), African grape (*Lannea sp.*), Mango (*Magnifera indica*), Marula (*Sclerocarya birrea*) and other fruit trees. Surrounding the farms and fallows, the landscape is a patchwork of tall grasses, meadows, interspersed with large African Ebony (*Khaya senegalensis*) and Baobab (*Adonsonia digitata*) trees, and shrub woodlands dominated by *Combretaceae*, wetlands, marshes, and riparian gallery forests.

5.2.2 Species Choice

A *Sclerocarya birrea* tree was selected to represent the large woody vegetation of the agricultural zone of the small watershed based on its high prevalence and local importance (Introduction and Conclusion). We are currently investigating the importance of these trees to the local social economy but in a rapid tree inventory of a representative hectare of the agricultural land, 6 of the 9 trees with a diameter at breast height (dbh) of over 10 centimeters were *Sclerocarya birrea*. Other species in the agricultural land include *Ficus thonningii*, *Magnifera indica*, *Piliostigma reticulatum*, and *Terminalia laxiflora*. The individual chosen is a medium tree with a dbh of 40 centimeters located in the agricultural upland. Comparison of large woody vegetation composition of representative 1-hectare plots in agricultural and savanna land cover revealed that there are important differences between the land cover types in terms of their tree densities, species diversity, and age class distributions. Where the agricultural plot only contained 9 individuals of 4 species, the savanna plateau site contained 254 individuals of 23 species, but fewer *Sclerocarya birrea*, and all trees were considerably smaller and shrubbier. This indicates clear preference for *Sclerocarya birrea* by cultivators and is evidence of their removal of small trees.



Figure 5-2. *Sclerocarya birrea* tree in unplanted millet field surrounded by components of wireless sensing network, sap flow sensors, and solar power energy supply.

The relative soil moisture model that we use (Equation 5.1) sets the change in relative soil moisture (ds) per time (dt) equal to the difference between the precipitation (R) or event depth (h) and the sum of losses from canopy interception (I), runoff (Q), evapotranspiration (E), and leakage (L) or deep infiltration averaged over the rooting depth (Z_r) and divided by the pore space (n). Values of soil moisture, rainfall, and interception as well as physical soil parameters were gathered during five months spanning the wet season.

$$\text{Relative Soil Moisture: } nZ_r \frac{ds(t)}{dt} = R(t) - I(t) - Q[s(t), t] - E[s(t)] - L[s(t)] \quad (5-1)$$

$$\text{Soil moisture model in detail}$$

$$R = h = \begin{cases} \lambda < p \rightarrow h = 0 \\ \lambda > p \rightarrow p(h) = \frac{1}{\alpha} e^{-h/\alpha} \end{cases}$$

$$I = \begin{cases} h < \Delta \rightarrow I = h \\ h > \Delta \rightarrow I = \Delta \end{cases}$$

$$Q = \begin{cases} R - I < (1-s) \cdot n \cdot Z_r \rightarrow Q = (1-s) \cdot Z_r \\ R - I > (1-s) \cdot n \cdot Z_r \rightarrow Q = 0 \end{cases} \quad (5-2)$$

$$E = \begin{cases} s < s_w \rightarrow E = \frac{s \cdot E_{\max}}{s_w} \\ s > s_w \rightarrow E = E_{\max} \end{cases}$$

$$L = K \cdot s^{2b+3}$$

This is a minimal model that can be coupled with other processes or expanded to include larger scales or higher complexity such as topography in the future. Each component of the model is calculated as shown in Equation 5.2.

Rainfall was calculated as a Marked Poisson process where time between events follows the exponential derivation, $\lambda e^{-\lambda}$, and the depth of rainfall events follows the exponential distribution of $1/\alpha e^{-h/\alpha}$. Values of λ and α were calculated for a single season, where λ is equal to the frequency of rainfall events and α is equal to the mean depth of event. Actual rainfall was recorded with a *Précis* transduction rain gauge with a resolution of 0.1 millimeter placed in an open area less than 100 meters from the tree of interest.

Interception prevents a part of each rainfall event from reaching the soil because the canopy intercepts it. The quantity of rainfall intercepted is complex and depends on the species, the rainfall intensity, and other seasonal and climatic variables such as wind speed or stage of leaf growth. In the past, interception has been modeled as a percent of rainfall, but this model uses a simplified threshold where Δ represents an amount under which no rain reaches the soil surface. Following the approach of Laio et al. (2001), who calculated interception when the rainfall event was greater than a value Δ , the amount Δ was subtracted from the depth of the event to equal throughfall, or the depth of rain reaching through to the soil surface, with $\Delta=2$ millimeters for (trees) and $\Delta=0.5$ millimeters for grasses (millet). Alternatively, we considered the method of Samba et al., (2001) who found interception to be 9-22% depending on distance from tree (.5 to 1 of the radius) in the case of *Cordyla piñata* (equation 5-3).

$$\text{Interception (Samba et al., 2001)} \quad I = 1.76 * h^{0.2971} \quad (5-3)$$

Runoff was taken into account when throughfall was in excess of the storage capacity. The storage capacity was calculated as the soil moisture subtracted from one and multiplied by the porosity multiplied by the rooting depth. When throughfall was greater than this storage capacity, then the runoff was calculated to be the difference between them. Leakage, or the amount of water that drains from the soil to the depth of the active roots was calculated as the rate of saturated leakage (K), which varies according to soil texture, multiplied by the soil moisture to a power of c , where $c = 2b+3$, and b is coefficient that is strongly related to soil texture (Clapp and Hornberger, 1978).

Evapotranspiration was considered equal to soil moisture (s) multiplied by maximum evaporation (E_{max}) over the point of onset of plant water stress (sw) until s equalled sw , thereafter it was considered to be equal to E_{max} , following the method of Federer (1979). E_{max} was calculated from evaporation measurements calculated using eddy covariance technique using vertical wind speed measured with a Campbell Sonic Anemometer and fluctuations in water vapor concentration measured with a Kipp and Zonar Licor gas analyzer less than 100 meters from the tree of interest in the agricultural field.

The relative soil moisture is the percent of the volumetric water content over the porosity, or in other words the volume of water in the soil over the sum of the volume of air and water. This model is only concerned with the soil in the active root space and averages over that depth. The values of soil moisture ranged between perfectly dry soil (0) and saturated soil (1). Initial soil moisture was estimated at the hygroscopic point, or as close to zero as possible since the model simulation began in January, in the dry season. Calculation was done at a time step of 1 day. All calculations were made in millimeters. Tables 5.1 and 5.2 show the values of all parameters used for the model.

Scenario	Vegetation	Infiltration Threshold Δ (mm)	Rooting Depth Zn (mm)	Wilting Point sw	Maximum Evapotranspiration E_{max} (mm/day)
1	Millet (<i>Pennisetum glaucum</i>)	0.55	1400	0.12	3.4752
2	Marula (<i>Sclerocarya birrea</i>)	2	3000	0.12	3.4752
Ref:		Laio et al. (2001)	Sivakumar et al. (1994), Smith et al. (1997)	Ong and Leaky (1999)	Measured

Table 5-1. Vegetation characteristics used in two scenarios.

Dominant Soil Texture	Pore Size Distribution Index b	Porosity n	Hygroscopic Point s(1)	Saturated Leakage K (mm/day)
Silty Loam	4.977	0.39	0.15	622.08
Appendix III	Fernandez-Illescas et al. (2001)	Sampled	Initial measurement	Clapp and Hornberger (1978)

Table 5-2. Soil characteristics used in two scenarios.

5.2.3 Measurements

The watershed adjacent to the village surrounding an ephemeral stream (3.5 km²) in South East Burkina Faso was instrumented with a network of 12 wireless sensor meteorological stations (Inglrest et al., 2010). Scientific equipment to measure a variety of hydrologic and meteorological variables was installed in 2009 and is still operational. Over the last three years, it has been continually maintained and monitored. Two of these stations were configured to monitor the hydrologic function of 2 individual *Sclerocarya birrea* trees (figure 1-3, Appendix II) For the purposes of this paper, one was fully functional and the other only partially functional. The fully functional station included soil moisture sensors at three depths along two axis of the tree, to the South and to the East. Interception of precipitation by the tree was measured by rain gauges dispersed under the tree canopy. In addition, sap flow sensors monitored the flow of water from the root zone to the canopy. Changes in leaf area index are currently being determined using solar radiation sensors that are set up beneath the tree canopy (following chapter). This particular analysis will focus on the results of the soil moisture monitoring and rainfall monitoring. The hydrologic importance of the *Sclerocarya birrea* tree was then determined by balancing the water balance around each tree using a simple bucket model.

Volumetric water content of soil was measured with the Decagon Devices EC-TM soil moisture and temperature sensor. It measures the volumetric water content between 0 and 1 m³/m³ with a resolution of 0.0008 m³/m³. Sensors were place along two axes running North and East from the base of the tree at radial distance of 0, 2, 5, and 7 meters and depths of 15, 30, and 70

centimeters following a general Doehler design. In addition, fifteen meters from the tree, sensors were installed in an agricultural field at 15 and 30 centimeters depth at a single point. For the purpose of this analysis, measurements at the depths are averaged for each point. Sensors were attached to a wireless sensing network of Sensorscope stations.



Figure 5-3. Decagon devices EC-TM soil moisture sensor installed under tree.

5.3 Results

Total rainfall for the season was 788 mm which is below the average for the nearest long term data record at Pama, 60 km away, from 1978 to 2007 (867.2 mm, Meteo Burkina Faso). Modeled rainfall did not demonstrate the same level of variation and irregularity that the actual rainfall did although the original values for frequency, 0.64495 /day, and mean, 9.0575, were used (Figures 5.5 and 5.6). For this reason, the subsequent model was calculated in response to actual rainfall so that resulting soil moisture could be compared. As shown in Tables 5.1 and 5.2, the only changes between the tree and millet scenarios were interception and rooting depth, however, we see that even these changes affect the sensitivity of the system. The leakage in particular is much higher in the case of millet, and the storage capacity is much higher for the *Sclerocarya birrea* tree.

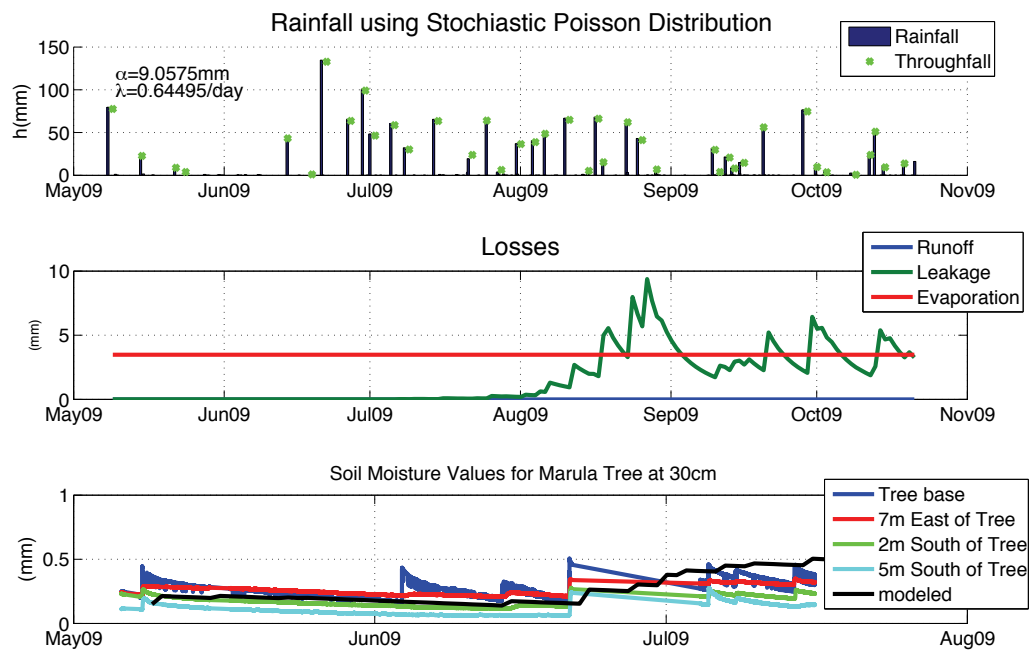


Figure 5-4. Comparison of inputs, losses, and final soil moisture under *Sclerocarya birrea*. Top plot shows modeled rain and throughfall that was used for an input as well as the calculated alpha and lambda values. Losses, middle plot, include runoff (blue), leakage (green), and evaporation (red). Soil moisture is the output, in black in the lower plot. The blue, red, green, and cyan lines show soil moisture measured around the tree at different distances from the trunk base.

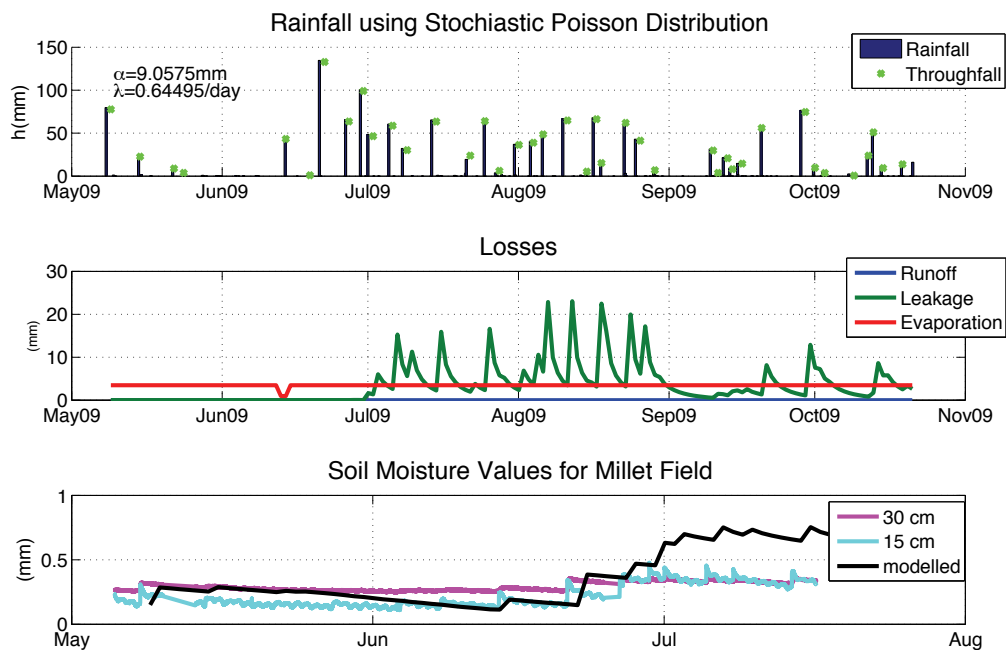


Figure 5-5. Comparison of inputs, losses, and final soil moisture under *Pennisetum glaucum*. Top plot shows modeled rain and throughfall that was used for an input as well as the calculated alpha and lambda values. Losses, middle plot, include runoff (blue), leakage (green), and evaporation (red). Soil moisture is the output, in black in the lower plot. The pink and cyan lines show soil moisture measured under the millet field at 30 and 15 cm respectively.

Figures 5.5 and 5.6 compare the actual response to precipitation and the modeled response. We see that in both cases, the predicted response is a good estimate until July when theoretical soil moisture content continues to rise whereas actual soil moisture decays. At the tree, we focus on the response at a mid point of the rooting depth, 30 centimeters. We see that position in relation to the trunk changes the response considerably. The stemflow, the rain flowing down the trunk at the base of the tree, which is neither the soil moisture nor the sapflow, is a much larger input to the system than the canopy infiltration that we accounted for in this model. Counter intuitively, the values at the edge of the canopy, at 7 meters, also are more important than the mid canopy (5 meters), which is even, less than the near canopy (2 meters). In the millet field, we observe that deeper soils are wetter until July when shallow soils respond much more quickly to the rain event.

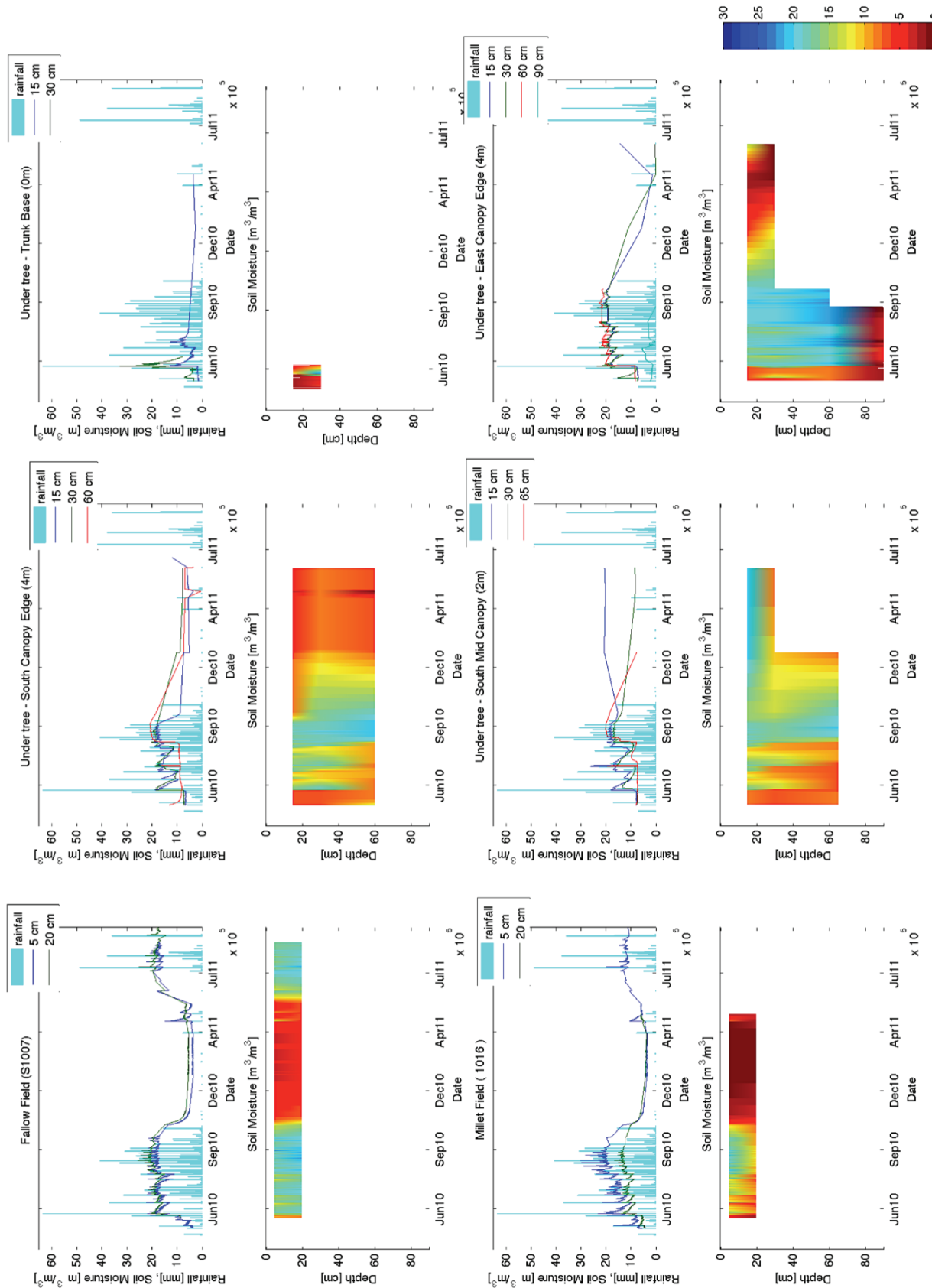


Figure 5-6. 5-7 Soil Moisture profiles compared between two stations in the open and four profiles under the tree. Note that each profiles is a set of 2 graphs – one where the soil moisture at each measured depth is laid over the rain fall, and one where linear interpolation has been used to depict the behavior of soil moisture over the depth of study. The depths are not identical at all sites, but the axis scale has been maintained to aid with comparison.

Observation of soil moisture with the wireless sensor network found considerably higher levels of drying at the fallow field and millet field sites than under the tree (5-6). In the millet field (1016), soil moisture at 20 cm never exceeded 15%, whereas at all sites under the tree, soil moisture exceeded this value after every rainstorm. Both sites in the open fields were apparently dry (soil moisture < 5%) in October and stayed dry until rains began in April and May, whereas beneath the agroforestry tree, soil moisture at what level stayed under the eastern Canopy edge until the end of December at these same depths and lasted all year long under the southern mid canopy. Unfortunately, deep probes were not functional at all sites for all seasons, but this has been corrected for future seasons.

Since the publishing of this chapter, we have collected new data. I'll briefly present that new data here with the goal of stimulating discussion. The general idea is to refine the previously presented modeling exercise using data from our innovative set up of a Sensorscope station around the tree. The quality of this data is not perfect, unfortunately, and some work still needs to take place to improve the compatibility of it with the over all tree water balance.

I begin by using the same soil moisture balance (equation 5-1). Each loss term will be explored separately. Canopy interception was measured with three Davis Rain Gauges under the tree canopy. Interception rained throughout the season, and occasionally reduced throughfall to nothing (figure 5-7). Actual throughfall seems higher than original modeled amount (figure 5-4). Comparing interception to rain, a general linear relationship is visible, with some interception absorbing all rain even at high levels of rain (figure 5-8). The threshold of 2mm for interception is much too low according to our data. Smallest quantities of rain produced no throughfall. Interception as a portion of rainfall is lowest in June - perhaps because the trees leaves are not fully developed yet and intensity is high (figure 5-9).

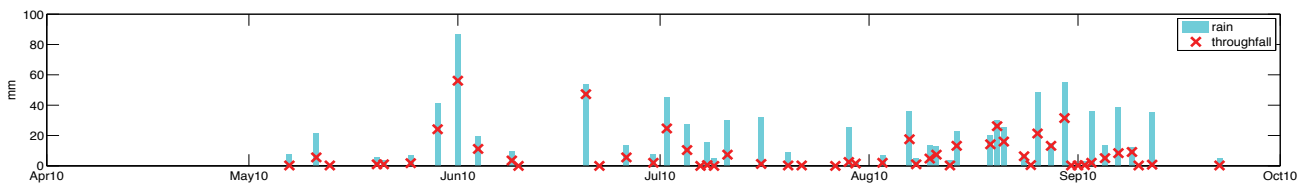


Figure 5-8 Rain & Throughfall. Rainfall is shown in turquoise and the measured interception is shown with red « x ». This is data from one rainy season, 2010. There is one bar for event.

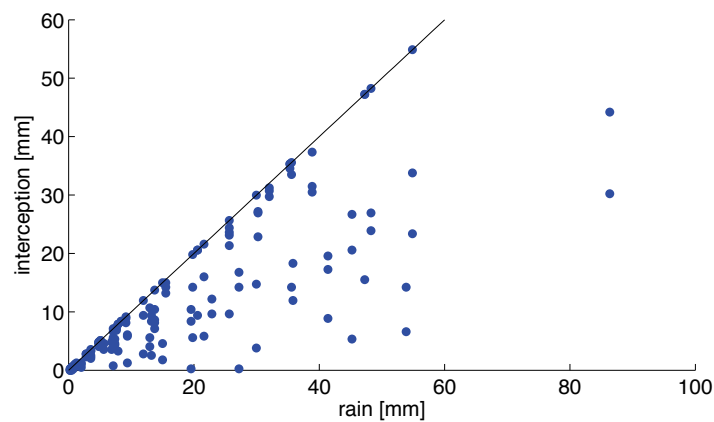


Figure 5-9 Interception compared to rain (mm). This is for the 2010 and 2009 seasons. Both are in mm. The black line is a 1 :1 line. There is one blue dot for event.

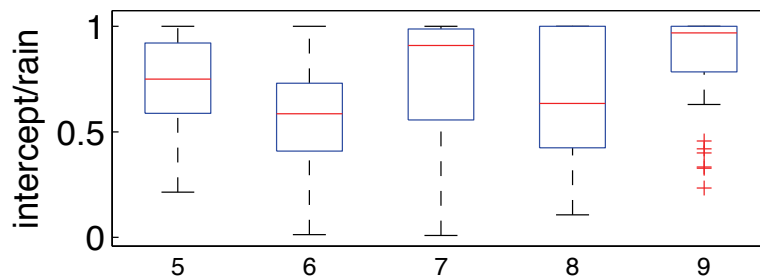


Figure 5-10 Ratio of interception to rain (unitless) according to month of rainy season (x-axis). Red line shows the median, blue box the 25 and 75th quartiles, whiskers the 5 and 95 quartiles, and red +'s the outliers. No clear seasonal trend is visible.

Runoff plots of a square meter were installed under 2 trees, one with relatively sparse understory vegetation (figure 5-10) and one with dense, tall grasses, and 2 open sites – a millet and a fallow field. Run off is expected to respond to the storage capacity at the time of precipitation. Although there is some trend to have increasing runoff with increase in storage capacity, it is not a strong relationship. As is visible in figure 5-11, there was considerable variation in the response of measured runoff. This suggests that it is a fairly nuanced relationship.

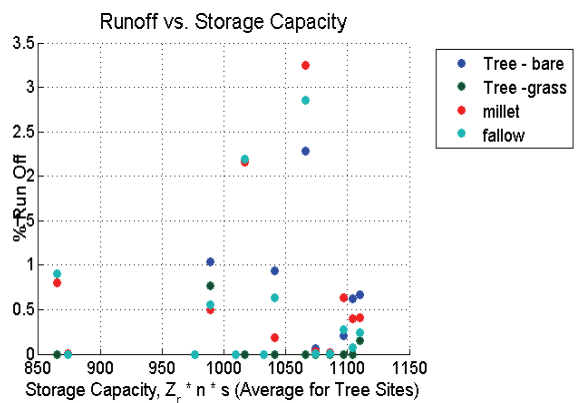


Figure 5-11. Plot of Measured Run-off compared to storage capacity of each site. A general trend is observed up to a point. Photograph of runoff plot to the right. Runoff plots located in 4 places, in the open and under tree as indicated by colors.

Further analysis of soil hydraulic conductivity both through the soil textural analysis and infiltrometer measurements together with the *in situ* soil moisture monitoring described in Appendix III will be used to approximate the deep leakage parameters. Soil moisture was measured at up to 4 different depths at 5 points along two radial axes, South and East for the Field tree (shown) and downslope/North and upslope/South for the Riparian tree. Evaporation is calculated from two eddy-covariance stations and a grainer sap-flow system described in Chapters 2 and 6. Tree transpiration is approximated from sapflow as explained in the following chapter.

5.4 Discussion

The simplistic soil moisture model correctly approximated a part of the response of soil moisture to rainfall, however it is inadequate as time continues. From examination of actual data, it is apparent that there is considerable spatial variation based on the direction and distance from the trunk because of the combined influence of water routing by the branches and trunk, exposure to direct sunlight, and possible small scale slope effects. The model of soil moisture in the open field similarly gives an average

response for soil moisture that it is approximately correct until late June. What happened around the transition from June to July that the model fails to include?

In both cases, the runoff component is zero for the entirety of the modeled time, however there was clear evidence of runoff in both cases in the field following rain events, particularly as the season progressed. In our model, runoff is formed when the amount of throughfall and intensity of throughfall received exceeds storage capacity. According to our current examination, this never occurred, but perhaps it did occur at different spatial parts of the soil, explaining the discrepancy between model and real values. The upper layer of soil may have been completely saturated, generating runoff, even if the vertically averaged storage capacity was not full. When rainfall intensity is high, it exceeds the infiltration capacity of the soil, pools and generates runoff (Brutsaert 2005). The infiltration capacity of the soil needs to be measured at different depths to improve estimations from the literature.

We see the importance of position under the canopy in the sub-tree moisture response (Figure 5-6). Settin et al. (2007) found that the spatial averages over a large basin of the proposed analytical model do describe the soil moisture dynamics, when seasonal dynamics are accounted for. According to their work, improved parameterization of our soil moisture model could be made, if we average all values spatially. For example, we have made estimations of wilting point and rooting depths based on literature for other species, however our model will be stronger if we can solve for these parameters with our individual tree.

Alternatively, we may need to further describe the spatial heterogeneity. Katul et al. (1997), propose a linearized Taylor series to explain the vertical variation in soil moisture loss due to root water uptake in a growth chamber. Their model will allow for the inclusion of diurnal recharge due to the nighttime slowdown of transpiration. Developing our model so that it accounts for root density variation and benefits from sap flux measurements and isotope monitoring may help reduce the observed error. We begin this step in the following chapter.

Isham et al. (2005) propose a method to account for the variability in space and time of the basic soil moisture model by breaking the model space into cylindrical cells. For our purposes their strategy might allow us to account for the variation in factors such as radial direction and distance from tree base, i.e. shading, however addition of throughfall must be calculated in relation to the canopy architecture. Baldocchi et al. (2004) found in their examination of oak savannas, that it is essential to account for variations in evaporative demand over the savanna space. Our current model used evaporation from a nearby eddy covariance tower, but in the future we should measure the latent heat flux at smaller scales and particularly to compare between and under canopies.

Caylor et al. (2006), propose representing savanna heterogeneity as an overlapping network of leaf and root canopies. In this way, they describe the spatial variability of soil moisture at a larger scale. However, there is no clear account for interaction between woody and herbaceous vegetation in their case of a natural savanna using a Poisson distribution to estimate the spatial arrangement of canopies in a Kalahari transect. In 2005, Caylor et al., examined the interaction between trees and grasses using a coupled soil moisture and energy balance method for the Kalahari Desert. They compare under canopy and between canopy levels of soil moisture in terms of the quantity of water stress on the vegetation. They found that areas between canopies experienced higher levels of stress than under canopies and in this way the trees shielded the water stress of understory vegetation in periods of drying. This is the opposite of what we found over the rainy season, that soil moisture was less under canopies, where there is presumably more root uptake.

Our preliminary results are not conclusive yet to make a strong recommendation to rural farmers in terms of managing soil moisture dynamics through woody vegetation. However, our data does show that water is more available in the between canopy spaces, as Ong et al. (2002) warned. Even so, there were still generous levels of soil moisture measured under canopy, particularly at the base of the trunk. The high level of soil moisture that our model produced in contrast to the actual measured soil moisture

show the potential soil moisture if run off was reduced to zero. Encouragement of pooling through artificial barriers is the most effective way to trap this moisture in both the open and subcanopy space. Our data suggests the importance of incorporating the spatial heterogeneity of sub-canopy into planting techniques. We thus recommend exploration of crop varieties that correspond to the moisture and light regimes under canopies, coupled with half moon techniques of stone lines to trap stemflow at the base of the tree trunk.

The soil moisture data used for this analysis was collected using soil moisture probes distributed throughout the rooting area of an agroforestry tree. These data were part of a wireless sensing network of Sensorscope stations. Currently data from 15 stations is sent to one of three base stations where it is collected biweekly with a memory card, however once a GSM network is available on the site, these data will be sent directly to a database on a central server and be available via a public website. This research would not have been possible without the option of multiplexing a large number of sensors on a single station, arranged around a tree. Over the three-month period, these stations required very little maintenance, however, once the rain season progressed into August, the combination of electricity and humidity rendered some of the components ineffective. Improvements are currently being made to prevent damage in future seasons. Solar energy provided all of the power for these stations without any problem, even over the course of the rainy season. Solar energy is well adapted to dry-land ecosystems as a minimal amount of daily solar radiation can be guaranteed.

5.5 Social Perspective

It is apparent that responses to the 2009 and 2010 interviews presented in the introduction disagree considerably. Although they both agree that *Sclerocarya birrea* is important for fruit and medicine in similar fashions - interviews did not concur on its place in the farming and ecological system. Even within the round of interviews, in 2010, there is some disagreement as to whether this species has a real impact on the local soil moisture, the location of its growth, and particularly the significance of its shade's improvement in the lives of people and animals. In this analysis, we have only presented the results of soil moisture monitoring, but subsequent analysis could focus on solar radiation, temperature, and possibly runoff changes due to the present of *Sclerocarya birrea* on the landscape. However, for soil moisture alone, we have already demonstrated that this species does effectively, extend the duration of soil moisture greater than 5% from early October to late December in some areas and through April in other areas. Additionally, the soil moisture reached higher levels under the tree canopy than out in the open. The observation with soil moisture sensors connected to a wireless sensor network demonstrates what some participants (76% in 2010) believed, but others refuted (all in 2009). Similar importance could be demonstrated with solar radiation sensors, runoff plots, and air and soil temperature sensors. In this study, no soil nutrient analysis was completed, but could be used for future studies.

How can this technology benefit the village in this context? Will people benefit from having technology inform them of what they already believe? Beyond the provision of knowledge, which is minimally interesting to subsistence farmers who are mainly concerned with the goal of obtaining food (as opposed to researchers), I propose two scenarios in which this technology, in this village, will benefit the farmers. First an immediate adaptation of farming practices to new observations, and second a payment for ecosystem service scheme that provides monetary incentives to farmers for the benefit of the keeping these trees in their fields that may either benefit them individually at a different scale than they are making decisions at or indirectly benefit other people who are not making the decisions and providing the labor to maintain these trees. Payments would come from people else where in the watershed or globe.

Farming practices could be improved using the knowledge provided by this new technology by optimizing the use of soil moisture below the canopy such as by gardening under the canopy (Rhoades, 1997; Rao *et al.*, 1998; Breman and Kessler, 1997; Buresh and Tian, 1998; Ewel, 1999; Noordwijk and Ong, 1999). As we observed in the interviews, there was some debate as to the possibility of

farming below the canopy of *Sclerocarya birrea*. In 2009, respondents agreed, that this was unproductive, however in 2010, they stated that it was useful for some crops. After observation of the soil profiles (Figure 5-6), I would recommend planting shade crops that use shallow water resources during the dry season, from October through April, in the middle of the canopy. The edge of the canopy and the base of the canopy are much drier, but the middle sustains significant soil moisture into the dry season. In order to transfer knowledge this knowledge to the community and in order for this practice to be accepted by the community, I recommend training sessions with specific interest groups such as the women's cooperative and youth association and eventual experimental plots focused on this goal of transfer. In Tambarga, we already have established the forum for both training sessions and experimental plots as part of the parallel outreach effort that has constructed a youth center and a botanical garden. Plans are underway for both seminar series and experimental gardens, however a plan to farm directly under the *Sclerocarya birrea* tree and observe the effect on soil moisture is not yet established.

An ecosystem service scheme might also be something that would interest local community groups and provide benefits both to local farmers and to the global environment. Several ecosystem benefits are directly linked to soil moisture, specifically, carbon sequestration and runoff, although the links need to be further established and confirmed in this environment. Carbon sequestration is valuable particularly to industrial countries that emit far more carbon dioxide than they sequester (Montagnini and Nair, 2012; Aquino *et al.*, 2011; Luedeling *et al.*, 2011). With current environmental treaties, they are often required to purchase carbon credits from organizations or individuals who can document and quantify the carbon that they sequester, forming the basis for the global carbon market. Without a method to monitor and quantify the carbon sequestered, it is impossible for a community like Tambarga to benefit from the carbon market. This wireless sensor network technology potentially provides a tool for farmers in Tambarga to document their soil moisture. The links between soil moisture and carbon sequestration have been discussed, but until now have not been established (Williams and Albertson, 2004; Porporato and D'Odorico 2003; Xu *et al.*, 2004). This may be a solvable problem that science could contribute to the village. If this link were closed, a farmer in Tambarga could use a Sensorscope station to monitor the soil moisture under their agroforestry trees, have that information delivered in real-time to clients in industrial countries, and receive direct payment for their work of maintaining trees in their fields.

In addition to carbon sequestration, maintaining *Sclerocarya birrea* trees in the fields, benefits downstream residents of the watershed by retaining soil moisture after rainstorms or by transpiring moisture, and thus reducing flash flooding. Again the links between deforestation and vegetation presence and flash flooding need to be further established. In the case of the Tambarga, downstream residents include those in the Singou basin, those in the Pendjari watershed, those in the White Volta basin, and those in the larger basin. In order for the payment for ecosystem service scheme to be successful, downstream users must have enough financial leverage and incentive to pay for the ecosystem benefit (Milder *et al.*, 2010; Jack *et al.*, 2008). In the past few years, flooding has destroyed many communities and contributed to outbreaks of waterborne diseases such as cholera and malaria (BBC, 2011; Opong, 2011); Although few of the downstream users are individually financially powerful enough to afford insurance such as this, perhaps international organizations or governments would be interested in providing the financial backing for this sort of system (Wenland *et al.*, 2010). In particular, downstream of Tambarga is the country of Ghana. Tambarga alone would not be able to set up a payment for ecosystem services scheme at this scale, but perhaps they could associate with surrounding villages. Again, a sensor network is essential to making this ecosystem service conservation documentable and quantifiable.

5.6 Conclusions

This chapter made an important first step in applying a simplistic soil moisture model to the *Sclerocarya birrea* agricultural parkland in Burkina Faso. Further work needs to be done to account for rainfall intensity and the subsequent run off levels. Spatial heterogeneity under canopy space should be examined in more detail in particular in relation to root and canopy architecture and

variations in evaporative demand. Our data suggests some preliminary agroforestry solutions that can optimize water use in this ecosystem such as under canopy planting of crops with lower light and water requirements and stone half moon placement to encourage run off infiltration particularly from stemflow.

This research represents an important first use of wireless sensing networks for environmental management in small-scale rural farms in West Africa. Data was successfully collected over the course of a rainy season. Subsequent work will make this technology more accessible to the farmers and community leaders themselves. The preliminary conclusions of this research already demonstrate the usefulness of this technology to find agroforestry solutions to the hydrologic problems presented by climate change for rural farmers.

In this chapter, we compare the results of the scientific measurement effort with the local perception of the Marula, and propose how innovative technology can be used for on going monitoring of the ecosystem services. Such a monitoring effort could be beneficial to set up additional incentive schemes to encourage farmers to maintain agroforestry trees, thus promoting a more diverse subsistence base, increasing carbon storage, and creating a more resilient social-agricultural system.

The Gourmantche people of South Eastern Burkina recognize marula, bunamangabu, or *Sclerocarya birrea* as a locally important agroforestry tree because of its cultural, agricultural, and nutritional value. Although it is known to provide hydrologic benefits to surrounding crops by local farmers, the larger scientific community had not yet verified its benefits. Using an easily deployable network of wireless meteorological stations, we observe the effect of these agroforestry trees on the local water balance. *Sclerocarya birrea* trees are found to promote deep infiltration of the surface precipitation into the ground water, enhancing recharge. On a patch scale, the highly vegetated surface is shown to conserve soil moisture after the rainy season and thus allows for longer crop cycles. In addition to the hydrologic services, the increased quantity of vegetation allows for marketable ecosystem services such as carbon sequestration or food production diversity.

5.7 References

- Aquino, A. R. D., Aasrud, A., & Guimarães, L. (2011). Carbon Sequestration Potential of Agroforestry Systems. (B. M. Kumar & P. K. R. Nair, Eds.)Development, 8. Dordrecht: Springer Netherlands.
- Baldocchi, D.D., Xu, L., & Kang, N. (2004). How plant functional-type, weather, seasonal drought, and soil physical properties alter water and energy fluxes of an oak-grass savannah and an annual grassland. *Agricultural and Forest Meteorology*, 123(1-2), 13-19.
- BBC. (2011). Deadly floods hit Ghana capital Accra. www.bbc.co.uk/news/world-africa-15475084
- Breman, H., & Kessler, J. J. (1997). The potential benefits of agroforestry in the Sahel and other semi-arid regions. *European Journal of Agronomy*, 7, 25-33.
- Brümmer, C., Brüggermann, N., Butterbach-Bahl, K., Falk, U., Szarzynski, J., Vielhauer, K., Wassmann, R., & Papen, H. (2008a). Soil-atmosphere exchange of N₂O and NO in near- natural savannah and agricultural land in Burkina Faso. *Ecosystems*, 11(4), 582-600.
- Brümmer, C., Falk, U., Papen, H., Szarzynski, J., Wassmann, R., & Brüggermann, N. (2008b). Diurnal, seasonal, and interannual variation in carbon dioxide and energy exchanges in shrub savannah in Burkina Faso. *Journal of Geophysical Research*, 113, G02030, 1-11.
- Brümmer, C., Papen, H., Wassmann, R., & Brüggermann, N. (2009). Fluxes of CH₄ and CO₂ from soil and termite mounds in south Sudanian savannah of Burkina Faso. *Global Biogeochemical Cycles*, 23(1), 1-13.
- Buresh, R. J., & Tian, G. (1998). Soil improvement by trees in sub-Saharan Africa. *Tropical Agriculture*, 51-76.
- Cannell, M.G.R., Noordwijk, M.V., & Ong, C.K. (1996). The central agroforestry hypothesis: the trees must acquire resources that the crop would not otherwise acquire. *Agroforestry Systems*, 34(1), 27-31.
- Caylor, K., D'Odorico, P., & Rodriguez-Iturbe, I. (2006). On the ecohydrology of structurally heterogeneous semiarid landscapes. *Water Resources Research*, 42(7), 1-13.

- Caylor, K., Shugart, H.H., & Rodriguez-Iturbe, I. (2005). Tree canopy effects on simulated water stress in Southern African savannas. *Ecosystems*, 8(1), 17-32.
- Clapp, R.B., & Hornberger, G.M. (1978). Empirical equations for some soil hydraulic properties. *Water Resources Research*, 14(4), 601-604.
- DeFries, R. 2008. Terrestrial vegetation in the coupled human-earth system: contributions of remote sensing. *Annual Review of Environmental Resources*, 33, 369-390.
- Delmas, R.A., Mraenco, A., Tathy, J.P., Cros, B., & Baudet J.G.R. (1991). Sources and sinks of methane in the African savannah. *Journal of Geophysical Research – Atmosphere*, 96(D4), 7287-7299.
- Donner, L.J., & Large, W.G. (2008). Climate modeling. *Annual Review of Environmental Resources*, 33, 1-17.
- Downing, T.E., Ringius, L., Hulme M., & Waughray, D. (1997). Adapting to Climate Change in Africa. *Mitigation and Adaption Strategies for Global Change*, 2(1), 19-44.
- Ewel, J. J. (1999). Natural systems as models for the design of sustainable systems of land use. *Agroforestry Systems*, 1-21.
- Falkenmark, M., & Rockstrom J. (2006). The new blue and green water paradigm: breaking new ground for water resources planning and management. *Journal of Water Resources Planning and Management*, 132(3), 129-132.
- Federer, C.A. (1979). A soil-plant-atmosphere model for transpiration and availability of soil water. *Water Resources Research*, 15(3), 555-562.
- Fernandez-Illescas, C.P., Porporato, A., Laio, F., & Rodriguez-Iturbe, I. (2001). The ecohydrological role of soil texture in a water-limited ecosystem. *Water Resources Research*, 37 (12), 2863-2872.
- Fries, J., & Heermans, J. (1992). Natural forest management in semi-arid Africa: status and research needs. *Unasylva*, 43(168), 9-15.
- Furley, P. (2004). Tropical savannas. *Progress in Physical Geography*, 28, 581-598.
- Griffith, A.L. (1961). Dry woodlands of Africa South of the Sahara. *Unasylva*, 15(1).
- Grote, R., Lehmann, E., Brümmner, C., Brüggemann, N., Szarzynski, J. & Kunstmann H. (2009). Modeling and observation of biosphere-atmosphere interactions in natural savannah in Burkina Faso, West Africa. *Physics and Chemistry of the Earth*, 34(4-5), 251-260.
- Hobbs, R.J., & Cramer, V.A. (2008). Restoration ecology: interventionist approaches for restoring and maintaining ecosystem function in the face of rapid environmental changes. *Annual Review of Environmental Resources*, 33(1), 39-61.
- Hulme, M., Doherty, R., Ngara, T., New, M., & Lister, D. (2000). African Climate Change 1900-2100. *Climate Research*, 17(2), 145-168.
- Isham, V., Cox, D.R., Rodriguez-Iturbe, I., Porporato, A., & Manfreda, S. (2005). Representation of space-time variability of soil moisture. *Proceedings of the Royal Society A*, 461(2064), 4035-4055.
- Jack, B. K., Kousky, C., & Sims, K. R. E. (2008). Designing payments for ecosystem services: Lessons from previous experience with incentive-based mechanisms. *Proceedings of the National Academy of Sciences of the United States of America*, 105(28), 9465-70.
- Jonsson, K., Ong, C.K., & Odongo, J.C.W. (1999). Influence of scattered néré and karité trees on microclimate, soil fertility, and millet yield in Burkina Faso. *Exploratory Agriculture*, 35(1), 39-53.
- Kallis, G. (2008). Droughts. *Annual Review of Environmental Resources*, 33, 85-118.
- Katul, G., Porporato, A., & Oren, R. (2007). Stochastic dynamics of plant-water interactions. *Annual Review of Ecology and Evolution Systematics*, 38, 767-791.
- Katul, G., Todd, P., Pataki, D., Kabala, Z., & Oren, R. (1997). Soil water depletion by oak trees and the influence of root water uptake on the moisture content spatial statistics. *Water Resources Research*, 33(4), 611-623.
- Kessler, J. (1992). The influence of karité (*Vitellaria paradoxa*) and néré (*Parkia biglobosa*) trees on sorghum production in Burkina Faso. *Agroforestry Systems*, 17(2), 97-118.
- Laio, F., Porporato, A., Ridolfi, L., Rodriguez-Iturbe, I. (2001). Plants in water-controlled ecosystems: active role in hydrologic processes and response to water stress II. Probabilistic soil moisture dynamics. *Advances in Water Resources*, 24(7), 707-723.
- Leenders, J.K., Visser, S.M., & Stroosnijder, L. (2005). Farmers' perceptions of the role of scattered vegetation in wind erosion control on arable land in Burkina Faso. *Land Degradation and Development*, 16(4), 327-337.
- Luedeling, E., Sileshi, G., Beedy, T., & Dietz, J. (2011). Carbon Sequestration Potential of Agroforestry Systems. (B. M. Kumar & P. K. R. Nair, Eds.) *Media*, 8(C), 61-83. Dordrecht: Springer Netherlands.

- Mahe, G., Olivry, J.C., & Servat, E. (2005). *Sensitivity of West-African Rivers to Climatic and Environmental Changes: Extremes and Paradoxes*. Wallingford: IAHS Press.
- Milder, J. C., Scherr, S. J., & Bracer, C. (2010). Trends and Future Potential of Payment for Ecosystem Services to Alleviate Rural Poverty in Developing Countries. *Ecology And Society*, 15(2).
- Miles, L., Newton, A.C., DeFries R.S., Ravilious, C., May, I., Blyth S., Kaspos, V., & Gordon, J.E. (2006). A global overview of the conservation status of tropical dry forests. *Journal of Biogeography*, 33(3), 491-505.
- Montagnini, F., & Nair, P. K. R. (2012). Carbon sequestration : An underexploited environmental benefit of agroforestry systems. *Agroforestry Systems*, 281-295.
- Murphy, P.G., & Lugo A.E. (1986). Ecology of tropical dry forest. *Annual Review of Ecology and Systematics*, 10(1):17, 67-88.
- Neumann, K., Kahlheber, S., & Uebel, D. (1998). Remains of woody plants from Saouga, a medieval West African village. *Vegetation History and Archaeobotany*, 7(2), 57-77.
- Noordwijk, M. V. A. N., & Ong, C. K. (1999). Can the ecosystem mimic hypotheses be applied to farms in African savannahs ? *East*, 131-158.
- Ong, C.K, Wilson, J., Deans, J.D., Mulayta, J., Raussen, T., Wajja-Musukwe, N. (2002). Tree-crop interactions: manipulation of water use and root function. *Agricultural Water Management*, 53(1-3), 171-186.
- Ong, C.K., & Leaky, R.R.B. (1999). Why tree-crop interactions in agroforestry appear at odds with tree-grass interactions in tropical savannahs. *Agroforestry Systems*, 45(1-3), 109-129.
- Oppong, B. K. (2011). Environmental Hazards in Ghanaian Cities: The Incidence of Annual Floods Along the Aboabo River in the Kumasi Metropolitan Area (KMA) of the Ashanti Region of Ghana. Methodology. Kwame Nkrumah University of Science and Technology.
- Payne, W.A. (2000). Optimizing crop water use in sparse stands of pearl millet. *Agronomy Journal*, 92(5), 808-814.
- Porporato, A., & D'Odorico, P. (2003). Hydrologic controls on soil carbon and nitrogen cycles . I . Modeling scheme. *Advances in Water Resources*, 26, 45-58.
- Rao, M. R., Nair, P. K. R., & Ong, C. K. (1998). Biophysical interactions in tropical agroforestry systems *. *interactions*, (5), 3-50.
- Rhoades, C. C. (1997). Single-tree influences on soil properties in agroforestry : lessons from natural forest and savanna ecosystems. *Agroforestry Systems*, 71-94.
- Richards, P. (1985). *Indigenous agricultural revolution: ecology and food production in West Africa*. London: Hutchinson.
- Rockstrom, J., & Falkenmark, M. (2000). Semiarid crop production from a hydrological perspective: gap between potential and actual yields. *Critical Reviews in Plant Sciences*, 19(4), 319-346.
- Rodriguez-Iturbe, I., Porporato, A., Ridolfi, L., Isham, V., & Cox, D.R. (1999). Probabilistic modeling of water balance at a point: the role of climate, soil and vegetation. *Proceedings of the Royal Society Academy of London Series A Mathematical Physical and Engineering Sciences*, 455(1990), 3789-3805.
- Samba, S.A.N.S., Camire, C., & Margolis, H.A. (2001). Allometry and rainfall interception of *Cordyla pinnata* in a semi-arid agroforestry parkland, Senegal. *Forest Ecology and Management*, 154(1-2), 277-288.
- Savadogo, P., Sawadogo, L., & Tiveau, D. (2007). Effects of grazing intensity and prescribed fire on soil physical and hydrological properties and pasture yield in the savannah woodlands of Burkina Faso. *Agriculture, Ecosystems & Environment*, 118(1-4), 80-92.
- Schuol, J., Abbaspour, K.C., Yang, H., Srinivasan, R., & Zehnder, A.J.B. (2008). Modeling blue and green water availability in Africa. *Water Resources Research*, 44(7), 1-18.
- Settin, T., Botter, G., Rodriguez-Iturbe, I., & Rinaldo, A. (2007). Numerical studies on soil moisture distributions in heterogeneous catchments. *Water Resources Research*, 43(5), 1-13.
- Sivakumar, M.V.K., & Salaam, S.A. (1994). A wet excavation method for root/shoot studies of pearl millet on the sandy soils of the Sahel. *Experimental Agriculture*, 30(3), 329-336.
- Smith, D.M., Jarvis, P.G., & Odongo, J.C.W. (1997). Sources of water used by trees and millet in Sahelian windbreak systems. *Journal of Hydrology*, 198(1-4), 140-153.
- Thomas, R.J. (2008). Opportunities to reduce the vulnerability of dryland farmers in Central and West Asia and North Africa to climate change. *Agriculture, Ecosystems, and Environment*. 126(1-2), 36-45.
- Turner, B.L., & Robbins, P. (2008). Land-changes science and political ecology: similarities, differences, and implications for sustainability science. *Annual Review of Environmental Resources*, 33, 295-316.

- Wallace, J.S., & Gregory, P.J. (2002). Water resources and their use in food production systems. *Aquatic Sciences*, 64(4), 363–375.
- Wendland, K. J., Honzák, M., Portela, R., Vitale, B., Rubinoff, S., & Randrianarisoa, J. (2010). Targeting and implementing payments for ecosystem services: Opportunities for bundling biodiversity conservation with carbon and water services in Madagascar. *Ecological Economics*, 69(11), 2093-2107. Elsevier B.V.
- Williams, C. A., & Albertson, J. D. (2004). Soil moisture controls on canopy-scale water and carbon fluxes in an African savanna. *Water Resources*, 40, 1-14.
- Williams, M. (2008). A new look at global forest histories of land clearing. *Annual Review of Environmental Resources*, 33(1), 245-367.
- Wittig, R., König, K., Schmidt, M., & Szarzynski, J. (2007). A study of climate change and anthropogenic impacts in West Africa. *Environmental Science and Pollution Research*, 14(3), 182-189.
- Xu, L., Baldocchi, D. D., & Tang, J. (2004). How soil moisture, rain pulses, and growth alter the response of ecosystem respiration to temperature. *Global Biogeochemical Cycles*, 18(4), 1-10.
- Zheng, X., & Eltahir, E. (1998). The Role of vegetation in the dynamics of West African Monsoons. *Journal of Climate*, 11, 2078-2096.

Chapter 6 Detection of seasonal leaf out and groundwater recharge with stable isotopes of water

The net benefit of agroforestry trees for small scale farmers in dry land agricultural systems is debatable because while they provide significant direct and indirect services to the farmer and crops, they also consume considerable amounts of scarce resources, specifically water. In this chapter, we monitor the stable isotopes of water to improve understanding of water use by a *Sclerocarya birrea* tree in a millet field in South Eastern Burkina Faso. Isotopic ratios were determined from water extracted from stems and sub-canopy soil, while nearby ground water, precipitation, and surface water was sampled weekly. Canopy leaf area index was first determined through photo documentation of the canopy and then correlated with shading observed with broad-spectrum solar radiometers placed under the canopy. Finally, sap flow monitored with a heat pulse system was used to directly observe transport in the trunk. This new use and configuration of the wireless sensor network, which measures the canopy temperature and humidity, soil moisture, and subcanopy light penetration. It provides a more simple and economical method to monitor vegetation change. The different sets of observations – stable isotopes, sap flow, canopy shading of radiometers, and photographic documentation – corresponded with each other regarding dates of senescence and leaf out, thus validating each other. This analysis proved the extreme seasonality of the *Sclerocarya birrea* tree corresponding to the shift between the wet and dry seasons and employed two novel techniques – stable isotopes to monitor source water and radiometers to observe changes in canopy cover. This research contributes to global understanding of agroforestry as a tool for climate change adaptation in dry-land ecosystems.

6.1 Introduction

6.1.1 Open question of agroforestry's benefit

Agroforestry refers to farming systems that mix woody perennials alongside herbaceous vegetation. There is a high potential benefit of diversifying land use in this way, because each component occupies a separate niche, uses different resources, responds differently to environmental stressors, and provides different services (Lott, Khan, Ong, & Black, 1996). However, before recommending pairing of particular species and systems, it is important to examine their interactions, both complementary and competitive. In semi-arid systems, water is the principle limiting resource. Thus an examination of the benefits of agroforestry in a semi-arid system must study the hydrologic flows through the components of the agroforestry system, including below ground interactions in the root system.

6.1.2 Review of Stable Isotopes in Water

As water moves through the environment and changes phase, the abundances of these different isotopes vary. Certain processes such as evaporation are known to differentiate between isotopes and thus fractionate the concentrations resulting in, for example, a liquid body that is enriched of heavy isotopes, and a vapor that is depleted in heavy isotopes (Gonfiantini, 1986). This is because

the heavier isotopes are less volatile. In contrast, other processes do not fractionate water. The uptake of water from the soil across the root surface does not fractionate water, nor does transport of water and infiltration of water through soil layers, therefore the water source of plant water use can be identified by examining the stable isotope composition of xylem water and comparing it to different sources of water because there is no fractionation across root surface as water is taken up into the xylem (Ehleringer, Phillips, Schuster, & Sandquist, 1991). However, it has been shown that water can become enriched in woody stems because of enrichment at the leaf surface from transpiration (Dawson & Ehleringer, 1993) which is a source of error.

Water exists in several common stable isotopes, or molecular rearrangements, other than the most common, $H_2^{16}O$; $H_2^{18}O$; $H_1^1H_1^2O^{16}$; $H_2^2O^{18}$; and $H_1^2O^{18}$. The fraction of each of these present in any given water can be expressed relative to the Vienna Standard Mean Ocean Water (V-SMOW).

$$\delta^{18O} \text{ or } \delta^{2H} (\text{‰}) = \frac{R_{\text{sample}}}{R_{\text{SMOW}}} - 1 \times 1000 \quad (6-1)$$

As Gonfiantini (1986) explains, according to the Craig-Gordon model of evaporation, water vapor that is released from liquid surface is depleted in heavy isotopes compared to the liquid because they are less volatile. A linear mixing model is the most basic way to calculate source water, as it assumes that the “product” water, for example the water at the stream outlet, will equal a combination of its sources, for example the glaciers, soil water, rain water, and lakes that feed it. However, Burgess (2000) found that a linear mixing model, or the end member method of assessing water sources to be insufficient for determination of plant water sources. Detailed profiling of δD is required to understand where the vegetation obtains its water. He advised that more aggressive studies using irrigation or direct injection into plant tissues should be considered, or else root excavations and soil moisture monitoring are required to understand under ground resource partitioning.

6.1.3 Monitoring of Stable Isotopes in West Africa

The isotopic signature of water is less documented in West Africa compared to other parts of the world, however we do know that there is variation that allows for stable isotopes to be used as tracers. Jean-Denis Taupin *et al.* (2000) analyzed the isotope signatures of all precipitation in the IAEA database through 1989. Only a small part of IAEA samples are over the African continent. They found that the Gulf of Guinea and re-evaporated water are the main sources of vapor in the Sudaneo-Sahelian zone of West Africa. The significance of re-evaporated water suggests the importance of land use to regional climate. West Africa's climate is characterized with a winter when dry air masses circulate southwards and a summer when humid air masses move from the South Atlantic towards the north and the inter tropical convergence zone extends up to about thirteen degrees north. North of which, precipitation occurs when the inter-tropical front changes structure at three-kilometer elevation. Evapotranspiration is an important contribution to moisture. Water that originates from the Gulf of Guinea will show a decreasing value of δO^{18} as the monsoon rains travel inland because heavy isotopes will be preferentially removed by falling rain because they are heavier. This creates regional variation that also results in enough of a range over the course of the rainy season that we can use stable isotopes as a tracer in this region. δO^{18} and δH^2 are essential indicators of evaporative enrichment and can be used to quantify evaporation rates in shallow ground water environments (Edmunds, 2010).

6.1.4 Stable Isotopes are useful tracers to understand plant water use

Stable isotopes can be used as tracers to observe how the underground resource is partitioned into soil water, water taken up by trees, water that will evaporate directly from the soil, and stored water (Ehleringer, Dawson, & City, 1992). For example, Smith, Jarvis, & Odongo (1997) investigated the groundwater access of trees in agroforestry, specifically windbreak, systems in Niger using stable isotopes of water sampled both in the xylem tissues and in the soil water. They contrasted two sites and found that near the

town of Majjia which received 544mm of rain, *Azadirachta indica* trees intercropped in a millet field could access the groundwater which was only 6-8 meters under the surface whereas in Sadoré which received 379mm of rain, windbreaks competed with millet fields for access to near surface soil water because groundwater was unattainable at a depth of 35 meters. Bertrand *et al.* (2012) used stable isotopes of water extracted from stems of riparian vegetation to look at trends in water uptake. Similarly to our study, they sampled groundwater, rainwater, soil water and tree water. However, they did not extract the water from the stems, but rather equilibrated the water vapor with the xylem sap in closed containers. Their measurements, therefore, might have less contamination for non-xylem water located in the stem tissue.

Isotopic analysis can reveal the origin of stem flow (Van Noordwijk *et al.*, 2004). Oxygen has 3 stable isotopes O-16, O-17, and O-18, which are found in various concentrations in the environment. The ratio between O-18 to O-16 is of particular interests to hydrologists because O-18 is enriched in water bodies with high levels of evaporation and depleted in high altitude water sources and cold precipitation. Hydrogen is found in two stable isotopes H-1 or H-2 (Deuterium). Similarly to O-18, H-2 concentrations are elevated in evaporated water (sea water, saline lakes), while polar ice and other less-evaporated water bodies contain lower concentrations. If evaporation and condensation are occurring in isotopic equilibrium, the relationship between the ratios of O-18 to O-16 and H-2 to H-1 will fall along the global meteoric water line (m-line), characterized by a slope of 8 and an intercept on the H-2 axes, referred to as the deuterium excess (Mook, 2000).

Evaporation, however, is a non-equilibrium process and results in a fractionation along a line with a slope of 4.5. By studying the ratios of isotopes of oxygen and hydrogen, we can deconstruct the story of how water has traveled and evaporated (Mook, 2000). If the isotopic ratios of water sources, such as surface water, ground water, and soil water, are sampled, the isotopic ratio in extracted xylem water in plant tissue can be used to determine the source water used by the plant (Dawson, 1993).

6.1.5 Research goals

Understanding water use by agroforestry trees in dry-land ecosystems is essential for improving water management. Agroforestry trees are valued and promoted for many of their ecologic and economic benefits but are often criticized as competing for valuable water resources. Much of the balance between benefits and costs depends both on the tree species and the environment where they are grown. By examining the seasonal evolution of the isotopic signature of flows through the watershed from precipitation through surface and groundwater, vegetation, and soil, we can determine when the tree is relying on soil moisture and ground water. We would like to investigate whether data collected using 4 innovative methods (stable isotope analysis, canopy observation, sap flow, and solar radiation attenuation), confer on times of leaf out, access to groundwater, and hydrologic connectivity.

6.1.6 Sampling and Measurement

The study site is shown relative to climatic zones, neighboring larger watersheds, and hunting concessions, as well as the position of the equipment in relation to the village, local topography and land cover in Figure 1-1. This study focuses on a single *Sclerocarya birrea* agroforestry tree. The tree is located in a mixed millet and fallow field, which is located near an ephemeral stream that flows into the Singou River, that is part of the Volta Basin. It is located in the Sudanian botanical and climate zone, and is farmed by the village of Tambarga, which is part of the commune of Madjoari. The 8 villages of this commune are isolated, inaccessible and surrounded by game reserves and national parks. The single *Sclerocarya birrea* tree is shown on the map (Figure 1-1). It is 13 m tall and has a 7 m canopy radius (Figure 6-1). The solar radiation sensors are arranged under the canopy at a height of 0.50 cm and the temperature/relative humidity sensors are arranged as a vertical profile in the center of the tree.



Figure 6-1 Sclerocarya birrea tree in June 2010. Sensors are visible under the tree canopy.

6.1.7 Sampling, Extraction

In order to monitor water uptake by the tree, we sampled xylem and soil for water extraction in parallel with water. Isotopes will serve as tracers to allow us to monitor water use. Water samples were collected directly and filtered with a 0.5 μm nylon syringe filter. Stem samples were collected from three points randomly distributed around the tree and soil samples were obtained from one point at 15 and 30 cm under the tree. Stem and soil samples were collected in hermetically sealed tubes. When possible, they were sealed a second time with parafilm and kept refrigerated. Water was obtained from stems using cryogenic vacuum distillation (Ehleringer, Roden & Dawson, 2000) conducted at the Paul Scherrer Institute in Villigen, Switzerland. Water from stem and soil samples was extracted by placing the samples in a warm water bath (80°C) under vacuum pressure of 10^{-3} Pa and then they are drawn into a liquid Nitrogen bath of -140°C for at least 2 h per sample. After extraction, the U-tubes with the frozen stem water were removed from the extraction line, sealed, the water thawed and transferred into 2 mL crimp cap vials (Edmunds, 2010).

6.1.8 Cavity Ring Down Spectroscopy

In order to know the isotopic content of each sample, we had to process and analyze the samples. Since isotopic values are relative, we chose standards that would be above and below our samples to compare them with. These standards were previously calibrated with the standard IAEA values, as is convention. All samples, both extracted and directly sampled, were analyzed with a Picarro L2130-i CRDS to obtain $\delta\text{O}18$ and $\delta\text{D}H$ fractions. All values are in relation to VSMOW standards. A few samples were also run on a standard Mass Spectrometer for reference (Paul Scherrer Institute, Villigen).

All samples were run with three standards whose values of deuterium and O18 were previously determined relative to IAEA delivered samples of Vienna Standard Mean Ocean Water 2 (VSMOW2: $\delta\text{O}18 = 0 \pm 0.02$; $\delta\text{D}H = 0 \pm 0.3$), Standard Light Antarctic

Precipitation 2 (SLAP2: $\delta\text{O}18 = -55.50 \pm 0.02$; $\delta\text{D}H = -427.5 \pm 0.3$), and Greenland Ice Sheet Precipitation (GISP: $\delta\text{O}18 = -24.76 \pm 0.09$; $\delta\text{D}H = -189.5 \pm 1.2$). Our house standards were calibrated on two separate Cavity Ring Down Spectrometers (CRDS). They were Hawaii Deep Blue water (HAW: $\delta\text{O}18_{\text{VSMOW}} = -0.1702$; $\delta\text{D}H_{\text{VSMOW}} = -2.1228$), Lausanne Millipore (LMP: $\delta\text{O}18_{\text{VSMOW}} = -12.1467$; $\delta\text{D}H_{\text{VSMOW}} = -90.3141$), and a mix of those two (HAWLMP: $\delta\text{O}18_{\text{VSMOW}} = -6.1565$; $\delta\text{D}H_{\text{VSMOW}} = -45.1072$). Early in our analysis, we used two other standards: BCS ($\delta\text{O}18_{\text{VSMOW}} = -14.24$; $\delta\text{D}H_{\text{VSMOW}} = -108.60$) and LRY ($\delta\text{O}18_{\text{VSMOW}} = -10.03$; $\delta\text{D}H_{\text{VSMOW}} = -70.44$), which were also both made at EPFL (M. Bensimon, EPFL, pers. comm).

Deuterium excess was also determined for each sample as the deviation from the Global Meteoric Water Line (Gat, 1996).

$$\text{Deuterium excess} \quad D_{ex} = \delta D - \delta^{18}\text{O} \quad (6-2)$$

In a tray of 54 vials, the first vial was always deionized water (DI) and the first three following the DI and the last three vials of the tray were standards. The HAW standard was always placed in first and last position since its difference was most likely to contaminate the samples. The standards were used to correct all samples along a standard curve. Variation between the first standards and the last standards was used as a measure of precision and drift. In addition, a controlled DI was run every six vials. This was used as a secondary control of drift (Lis, 2008). If the needle malfunctioned or if there was a high amount of drift or variability, the run was rerun. If there was an isolated sample that caused a problem, that sample was rerun if possible along with its duplicate.

6.1.9 Sap flow

A heat pulse Granier probe (UpGmbH Sap Flow System, User Manual: 2001) was used to measure sapflow. The instrument measures the difference in temperature between the upstream and downstream probe. The probes are made up of thermocouples (copper-constantan and are 10 cm away from each other. The top needle is heated constantly and will cool down more when the velocity is high, providing the difference in temperature and thus the signal. The temperature difference will be greatest without any sap flow. This temperature difference is converted to sap flow by multiplying by a dissipation coefficient.

$$\text{Sap Flow} \quad F = SA * 0.714 \left(\frac{\Delta T_{max}}{\Delta T} - 1 \right)^{1.231} \left[\frac{ml}{min} \right] \quad (6-3)$$

We used a sapwood area (SA) of 0.1243 m^2 based on a circumference of 125cm (measured, 2009) and a maximum temperature value for each 24 hour period from noon to noon to be the “night or no flow” value (6-3).

6.1.10 Additional Measurements

Additional meteorological measurements were taken with a network of wireless, autonomous stations that communicate through the GSM network (Sensorscope, see previous chapters) and 2 energy balance and eddy-covariance stations. The same wireless sensor network stations (Appendix IV) were uniquely configured around the *S. birrea* tree to collect and transmit the sub-canopy solar radiation, through fall, stem flow (Davis Instruments, see previous chapters), and soil moisture (Decagon, see previous chapter).

6.1.11 Canopy Shading

Canopy shading was obtained through 3 different means. First, the difference between the solar radiation sensors situated under and outside of the canopy were taken as a difference in shading. Theoretical solar radiation was calculated according to Whiteman and Allwine (1986). Second, photographs were taken daily from under the canopy, looking up at the canopy. These were analyzed for pixels of sky, green, and other and the ratio was used as a measure of leaf area index (LAI, equation 4-4) according to Korhonen

et al. (2009). Finally, an areal measurement of vegetation presence was used by using the extracted pixels from the NDVI product of MODIS, as described previous chapters.

$$\text{Canopy Cover Fraction (CCF)} = \frac{\text{leaf area}}{\text{leaf area} + \text{sky area}} \quad (6-4)$$



Figure 6-2. Sub-canopy view providing pixels to be analyzed.

Daily documentation of canopy leaf cover was done through inverse canopy photographs like this one. The photos that we used were taken at 2.5 m from the trunk in full sunlight if possible. There were also photos taken at the tree base and at the edge of canopy. They were always taken in the same place, marked by the solar radiometers. These areas were considered to be representative of the canopy.

6.2 Results

All together, there were 13 points of soil sampling, 8 points of tree sampling, 13 wells, 5 pumps, 3 surface water (stream) points, 4 locations of rain sampling, and 6 springs that were sampled. Some of these points were more continuously and maintained, others were changed by choice or obligation (for example one well went dry) as demonstrated by the colors in figure 6-3. We sampled the ground, surface, rain, plant and soil water a total of 2194 times. These samples were distributed among soil, trees, wells, pumps, surface water, rain, and springs. In general, we sampled more frequently in the rain season, especially for the surface water and rain that was impossible to sample during the dry season.

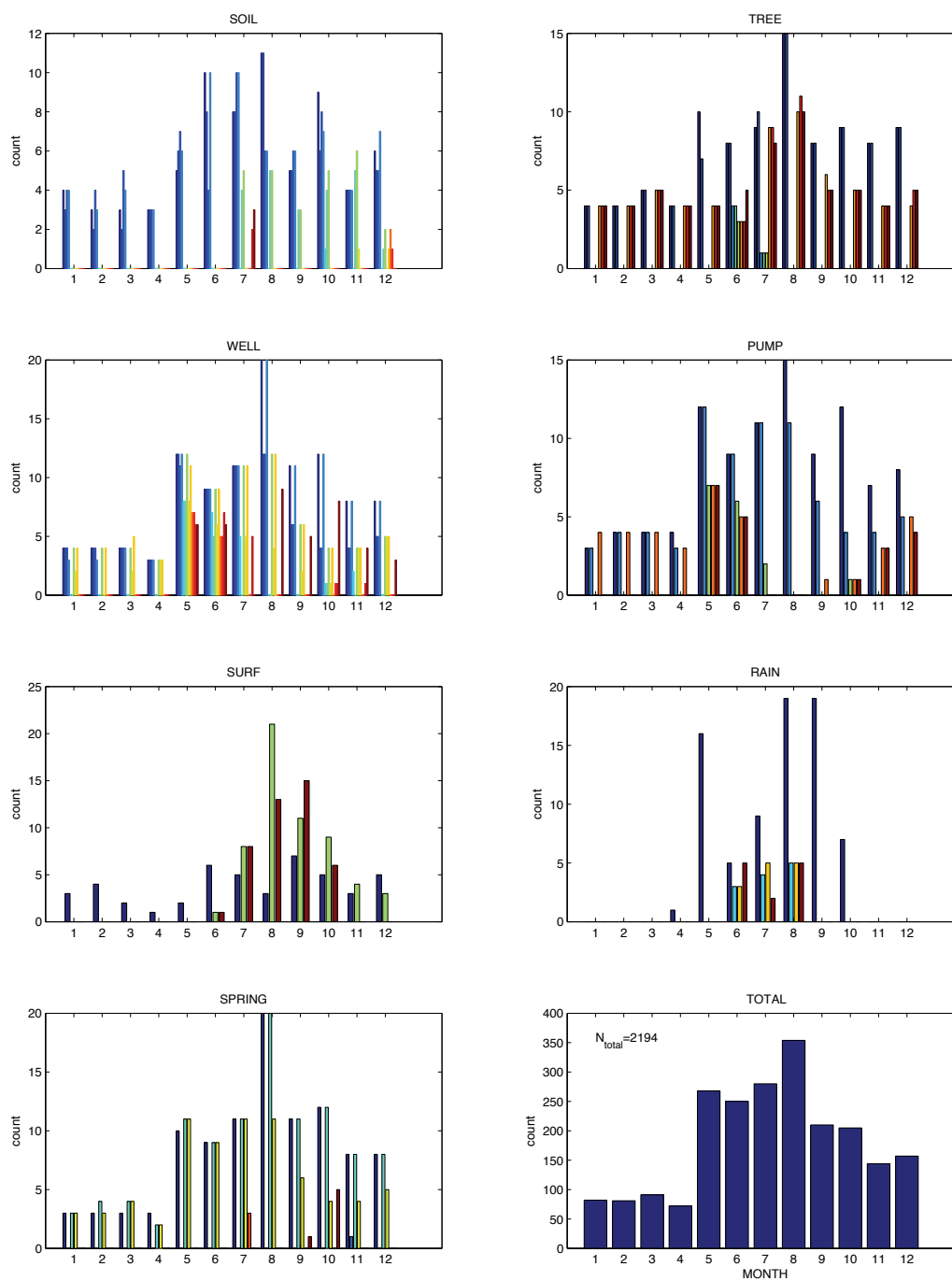


Figure 6-3. Monthly distribution of samples for isotope analysis between 2009 (68 days), 2010 (78 days) and 2011 (44 days). X-axis refers to month of the year and colors show the different points. Count is that particular locations for that month.

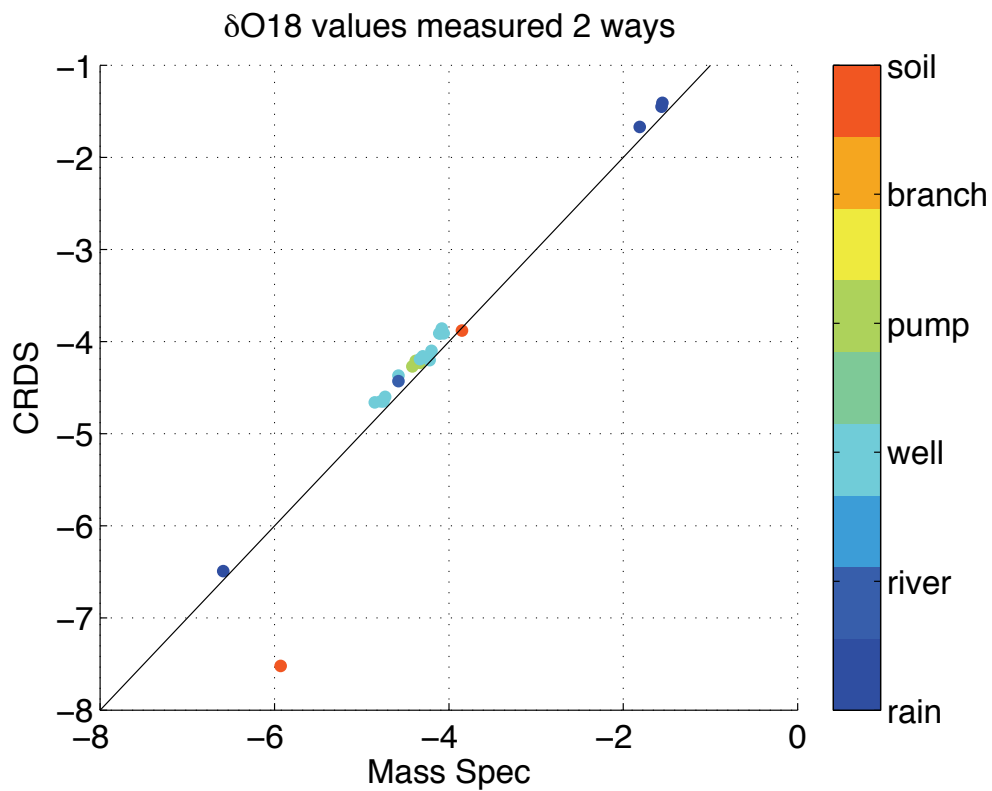


Figure 6-4. Scatter plot comparing measurements of $\delta\text{O}18$ made with the cavity ring down spectrometer and mass spec. The overall correlation is not strong, but by separating water extracted from vegetation from that from other sources, we see that vegetation is responsible for most of the discrepancy.

Cavity Ring Down Spectrometer (CRDS) and Mass Spectrometer (MS) measure a higher agreement for water and soil samples (98.6%) than for vegetation (80.3%). This is likely due to organic contaminants in samples, which alters the absorbance, but there is a strong enough relationship and only one outlier to proceed with analysis (figure 6-4).

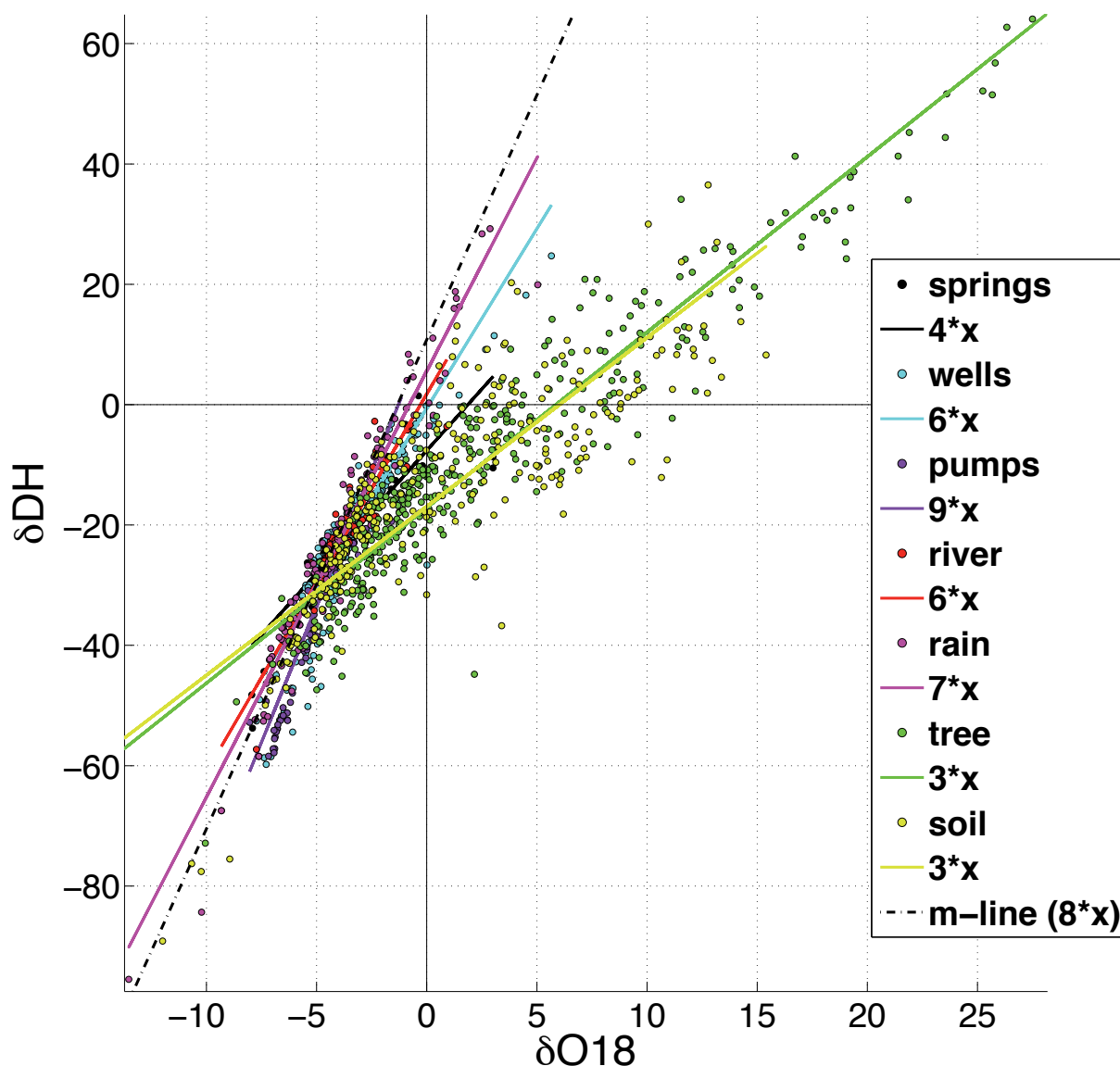


Figure 6-5. Meteoric Water Lines of All Samples. Each source is shown in a different color. Deuterium is on the y-axis and O-18 on the x-axis. The slopes of each line are in the legend. The global meteoric line is shown in black dashes.

The meteoric water line is expected to be standard for global precipitation because deuterium is preferentially removed in a fixed proportion to O18 from water during evaporation (Bowen, 2010). The local meteoric water line based on our precipitation data has a slope of 7.08 and an intercept of 5.58 whereas the global meteoric water line has a slope of 8 and an intercept of 10. Open surface evaporation accounts for the variation along the line but not for the departure from the line (Brooks et al., 2009). The best fit line of the wells, pumps, and rain are all close to both the local and global meteoric water lines, however the spring water has a slope of 4 and the tree and soil best fit lines have slopes under 3 (figure 6-5). The river water's slightly lower slope can be explained by it being fed by the spring water in addition to the rainwater and perhaps.

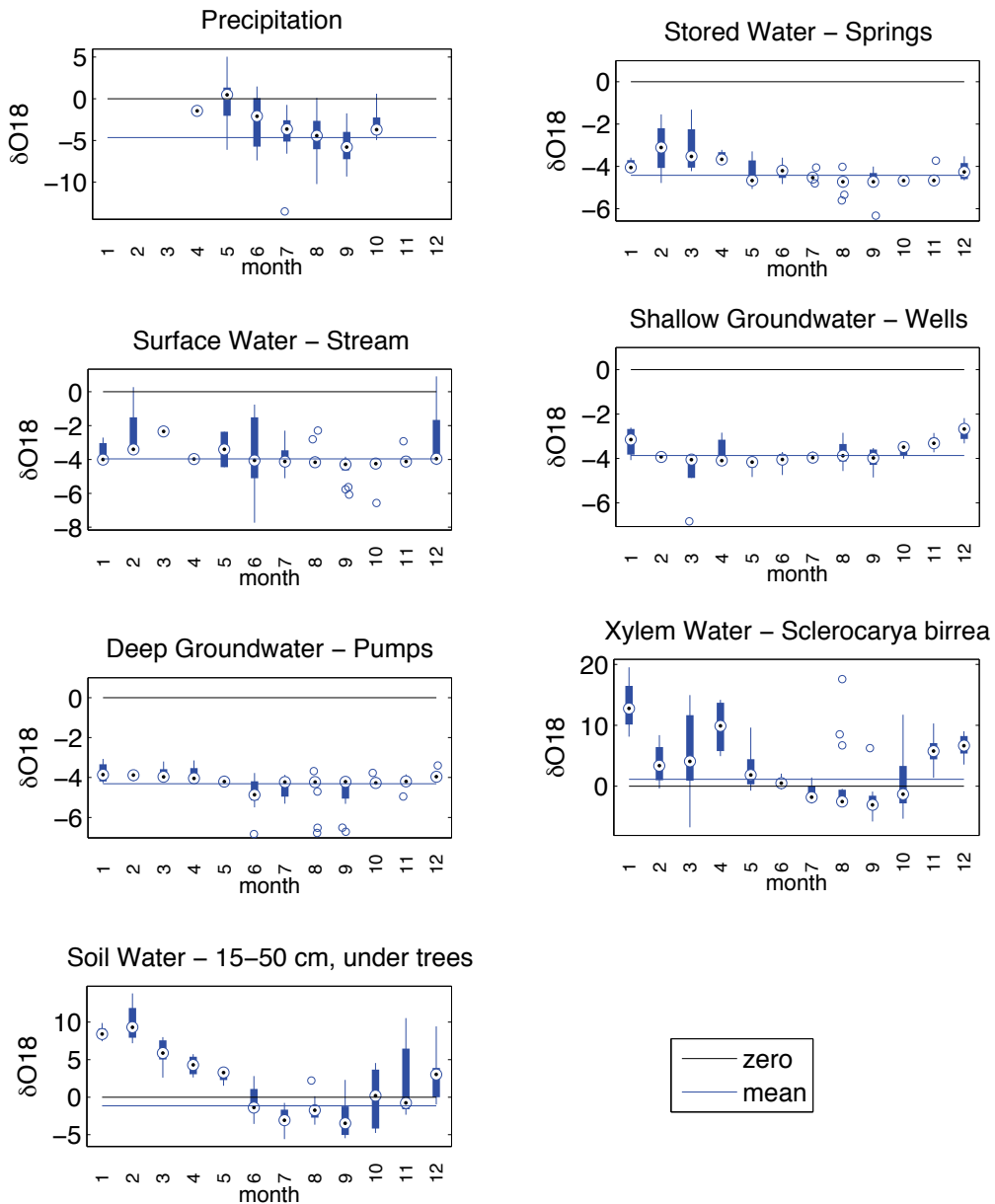


Figure 6-6. δO_{18} signatures of all water sources in the basin. From left to right, top to bottom, each subplot shows a different source : Precipitation, Springs, Stream, Well, Pumps, Xylem, and Soil. All values are plotted on an annual cycle, lumping together all sources of that type. This includes data from all the years of sampling. Each box plot shows the median (dot), 25 and 75 quartiles (box), 5 and 95 % (whiskers), and outliers (asterisks). The black horizontal line is the zero line on the plot for $y=0$ and the blue line is the mean of all data on that subplot. Months are numbered on x-axis from 1-12.

Rainwater is depleted (figure 6-6), or drops in δO_{18} over the course of the rainy season (May – October), supporting understanding of the African Monsoon system described in the introduction. The early rains are enriched, whereas the full rainy season monsoon rains with a large quantity of water are lower (Goni et al., 2001; Gallaire, 1995; Nijchoua et al., 1999).

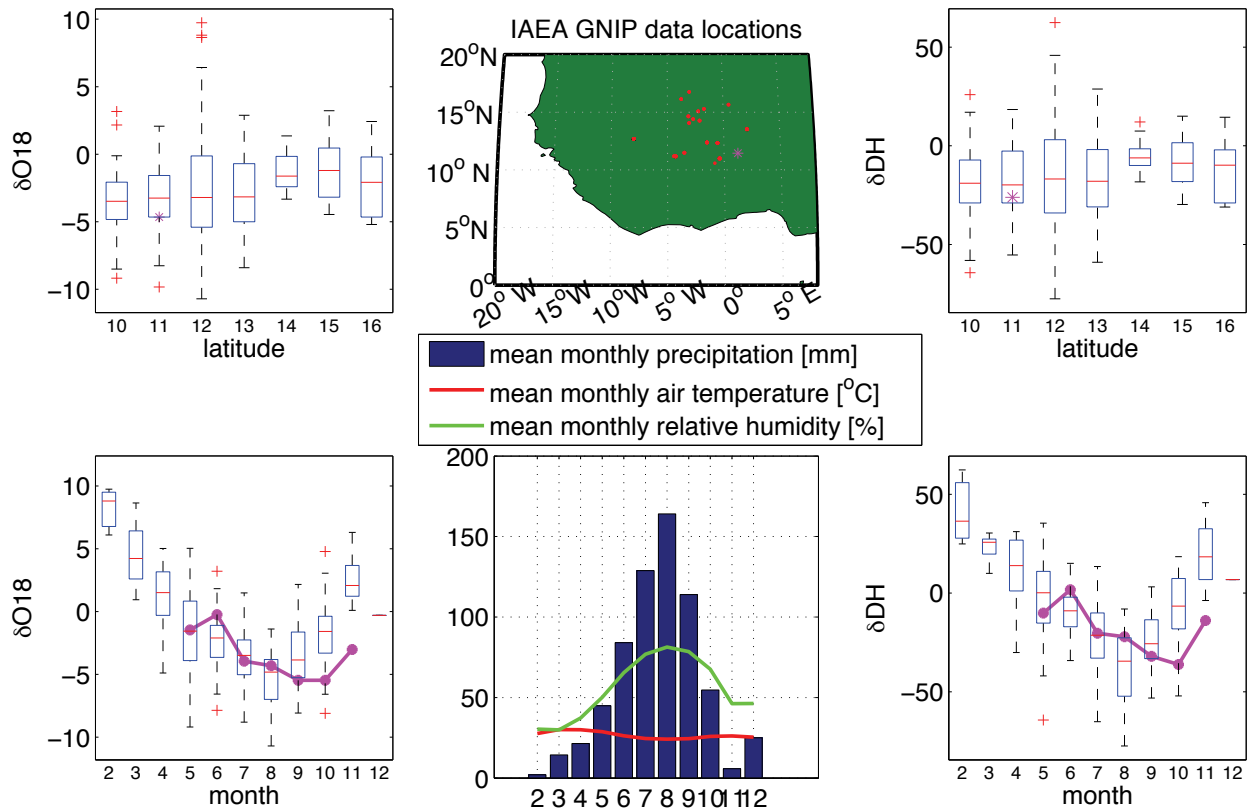


Figure 6-7. Overview of IAEA Global Network of Isotopes of Precipitation database for all West African sites. Upper left corner shows the O-18 distribution according to latitude, and lower left according to month. Right hand plots show the deuterium plots by latitude and month in the same way. Our site's average values are shown with the pink asterisk or bar. Our site is near 11°N. The other boxplots show the median (red), 25-75 quartiles (box), 5-95 spread (whiskers), and outliers (red plus) of all West African sites. The distribution of all sites included is in the upper center subplot. Other's are in red and ours is in pink. The lower center graph shows the mean monthly precipitation, air temperature, and humidity for all sites, to remind us of the seasonality of this region.

In order to assess the similarity of our measurements to those regionally, we plotted them against all of the West African values available in the current IAEA global network of isotopes in precipitation (GNIP) database. In figure 6-7 we compare our values of rainfalls with those from the IAEA GNIP database for Sudanian and Sahelian West Africa. Our values of precipitation follow regional patterns. In this figure, values of $\delta\text{O}18$ and $\delta\text{D}H$ are plotted by latitude and month. Trends of $\delta\text{O}18$ in our rainfall shown (in pink *) agreement seasonally and according to latitude with those in the IAEA database. Explained by movement of the African Monsoon regional pattern of rain movement (Taupin et al., JGR, 2000). Bowen (2010) predicts that the average O18 value for our site will be between -6 and -2 ‰ with variability between 10 and 16. This conforms to what we measured.

Figure (6-9) shows that stored water from the springs is fairly constant, with a slight enrichment from January to April. Surface water is enriched as it becomes disconnected from the ground water, due to the effect of water loss to evaporation, January to March. Shallow groundwater is enriched October to January, when recharge occurs. Deep groundwater is constant. Xylem water is enriched from November to April. Soil water is enriched from December to May. This extreme enrichment in the sub canopy soil water and the xylem does not resemble any of the sources. What is particularly interesting is that the soil and xylem water do not follow the same pattern. In particular, the xylem water dips down in February to near zero, while the soil water stays high. The change from the January value to a lower February value suggests that new water is moving into the stems, but since it is not mirrored in the soil, it must be coming from another source.

The relationship between the DH and O18 concentrations of water extracted from Soil and Tree samples do not fall along the meteoric water with a slope of 8 and y-intercept of 10. In order to explore whether this was a seasonally driven test, we grouped samples into an “evaporated group” or a “meteoric” group based on the smaller residual to the m-line or to the evapotranspiration (e-) line with a slope of 2.76 and an intercept of -17.13, determined as the best-fit line. Although more soil samples were found along the m-line during the rainy season than tree samples or dry season soil samples, there was no significant difference in days since rain for any group, suggesting that xylem water is always under evapotranspiration stress and soil water has undergone evaporation soon after a rain event, as expected.

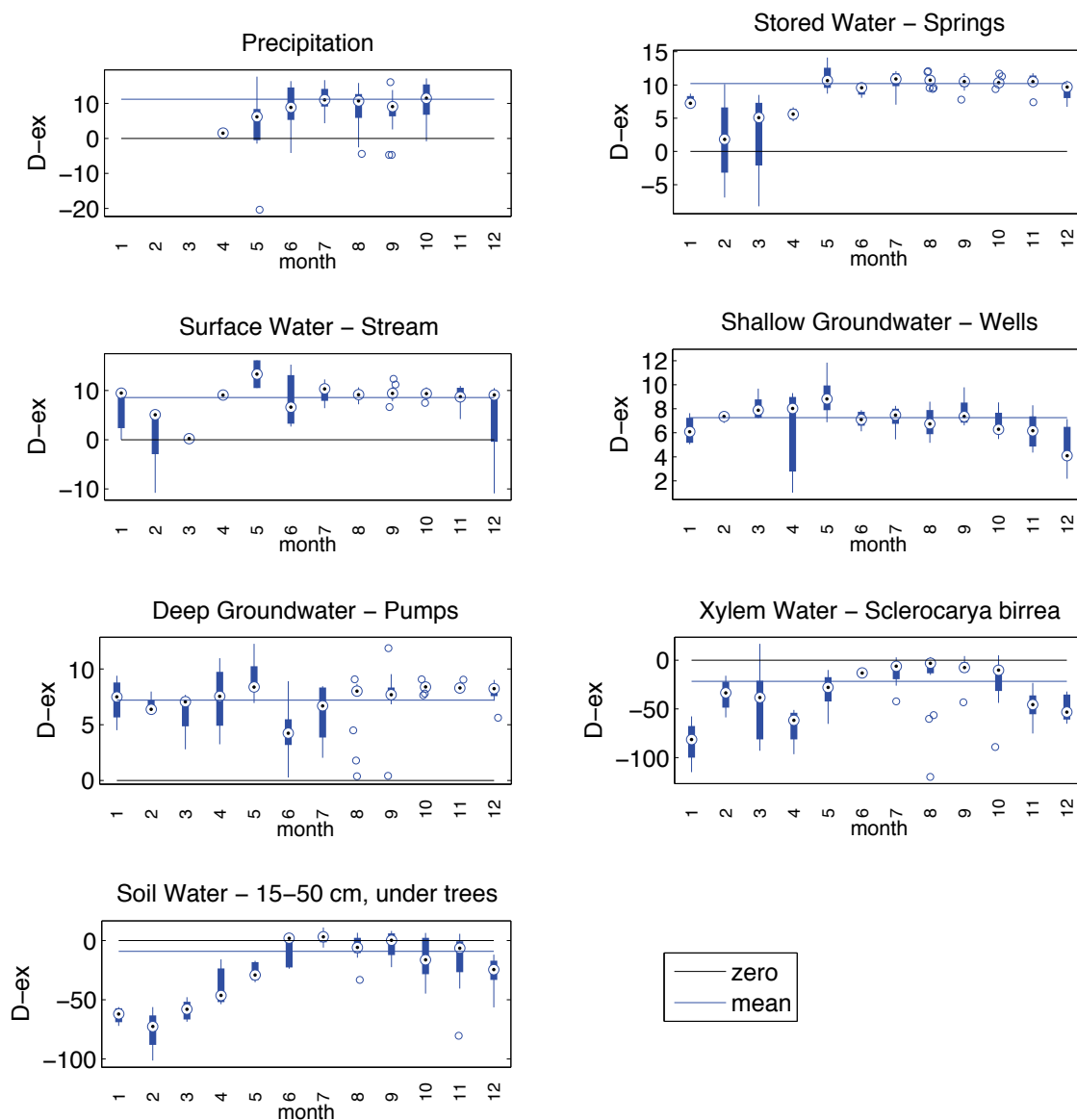


Figure 6-8. Signature of deuterium excess in all sources in the water basin. From left to right, top to bottom, each subplot shows a different source : Precipitation, Springs, Stream, Well, Pumps, Xylem, and Soil. All values are plotted on an annual cycle, lumping together all sources of that type. This includes data from all the years of sampling. Each box plot shows the median (dot), 25 and 75 quartiles (box), 5 and 95 % (whiskers), and outliers (asterisks). The black horizontal line is the zero line on the plot for $\gamma=0$ and the blue line is the mean of all data on that subplot. Months are numbered on x-axis from 1-12. .

Examination of the deuterium excess confirms many of the same patterns, though they will appear opposite – as more depleted waters in O18 with have a higher level of deuterium excess. Early season rainfall, which is probably from convective storms, is lower

than later season rainfall, that is more constant along the global meteoric water line (GMWL), 10. Stored water is also very constant on this line from May on, but in the dry season, from January to April, it is much closer to zero. This suggests that the springs are sourced from a different reservoir in the dry season that does not mix with the precipitation. In the rainy season, they are sourced from the rainfall. The surface water resembles the precipitation from June, when its primary recharge occurs. In February it has a dip, which is close to the spring water, suggesting that during this time it is sourced from the springs and this deep reservoir. The groundwater is again constant. The decrease in November and December is most likely due to surface evaporation from some wells that are disconnected from the groundwater. The deep groundwater's deuterium excess values are less constant than its O18 fraction. The decrease in June, and the values much lower than 10, suggest that evaporation occurs in rainwater before it recharges the groundwater; and that recharge does not begin until July. The xylem and soil water is near zero during the rainy season, but again their patterns deviate during the dry season. The xylem water drops sharply in November and stays at that level or lower until February when it increases sharply again, possible due to mobilization of another water source, in February and March before dropping again in April. The soil water on the other hand, increases slightly and continuously between February and June, suggesting that it is slowly becoming less depleted. Examination of the full time series for xylem (green) and soil (black with error bars and standard deviation) compared to rain (blue), groundwater (range in grey, mean in red), shows that xylem and soil water and precipitation started to converge on the values of groundwater in July. In the dry season, both the soil and xylem water values increase starting in November and reaching a peak in January. However, in February and March, groundwater is very consistently returning to zero. But at the same time, the tree xylem isotopic values seems to drop suddenly in most samples, although some remain high.

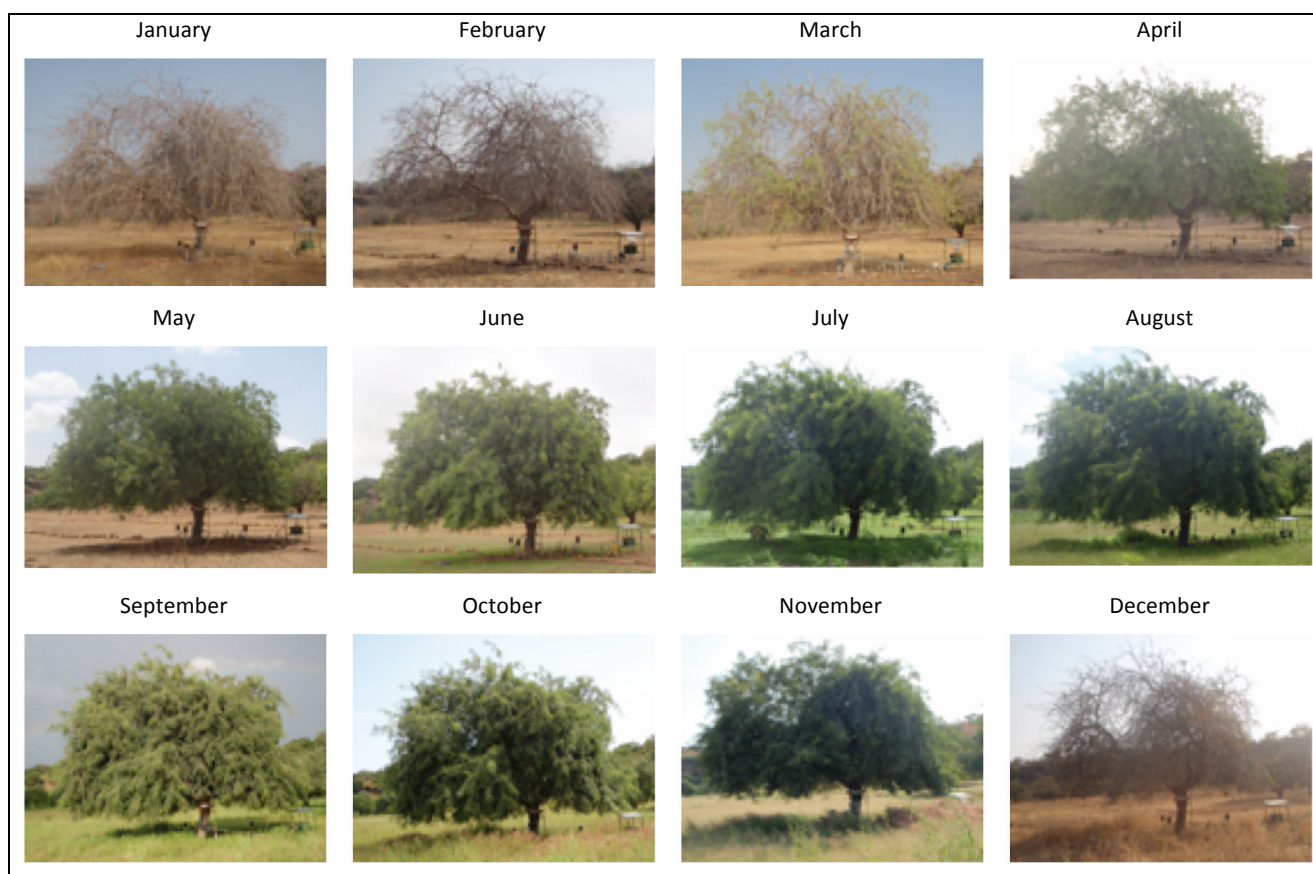


Figure 6-9. Photographic documentation of annual cycle of tree. Each photograph shows the mid month state of greening for each month of 2010. On the top: January through June; On the bottom: July through December.

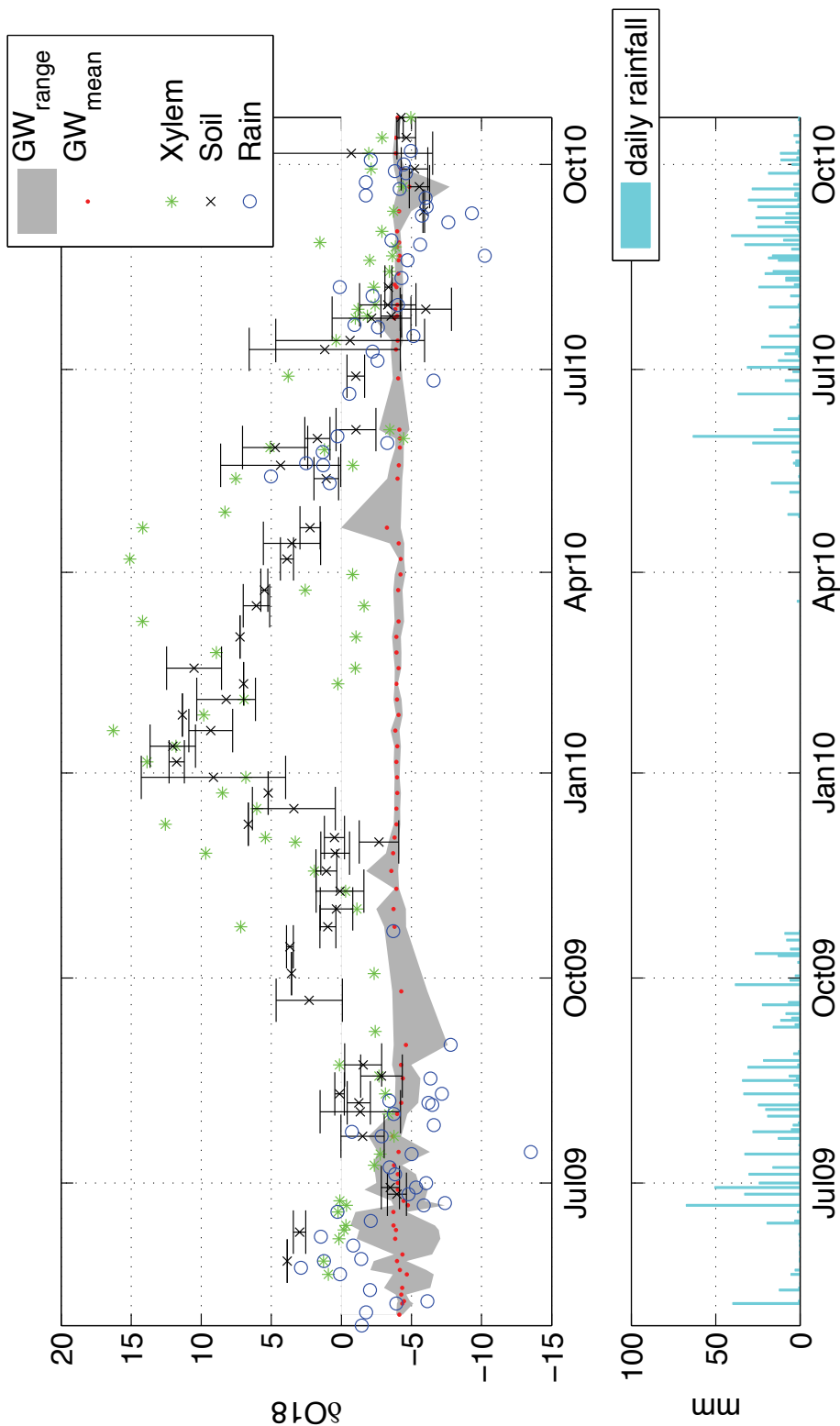


Figure 6-10 Time series of O18 values comparing groundwater with xylem (green asterisks), soil (black x's with error bars showing standard deviation since multiple samples), ground water (red dots with range in solid grey) and rain water (blue circles, when it rained). Lower bar graph shows rain fall over same period in cyan in mm. Months are indicated on x-axis. The series of photographs (figure 6-10) demonstrates what we observe in the isotope data – that there is a depletion occurring in March. Already in February, but mainly in March, we observe some green on the tree canopy. The dates of leaf out according to isotopic changes are 10-Feb-2010; 17-Feb-2010; 03-Mar-2010; 17-Mar-2010; 24-Mar-2010; and 31-Mar-2010. These are the dates when the values drop. Note that since our sampling is discontinuous, and only of a small subset of branches on any one day, we are not able to observe all intermediary dates. Upon examination of the growth of leaves, or leaf out, between February and May, we see that there are small increases in canopy cover fraction shortly after we observe the increase in δ O18.

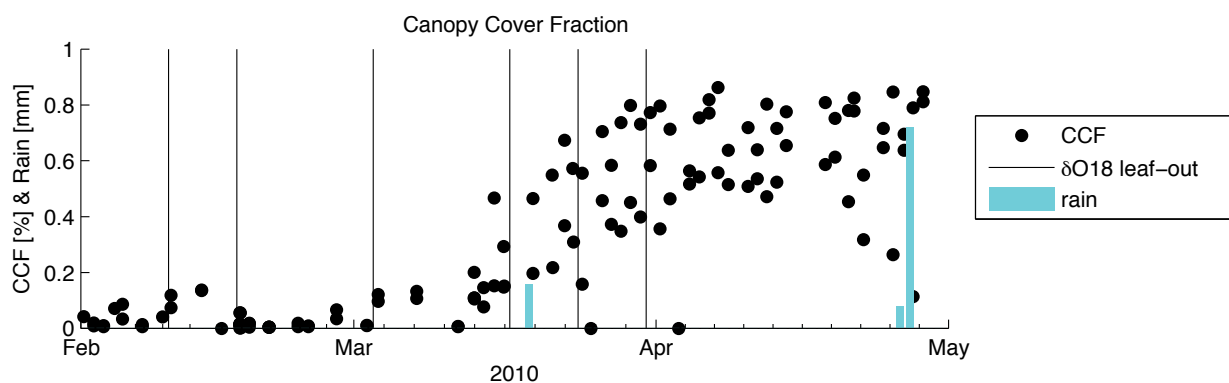


Figure 6-11. Canopy Cover Fraction for Leaf-Out in 2010. Black dots show canopy cover calculation over time series. Cyan bars show rainfall. Y-axis is mixed in percent and mm. The black vertical lines show the dates corresponding to the drop in isotopic values in xylem from the 2009 data shown in figure 6-10.

Figure 6-12 shows all the days with overlapping samples of xylem and roots to shed light on water movement within the trees. On May 26, 2010, when the root of the field tree was cored, we see that the tap root is cut off because its isotopic signature is so different from the rest of the samples. The water of the lateral and trunk seem to be intermediary between the water in the soil and the ground and surface water. It appears that they are mobilizing ground water, but are somewhat enriched, perhaps due to transpiration. On May 21, 2009, we see that the variation between the tree by the river and that in the field is significant. The tree by the river is more enriched and the soils are intermediary. Again this suggests the trees are accessing groundwater, releasing some of it in the soil (hydraulic redistribution), but that the xylem water has had some residual enrichment from the transpiration. The higher level of enrichment in the river tree supports this hypothesis because it is so much larger than the field tree. Because of the size difference, the water has to travel much further before it reaches the branches, if any transpiration or water loss occurs on the path, it will lead to enrichment. The more water loss, or the longer the path, the more enriched the sample will become. This is very early in the season before there was significant soil moisture, further confirming our hypothesis of hydraulic redistribution. Finally, the plot from December 1, 2009 shows that the stems are far more enriched than the roots – which are in the same range as the soils – but all tree water is very different from the water. Based on my understanding of the effect of “travel time” within the tree’s vessels, this supports my understanding that the tree is accessing groundwater, redistributing some to the soil (or equilibrating with the soil) and then transpiring or experiencing some unintended water loss from its branches.

Figure 6-13 tracks the isotopic values of five different trees over the basin. Their locations are shown in the map (Figure 1-3) as green circles. In the O18 plot, in April 2009, we see that we only have the first two trees, which have positive values. Values are slightly more enriched in the large tree, supporting our travel time hypothesis. In May 2009, they return closer to zero, but still are positive for the big tree but below zero for the field tree. In June through September, all values are negative for all trees and mostly constant for the duration of the rainy season, when there is plenty of available moisture and flow. The exception is the smallest tree, but the spring (green) in September, which has a lot of variation, suggested that it has already started becoming enriched, and drying out. By October all the trees have started to enrich or dry out. The tree in the field has the most variation. The large tree by the river becomes the most enriched in January, perhaps due to its size, but it also becomes the most depleted in February. The field and river trees, which have been the focus of our discussion and study, show the most decrease in February and March and then enrichment in April, suggesting “leaf out”. The tree by the upper spring only shows depletion in February, and then return to enriched state in March and April, perhaps suggesting that because of its small size, “leaf-out” is a shorter process. All trees return to more average levels in May. The deuterium excess subplot further reinforces that the tree in the field and the tree by the river become the most enriched in the dry season. All trees undergo the February depletion (coinciding with “leaf out”).

Some of them maintain those levels through March, but others do not. Only the tree in the field revert for the month of May, suggesting that it is moisture limited. By June in the field, upper spring, middle spring, and hill July by the river, the trees have returned to a ground water level. Values of isotopes in the soil were highly correlated between 15 and 30 cm under the two trees sampled (figure 6-14).

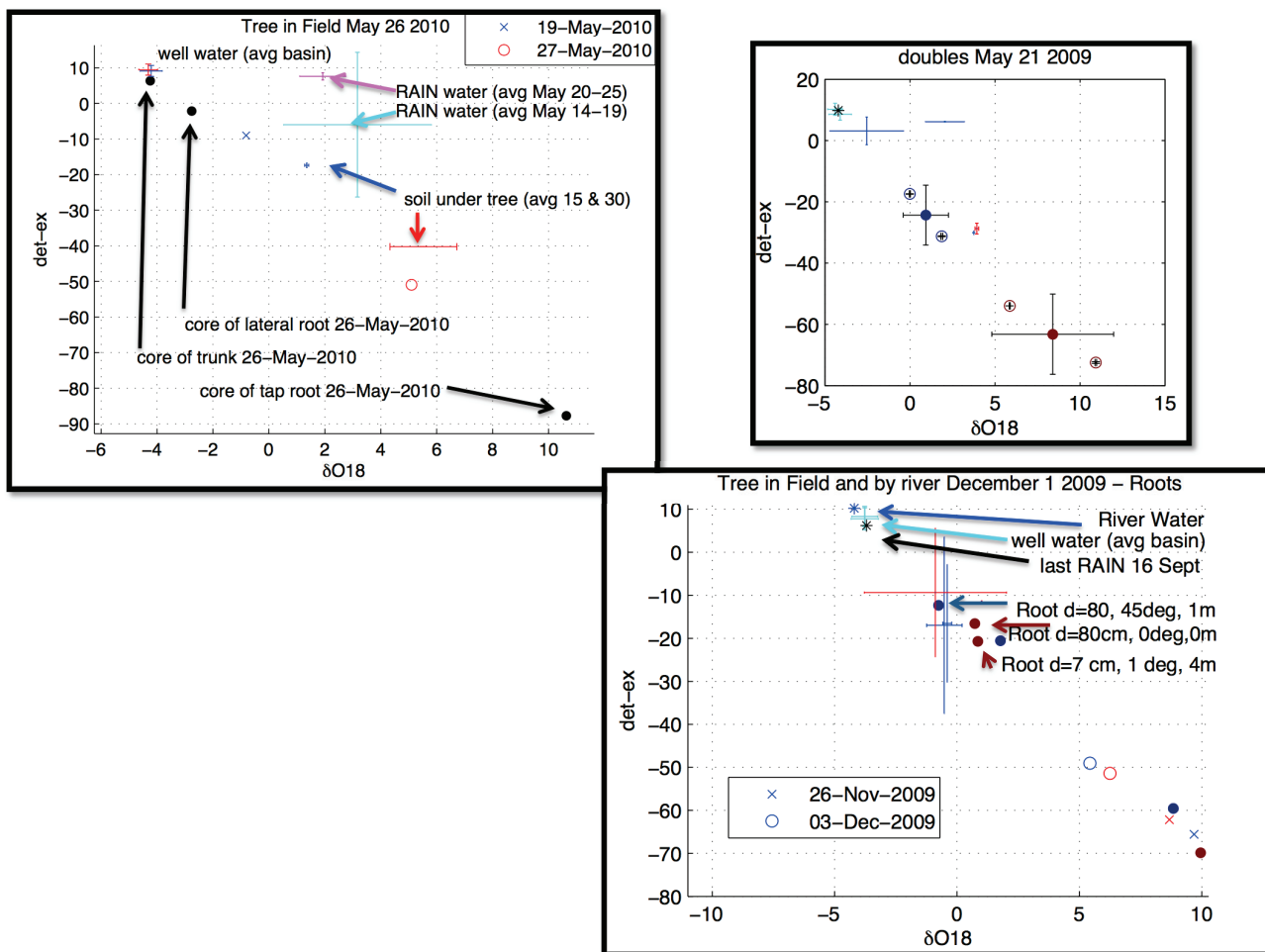


Figure 6-12. Subplots showing days with multiple measurements. (a) Upper left corner shows the days surrounding May 26, 2010. On this day, the root was cored. All of the samples are from or near the field tree. The solid black dots show the values of deuterium excess and $O18$ of the trunk, lateral root, and taproot. In addition, the average well water is plotted for the whole basin for the 19 of May (blue) and the 27 of May (red), the closest sampling dates, with a cross indicating the average and range of all values on that day. The values of soil water are shown for this same day – in those same colors and annotation, averaged for 15 and 30 cm. The normal xylem water sampling is shown by a blue x and a red circle for these same days. Finally the rain is shown for the preceding periods in pink and cyan for May 20-25 and May 14-19 respectively. (b) The upper right subplot shows double values for May 21, 2009. This is the first day of sampling for xylem, and so single branches were sampled in separate vials. Individual values are shown as asterisks inside colored circles (blue for small tree in field, maroon for large tree by river). The solid dots with error bars show the average and range of the samples – showing that they are distinctly different. Cyan crosses indicate ground water, black asterisk, rain, and blue line, surface. (c) Lower right plot shows the comparison between the roots of the tree in the field and that by the river on December 1, 2009. The red is for the river tree and the blue is for the field tree for the xylem and soil water. The normal xylem samples are shown by the x (November 26), circles (December 3), and solid dot (December 1). The roots at 2 different depths are shown for the two trees in solid dots with arrows. Or text. The unlabeled Root is from the second tree at 7 cm. The river water is shown as a blue asterisk, the well water as a cyan range cross for the whole basin, and the black for the last rain (2 and a half months earlier).

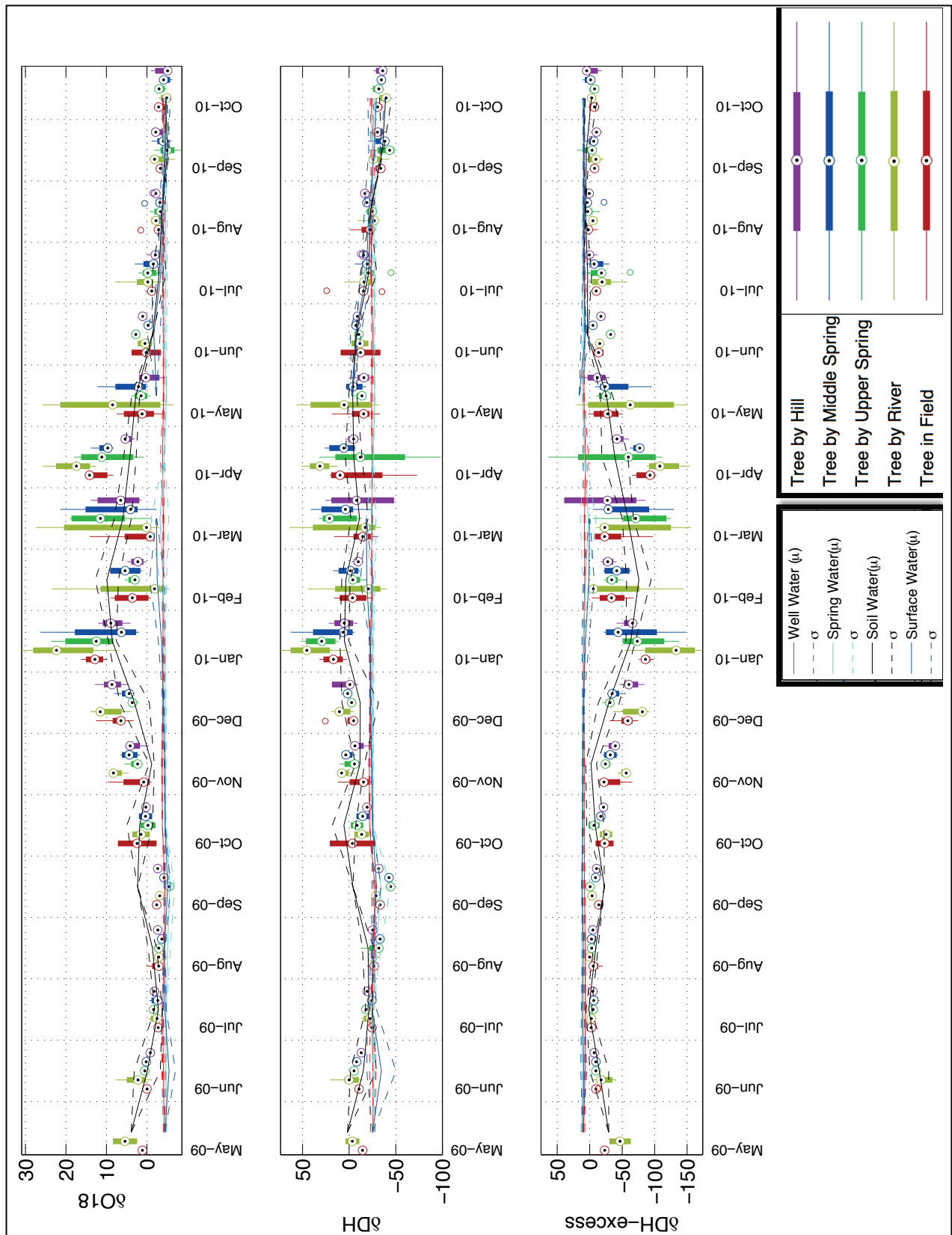


Figure 6-13 Comparison of five trees sampled for xylem water. Five trees shown by 5 colors in legend with specific locations shown in map (figure 1-3), show the median (dot), 25-75% distribution (box), 5-95% distribution (whiskers), and outliers (circles) for all samples collected during months from May 2009 to October 2010. Additionally, well water over basin is shown in red (solid mean, dashed standard deviation), spring water in cyan, soil water in black, and surface water in blue. Values of O18, Deuterium and Deuterium excess are shown. The main field tree we have discussed is shown in red, and the large tree by the river is in yellow. The green, blue, and purple trees have been less assessed and have no additional measurements surrounding

Unfortunately, it was not possible to look at additional variables at the same time as isotope sampling, but we looked at corresponding variables in the following year (figures 6-15 and 6-16). In 2011, the average daily vapor pressure deficit (VPD) as calculated at 5 heights (0.3m, 1.3m, 3.7m, 5.3m, and 7.3m) in the canopy was compared to the sap flow in ml/day, and the relative soil moisture averaged at 4 depths under the tree. Lines indicating the dates of leaf out in the previous year are placed for comparison. Canopy VPD was inversely related to sapflow and soil moisture and rainfall, as would be expected. The end of the previous year's leaf out period corresponds exactly to the moment when sapflow starts flowing, a jump in soil moisture and, surprisingly, a peak in VPD. Additionally, there seems to be more variation in VPD in the dry periods, and more fluctuations of daily sapflow in the wet periods.

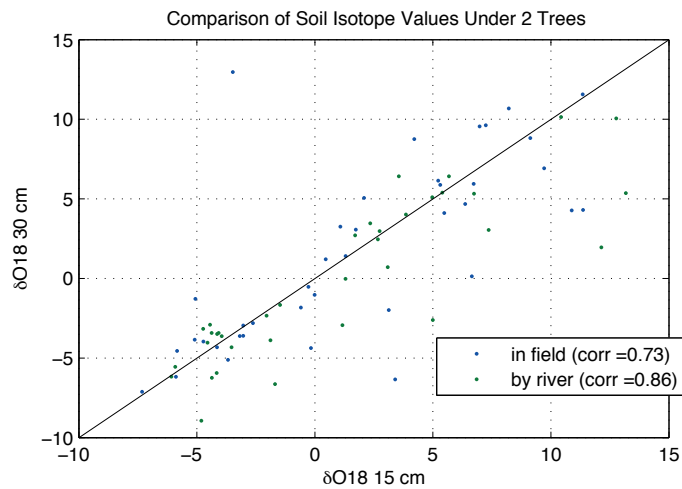


Figure 6-14 compares the isotopic (O18) values in the soil water for the two depths sampled, for the whole period of sampling. Blue dots show the samples under the field tree while green dots show by the river. Values of correlation are shown. Both are relatively high with a few outliers and scatter.

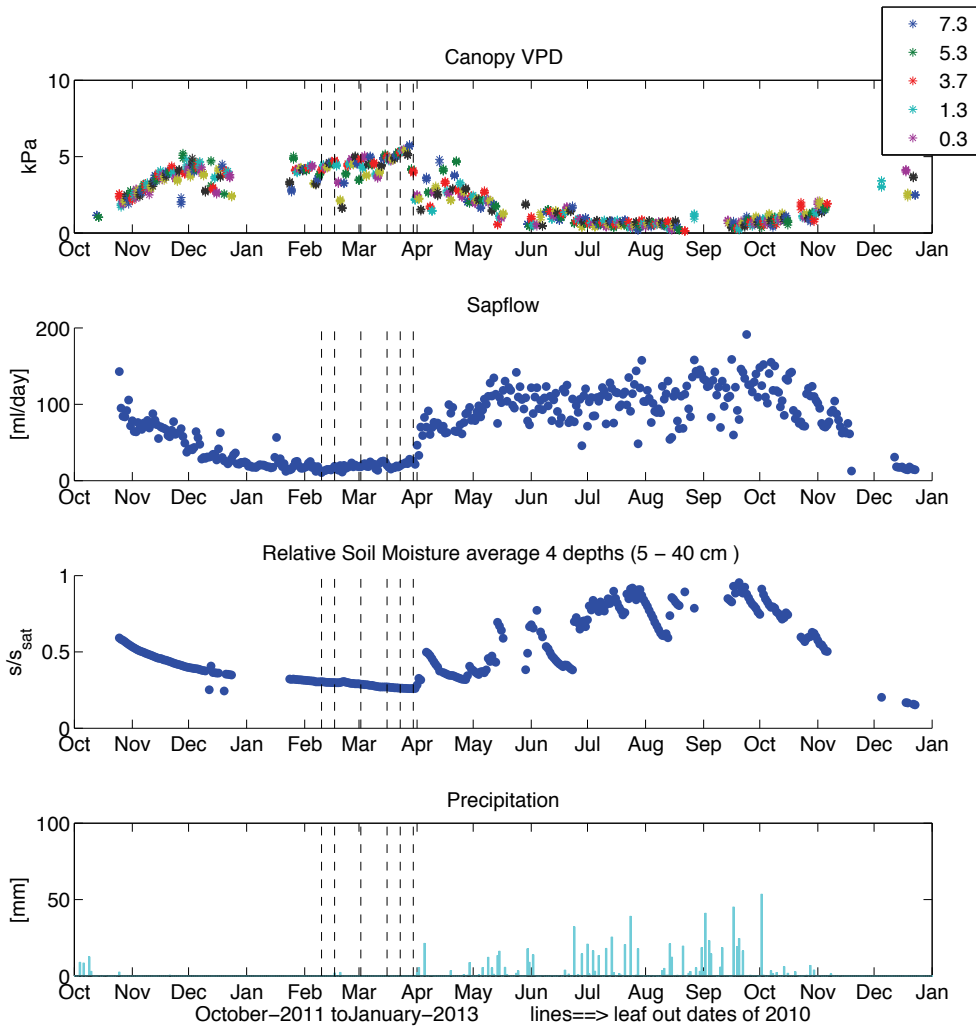


Figure 6-15 . Comparison of Vapor Pressure Deficit (top), Sapflow (second), Relative Soil Moisture (third), and Precipitation (fourth). All plots are on the same date line from October 2011 to January 2013. Lines indicate leaf out dates of 2010 according to isotopic depletion. Canopy VPD is in kPa and the 5 heights of sensors are indicated by the 5 colors in the legend, which is in meters. Sapflow is in ml/day – this is a daily total. And Relative soil moisture is unitless. Precipitation shows the height of each rain event.

The correlation between vapor pressure (VPD) deficit and sapflow was -0.78, to soil moisture was -0.87, and between sapflow and soil moisture was 0.77. Sapflow seems to be more highly correlated to both VPD and soil moisture during the transitions between wet and dry periods. At times of high sapflow, there is less dependence with both the VPD and the soil moisture, and similarly at times of high sap flow, there is less dependence with the VPD in particular. Between the VPD and soil moisture, there is an outline of an annual hysteresis loop (figure 6-16).

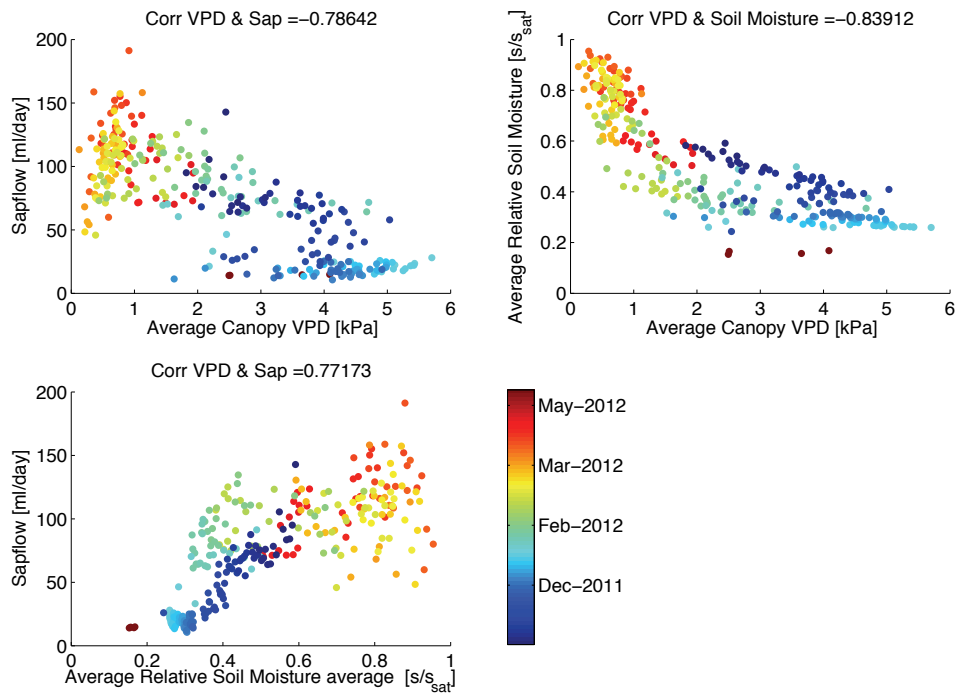


Figure 6-16. Correlation between Sapflow, Soil Moisture, and Canopy VPD according to month (color bar ranging from November 2011 to May 2012). Correlations between variables are written at the top of each plot. In upper left subplot is the correlation between Sapflow and Canopy Vapor Pressure Deficit. All values are daily averages. In upper right is the correlation between vapor pressure deficit in the canopy and soil moisture. In lower plot is the correlation between vapor pressure deficit and sap. Soil moisture values are unitless, divided by saturation value. Sapflow is in milliliters per day and canopy vapor pressure deficit is in kilopascals.

6.3 Discussion

6.3.1 Enrichment

What is striking about our data is that both water extracted from sap and water extracted from soil is extremely enriched in the dry season. This supports the hypothesis that they are disconnected from the groundwater, but their initial similarity suggests that they are connected to each other. The continued enrichment over the course of the dry season suggests that they continue to experience some water loss even after leaf loss, but more clearly it shows that the moisture reservoirs in the xylem and soil are not being recharged. Although, as demonstrated by the plots in figure 6-12, it is possible that there is significant water loss as the water travels through the vessels leading to a “travel time” enrichment. If this were the case, the hypothesis of accessing ground water would be supported. The difference between ground water and xylem values would be caused by enrichment that took place during travel. Intermediary soil isotope values further support this hypothesis, caused by hydraulic redistribution, or the tree distributing the ground water under the canopy through its root system.

The other interesting key finding is that the return to a non-enriched state towards the start of the rainy or growing season happens at different times and differently in xylem and soil. Upon examination of the photo documentation and pixel analysis of canopy cover data, it seems that the xylem’s early depletion events correspond to moments of leaf growth or leaf out.

The question is, where are these trees obtaining the water to flush out the system. It is not close enough in δO_{18} or deuterium excess to the groundwater to indicate that the tree is obtaining its water from there. It is deviating from the soil water values too

much to be stored there, unless of course it is from reservoir that we did not sample. But, more likely, it is mobilizing water that has been stored in the tree over the dry months.

Cappa et al. (2003) found that in their experiments of kinetic fractionation, as opposed to the standard equilibrium fraction, that the slope of the meteoric water line resulting from water circulating in saturated conditions and evaporation taking place with molecular diffusion as opposed to turbulent diffusion. The variation in slopes between deuterium and O18 suggests the fractionation that takes place in the xylem, soil, and water reservoir that exits in the springs is different than the direct evaporation into the atmosphere. I'll return to the examination of deuterium excess after, first examining the variation in the δ O18 signatures.

6.3.2 Water Storage

Water can be stored in plants due to the elasticity of tissues, capillarity, and cavitation (Tyree and Zimmerman, 2002). The elasticity of tissues, or the swelling of various parts of the plant, accommodates large amounts of water and has been measured (dendrometer) as a proxy for the diurnal and seasonal flows. Some species show an increase in water content after the leaf fall for example. Some water is stored in the elasticity of the stem or there may be specialized capillary structures. Or, yet another hypothesis is that there are gas spaces present in the wood. Changing the radii of the air-water interface can provide storage space in cracks between solid surfaces. Wood consists of bundles of perfect cylinders, and up to 6% of the total volume may depend on their hydraulic tension. Intercellular spaces not seen between axial elements can provide very effective water storage in wood – by changing meniscus radii but the location of that space will be static.

Gibbs (1958) describes very carefully the water content of many different species of temperate tree, where he observes that in many species there is a refilling of the wood just before leaf-out or just after leaf fall. In general, water content of wood is low all summer (temperate summer) and is at a low before leaf fall. It remains low for about a month after leaf fall, when some of the species seem to “refill” stems. Although the trees that he examines are not in a semi-arid system, he does highlight what is possible physiologically. Ring porous species commonly do not refill, maybe because early wood vessels become embolized, in the fall, in some species before winter. Zimmerman (1983) also document that in New England forests the water content of wood drops throughout the summer and reaches a low just before the leaf fall and some species seem to refill their stems but others do not.

The early depletion of xylem water could demonstrate the mobilization of water stored in the tree's intercellular spaces, instead of hydraulic redistribution or pre-rainy season access to ground water that it distributes in the rooting space as previously thought. Thus, it is possible that our data shows that *Sclerocarya birrea* is mobilizing stored water in the months of February and March for its spring leaf-out. This is very different than our original suspicion that it accesses the groundwater before the rains began.

6.3.3 Root groundwater access

There is some evidence that this tree has access to groundwater as well. Although *Sclerocarya birrea* is not a halophytic or xerophytic species, the high levels of enrichment found in the stems support the work of Ellsworth and Williams (2007) who found that many xerophytic and halophytic species exhibit fractionation of hydrogen isotopes in water during uptake by roots. Xerophytes are plants adapted to survive where there is no water and a halophyte survives in high salt content. If we are observing a fractionation at the root surface, it is possible that this is also a technique to survive in a highly arid period.

Isotope analysis done by Brooks et al. (2010) similarly found that trees accessed unexpected reservoirs of water. In their case, they found the tree to mobilize water stored in the interstitial spaces of the soil. Ehleringer et al. (1991) also discuss the seasonal differences that they found in stable isotopes of water. Herbaceous and woody perennials store early rainfall for use later on.

Since it is not clear what water they access, it is also not clear what neighboring plants would compete or benefit from having *Sclerocarya birrea* as a neighbor and when. Before we can fully recommend any this species for agroforestry on the basis of partitioning the water resource, a detailed analysis of root structure and distribution needs to be completed (Akinnifesi et al., 1999).

6.3.4 Monsoon Effect

Our precipitation data does shows a seasonal trend that agrees with the trend that is found throughout West Africa, which suggests that it is related to the movement of the monsoon. As Taupin (2000) and Bowen (2000) describe, this is very likely a function of two things – first whether the rain is arriving with a convective or an advective storm, i.e. from where the moisture transported by the storm originated; and second – how many times that water has gone through the precipitation – evaporation cycle. These are clearly interrelated, but in this way the isotopes of rain in West Africa and show a “travel time”. Risi et al. describe how isotopes in precipitation are controlled (2010). They found that in wet regions, vapor and rain could be determined by convection based on the number of times the rain has been evaporated. However, in dry regions it is primarily controlled by the air dehydration – thus it provides a record of the dehydration pathways. In fact, they found that the diurnal cycle plays an important role in isotope variability because late afternoon rain will have undergone “hotter periods” more recently that would have affected its isotopic signature.

6.3.5 Innovative tool

Isotopes have not been used extensively, if at all, to study the water movement in trees in West Africa, although they have been used for this purpose elsewhere. This study did provide a new set of before un-accessed data regarding the trees access to water. In addition, the other tools of sapflow sensors, in-canopy vapor pressure deficit measurements, canopy cover fraction, and soil moisture measures all proved useful for monitoring trees behavior. The solar radiation sensors, the soil moisture sensors, and the vapor pressure deficit sensors were all attached to a wireless sensor network that transmitted data in real time. The sapflow sensor could not be put on this system due to its energetic needs, but since it was so highly correlated with some of the other measurements – perhaps it is unnecessary. The manual photographs also overlapped in knowledge with the solar radiation sensors. The monitoring of isotopic content of xylem was the most time consuming and labor intensive, but none of these indicators are clearly enough correlated to suggest that we can abandon our study of isotopes. More work needs to be done to understand the specific of the isotope uptake in terms of water source, diurnal timing, and species level differences. In addition, monitoring of the isotopes of nearby herbaceous vegetation could shed light on the competition as well. Thus this study provided a basis for more rigorous, focused use of some of these tools to improve the water resources use by agroforestry trees.

6.3.6 Indicators

The analysis of the correlations between the sapflow, vapor pressure deficit and soil moisture indicates of water stress since it shows that when moisture is low, it will coincide in all three « pools ». Some plant physiologists suggest that these patterns are ways that trees communicate with their immediate environment (Gurovich, 2012). Perhaps the trees “decision” to take up water or not communicates by sending electrophysiological signals. These signals serve to synchronize between different organs in the single plants but also may exchange with soil organisms. The trees are signaled to begin this transition, not because of a change in soil moisture, but because of something constant like the photoperiod or a peak in vapor pressure deficit.

In fact, the early leaf out phase of this and other plants has long been a tool in traditional indigenous knowledge in Tambarga. Many elders told me that they knew when the rains were going to come based on watching the growth of the buds. The failure of traditional knowledge is one of the key failures of local farming as the climate begins to change. This proves yet another reason

why it is important that we understand the functioning of the tree from a scientific perspective – to provide a scientific version of the traditional knowledge that may be able to adapt to new realities.

6.4 Conclusions

The relationship between the δD and $\delta\text{O}18$ concentrations of water extracted from soil and xylem samples do not fall along the meteoric water line, and thus their source cannot be solved with a simple linear mixing model. However their highly enriched state suggests that they draw on self-created reservoirs or ground water into the dry season. Water may be stored in cavities in the xylem wood. However examination of the isotopic signatures of the roots suggested that this tree is performing hydraulic redistribution, or lifting the ground water and “sharing it” with soil in the rooting zone in the dry season. The enriched level of xylem in this case is a product of water loss, and enrichment, along the travel path of the water from the roots to the tip of the stem. Another interesting piece of evidence is that the tree mobilizes water in March and April, before rain begins. Vapor pressure deficit, soil water, and soil moisture interactions support this picture of interacting controls, separate from hydrologic triggers on the water movement in the tree. This is perhaps indicative of other signals in the tree and environmental changes, such as the movement of the sun that may be related to its early leaf out or a peak in vapor pressure deficit. We leave this analysis wondering how changing precipitation patterns may affect this tree’s annual cycle that forms the basis for gourmantche traditional knowledge to predict rain.

6.5 References

- Akinnifesi, F.K., Smucker, A.J.M., Kang B.T. (1999), Below-ground dynamics in agroforestry systems. *Annals of Arid Zones*, 38, 239–273.
- Bertrand, G., Masini, J., Goldscheider, N., Meeks, J., Lavastre, V., Celle-Jeanton, H., Gobat, J.-M., Hunkeler, D. (2012). Determination of spatiotemporal variability of tree water uptake using stable isotopes ($\delta^{18}\text{O}$, $\delta^2\text{H}$) in an alluvial system supplied by a high-altitude watershed, Pfyn forest, Switzerland. *Ecohydrology*.
- Bowen, G.J., (2010). Isoscapes: Spatial Pattern in Isotope Biogeochemistry. *Annual Review of Earth and Planetary Science*, 38, 161–187.
- Brooks, J.R., Barnard, H.R., Coulombe, R. & McDonnell, J.J. (2010). Ecohydrologic separation of water between trees and streams in a Mediterranean climate. *Nature Geosciences*, 3, 100–104.
- Burgess, S. (2000). Characterisation of hydrogen isotope profiles in an agroforestry system: implications for tracing water sources of trees. *Agricultural Water Management*, 45(3), 229–241
- Cappa, C. D., Hendricks, M. B., DePaolo, D. J., & Cohen, R. C. (2003). Isotopic fractionation of water during evaporation. *Journal of Geophysical Research*, 108(D16), 4525.
- Dawson, T. E. (1993). Hydraulic lift and water use by plants: implications for water balance, performance and plant-plant interactions. *Oecologia*, 95(4), 565–574.
- Edmunds, W. M. (2010). Conceptual models for recharge sequences in arid and semi-arid regions using isotopic and geochemical methods. In H. S. Wheatler, S. A. Mathias, & X. Li (Eds.), *Groundwater Modelling in Arid and Semi-Arid Areas* (pp. 21–37). Cambridge University Press.
- Ehleringer, J. R., & Dawson, T. E. (1992). Water uptake by plants: perspectives from stable isotope composition. *Plant, Cell & Environment*, 15(9), 1073–1082.
- Ehleringer, J. R., Phillips, S. L., Schuster, W. S., & Sandquist, D. R. (1991). Differential utilization of summer rains by desert plants. *Oecologia*, 88(3), 430–434.
- Ehleringer, J. R., Roden, J., & Dawson, T. E. (2000). Assessing ecosystem-level water relations through stable isotope ratio analyses. *Methods in ecosystem science*, 181–198.
- Ellsworth, P.Z., Williams, D.G. (2007). Hydrogen isotope fractionation during water uptake by woody xerophytes. *Plant Soil*, 291: 93–107.
- Gallaire, R., Fontes, J. C., & Zuppi, G. M. (1995). Isotopic characterization and origin of rainwater on the Air massif (Niger). Application of Tracers in Arid Zone Hydrology (Proceedings of the Vienna Symposium, August 1994). IAHS Publ.(232).

- Gat, J. R. (1996). Oxygen and hydrogen isotopes in the hydrologic cycle. *Annual Review of Earth and Planetary Sciences*, 24(1), 225-262.
- Gibbs, R.D. (1958). Patterns of the seasonal water content of trees. *In: Thimann KV (ed.) The physiology of forest trees*. Ronald Press, New York, 43-69.
- Gonfiantini, R. (1986). Environmental isotopes in lake studies. *In: Fritz, P. & Fontes, J.C. (Eds.) Handbook of Environmental Isotope Geochemistry*, vol 3 (p. 113-168). Elsevier, New York.
- Goni, I.B., Fellman, E., and Edmunds, W.M. (2001). Rainfall geochemistry in the Sahel region of northern Nigeria. *Atmospheric Environment* 35 (2001) 4331-4339.
- Gurovich, L.A. (2012). Electrophysiology of Woody Plants. *Electrophysiology – From Plants to Heart*. Ed: Saeed Orali. InTech: <http://www.intechopen.com/books/electrophysiology-from-plants-to-heart/plant-electrophysiology>
- Korhonen L Heikkinen J. 2009 Automated analysis of in situ canopy images for the estimation of forest canopy cover. *Forest Science, Society of American Foresters*. 55 (4) 323-334.
- Lis, G., Wassenaar, L., Hendry, M.J., (2008). High-Precision Laser Spectroscopy D/H and 18O/16O Measurements of Microliter Natural Water Samples. *Analytical Chemistry*, 80 (1), 287-293.
- Lott, J. E., Khan, A. A. H., Ong, C. K., & Black, C. R. (1996). Sap flow measurements of lateral tree roots in agroforestry systems. *Tree Physiology*, 16(11-12), 995-1001.
- Mook, W.G., (2000). *Environmental Isotopes in the Hydrological Cycle: Principles and Applications*, Vol. I: Introduction - Theory, Methods, Vol. 1. International Atomic Energy Agency and United Nations Educational, Scientific and Cultural Organization.
- Njitchoua, R., Sigha-Nkamdjou, L., Devera, L. Marlin, C., Sighomnou, D., Nia, P. (1999). Variations of the stable isotopic compositions of rainfall events from the Cameroon rain forest, Central Africa. *Journal of Hydrology*, 223, 17–26.
- Risi, C., Bony, S., Vimeux, F., Frankenberg, C., Noone, D., and Worden, J. (2010). Understanding the Sahelian water budget through the isotopic composition of water vapor and precipitation. *Journal of Geophysical Research*, 115, 1-23.
- Smith, D. M., Jarvis, P. G., & Odongo, J. C. (1997). Sources of water used by trees and millet in Sahelian windbreak systems. *Journal of hydrology*, 198(1-4), 140-153.
- Smith, D.M., Jarvis, P.G. (1998). Physiological and environmental control of transpiration by trees in windbreaks. *Forest Ecology and Management*, 105, 159-173.
- Taupin, J.-D., Coudrain-Ribstein, A., Gallaire, R., Zuppi, G. M., & Filly, A. (2000). Rainfall characteristics ($\delta^{18}\text{O}$, $\delta^2\text{H}$, ΔT and $\Delta H r$) in western Africa: Regional scale and influence of irrigated areas. *Journal of Geophysical Research*, 105(D9), 11911.
- Tyree, M. T., & Zimmermann, M. H. (2002). *Xylem structure and the ascent of sap*. Springer.
- Van Noordwijk, M., G. Cadisch and C.K. Ong. 2004. *Below-ground Interactions in Tropical Agroecosystems: Concepts and Models with Multiple Plant Components*. CABI Publishing. Cambridge, MA.
- Whiteman, C. D., Allwine, K. J., Fritzchen, L. J., Orgill, M. M., & Simpson, J. R. (1989). Deep valley radiation and surface energy budget microclimates. Part I Radiation. *Journal of Applied Meteorology*, 28, 414.
- Zimmermann, M.H. (1983). *Xylem structure and the ascent of sap*. Springer-Verlag, Berlin.

Chapter 7 Conclusion

7.1 Current Research

This study presents a significant observation of the energy balance in the Sudanian savanna, which previously had only been studied a few, shorter times. In addition, it is the first documentation of the fluxes of sensible and latent heat flux over a gallery forest in the Sudanian ecosystem. Fluxes were higher over both the gallery forest and the semi-cultivated fields than those previously measured in the region, suggesting the significance of this site's location inside a semi-protected area. And fluxes over the forest were higher than those over the dried grasses or in the agricultural field for both sensible and latent heat flux.

It is possible to successfully model the energy balance from data available from low-cost, portable Sensorscope stations in semi-arid West Africa. Variation in vegetation exerts a strong control on evaporation because of its effect on the conversion of net radiation to ground heat flux, roughness length, and albedo. Future work will focus on predicting these parameters based on seasonal and spatial changes in vegetation. This work presents a significant step towards developing tools that could provide farmers with real time estimates of evaporation and thus the coupled energy and water budgets in real time.

Evaporative fraction was found to be consistent over mid-day. Removal of the influence of dry air entrainment revealed the land surface controls on evaporative fraction to be significant, particularly in the agricultural field. Cloud cover in addition to the land surface parameters of the vegetation index and the soil moisture had an effect on evaporative fraction. This work provides a foundation for upscaling evaporation estimates to a larger by using satellite derived data of surface temperature, vegetation index, soil moisture, and cloud cover based on our field measurements.

The model and observation soil moisture under the tree and in the open improves our understanding of the *Sclerocarya birrea* agricultural parkland. The rainfall intensity, interception, run off quantity, and spatial heterogeneity under the canopy should be examined in more detail, our data suggests some agroforestry solutions that can optimize water use in this ecosystem such as under canopy planting of crops with lower light and water requirements and stone half moon placement to encourage run off infiltration particularly from stemflow. In addition to the tangible farming recommendations, we also proposed some new approaches to motivating farmers to take on the challenge of a more integrative practice with the downstream users in mind.

The relationship between the $\delta D H$ and $\delta O 18$ concentrations of water extracted from soil and xylem samples do not fall along the meteoric water line, and thus their source cannot be solved with a simple linear mixing model. However their departure from their highly enriched state suggests that they draw on either ground water or reservoirs created by the tree in the dry season for leaf 2-3 months prior to the first significant rain. Vapor pressure deficit, soil water, and soil moisture interactions support this picture of interacting controls, separate from hydrologic triggers on the water movement in the tree. We leave this analysis wondering how changing precipitation patterns may affect this annual tree cycle that forms the basis for gourmantche traditional knowledge to predict rain.

This research represents an important test of many new technologies and approaches in addressing the questions and needs of sub-Saharan African, particularly the Sudanian agroforestry – savanna. Together these technologies provide tools necessary to

move from a high tech system to a more widely distributable but equally informative design. This will eventually allow for environmental data to be collected at a much higher quality over a larger area while maintaining an appropriate scale of resolution. In addition, this presents an enormous opportunity for local farmers to benefit even more directly from environmental management. The next major step in this exchange is to develop the tools that they can use to access this information.

7.2 Future Research

Broadly, future work could go deeper and more specific or broader and more comprehensive; And it should provide solutions to this particular community or make replicable products that can be generalized – to provide answers to regional or theoretical questions. It could take the form of improved calculations, data mobilization, filling the gaps in data, improved technologies at tree to watershed scale, and improvements to the participatory process and development of applications. We are still far from our goal of providing an integrated, holistic vision of the ecohydrologic processes present in a West African savanna and the management necessary to increase resilience. Below are my suggestions to move us towards that goal.

The most obvious improvement that future research should address is to improve the calculations. The evaporation models should be compared between the evaporative fraction and the similarity theory methods presented here. The quality of output compared to different input data including various levels of field data in addition to satellite and historic data sets should be systematically analyzed. Other simple models such as advection aridity can be incorporated into this analysis.

Second, more data from the current dataset should be mobilized. The CO₂ flux measurements should be integrated into this assessment of the land surface controls on atmospheric properties. The two main questions that I perceive at this site, with this data are: (1) what are the current patterns of water use efficiency, carbon sequestration, and net primary productivity on this site? ; And (2) what is the impact and magnitude of fire in the energetic and nutrient pathways?

Third, gaps need to be filled. A crucial link that is missing is a measurement of the stable isotope fraction of water vapor. This would allow us to resolve the complete hydrologic cycle. Along those same lines, I would recommend an intensive campaign where the spatial pattern of isotopic enrichment is more carefully studied in the canopy and in the root zone during the leaf out period.

7.2.1 Improved Technologies and Use of Equipment

Several improved technologies and processes emerged from this work. First, current research and measurements could be improved, learning from the work in this thesis. Specifically, the components of measurement of the tree water balance could be resolved more completely and meticulously. Sap flow sensor technology should be incorporated into the wireless sensor network. This would allow simultaneous monitoring of more individuals in the system. Similarly sensor choice on the tree should be refined to avoid redundancy based on the data present here. The current set up was too “heavy” i.e. there were so many sensors that they frequently failed. Soil moisture measurement under the tree was compromised because of the quantity of sensors, and in retrospect, a simplified measurement scheme that worked for more time would have been more useful. Measurements of subcanopy runoff, throughfall, and stemflow were all attempted, however the sensors used were not specifically adapted for these measurements. More work has been done to develop throughfall and runoff measuring tools elsewhere, but again; the product needs to be a simple, scalable technique that can be incorporated in the wireless sensor network. Our use of the subcanopy solar radiation sensor proved valuable data that perhaps would replace the need for other canopy measures. One sensor would provide adequate information and more work could be done to link this measurement to actual leaf area index and transpiration.

This improvement would allow our understanding to go deeper on specific trees, but more interesting, would make replicating this experience on many individual trees of different species more realistic. A simple “tree water balance” station could be placed around the trees in actively farmed fields. Species of future interest would include: *Vitellaria paradoxa*, *Parkia biglobosa*, *Magnifera indica*, *Azadirachta indica*, *Vitex doniana*, and *Tamarindus indica*. These are all trees that were found to be especially valued in farms, despite the fact that some of them have no sub-canopy farming. In addition species of *Ficus* and *Mitragyna inermis* are often sited as “bringing water”. This sort of station would be essential for a payment for ecosystem services scheme as proposed in the conclusions. Next to the station, the models and software to access this station would be essential. This expansion would collect important data that would allow for data to be directly relevant to the farmers and for a much broader understanding. Finally this improvement could also provide a database that could answer some more theoretical questions. For example, how to individual trees, as part of a community of trees, respond to drought stress and create resilience?

Second, new technologies could be brought to the site along with better use of those technologies. Through our entire measurement campaign, we struggled with the soil moisture sensors. Dielectric sensors tend to break whenever the ground moves and it moves often. Alternatives need to be explored. Also, ground water needs to be carefully monitored. We measured the groundwater entirely by hand, which led to use biases, in particular in regards to the diurnal cycle. Finally, to move beyond the point measurements to a spatial resolution, while still acting as an intermediary to satellite images, the use of small-unmanned aircraft needs to be explored. They present a valuable opportunity to get NDVI, thermal, or visual data at a high resolution over our catchment.

The research presented in this paper, in isolation, does little to contribute to local knowledge or local benefit. We did make an effort to reach out to local communities through interviews and a participatory process, but we have not communicated any definite results of our research or offered any tangible tools that came from our research. There is no potential for transfer without both increased communications and tools. With the correct systems, the local village can receive knowledge to improve their farming systems and tools to improve their environmental management both through incentive schemes and monitoring systems. The co-creation of knowledge, however, is still evading us. The first steps have been taken by inventorying local and scientific knowledge, but future steps need to bring these two bodies of knowledge together. As we continue with this project, we will proceed with this iterative process of knowledge sharing and refinement.

Finally, future work needs to learn from our experiences in this project to improve the participatory process so that applications can be relevant and useful. I began by evoking Wangari Maathai’s role model, and I’ll close by saying that I hope in the future we aspire to do an even better job of not only understanding the soil – vegetation – atmosphere transfer processes, but also passing on concrete tools and development for increased resilience to our colleagues and counterparts in the village.

Postface: Lessons Learned

From a North-South, International, Cross- Cultural, Inter-Institutional, and Interdisciplinary Research-Development Project Aimed to Benefit Base of the Pyramid Farmers with Hi-Tech Research

The goal of this postface is to share some of my perspective as one of the doctoral students working on this project. I use an ethnographic methodology of participant – observation in order to critically examine this project in such a way that future projects with similar aspirations and in similar contexts can learn from our experience. It is important to note that this method of analysis is not objective but rather full of my own bias. To balance the bias, I will draw in the results of some interviews conducted in 2010 in the village of Tambarga. I will write this somewhat backwards, beginning where the conclusions left off.

Looking forward

Perhaps most importantly, future work at this site needs to focus on the improving the participatory process and application. We do not achieve this goal of social – collaborative research. As Wangari Maathai experienced, environmental resource management can provide a tool for collective mobilization and empowerment. In learning to use the technologies offered by science, community member can become more autonomous and free to make their own decisions. Our intentions to do this were there, but we had to understand our own goals and objectives before we could be pure change agents. My interviews with villagers in 2011 give some insight into this challenge.

Villagers described that from 2008 to 2011, the time that our project had been present in the village, there had been tremendous development. The maternity clinic was nearly finished (3 women had died the year before), there was the new market building and a new pump, fewer water born diseases, speakers at the youth house, flow breaks in the stream, white people in the village, more tomatoes and cabbage, a secondary school, a training house, farming material, cell phone network, many more white people coming to the village, our stations are there, and increased understanding of them, people, and research. They told how people initially thought that our stations were tools to find gold or that they would kill them. They also talked about how people are more open to new ideas now and are more willing to take the advice of others. At the same time, people said that there is less cotton production now, and that more young men and children are dying from snake bites because traditional healers have either forgotten their craft or that their skills stopped working. But most said that fewer people are dying now. Children don't listen to parents anymore because parents don't raise them well.

The overall message I take from this summary is that the last few years have been a time of change and education. Based on this, I would say we haven't failed at all, but rather, we have to be patient with the time scale with which change occurs. People see a growth not only in the infrastructure of the village but also in the awareness of the village. This is a huge step in the right direction. However, I would be surprised if very many villagers could articulate what, besides the physical infrastructure of stations and buildings, they gained. Some would tell us that they learned from us, that they learned how our weather stations worked, but I don't think any would tell us how they could benefit from that knowledge concretely.

To rise to this challenge, we need to find concrete questions that farmers need to know that our technology can answer. Also, we need to reexamine our site. The fields where our research takes place are the "house gardens", located near the house and often

farmed by the older family members or women with young children who cannot make the journey to the real fields. If we really want to draw conclusions about the state of agriculture in this village, we need to direct our attention to those fields. Our work in the “house gardens” is important as a first step. They had many advantages – were close by, were protected, and were situated in a catchment. But from this point forward, we have to adapt our research to the local need.

Villagers told me that they needed to know what crops they should plant. How should they change their current practices to a changing problem? They thought that legumes and groundnuts were more adapted to difficult rainy seasons. They wanted to know if their specific farm was good in terms of soil, water, and climate. They asked how many trees they should leave in their field. They said that some trees would prevent growing around them, and wanted to know exactly which trees were good and bad for their crops. Also which trees could impact your health if you ate or cut them, and which ones could be burned and which could be debarked. Most universally, they wanted to increase production. And if possible, wanted technology to increase and manage rain fall.

These are all good questions – many of which we can answer with by collaborating more closely with the members of the community. We also have much to learn from them, and can forage new ways to collaborate on some of these issues.

The big change in the village, over the lifetime of most adults in the village is the water source. When they were young, they fetched water from the springs, but now there are lots of wells and pumps. However, before, those wells never when dry, and now they go dry frequently. Some explained to me that this is because the construction of the wells brought more people to the village that now use more water. There also are more children born, because people marry young and want children. The population increase also leads to more land conflicts between herder and farmers, and more elephants.

Also, the former farmland was more fertile, covered less area, and only millet and groundnuts were farmed. But now there are more farms and they are more diverse including corn, millet, cotton, beans, potato, yam, and rice. In the future, more melon would be nice. The rice has also changed since before have short season rice and corn. If the rain lasts long, it is better to grow long season plants. If it is a dry season, then millet and cotton are better crops, but if it is a humid year, then plant corn and legumes. Some explain that herbicide and insecticide that degraded land, and increased diseases in people and animals that are hard to heal and stuck in the water. The wind today carries disease, which it didn't before. And in general there are more diseases.

The rain arrives later now – and we know because gourmantche months refer to the stage of the rainy season. And the rain that used to correspond to August now comes in September. Others said that there was more rain before or that the rainy seasons today stop in the middle and the soil never saturates. The water runs off quickly now, leading to erosion, whereas before it stayed on the fields more. There was also more flooding that sometimes ruined the fields. Others explained that these changes in rain are because of God. Wind is less regular now, although some say stronger, and blows less in the dry season, which is hotter.

The ancestors of this village came from Fada and Madjoari, and arrived when there was a war. They left from Madjoari, where there was a smith who made canary. Madjoari was crowded so came to Tambarga, which means hill. The hill was an important part of why this site was chosen, because people could flee up into the hill and hide during the time of war and frequent visits by soldiers (~1875). During that time some people even fought in the Niger army. Before there were no fields far away, they were all close to the houses and only contained millet and groundnuts. Hunting wild animals and honey complemented the diet. People ate raw meat and raised chickens. There were magic products that today would bring problems. When hunting was forbidden, and there was no more honey, people turned to farming. They had to expand the farms to far from the houses. Especially in the site of Botchandi, which is now forbidden. Now there are also tractors and animals that help plow – whereas before, it was just with the manpower.

Perhaps together, we can find ways to extract our own data and our own needs from their knowledge. Perhaps we need to set up some sort of scientific advisory board in village that would discuss these matters. The project had the original goals to first build an innovative planning support platform specifically adapted to rural development and second to help people live more sustainable through information.

Neither of those two goals, or the following more specific versions of those goals, necessitate any more technology than what we have on site. To our credit, the introduction of the current set up of sensors and monitors is extremely valuable and will serve to provide information. But the next step needs to focus on the delivery and use of that information. To shed light on that goal, I begin with a story that highlights many themes. Before we begin, it is important to note the players in this project and the start of the project.

In 2008 residents of the villages surrounding the Singou River Basin gathered for a participatory mapping workshop (Figure 1-1). Discussions directed research towards understanding hydrologic consequences of conversion of savanna to agriculture and mitigating those consequences through education, information exchange, and reforestation out reach projects focused on the commune of Madjoari. From this meeting the site was chosen and the players became clear. There were 2 academic institutions – one in Switzerland and one in Ouagadougou. In one of the institutions, there were three different scientific entities – one devoted to cooperation, one to environmental science, and one to information technology. The scientific interests of the group in Ouagadougou were most closely aligned with the environmental scientists, but the habitual cooperation happened through the entity devoted to cooperation. In addition to the academic institutions, there was an organization based in Ouagadougou that normally worked to improve access to water infrastructure in the city. Finally, there were the partners in the village, led by the mayor but in volume a whole diversity of people with different interests in the project.

Personal Story

One day, I climbed up to the top of our hill; I found that the wire to the base station on top of the hill, that is responsible for communicating all of our data to the server in Switzerland, had been cut with a rock. Further over the plateau, I found that the wires connecting the rain gauge to the sensor box had been chewed. My field assistant was furious – he knew that this reflected badly on him, as it is his responsibility to keep the station free of harm. This happened in mid June, which is a very important time in this part of West Africa, as it corresponds to the passage of the nomadic Fulani and their herds of cattle from the southern countries of Ghana and Benin back up to their homelands in Niger and Mali. Our village, Madjoari (Burkina Faso), is one of the last passages that is relatively open and free of harm. It is situated in the middle of a group of trans-national parks that are shared between Burkina, Benin, and Niger. The herders and their cattle are allowed to cross the area as long as they do not let their cattle stray too far from the road and eat the vegetation reserved for the wild animals. Along the way, villages such as ours welcome them and benefit from the influx of money and resources that they transport, even if farms occasionally get trampled, and in our case, meteorological stations get chewed or knocked down. When I returned to the village, I immediately went to see the local Fulani chief, a man who decided to take up permanent residence in the village years ago and had become of friend of mine because I frequently buy his milk, practice my rudimentary Fulfulde with his wives, and encourage his daughter to stick with her studies in French. Luckily it was Friday, so following the mid-day prayer, he convened all the Fulani who were in the village to meet under the large Tamarind tree in the communal hotel where we stay. I watched in amazement as hundreds of men and boys in turbans, sirwaal, and holding little sticks gathered in my yard. I spoke in French before the crowd, asking them to “please try and keep their cattle away from our stations, which were very important for our research”, which my assistant translated into Gourmantche along the lines of “this equipment is extremely valuable, is responsible for bringing the rain this season, and if anyone or their cattle ever so much as comes near it again, they will be immediately executed or sent to prison”, which the chief then translated in to Fulfulde with something

undoubtedly more severe. After the speeches, everyone applauded and we never had any more problems with cattle disturbing our sensors, although part of me will always feel that an educational opportunity was missed.

The fundamental conflict in this story is between the cows and the stations. On a certain level, this demonstrates the conflict between the production of food and income and the production of knowledge. The tools for our research are not immediately useful. They have no practical value. The time scale of knowledge conflicts with the scale of production. In terms of concept, it has been hard to balance the abstract theoretical and scientific research objectives with the immediate needs of the village. For me personally, I felt like I had to ask research questions that directly responded to the needs of the village, but that were also interesting to the scientific community. This has not been easy, and I feel like I more often am disappointing one party than satisfying both. This frustration is a symptom of the different interests and time lines. Science has one time line and farming has another, and political change has yet another.

This is a conflict between not only the village and the scientists, but also can be observed at the scale of the different institutions. In order to overcome these challenges, we need to make it more relevant to each of the players from the start. This means, address disagreements and conflicts of scale vocally. We need to identify common objectives and needs and not aspire to unrealistic goals. We need to follow through with the participatory process that has an important role in bring us together throughout the process. An ideal participatory process will not happen just once, but will happen over and over in an iterative fashion. Finally, it is essential that we develop information sharing tools that everyone can use.

The second big lesson is demonstrated by this story is the translation. The specific meanings were lost. This brings me to my second major lesson learned, that communication must be clear. A realistic time line must be agreed upon at the beginning and reevaluated as the project continues. The budget and objectives need to be similarly established and monitored and reevaluated. One participatory workshop was not enough. Communication has to overcome many barriers, and language is just the beginning – culture, economics, education, lifestyle, and worldview to name a few. Even between scientists in the same institution, we had to overcome our disciplinary differences.

My major recommendation out of this project is to have someone specifically studying these exchanges guided by the question: “How do we do science, so others can benefit?” This question will benefit not only the cooperation and development community but will benefit the growing number of interdisciplinary collaborations. In the future, a careful, well planned project with only a few clear, shared goals, and a few collaborators who agree on the procedure and invest time collaborating might be able to take our baton and make something truly beautiful from it. Project diversity should be turned into a benefit, not a challenge.

Appendices

Appendix I. Species Inventory

- Plot 1: 100 m x 100 m, on hill, near Sensorscope 1009.
- Plot 2: 100 m x 100 m, in farmland, near Sensorscope 1012.
- Farmland Survey: Identification and measurement of all trees in farmland area (~3.4 km²)
- Gallery Forest Survey: Identification of all trees in gallery forest.
- Groundcover and shrubs on Hill: *Annona senegalensis*, *Chlocospermum*, *Vernonia*, geophyte bulbs, *Strychnos innoca*, *Andropogon sp*, *Amorphallus sp*.
- Groundcover in farms: millet fields, riparian shrubs, fallow scrub
- Gallery forest groundcover: *Oxytenanteia abissineica*
- Tree height: up to 14 m on hill and 18 m in fields
- Dominant Shrub layer height on hill: 3 -7 m tall (19 June 2009)
- Canopy Cover on Hill: 30% trees
- Ground Cover on Hill: 60% herb 40% bare
- Average Canopy size on farms of *Sclereocarya birrea*: 69.3m²
- Average Canopy size on farms of all trees: 68.7m²


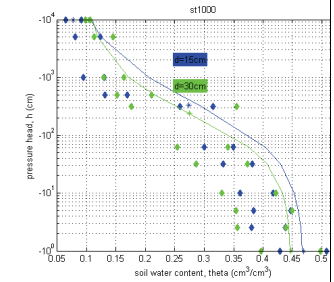


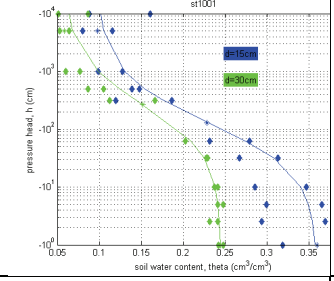

Table below shows number of individuals present in each plot.


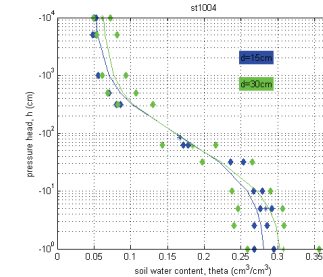


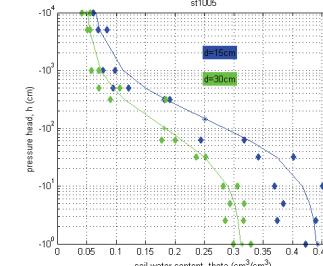


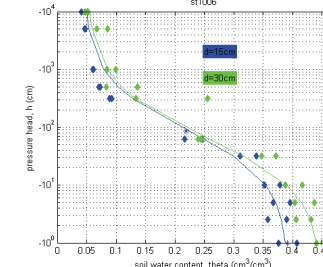


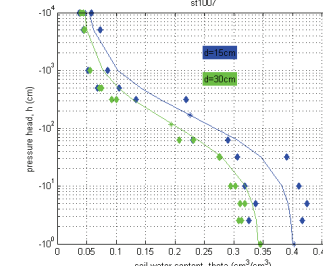

	Local Name (Gourmantche)	Individuals present			
		On Hill (100m x	In Farmland (100m x	In Farmland Total	Gallery Forest
<i>Acacia macrostachya</i>	<i>o calipangpangu</i>	6		1	1
<i>Acacia sieberiana</i>	<i>li konmoanli</i>			2	
<i>Adonsonia digitata</i>	<i>butuoabu</i>			4	
<i>Albezia chevalleri</i>	<i>ocarkpangbayaro,</i>	5		6	
<i>Angeiossus leiocarba</i>	<i>busiebu</i>			1	
<i>Azardica indica</i>	<i>butu tombo</i>			1	
<i>Balenites aegyptiaca</i>	<i>bupkam pkagibu</i>			7	
<i>Bombax costatum</i>	<i>bufuoubu</i>		1	3	
<i>Burkea africana</i>	<i>okpangabou</i>	2			
<i>Citrus sp.</i>	<i>lomuli</i>			1	
<i>Combretum nigricans</i>	<i>okadjamon</i>	1		3	
<i>Daniella oliveria</i>	<i>bunalinlinga, linobili</i>	10			2
<i>Detarium microcarpum</i>	<i>bunapagibu</i>	84		2	
<i>Dichrostachys cinera</i>	<i>linajagali</i>				1
<i>Ficus abatifolia</i>	<i>bukankanbu</i>			9	
<i>Ficus sycamorus</i>	<i>kukargo, likakasagli</i>			15	
<i>Ficus thonningii</i>	<i>sidia</i>			1	
<i>Gardenia erubecens</i>	<i>bunasotibu</i>	1			
<i>Gardenia tenifolia</i>	<i>nimbelbilinga</i>				1
<i>Grewia flavescens</i>	<i>liyompienti</i>	9			1
<i>Guiera senegalensis</i>	<i>ipuenpieni</i>	41			
<i>Hymenocardia acida</i>	<i>ipujamanga</i>	4			
<i>Hyphaene thebaica</i>	<i>I kaarikpe</i>			1	
<i>Lanea acida</i>	<i>limantchabili</i>			5	
<i>Lannea microcarpum</i>	<i>oomanchanouga</i>			25	
<i>Magnifera indica</i>	<i>mangili, bunasarsambu</i>			15	
<i>Parkia biglobosa</i>	<i>odoubu</i>	1			

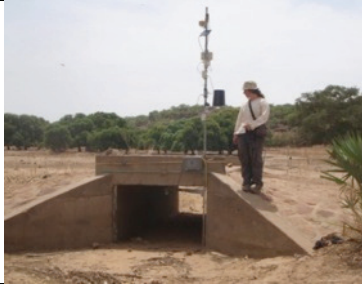



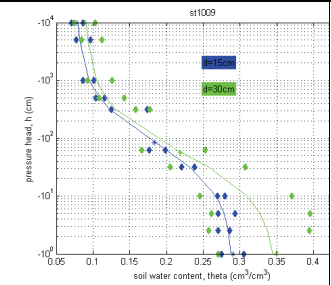


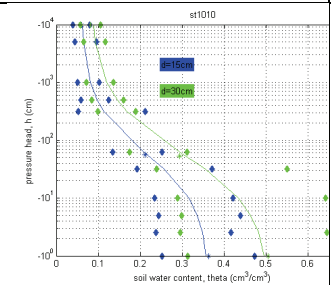




<i>Periopsis laciflora</i>	<i>bunalinlinbu</i>				1
<i>Piliostigma reticulatum</i>	<i>unabangu</i>		1	88	
<i>Prosopis africana</i>	<i>ikpandongu</i>	4			
<i>Psychotria psychotrioides</i>	<i>okpenagagu</i>				1
<i>Pteleopsis subrosa</i>	<i>ogbelu</i>	110			1
<i>Pterocarpus erinaceus</i>	<i>bunatombu</i>	7			
<i>Sclerocarya birria</i>	<i>bunamaribu</i>	2	6	116	
<i>Sterculia setigera</i>	<i>bunafocabu</i>	2		2	
<i>Strychnos spinosa</i>	<i>bukpankpalimbu</i>	19			1
<i>Tamarindus indica</i>	<i>bupubu</i>			1	
<i>Terminalia avicennioides</i>	<i>lifapebli moili</i>	54		1	
<i>Terminalia glaucescens</i>	<i>oungagbubobotiegu</i>	10		4	
<i>Terminalia laxiflora</i>	<i>ufapubli</i>	79	1	55	
<i>Terminalia mollis</i>	<i>lisididuali, lisikuali</i>	1		7	
<i>Vitellaria paradoxa</i>	<i>busaambu</i>	9			
<i>Vitex donania</i>	<i>bunambu</i>				1
<i>Ximenia americana</i>	<i>bumidenbu</i>	13			1
<i>Ziziphrus mauritania</i>	<i>omandibu, buyumbu</i>			4	


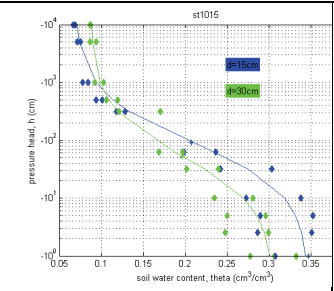

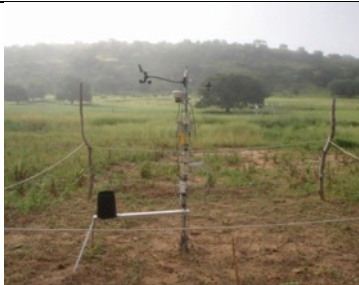
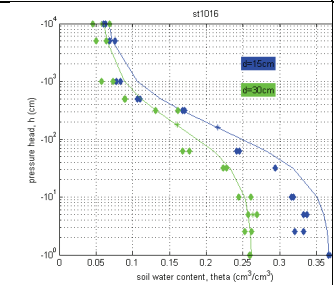


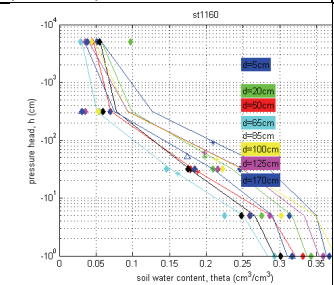


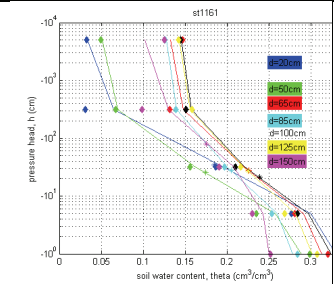

Appendix II. Sensorscope Station Inventory





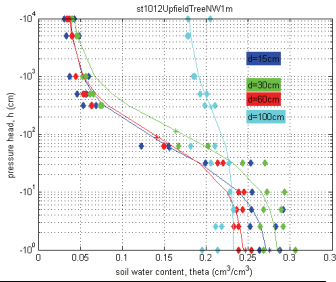




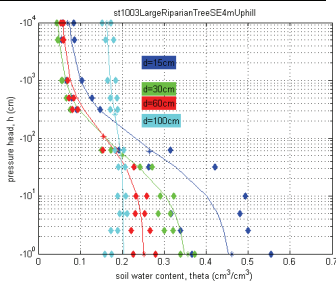
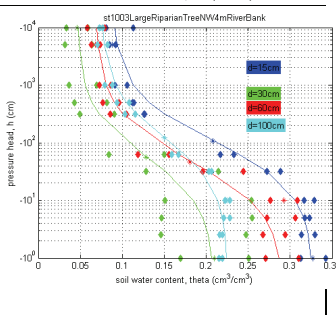
Soil and pictorial documentation of different stations in watershed. First column shows station number(s), then pictures, a brief description, and soil conductivity plot. If there are multiple numbers, then the station has changed names over the course of the experiment, and it is still potentially in operation through the beginning of 2014. Some changes have been made regarding the sensors present, but the location has stayed consistent. Discontinued dates are notes. See subsequent Appendices for more information regarding the soil and the technology.

1000 1260 1264			
	Close to Village, South-facing slope. Not far from Forage 1.	Degraded soil, lots of runoff from village, near to village waste sites. Soil is sandier at the surface but is a sandy loam at both 15 and 30 cm.	In short cycle millet field that is fallow much of the year. Fallow species include many grasses and vines. Closest tree is a <i>Ficus sycamorus</i> (200 m, ~20 m high).
1001 1267			
	Near Bridge, Flat, Near Source 1, Near River,	Saturated for rainy season, but still sandy loam, darker color (black) compared to others	Surrounded by wetland plants and rice fields.

<p>1004 (discontinued. Oct. 2011)</p>			
	<p>North Facing slope, Near transition from fields to canyon.</p>	<p>Sandy Loam soil.</p>	<p>In short cycle millet field that is fallow much of the year. Fallow species include many grasses and vines. Trees nearby include Boobab (<i>Adonsonia digitata</i>, <i>Lannea microcarpa</i>, <i>Ficus sp.</i>, and <i>Sclerocarya birrea</i>).</p>
<p>1005 1265</p>			
	<p>North Side of River, on River bank, just downstream of large tree (1003). Riverbank slopes to River</p>	<p>Sandy Loam soil.</p>	<p>In grass shrub on river bank between millet/fallow field and river.</p>
<p>1006</p>			
	<p>In curve in river where DTS was rerouted through river bank.</p>	<p>Sandy soil.</p>	<p>In shrubby vegetation that is on the river bank</p>
<p>1007 1266</p>			
	<p>In Fallow field near small tree. Additional Equipment: closest complete station to 2069 energy balance station</p>	<p>Sandy soil.</p>	<p>Fallow grass species, near <i>Piliostigma reticulata</i> tree, <i>Sclerocarya birrea</i></p>

<p>1008</p>			
	<p>On Bridge. Other Equipment: pressure gauge for stage under bridge. Closest station to Weir 1.</p>	<p>No Soil, sandy in river bottom.</p>	<p>Fallow grass species, <i>Jatropha</i> and <i>Hyphaene thebaica</i> tree near bridge.</p>
<p>1009 1261</p>			
	<p>High on plateau.</p>	<p>Wind deposits from the whole region here. Loamy Sand at 15 cm and Loam at 30 cm. A fair amount of cobble in upper soil layers as well.</p>	<p>Sudanian savanna, remarkable <i>Prosopis africana</i> tree nearby, also lots of <i>Crossopteryx</i> and <i>Terminalia</i>. Average tree height 10 m. Veg inventory available.</p>
<p>1010</p>			
	<p>North Facing slope (18%). Lowest of 3 upper stations. In wooded area near dry stream bed (only observed disconnected water in bed once, in September)</p>	<p>Rocky soil with lots of boulders and cobble. Sandy Loam.</p>	<p>In forested area. Trees include <i>Vitellaria paradoxa</i>, <i>Lannea barteri</i>, <i>Burkea africana</i>, <i>Chloclopermum</i>, <i>Sapium</i>, <i>Terminalia laxifolia</i>, <i>Detarium</i></p>
<p>1014, moved to a nearby higher rock in October 2011</p>			
	<p>On rocky peak along ridge. closest station to 1828 energy balance station, similar position.</p>	<p>Rocky out cropping covered with black lichen.</p>	<p>Nearby <i>Ficus abustifolia</i> tree growing in crevice and overlooking <i>Detarium</i> and <i>Terminalia</i> trees</p>

<p>1015 (discontinued Oct. 2011)</p>			
	<p>Near transition from fields to canyon. Closest station to Weir 2 – and pressure gauge.</p>	<p>Sandy Loam soil.</p>	<p>In fallow field that has grown peanuts and melon. Large <i>S. birr</i> tree near by.</p>
<p>1016</p>			
	<p>on flat area above river, across from 2069 EC station, near village</p>	<p>Sandy Loam soil. In Fallow area degraded from village proximity, lots of erosion.</p>	<p>In short cycle millet fallow field. Degraded fallow vegetation.</p>
<p>1160 (discontinued . Oct. 2011)</p>			
	<p>Flat area near 2069 EB station 10 ECTM sensors vertically spaced. Ground level rain gauge – interception. Additional Equipment: EC station, Precis rain station, Runoff plot.</p>	<p>Sandy Loam soil.</p>	<p>In short cycle millet field that is fallow much of the year. Left fallow this year. Not far from <i>Piliostigma reticulata</i> tree.</p>
<p>1161 (discontinued . Oct. 2011)</p>			
	<p>North facing slope, Near base of hill coming down, near <i>cordon pierreuse</i>. 10 ECTM sensors vertically spaced. Ground level rain gauge – interception. Additional Equipment: Runoff plot.</p>	<p>Sandy Loam soil in upper 40 cm, deep layers loam and clayey loam.</p>	<p>In short cycle millet field that is fallow much of the year, farmed this year. Downslope from <i>S. birr</i> tree.</p>

<p>1012 1013 1263</p>					
	<p>Small <i>Sclereocarya birrea</i> tree</p>	<p>13m tree, understory disturbed by research and animals. Surrounded by fallow field. Many neighboring <i>S. birr</i> trees.</p>	<p>3 throughfall, 1 stemflow, 3 canopy light penetration, 1 PAR, soil moisture sensors arranged along South and East Axes in 4 depths, at 3 radial distances from trunk. Canopy Mast holds 5 air temperature/humidity,</p>	<p>Runoff plot under its canopy and neighboring tree, sapflow probes</p>	<p>Sandy Loam soil, over a cemetery (2 graves discovered), likely site of former village. At a meter, Loam and near surface Sandier.</p>
<p>1003 1011 1262</p>					
	<p>Large <i>Sclerocarya birrea</i> tree, 7 meters from river bank.</p>	<p>Sandy Loam or Loamy Sand even up to 1 meter depth. Higher clay content at depths deeper than 1 meter.</p>	<p>Surrounded by short season millet and then fallow fields.</p>	<p>3 SOLA under canopy for light penetration, MPS1 & ECTM at 4 different holes and 4 different depths: 1 uphill, and 3 downslope holes towards river</p>	

Appendix III. Calculation of the Hydraulic Properties of Soils

Soil Hydraulic Properties were determined using the Mualem Model to determine the Van Genuchten parameters using Hydrus software (1980). These were determined in the laboratory for 100 cm³ samples taken in the dry season at four depths from 3 holes under the 2 trees in duplicate. Shown here are the characteristic curves averaged for duplicate samples at the 11 pressure heads. The triangle shows the determined textures from the soil from the different stations. Plots of the Van Genuchten parameters are in Appendix III for each station and below in more detail.

$$\theta = \theta_r + \frac{(\theta_s - \theta_r)}{[1 + (\alpha h)^n]^m}$$

$$m = 2 - \frac{1}{n}$$

$$K_r(h) = \frac{1 - (\alpha h)^{n-2} [1 + (\alpha h)^n]^{-m}}{[1 + (\alpha h)^n]^{2m}}$$

In addition to automatic sensing, soil samples were taken for analysis of volumetric water content by drying in an oven at 105°C for 24 hours. The volumetric water content was calculated by subtracting the dry weight from the wet weight and dividing by the dry weight. Soil porosity was calculated by weighing samples of 100 cm³ after drying in a drying oven at 105 °C for 24 hours. The weight over the volume or apparent density was divided by 2.65 to obtain the soil porosity. These values were used to verify automatic sensor values. Calibration between the manual measurements and the dielectric sensors was done using the Topp equation (Topp et al., 1980).

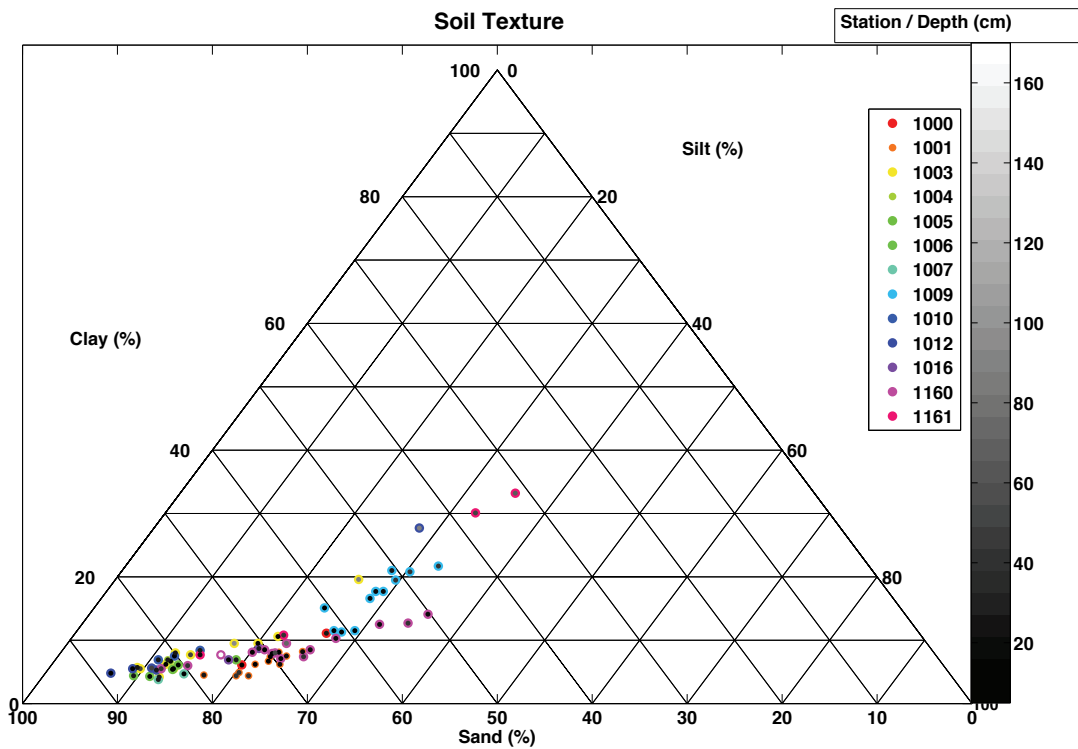


Figure III - 1: Soil Texture Triangle by depth and station (colors and shading) determined in the laboratory.

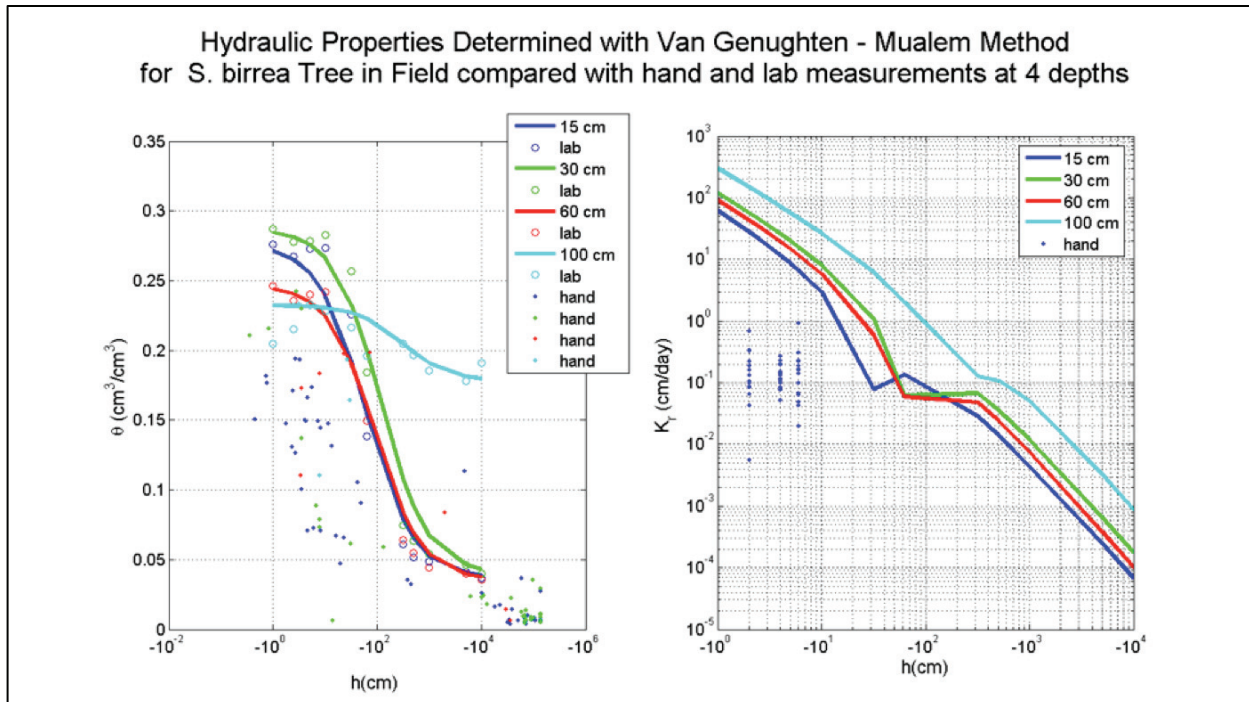


Figure III – 2. Soil Hydraulic Properties determined at tree for fourth depths. On the left is the volumetric water content and on the right is the hydraulic conductivity both over hydraulic head.

Reference

- Topp, G. C., Davis, J. L., A. P. Annan. (1980). Electromagnetic determination of soil water content: Measurements in coaxial transmission lines. *Water Resources Research*, 16(3), 574-582.
- Van Genuchten, M.Th. (1980). A closed-form equation for predicting the hydraulic conductivity of unsaturated soils. *Soil Science Society of America Journal*, 44, 892-898.

Appendix IV. Wireless Sensor Networks²

Wireless sensor networks (WSN) are a new generation of measurement systems with a built-in capacity to produce high temporal and spatial density measurements (Szewczyk et al., 2004; Langendoen et al., 2006; Barrenetxea et al., 2008). They are composed of multiple autonomous sensing stations, which typically operate in a self-organized manner and communicate together using low-power radio modules. Sensing stations regularly transmit data (e.g., air temperature and humidity, wind speed and direction, soil moisture) to a sink, which in turn, uses a gateway to relay the data to a remote server. Due to their capability to produce high temporal and spatial density data, WSN have a high potential for improving environmental data acquisition and for interfacing with scientists, managers, and farmers (Martinez et al., 2004; Werner-Allen et al., 2005; Sikka et al., 2006; Selavo et al., 2007).

² This originally appeared as a section of the following publication : Ceperley, N., Repetti, A., & Parlange, M. (2012). Chapter 15: Application of Soil Moisture Model to Marula (*Sclerocarya birrea*): Millet (*Pennisetum Glaucum*) Agroforestry System in Burkina Faso. In J.-C. Bolay, M. Schmid, G. Tejada, & E. Hazboun (Eds.), *Technologies and Innovations for Development* (pp. 211-229). Paris: Springer Paris.

One of the unique features of WSN is multi-hop routing (Buonadonna et al., 2005; Barrenetxea et al., 2008), which, under some restrictions, allows sensing stations to be placed farther away from the sink than the communication range of the low-power radio module. In this kind of routing mechanism, data packets are forwarded along a chain of stations, from the slave station to the sink. This feature has the advantage of enabling data gathering over a wide area with only one single sink. The sink usually relies on the GPRS network, largely available worldwide, to transmit the collected data from the deployed stations to any computer connected to the Internet.

Self-organization and multi-hop routing make WSN highly versatile, which means their use will be favored in place of, older, less user-friendly technologies. Thus, they offer potential for widespread environmental monitoring. Given the severity of potential climate change, natural habitat fragmentation by agricultural conversion, human population increase and migration, soil salinization, erosion in seasonally dry regions, and active management require; WSN can provide appropriate monitoring systems for producing high temporal and spatially dense measurements. Moreover, as the cost for building WSN gets lower, they can cover larger monitoring areas with minimal costs, which meets the application requirements of high quality and wide coverage data, in various environmental sciences (Inglerest, F. et al., 2010).

References

- Barrenetxea, G., Ingelrest, F., Schaefer, G., & Vetterli, M. (2008). SensorScope: The hitchhiker's guide to successful wireless sensor network deployment. *Proceedings of the 6th ACM Conference on Embedded Networked Sensors Systems (SenSys 08)*.
- Buonadonna, P., Gay, D., Hellerstein, J., Hong, W., & Madden, S. (2005). TASK: sensor network in a box. *Proceedings of the Second IEEE European Workshop on Wireless Sensor Networks and Applications*.
- Ingelrest, F., Barrenetxea, G., Schaefer, G., Vetterli, M., Couach, O., & Parlange, M. (2010). SensorScope. *ACM Transactions on Sensor Networks*, 6(2), 1-32.
- Langendoen, K., Baggio, A., & Visser, O. (2006). Murphy loves potatoes: experiences from a pilot sensor network deployment in precision agriculture. *Proceedings of the 20th IEEE International Parallel and Distributed Processing Symposium*.
- Martinez, K., Hart, J., & Ong, R. (2004). *Environmental sensor networks*. *IEEE Computer Society*, 37, 50–56.
- Selavo, L., Wood, A., Cao, Q., Sookoor, T., Liu, H., Srinivasan, A., Wu, Y., Kang, W., Stankovic, J., Young, D., & Porter, J. (2007). LUSTER: Wireless sensor network for environmental research. *Proceedings of the 5th ACM International Conference on Embedded Networked Sensor Systems*, Sydney.
- Sikka, P., Corke, P., Valencia, P., Crossman, C., Swain, D., & Bishop-Hurley, G. (2006). Wireless adhoc sensor and actuator networks on the farm. *Proceedings of the 5th ACM/IEEE International Conference on Information Processing in Sensor Networks*.
- Werner-Allen, G., Johnson, J., Ruiz, M., Welsh, M., & Lees, J. (2005). Monitoring volcanic eruptions with a wireless sensor network. *Proceedings of the 2nd IEEE European Workshop on Wireless Sensor Networks and Applications*, Istanbul.

NATALIE CLAIRE CEPERLEY

Born: 21 February, 1981 in California, USA
Contact: natalie@ceperley.com



OBJECTIVE

Environmental scientist with multi-disciplinary skills drawn from micrometeorology, hydrology, ecology, forestry, and ethnography as well a contextual understanding of international development work, particularly in West Africa. I study links between water and plants and the communities that depend on them based both on scientific and traditional knowledge.

EDUCATION

SWISS FEDERAL INSTITUTE OF TECHNOLOGY –LAUSANNE (EPFL), PHD CIVIL & ENVIRONMENTAL ENGINEERING 2008-2013

- Thesis: Ecohydrology of a Mixed Savanna-Agricultural Catchment in South-East Burkina Faso;
- Advisors: Marc B. Parlange, Laboratory of Environmental Fluid Mechanics and Hydrology & Jean-Claude Bolay Center of Cooperation and Development
- Management & Operation of Info4Dourou Research-Development Project and Field Site in Cooperation with 2iE & PRCCU in Ouagadougou, Burkina Faso and the Commune & Residents of Madjoari, Burkina Faso; Supervise Master Thesis's (7), Semester Projects (8), & Internships (9) in Switzerland & Burkina Faso; Teaching Assistant for Travaux Pratiques, Bachelor Semester 2 Environmental Engineering; Responsible for Liquid Water Stable Isotope Lab; Advances in Ecohydrology Summer School, Palermo, Italy (2010); Stable Isotopes for Ecological Research Course, Paul Scherrer Institute, Villigen (2010)

YALE SCHOOL OF FORESTRY AND ENVIRONMENTAL STUDIES, MESC ENVIRONMENTAL SCIENCE, AFRICAN STUDIES (CERT.) 2006-2008

- Thesis: Conservation Importance of Sacred Forests for Riparian Ecosystems in Central Benin
- Teaching Assistant (Local Flora), Environmental Education Intern (Urban Resources Institute), Urban Youth Science Mentor, Translator/Interviewer for Supply-Chain Analysis of Congolese Timber (WWF/Yale); Research Assistant (Geology Department - Stable Isotope Laboratory)

GRINNELL COLLEGE, BA BIOLOGY, GLOBAL DEVELOPMENT STUDIES (CONC.) 1999-2003

- Independent Research: Tree Ring Analysis Along Floodplains of the Rio Grande River, NM
- Internships: The Alaska Sea Otter and Steller Sea Lion Commission, Anchorage, AK; White Mountain Research Station, Bishop, CA; Social Commitment Preparatory Program (200 hours community service); Studies in International Development Dakar, Senegal (U of MN); Earth Systems Field School (U of AK); Wilderness Field Station: Behavioral Ecology (ACM, Ely, MN); Terrestrial & Marine Tropical Biodiversity Field Course (Belize).

EXPERIENCE

U.S. FULBRIGHT STUDENT, UNIVERSITY OF ABOMEY-CALAVI, BENIN, LABORATORY OF APPLIED ECOLOGY 2005-2006

- Research: Role of Traditional Healers in Resource Management around the Pendjari Biosphere Reserve; Coursework towards D.E.S.S. of Natural Resource Management

U.S. PEACE CORPS VOLUNTEER, ISLAMIC REPUBLIC OF MAURITANIA, ENVIRONMENTAL EDUCATION 2003-2005

- Taught (500+ hours) in Primary School, prepared lesson plans, organized outside of class activities; Initiated & Led Community Environmental Activities (beekeeping, youth, forestry, school expansion)

PUBLICATIONS

1. Application of Soil Moisture Model to Marula (*Sclerocarya birrea*): Millet (*Pennisetum Glaucum*) Agroforestry System in Burkina Faso, Ceperley, N.C., A. Repetti, and M. B. Parlange; 211-229. In: Bolay, J. -C., M. Schmid, G. Tejada, and E. Hazboun (Eds.). 2012. *Technologies and Innovations for Development: Scientific Cooperation for a Sustainable Future*. Springer University Press, Paris, France.
2. *Ibu Odu* of Central Benin, Ceperley, N.C. In: Pungetti, G., G. Oviedo, and D. Hooke (Eds.). 2012. *Sacred Species and Sites: Advances in Biocultural Conservation*. Cambridge University Press, Cambridge, UK.
3. Significance of sacred sites for riparian forest conservation in Central Benin. 2010. Ceperley, N.C., F. Montagnini, and A. Natta. *Bois et Forêts des Tropiques*. **303** (1): 5-23.
4. The Role of *Íbú ódó* Sacred Pools in Preserving Riparian Forest Structure and Diversity along the Ouémé and Okpara Rivers of Central Benin. Ceperley, N.C. 2008. *Tropical Resources: The Bulletin of the Yale Resource Center*, **27**.
5. Les Noms Locaux du Nord Du Bénin, Ceperley, N.C., In: DeSouzo, S. 2008. *La flore du Bénin, 3rd Ed.* Paris, France.

SKILLS

- **Language:** English (native), French (fluent), Spanish (int.), Hassaniya-Arabic (adv. oral, beg. writ.), Yoruba (int.), Wolof (int.), Gourmantche (beg.)
- **Instrumentation:** Campbell Scientific, Licor, Kipp & Zonen, Sensorscope, Decagon, Davis, Sensirion, Apogee, MADD, UP-Sapflow, Precip, Picarro, Los Gatos Research, and Solar Energy Supply
- **Computer:** Matlab, Microsoft Office, ArcGIS, QGIS, ERMapper, HEC-RAS, SAS, R, Minitab
- **Botanical:** Identification of the Flora of West Africa, North America, Europe, and Neotropical (Belize)
- **Outdoor:** Trained in Avalanche and Glacier Safety, Wilderness First Aid, Lifeguarding, Rope Rescue, Backcountry Recreation (skiing, mountaineering, climbing, hiking, canoeing), Swim Instructor

FELLOWSHIPS & GRANTS

1. Planet Action: A Spot Image Initiative, 2010, *Ecohydrology of Heterogeneous Mixed Savanna (Satellite Data)*.
2. KFPE Young Researcher Fellowship, 2009-2012, *Info4Dourou: Ecohydrology of a mixed savanna agricultural Catchment*.
3. Tropical Resources Institute, Agrarian Studies Fellowship, Globalization Fund, Master's Student Travel Fund, 2007, *Role of Sacred Forest in Riparian Forest Conservation*, Save Region, Benin.
4. Foreign Languages and Area Studies Fellowship, 2006-08, *African Studies – Yoruba*, Yale University (2 years).
5. Fulbright Fellowship, 2005, *Role of Traditional Healers in Resource Monitoring*, Benin.
6. U.S. Embassy to Mauritania, Self-Help Program, 2004, *School Improvement Project*, Jidrel Mohghuen, Mauritania.
7. San Diego Peace Corps Partnership, 2004, *Small Project Assistance for village beekeeping*, Mauritania.
8. Grinnell College Environmental Studies Grant: WMRS, Bishop, CA (2001); TASSC, Anchorage, AK (2002).
9. Grinnell College Trustee Honor Scholarship, 1999-2003, Grinnell, IA (4 years).
10. Tallen Award for Women in Science, ACM Wilderness Field Station, 2000, Ely, MN.

ASSOCIATIONS

- American Geosciences Union. *Student Member*. 2009 – 2013
- European Geosciences Union. *Student Member*. 2010 – 2013
- International Society of Tropical Foresters. *Student member, Conference Organizer for Yale Chapter*. 2006 - 2008.
- Society of American Foresters. *Student member*. 2006-2008.
- Sustainable Environment & Development Student Interest Group, Yale University. *Treasurer, Member*. 2006-2008.
- Environmental Action Group, Grinnell College. *Coordinator, Member*. 2000-2003.